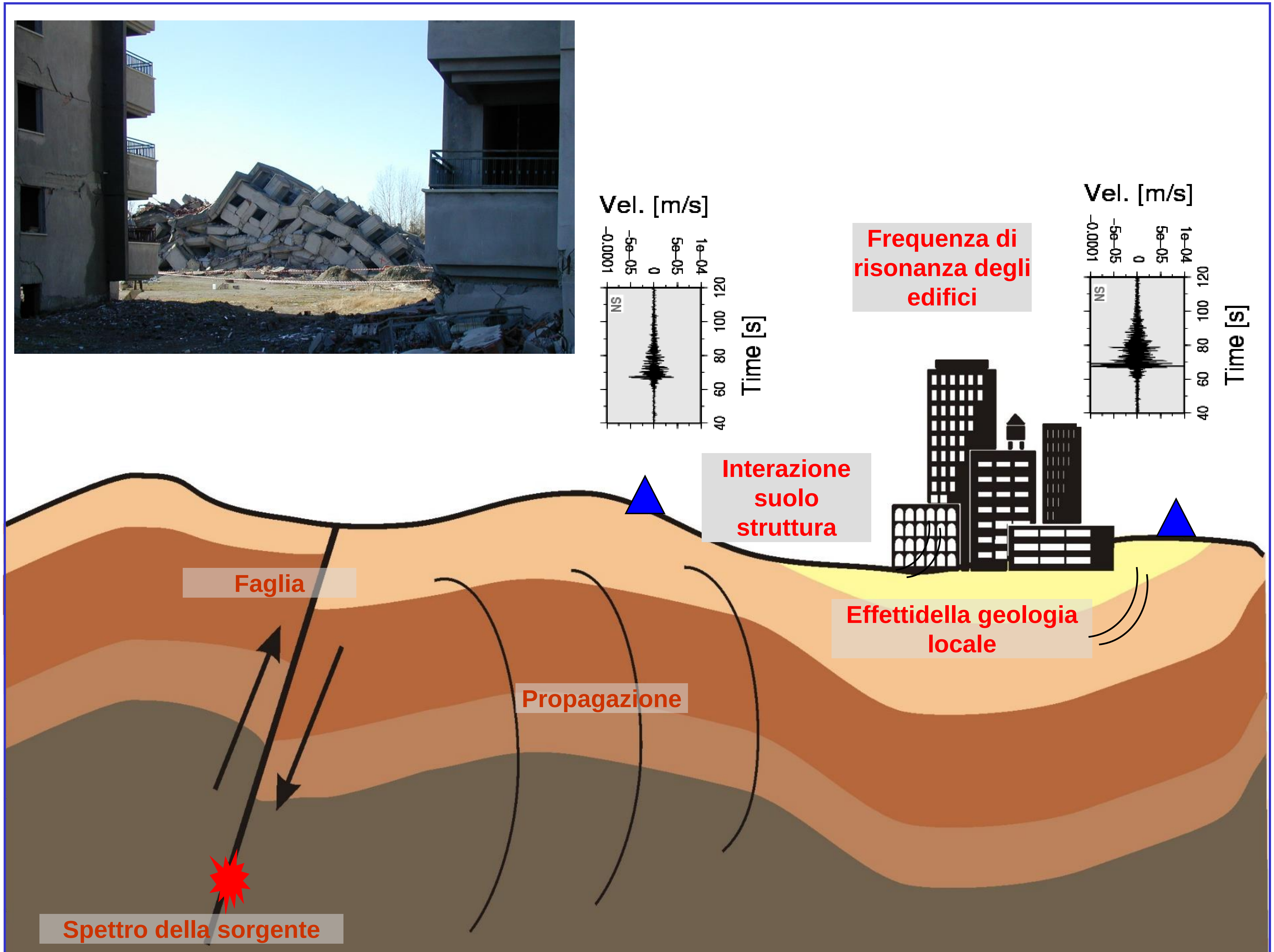

UNIVERSITÀ DEGLI STUDI DI TRIESTE

Effetti di sito: Valle di Gubbio

L'ampiezza delo scuotimento AUMENTA!
all'aumentare della distanza dalla sorgente!

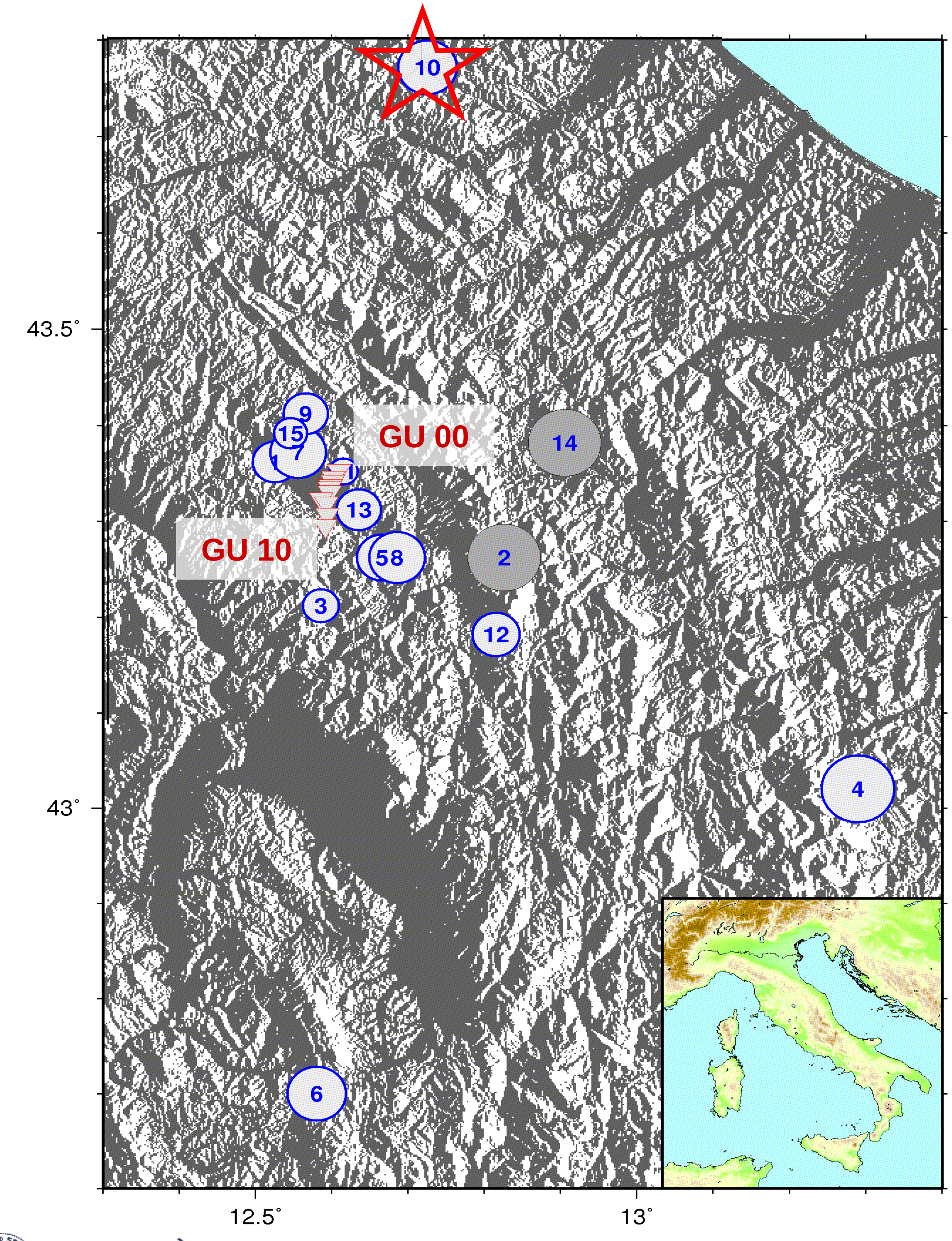

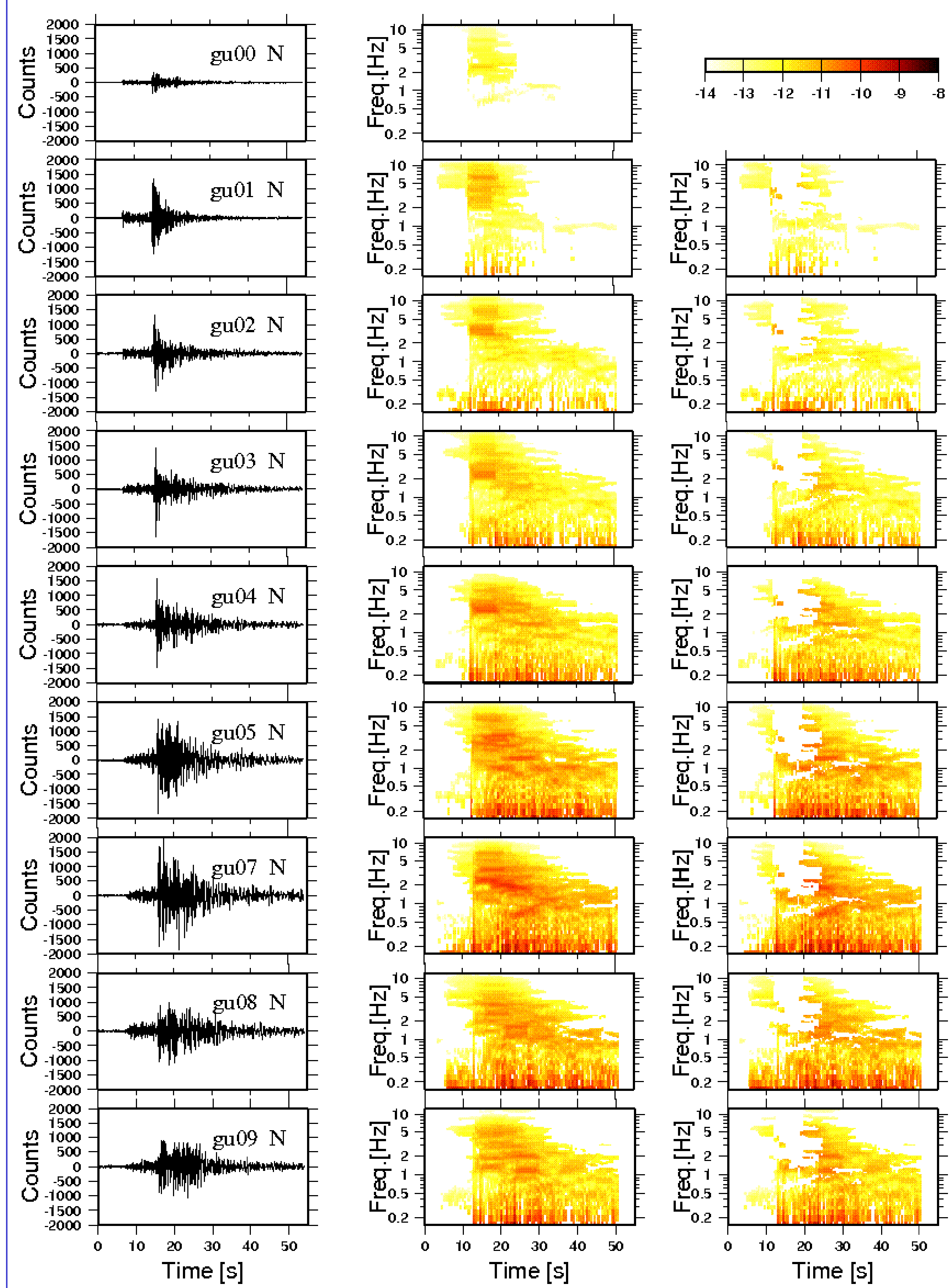

La banda di frequenza amplificata dipende dalla struttura del sottosuolo

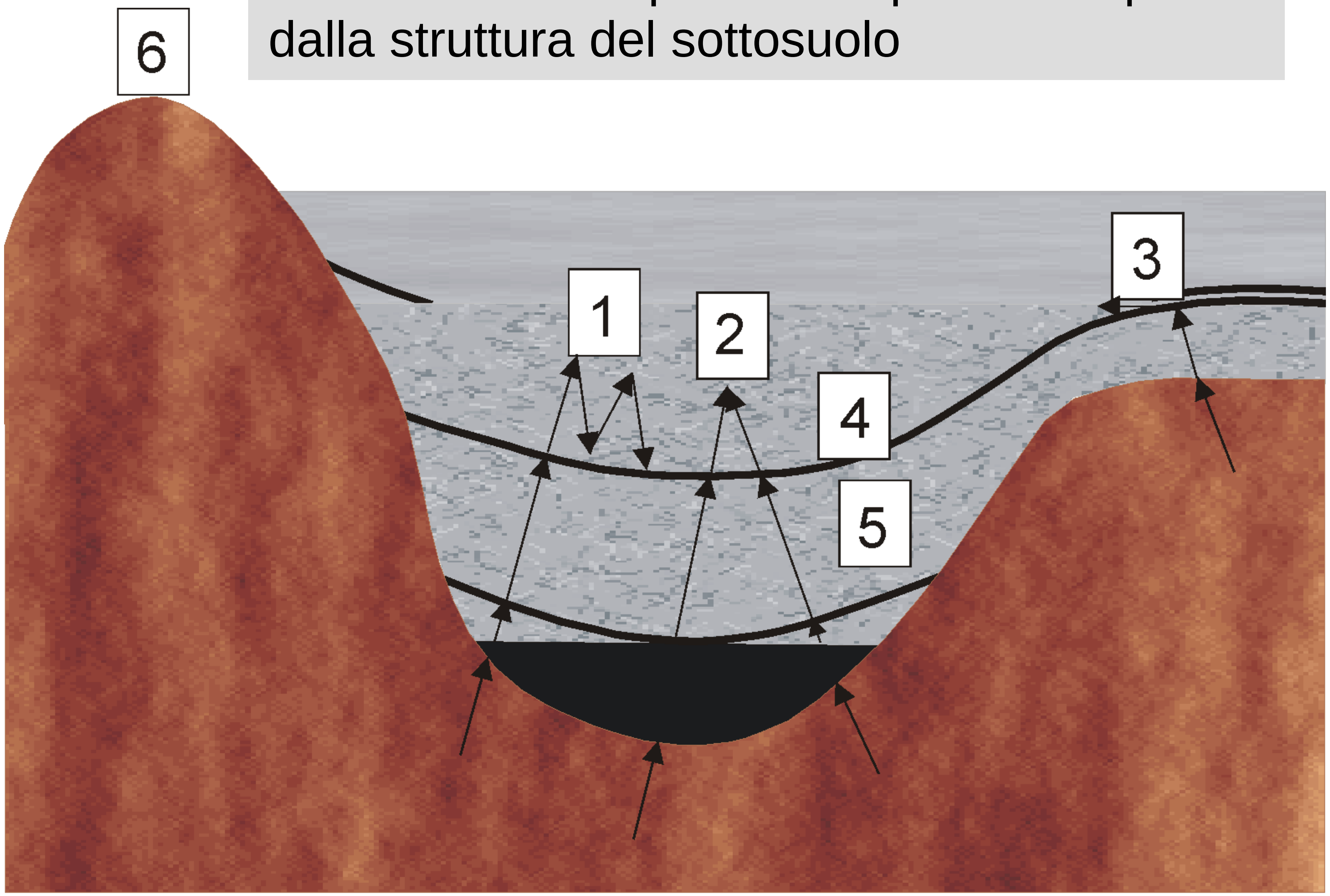

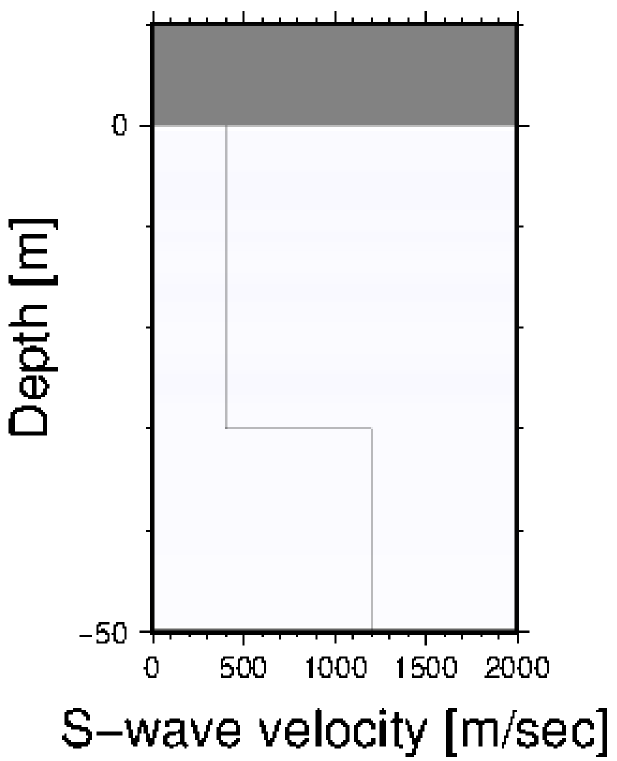

1 - Resonance due to impedance contrasts, 2 - Focusing due to subsurface topography, 3 - Body waves converted to surface waves, 4 - Water content, 5 - Randomness of the medium and 6 - Surface topography

Modified after Safak (2001)

MZS - Engineering Seismology

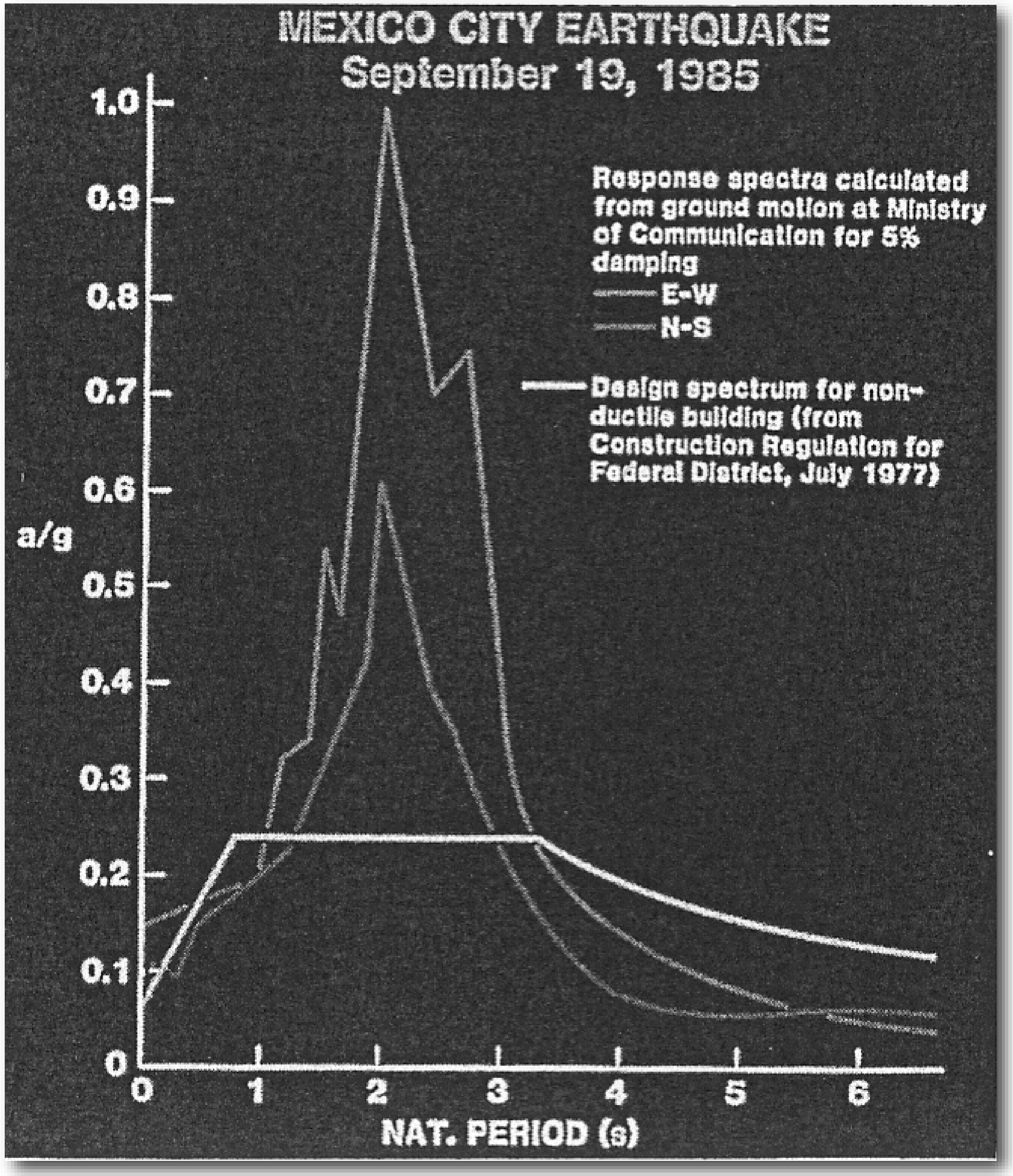

Michoacan 1985 event: way to DF...

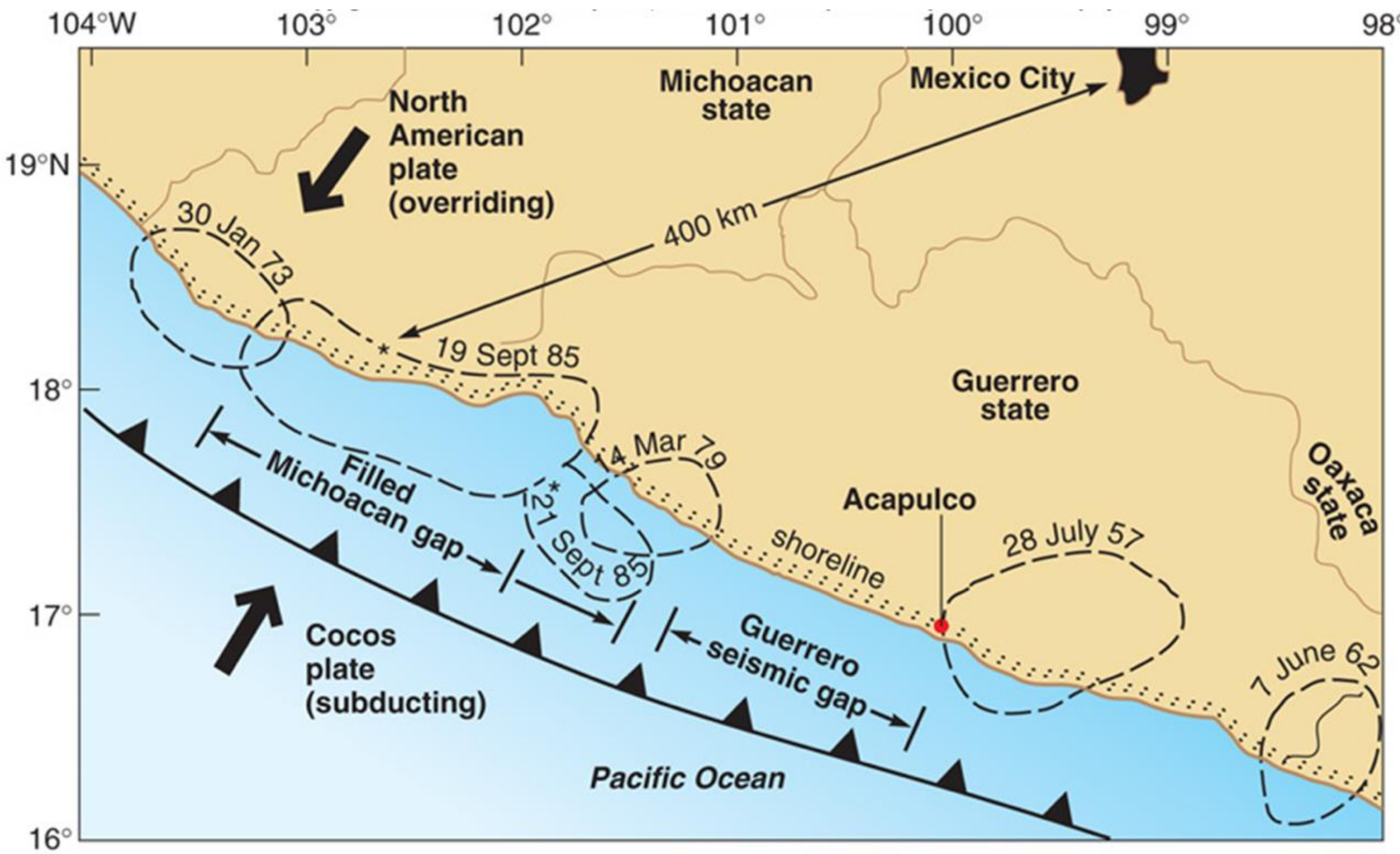

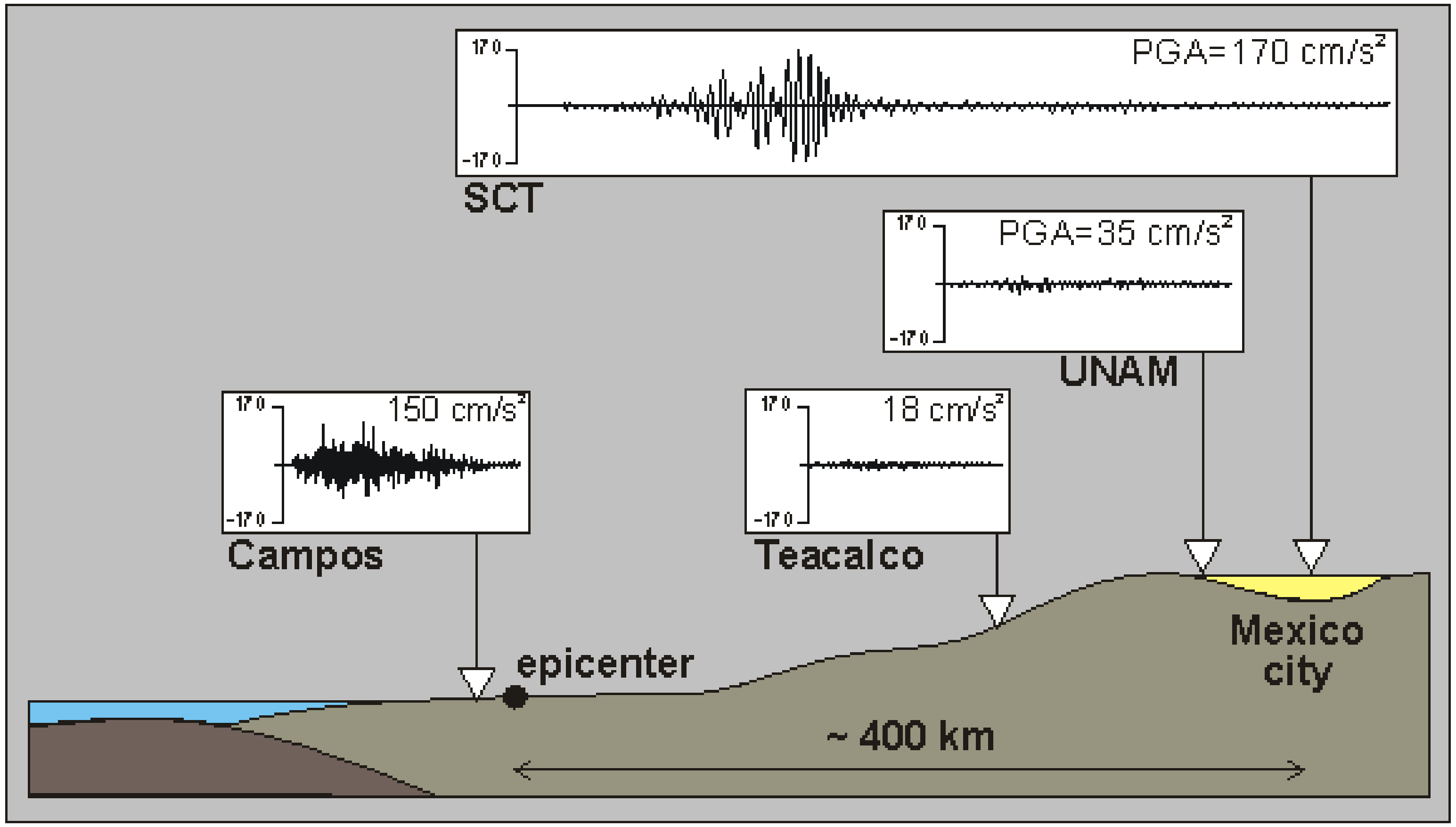

Tenochtitlan and Mexico City (DF)

La ciudad de Tenochtitlan y su entorno en el siglo XVI Pintura de Miguel Covarrubias, Museo Nacional de Antropología, México DF

The actual boundaries of the World Heritage Property follows the boundaries of the Historical Monuments Zones, according to the limits of the city in the 19th century (perimeter A), and a buffer zone (perimeter B)

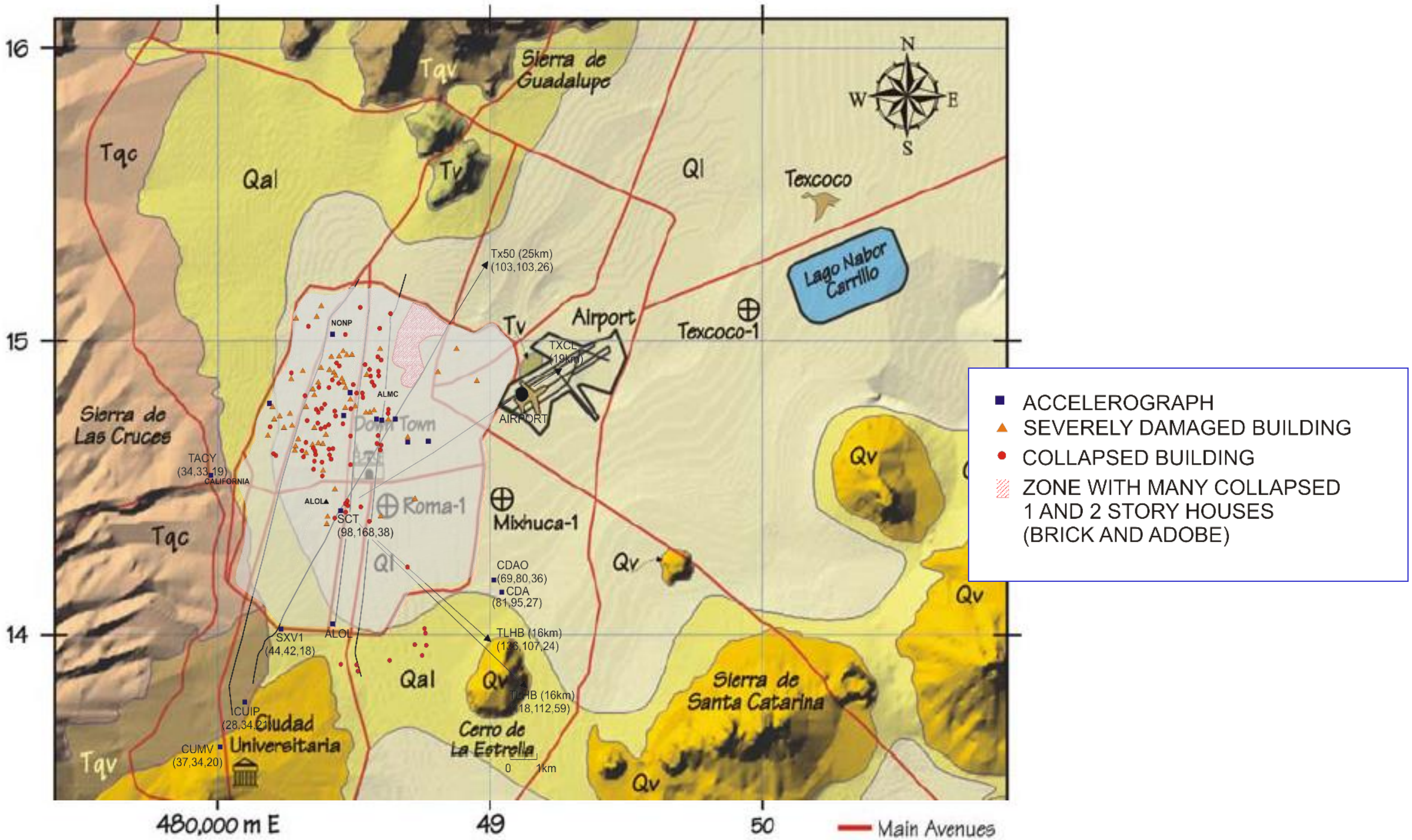

Modified Flores-Estrella et al. (2007) and Singh et al.(1989)

Michoacan 1985 event: GM in DF

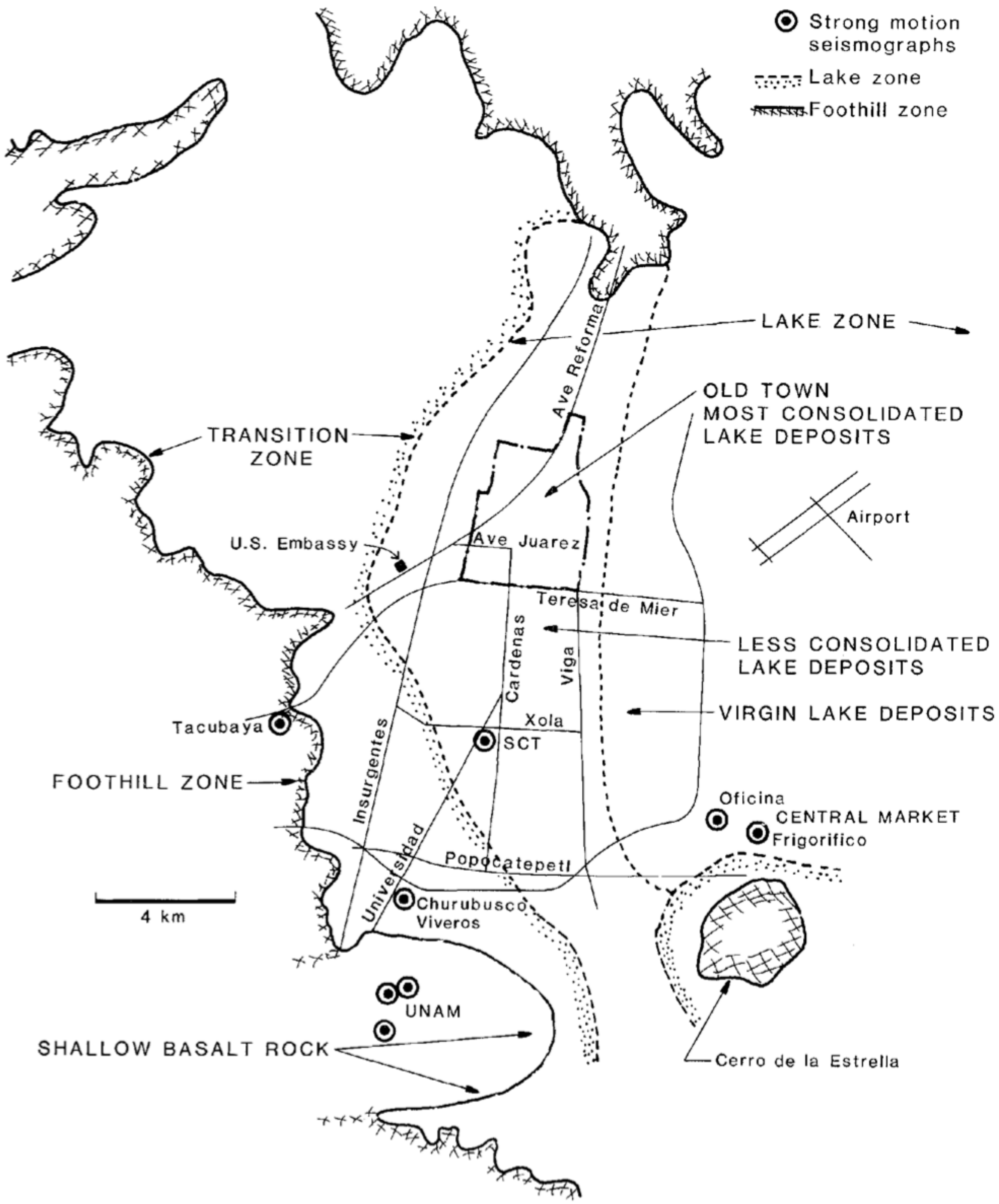

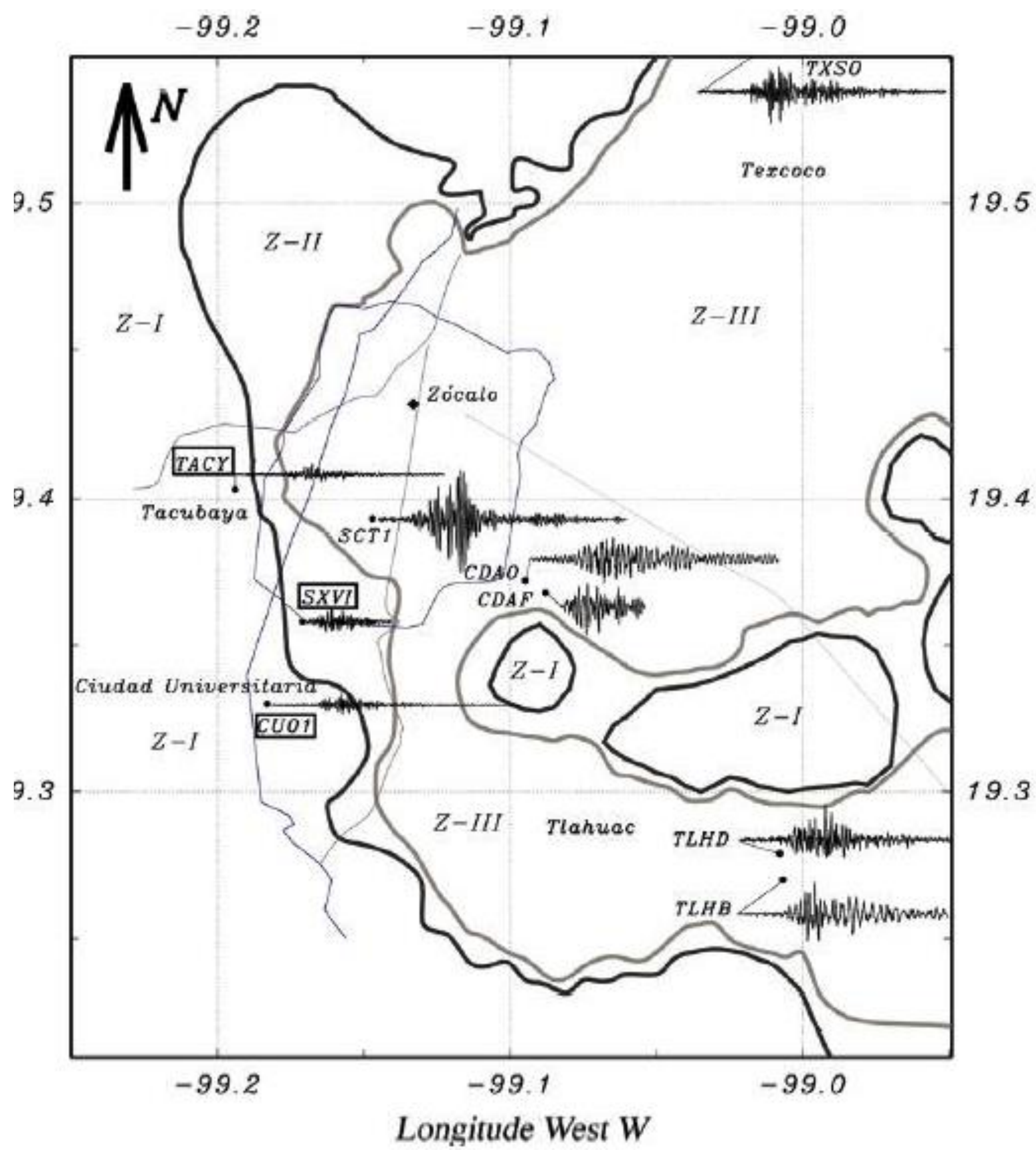

Michoacan 1985 event: damage in DF

Wreckage of a twenty-one-story building in
Conjunto Pino Suarez Complex

Totally destroyed office building in the foreground,
while the 44-floor Torre Latinoamericana office
building, in the background on the right, stands

Response spectra

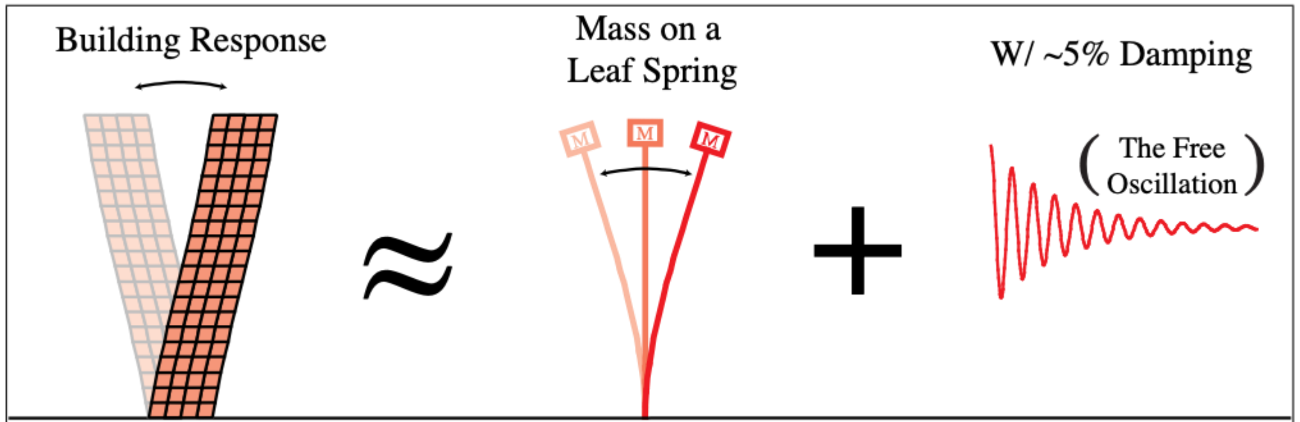

Figure 1. The response-spectrum value is the peak motion (displacement, velocity, or acceleration) of a damped single-degree of freedom harmonic oscillator (with a particular damping and resonant period) subjected to a prescribed ground motion.

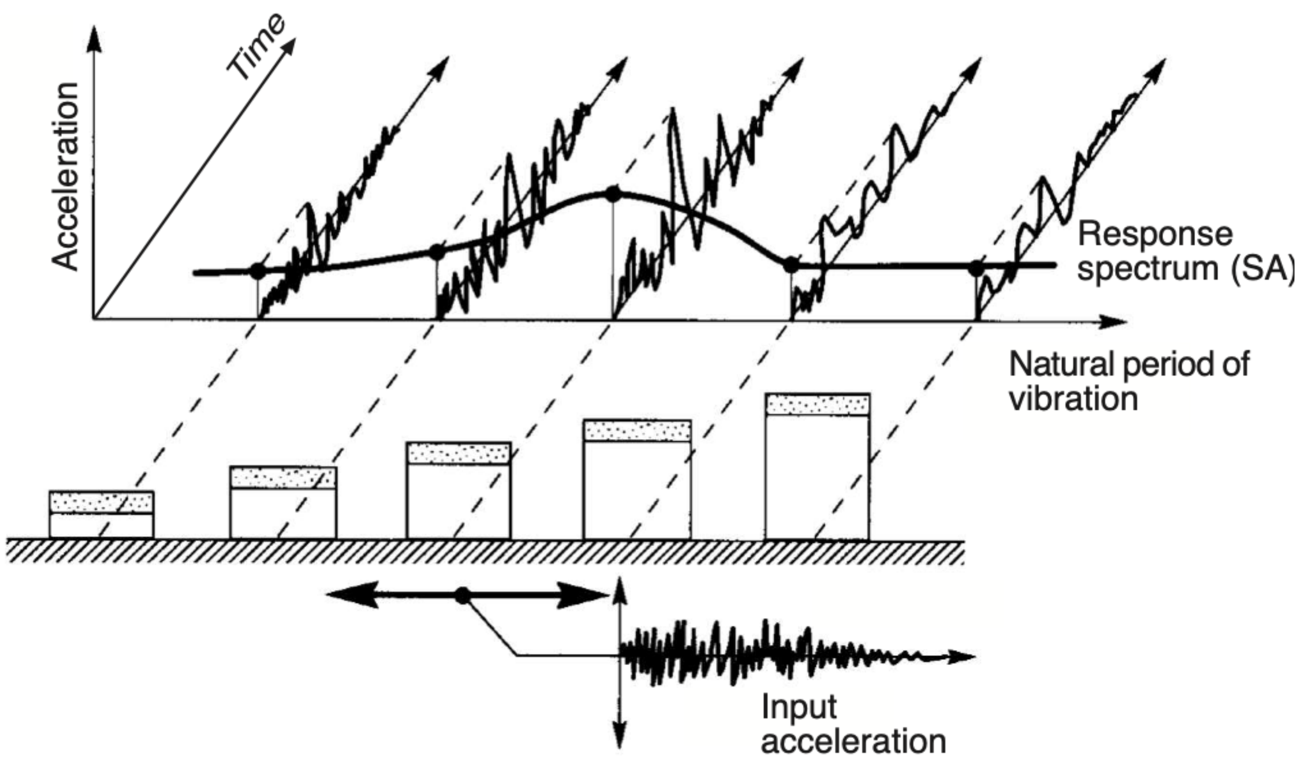

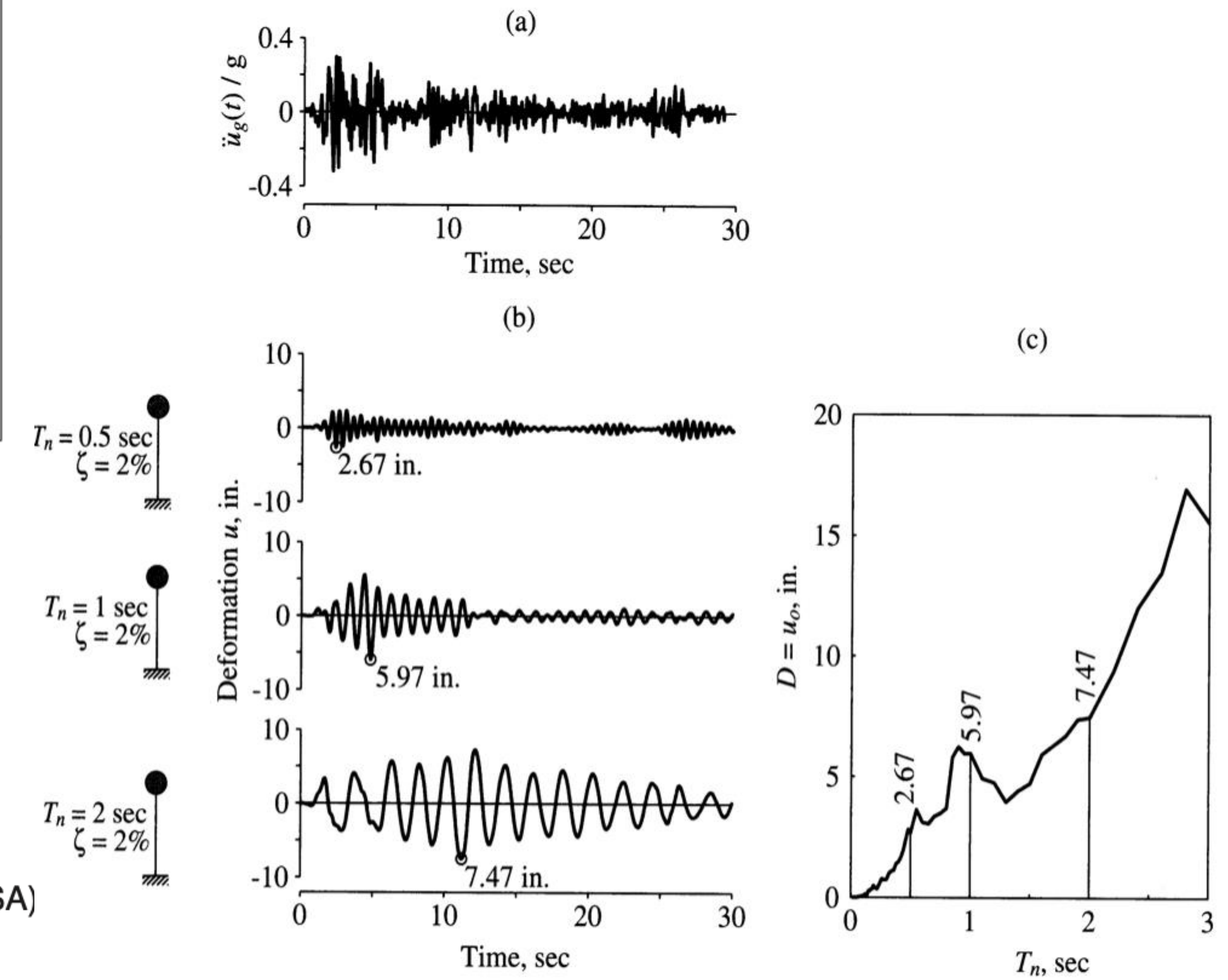

Figure 6.6.1 (a) Ground acceleration; (b) deformation response of three SDF systems with $\zeta = 2\%$ and $T_n = 0.5$, 1, and 2 sec; (c) deformation response spectrum for $\zeta = 2\%$.

Relative displacement

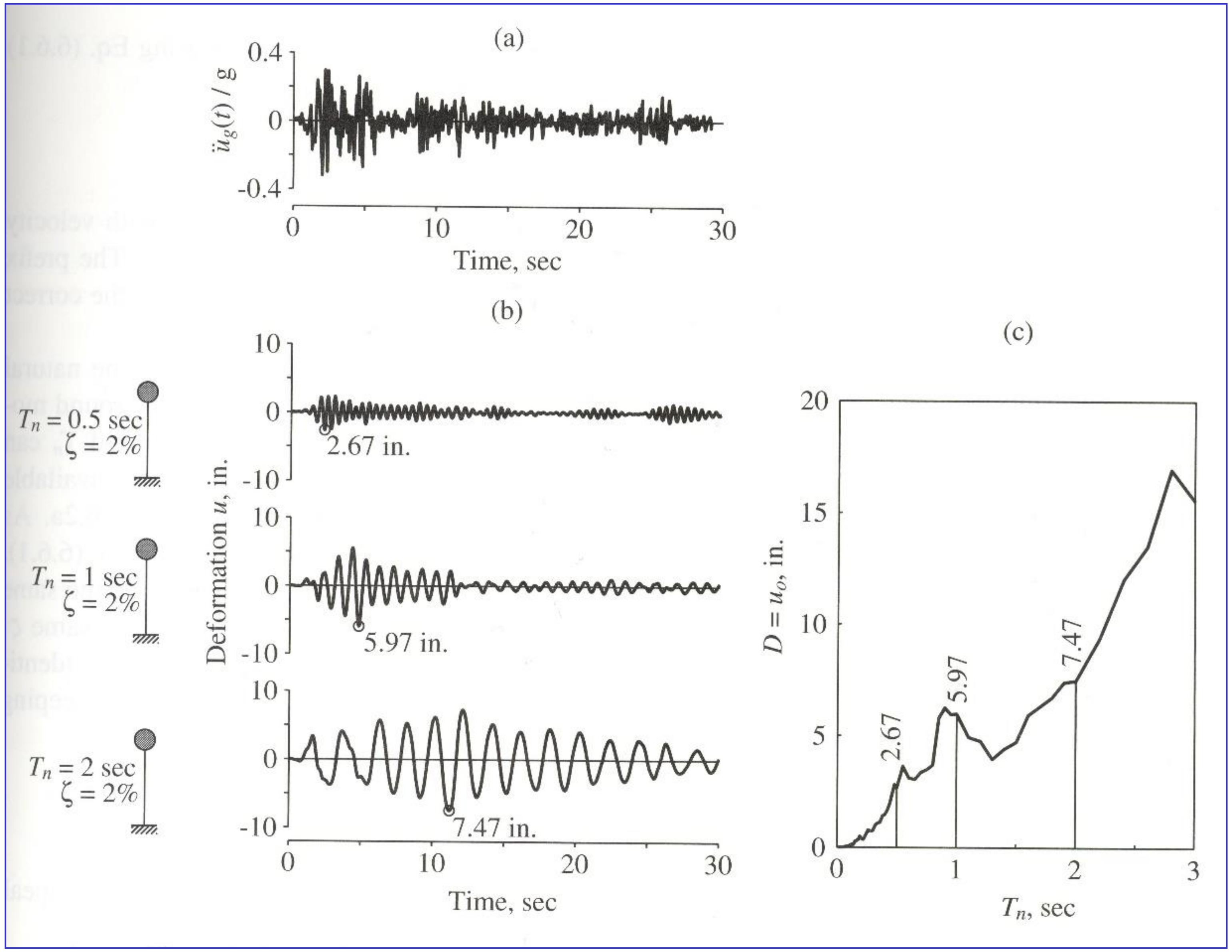

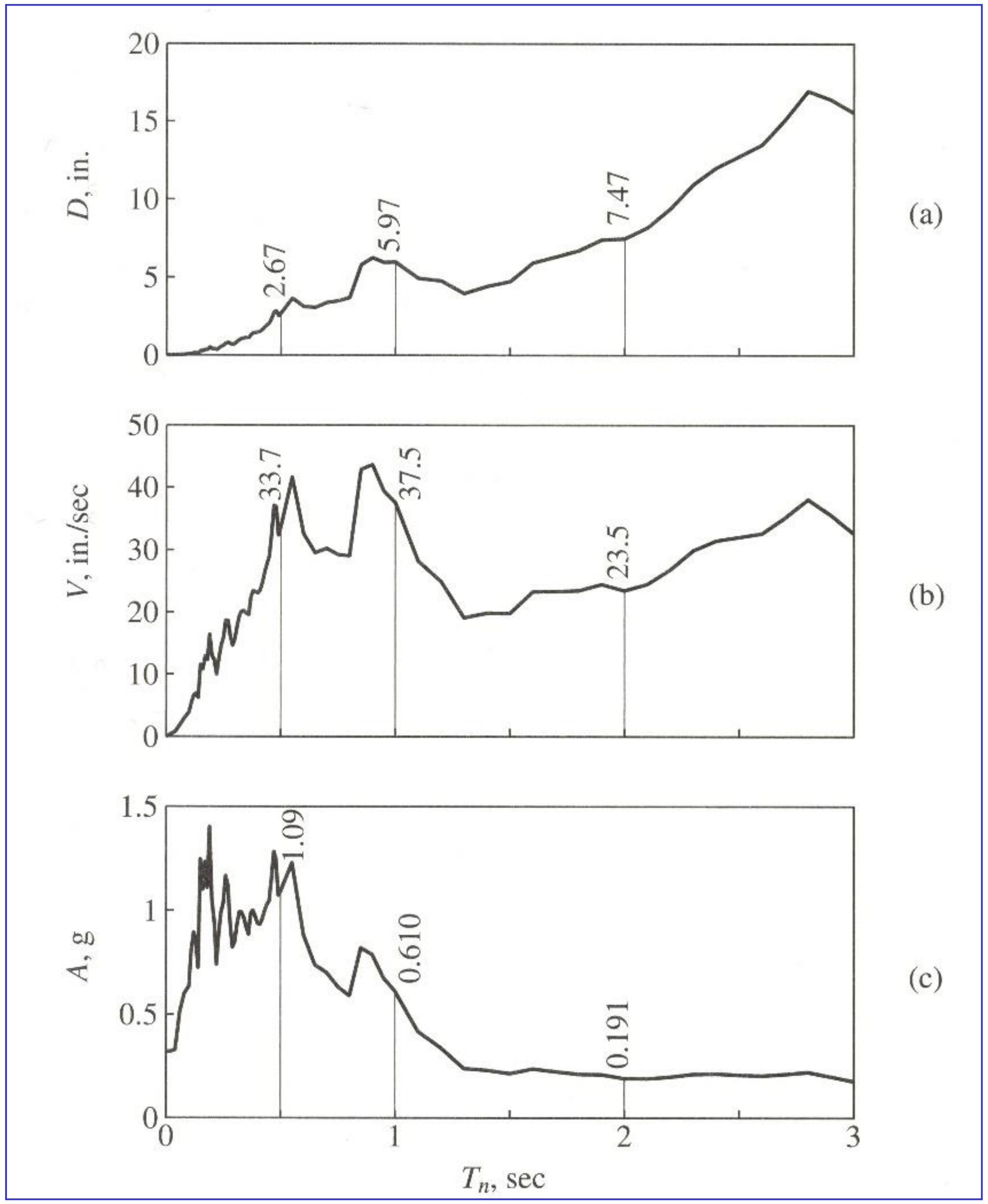

Pseudo Velocity and
Pseudo accelerations

UNIVERSITÀ DEGLI STUDI DI TRIESTE

Since PSV and PSA are obtained by SD simply multiplying for a factor □

The 3 spectra can be diplayed on the same plot

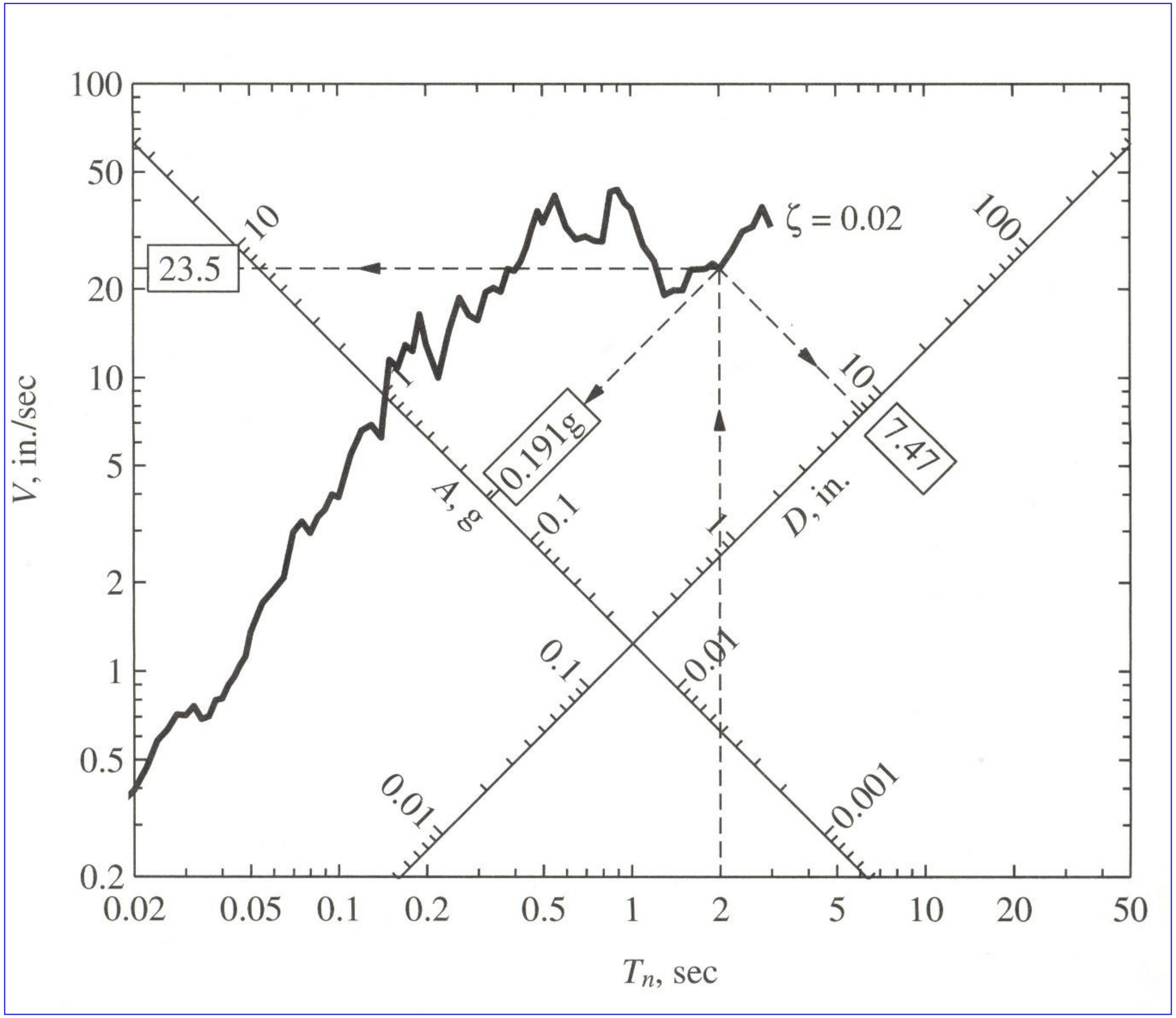

Response spectra

Critically damped system $(\xi = 1)$.
2. Overdamped system $(\xi > 1)$.
3. Underdamped system $(\xi < 1)$

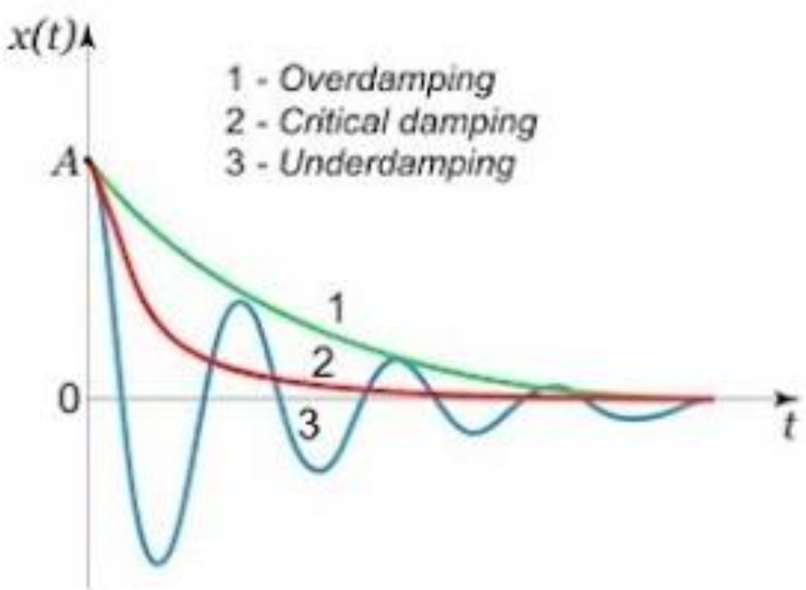

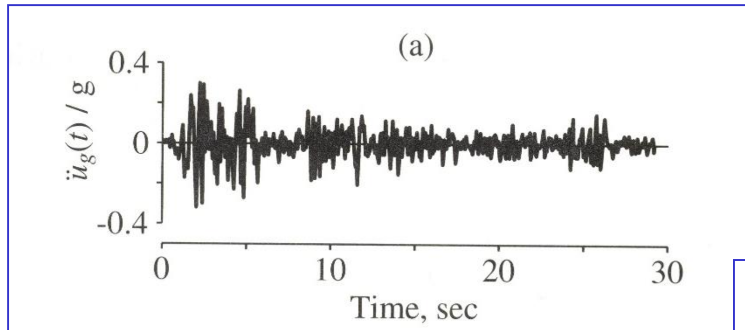

La risposta dell'oscillatore dipende dalla sua frequenza e dallo smorzamento!

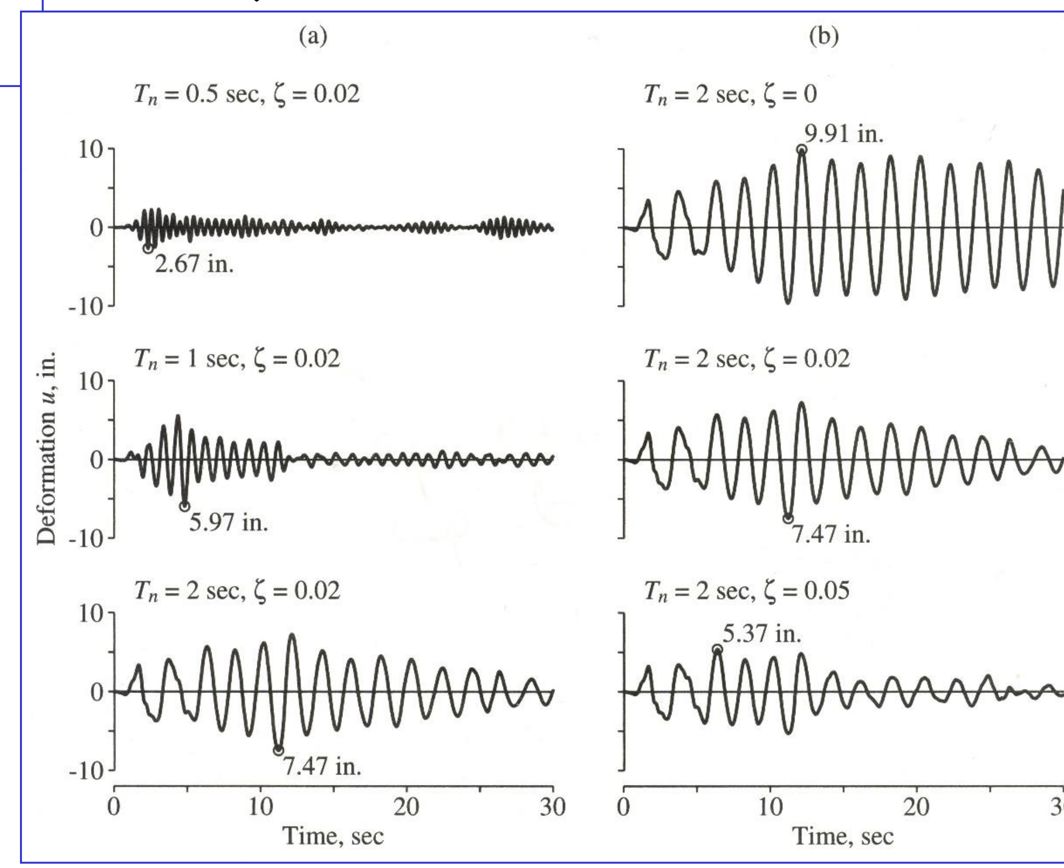

Born: 21 March 1768 in Auxerre, Bourgogne, France

Died: 16 May 1830 in Paris, France

$$\frac{1}{2\pi}\sum |A(\omega)| e^{i[\omega t + \phi(\omega)]} \Delta\omega$$

$$=$$

$$f(t)$$

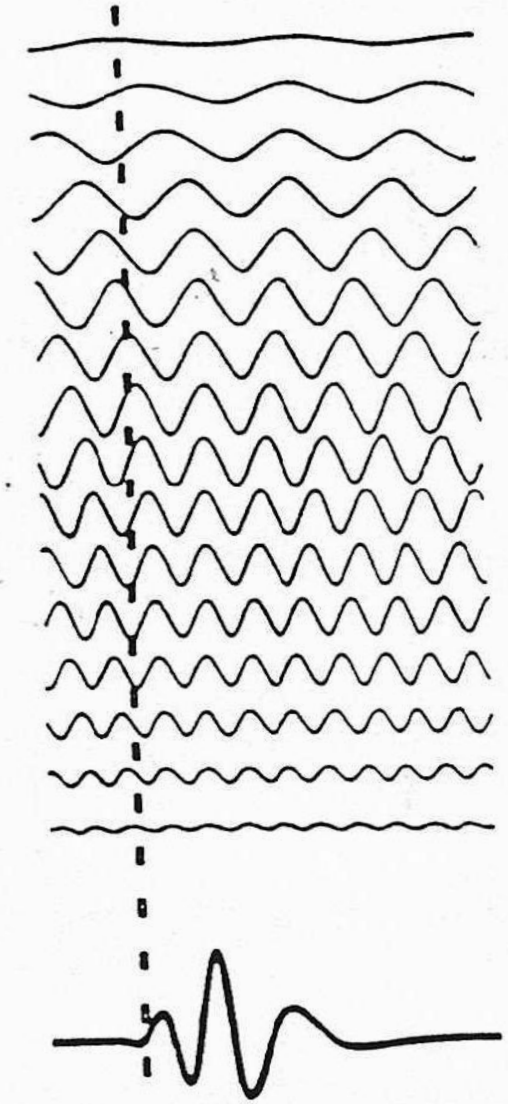

FIGURE 5.B1.2 A discretized version of Eq. (5.1.1), showing how a sum of harmonic terms can equal an arbitrary function. The amplitudes of each harmonic term vary, being prescribed by the amplitude spectrum. The shift of the phase of each harmonic term is given by the phase spectrum.

Fourier spectrum: $G(\omega)=\int_{-\infty}^{\infty} g(t)\exp(i\omega\, t)\,dt$

- In what way are there two numbers at each frequency? From basic complex number theory:

$$e^{i\theta} = \cos\theta + i\sin\theta$$

- Using this, the definition can be rewritten as:

$$G(\omega)=\int_{-\infty}^{\infty} g(t)\left[\cos(\omega\, t)+i\sin(\omega\, t)\right]dt$$

- Thus, the definition can be rewritten as:

$$a(\omega)=\int_{-\infty}^{\infty} g(t)\cos(\omega\, t)\,dt$$

cos(□t) even function

$$b(\omega)=\int_{-\infty}^{\infty} g(t)\sin(\omega\, t)\,dt$$

sin(□t) odd function

- The two numbers at each frequency are a(ω) and b(ω) (for g(t) real).

$$G(\omega)=a(\omega)+ib(\omega)$$

Modified from D. Boore, 2004

$$f(t) = \frac{a_0}{2} + \sum_{n=1}^{\infty}\left[a_n \cos\left(\frac{n2\pi t}{T}\right) + b_n \sin\left(\frac{n2\pi t}{T}\right)\right]$$

$$a_n = \frac{1}{T}\int_{-T/2}^{T/2} f(t)\cos\left(\frac{n2\pi t}{T}\right)dt$$

$$b_n = \frac{1}{T}\int_{-T/2}^{T/2} f(t)\sin\left(\frac{n2\pi t}{T}\right)dt$$

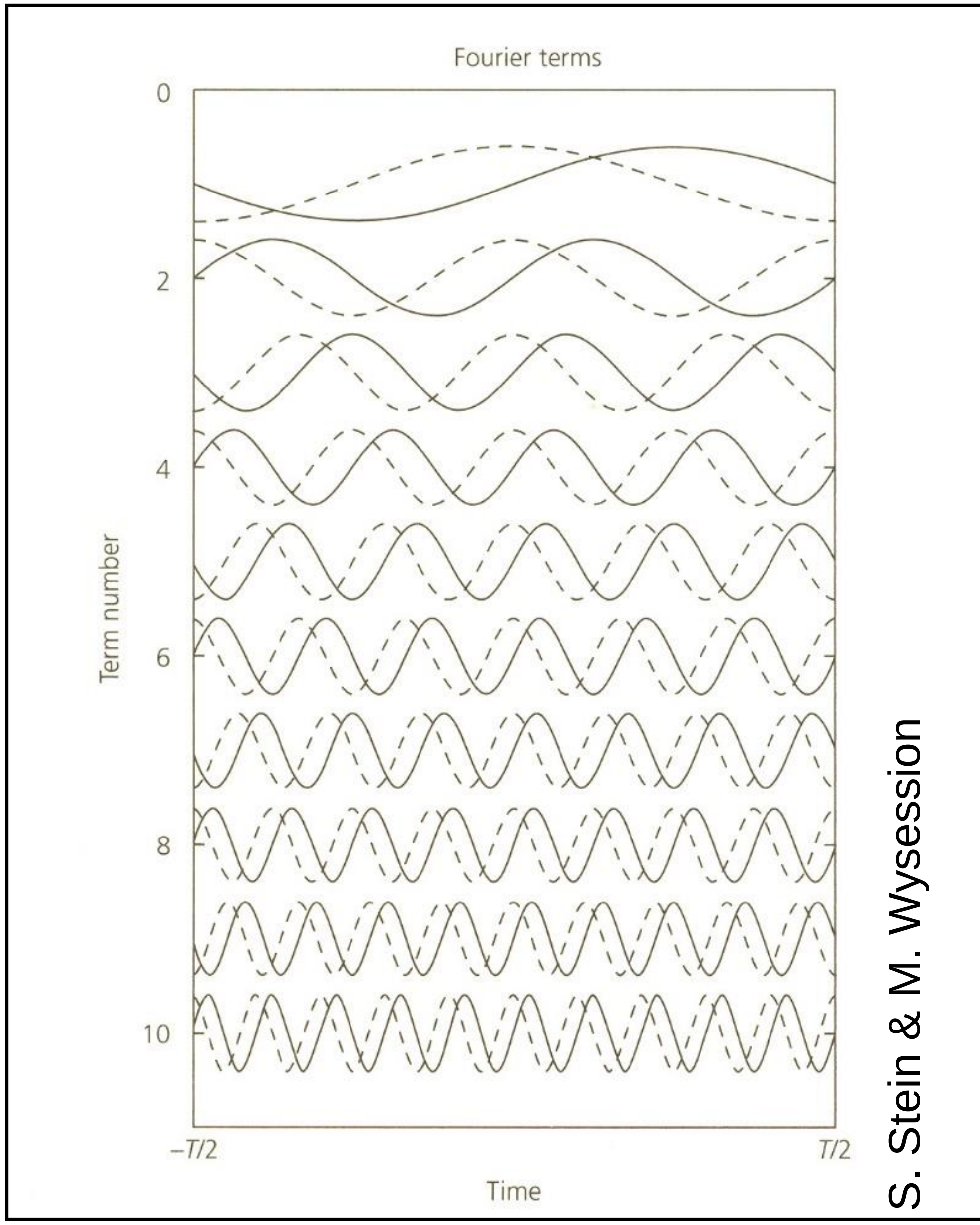

S. Stein & M. Wysession

with
n positive integer

Fourier spectrum: $$G(\omega) = \int_{-\infty}^{\infty} g(t) \exp(i\omega t) dt$$

$$a(\omega) = \int_{-\infty}^{\infty} g(t) \cos(\omega t) dt$$

$$b(\omega) = \int_{-\infty}^{\infty} g(t) \sin(\omega t) dt$$

$$G(\omega) = a(\omega) + ib(\omega)$$

It is very useful to define the Fourier Amplitude Spectrum:

$$|G(\omega)| = \sqrt{\left(a^2(\omega) + b^2(\omega)\right)}$$

and the Fourier Phase Spectrum:

$$\phi(\omega) = \tan^{-1} \frac{b(\omega)}{a(\omega)}$$

Modified from D. Boore, 2004

Some properties of the Fourier Transform $\Im$

-Linearity: $$\Im[a_1 f_1(t) + a_2 f_2(t)] = a_1 \Im f_1(\omega) + a_2 \Im f_2(\omega)$$

-Derivative: $$\Im\left[f^{(n)}(t)\right] = (i\omega)^n \Im f(\omega)$$

-Shift: $$\Im[f(t-a)] = e^{-i\omega a} \Im f(\omega)$$

-Convolution: $$\Im[f_1(t) * f_2(t)] = \Im \int_0^t f_1(\tau) f_2(t-\tau) d\tau = \Im f_1(\omega) \Im f_2(\omega)$$

Applications: linear system (source*path*site*instrument), time-delay of propagation (e.g. array analysis), solving differential equations, etc…

Parseval identity
(sum of the square values)

$$\| f(t) \|_2 = \| \Im f(\omega) \|_2$$

Fourier spectrum

Add the following 3 sinusoids:

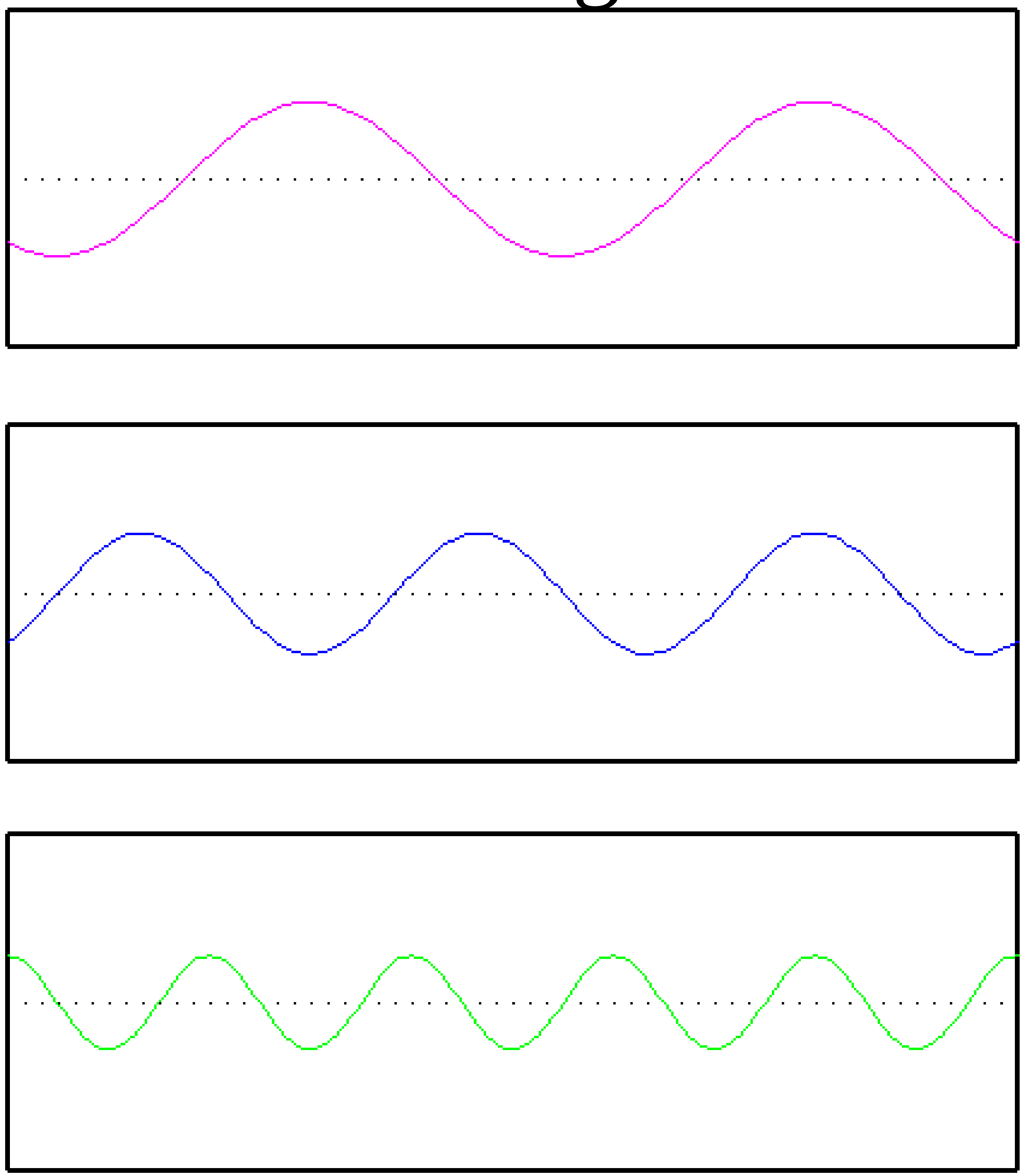

Courtesy of D. Boore

Fourier spectrum

This shows the summation of the 3 sinusoids to produce the total signal (top) and the Fourier amplitude (bottom)

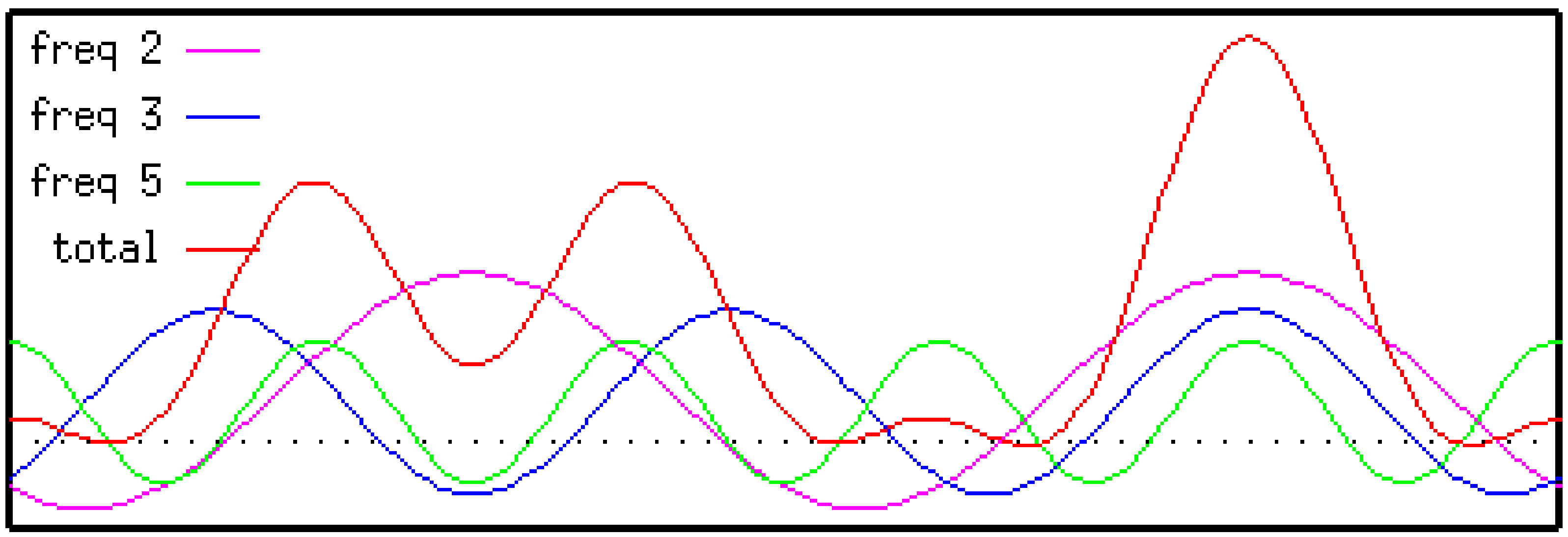

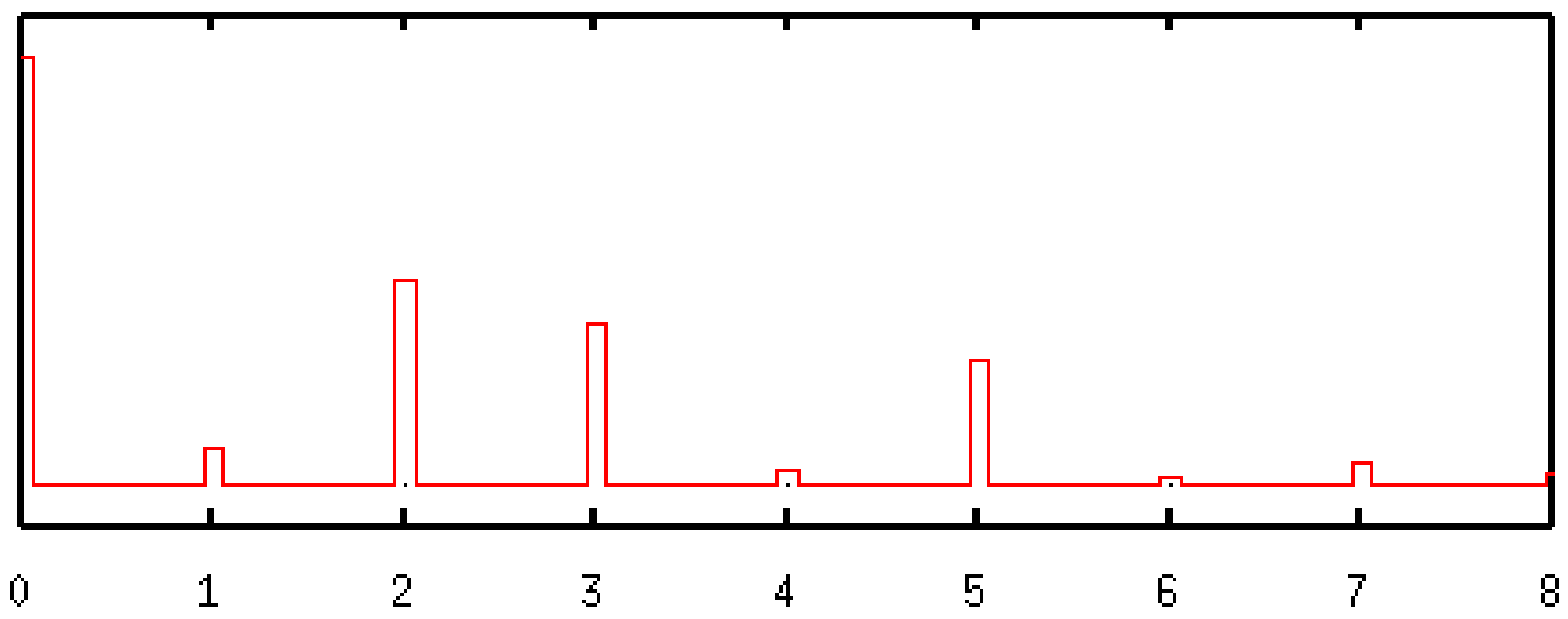

Courtesy of D. Boore

Some properties of the Fourier Transform $\Im$

-Linearity: $$\Im\left[a_1 f_1(t) + a_2 f_2(t)\right] = a_1 \Im f_1(\omega) + a_2 \Im f_2(\omega)$$

-Derivative: $$\Im\left[f^{(n)}(t)\right] = (i\omega)^n \Im f(\omega)$$

-Shift: $$\Im\left[f(t-a)\right] = e^{-i\omega a} \Im f(\omega)$$

-Convolution: $$\Im\left[f_1(t) * f_2(t)\right] = \Im \int_0^t f_1(\tau) f_2(t-\tau) d\tau = \Im f_1(\omega) \Im f_2(\omega)$$

Applications: linear system (source*path*site*instrument), time-delay of propagation (e.g. array analysis), solving differential equations, etc…

Parseval identity
(sum of the square values)

$$\left\| f(t) \right\|_2 = \left\| \Im f(\omega) \right\|_2$$

Amplitude spectra

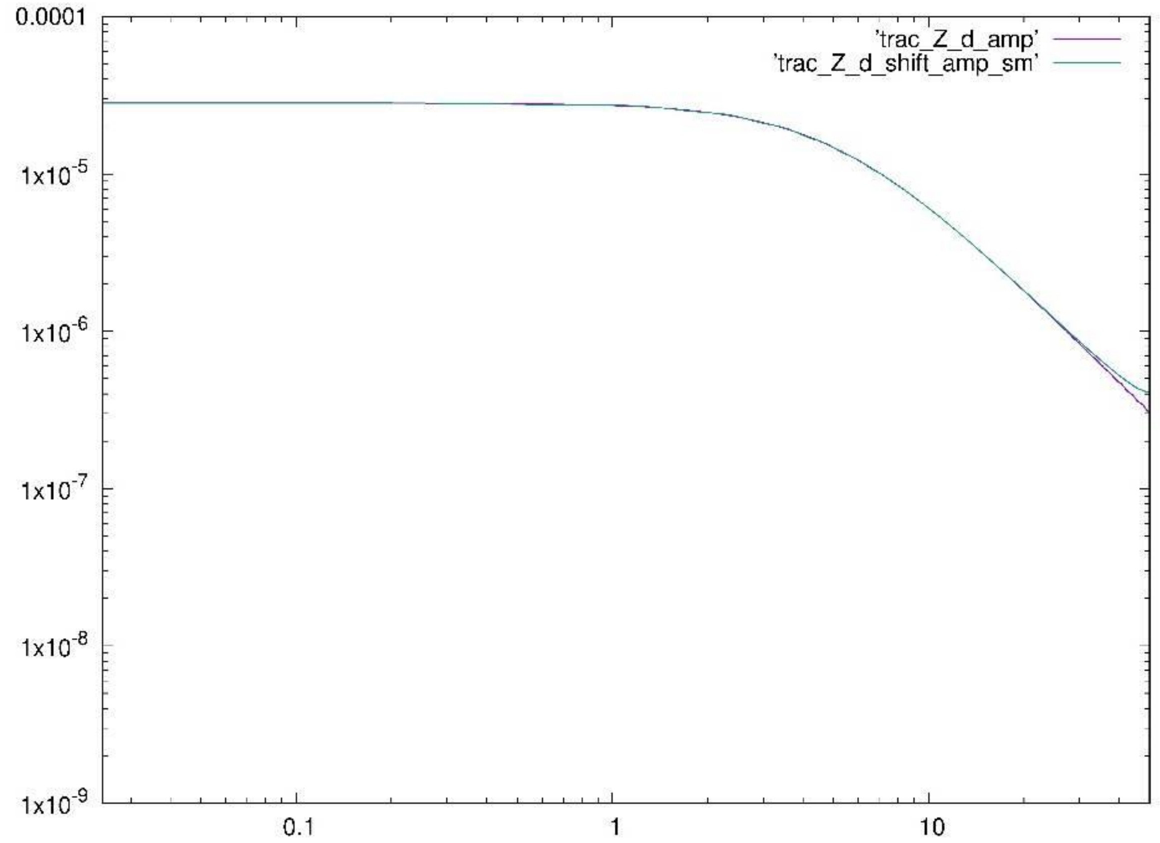

Time Series

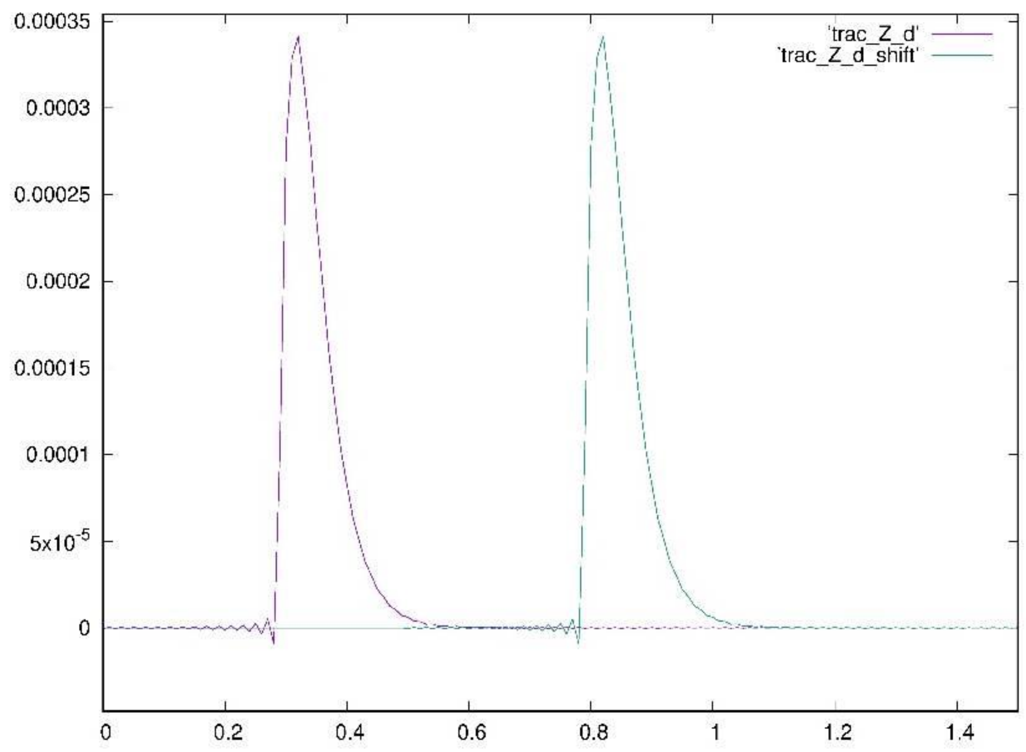

Phase spectra

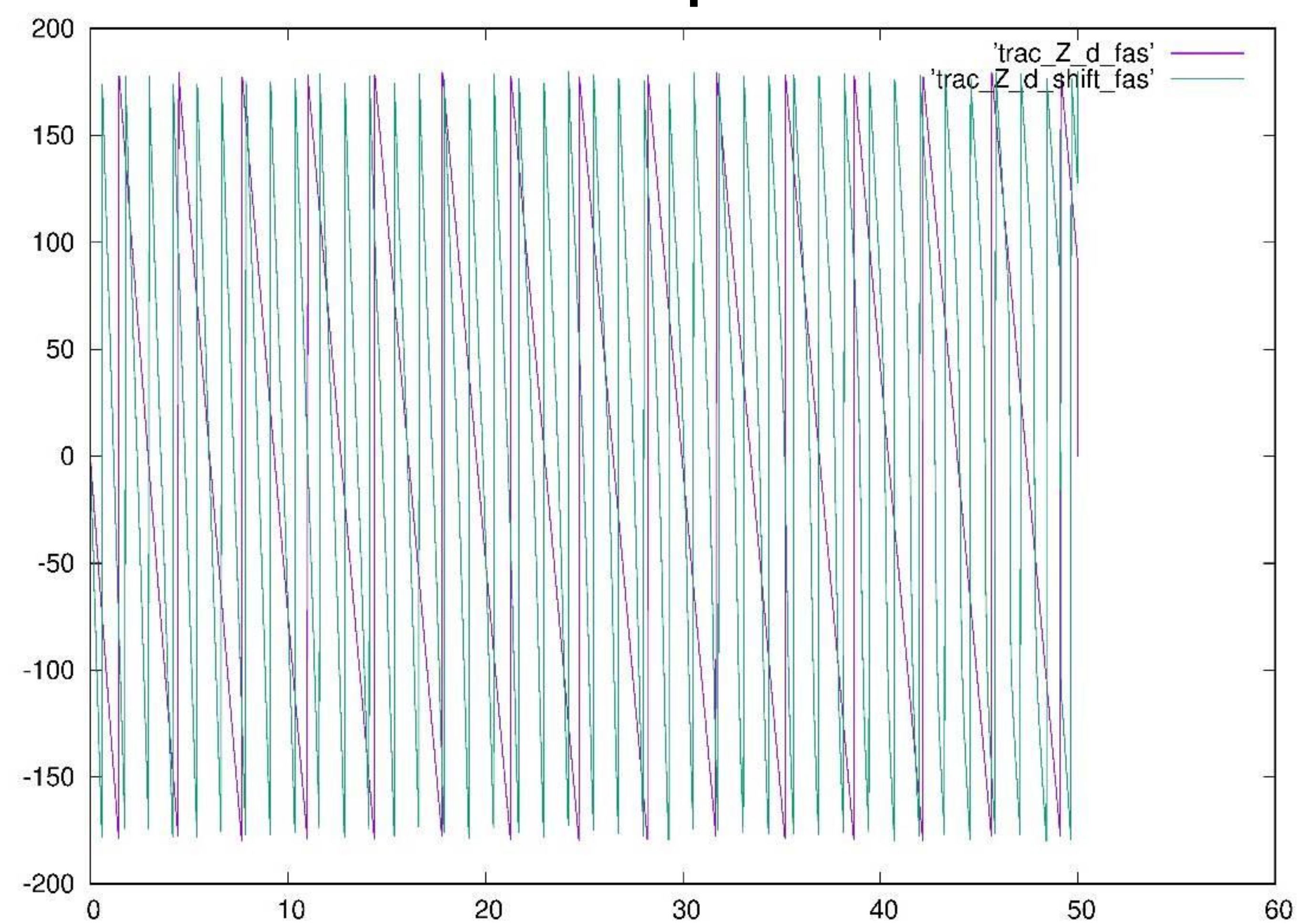

UNIVERSITÀ DEGLI STUDI DI TRIESTE

0 1 2 .... N

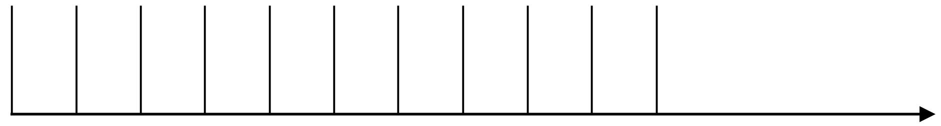

sampling

0 dt 2dt .... Ndt=T

Timet [s]

N intervals with spacing dt
Duration T of the whole signal
T=N*dt

Sampling

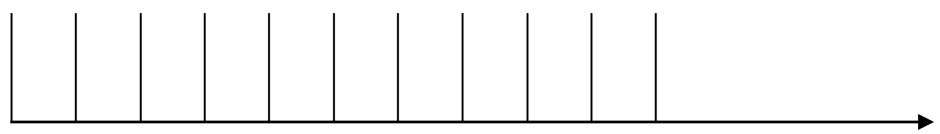

$-f_N$ $-f_N+df$...... f_N

Frequency [Hz]

N intervals of width df

Nyquist frequency: $f_N=1/(2*dt)$

$N*df=2f_N$ □

$df=2f_N/N=1/Ndt=1/T$

df=1/T

df depends on the window length

df dt=1/N

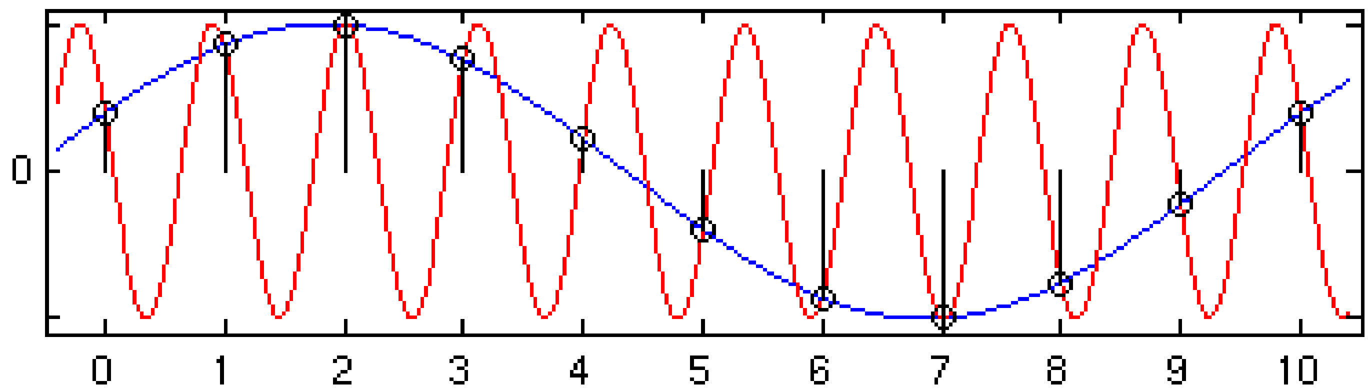

dt=1s;

f_N=0.5Hz

f>0.5Hz cannot be retrieved en

(Periods T< 2 s)

The red curve has a period of T=1.1s

red: freq>Nyquist

Look at the blue curve!!!

Due to Aliasing the data must be low-pass filtered before the analog to digital conversion (anti-alias filter). The corner frequency of the filter $0.8f_{N.}$

Input: Time signal

signal $y(t_n)$ — Fourierspectrum $Y(\omega)$ — Sinus form **Period T**

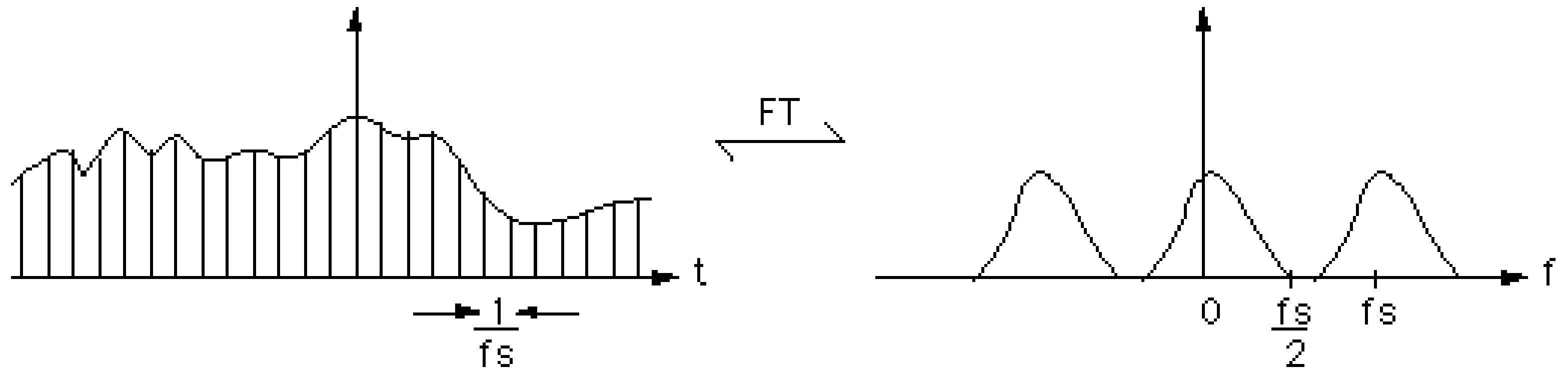

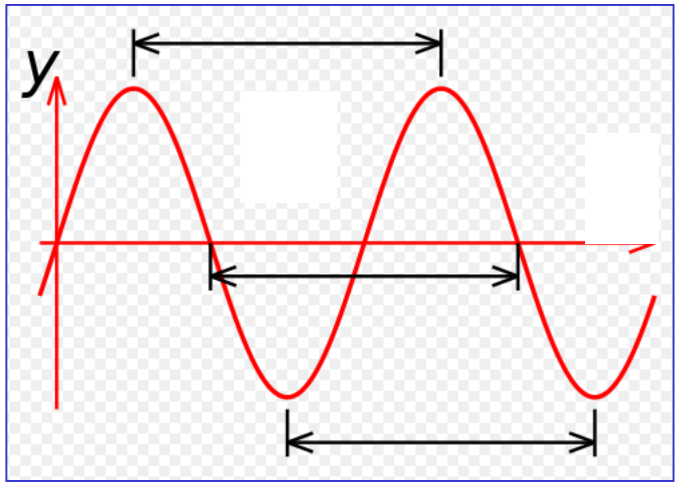

$fs=1/dt$ $f_{Nyquist}=fs/2$ $\omega=2\pi f=2\pi/T$ (angular frequency [rad/s])

(time) Aliasing

Signal $y(x_n)$ — Fourierspectrum Y(□) — Sinus form **wavelength** □

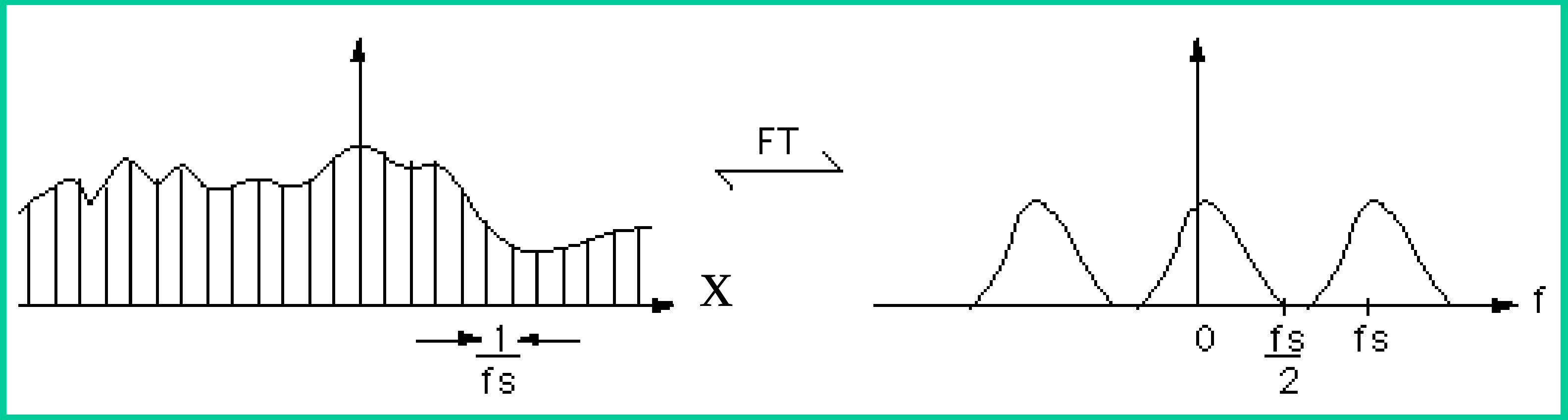

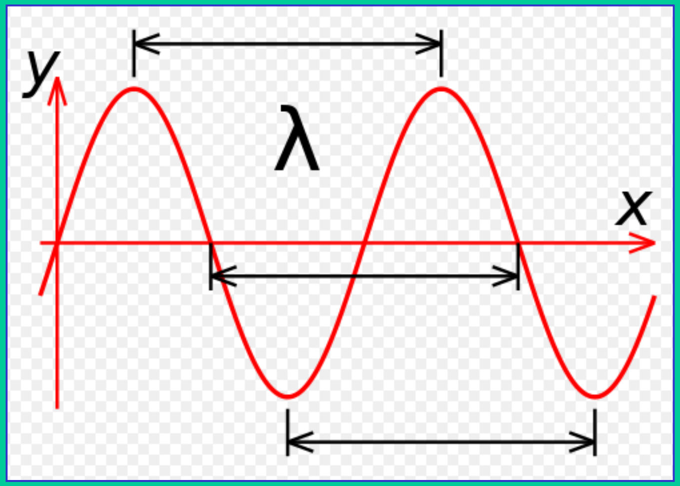

$fs=1/dx$ $f_{Nyquist}=fs/2$

$\kappa=2\pi f=2\pi/\lambda$

(Wavenumberl [rad/m])

(spatial) Aliasing

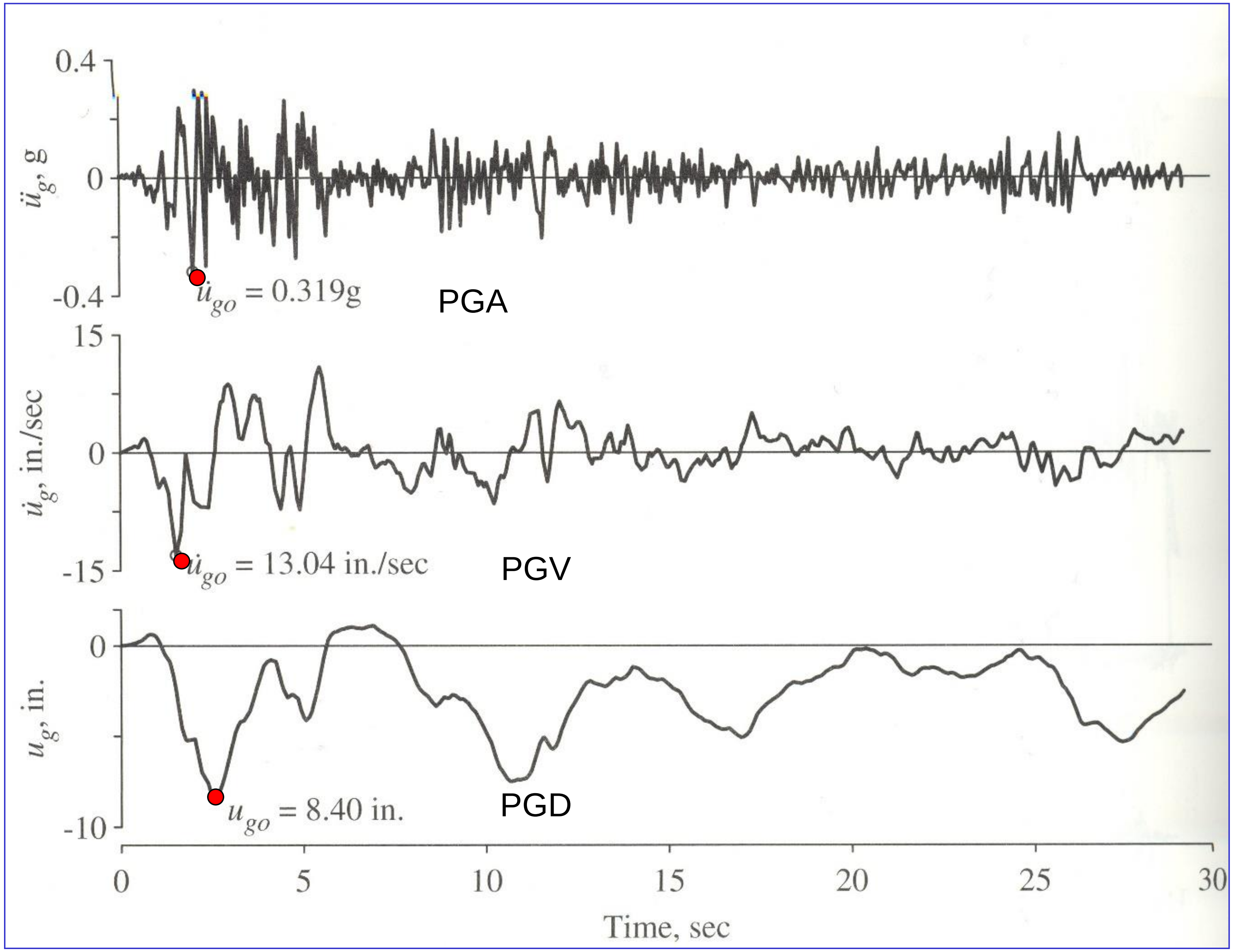

0.4
0
-0.4
$\ddot{u}_g$, g
$\ddot{u}_{go}$ = 0.319g
PGA
15
0
-15
$\dot{u}_g$, in./sec
$\dot{u}_{go}$ = 13.04 in./sec
PGV
0
-10
u_g, in.
u_{go} = 8.40 in.
PGD
0
5
10
15
20
25
30
Time, sec

Some properties of the Fourier Transform $\Im$

-Linearity: $\Im[a_1 f_1(t) + a_2 f_2(t)] = a_1 \Im f_1(\omega) + a_2 \Im f_2(\omega)$

-Derivative: $\Im\left[f^{(n)}(t)\right] = (i\omega)^n \Im f(\omega)$

-Shift: $\Im\left[f(t-a)\right] = e^{-i\omega a} \Im f(\omega)$

-Convolution: $\Im\left[f_1(t) * f_2(t)\right] = \Im \int_0^t f_1(\tau) f_2(t-\tau) d\tau = \Im f_1(\omega) \Im f_2(\omega)$

Applications: linear system (source*path*site*instrument), time-delay of propagation (e.g. array analysis), solving differential equations, etc…

Parseval identity
(sum of the square values)

$$\left\| f(t) \right\|_2 = \left\| \Im f(\omega) \right\|_2$$

UNIVERSITÀ DEGLI STUDI DI TRIESTE

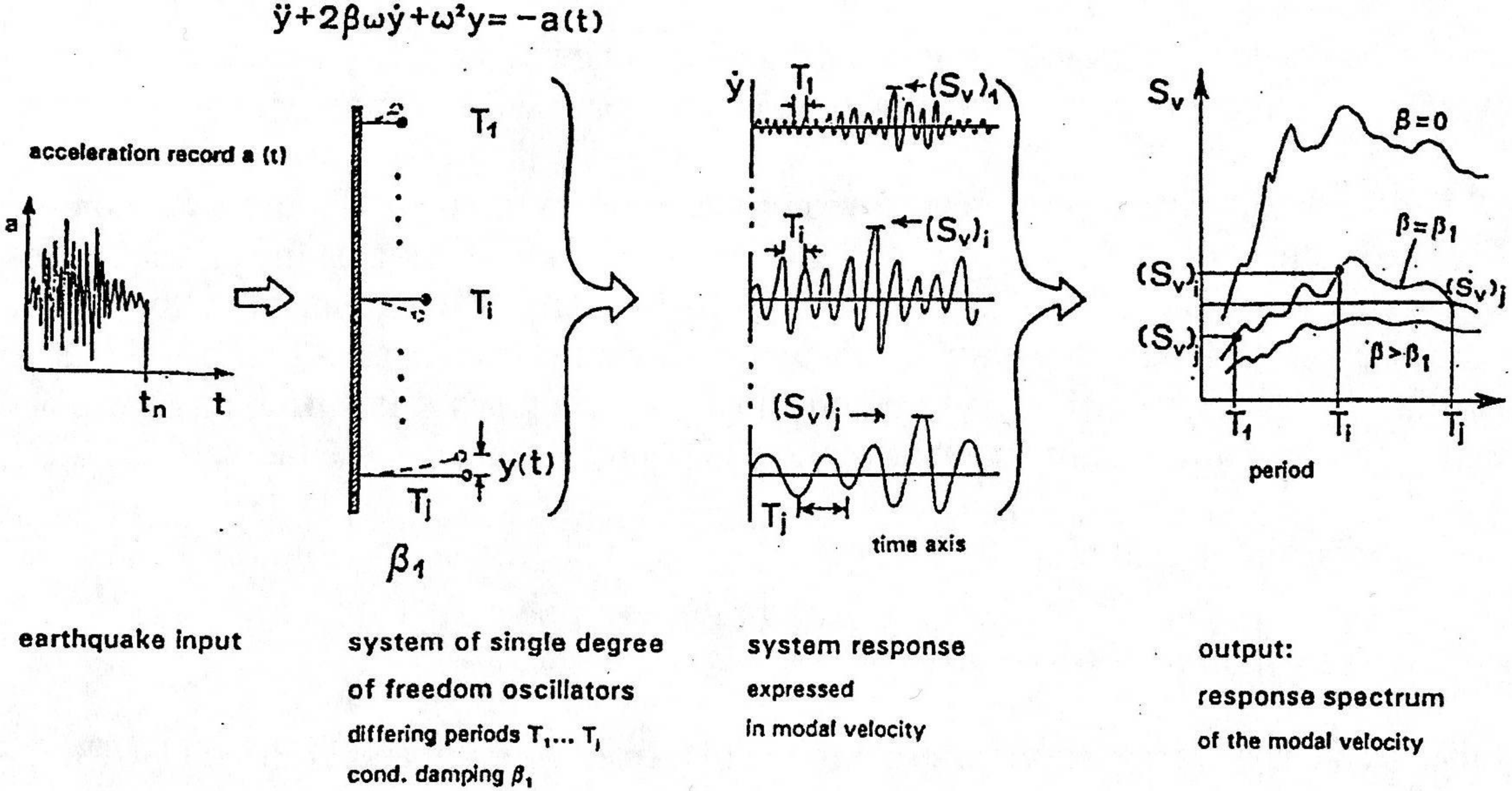

Fig.7: Schematic presentation of the construction of response spectra.

Courtesy of G. Grünthal

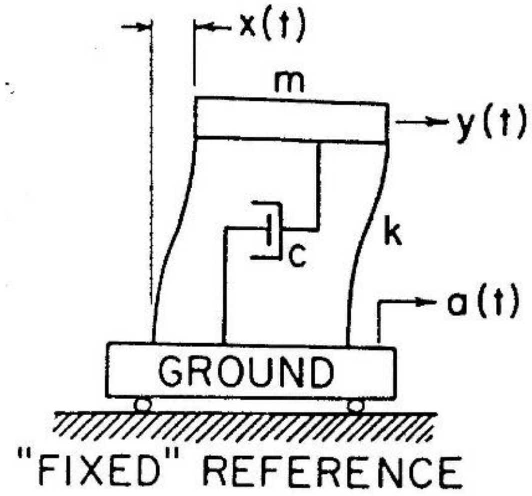

$x(t)$ = RELATIVE MOTION OF m WITH RESPECT TO GROUND

$y(t)$ = ABSOLUTE MOTION OF m WITH RESPECT TO "FIXED" REFERENCE

$a(t)$ = ABSOLUTE ACCELERATION OF GROUND WITH RESPECT TO "FIXED" REFERENCE

ritically damped system $(\xi = 1)$.
2. Overdamped system $(\xi > 1)$.
3. Underdamped system $(\xi < 1)$

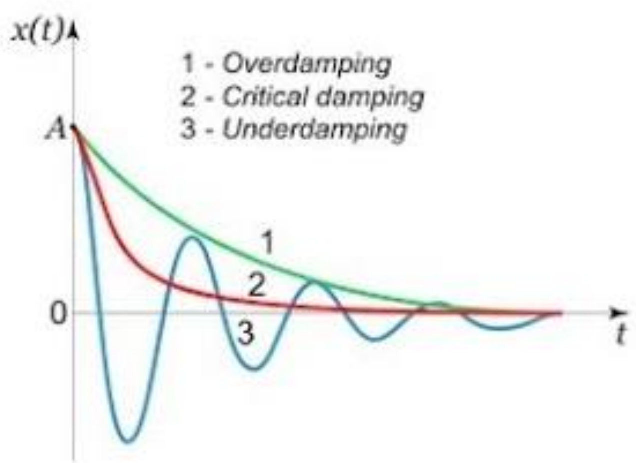

EQUATION OF MOTION OF m: $\ddot{x} + 2\omega_n\zeta\dot{x} + \omega_n^2 x = -a(t)$

WHERE: $\omega_n = \sqrt{k/m}$ = NATURAL FREQUENCY; $T = \frac{2\pi}{\omega_n}$ = PERIOD

$\zeta = c/2m\omega_n$ = FRACTION CRITICAL DAMPING

GENERAL SOLUTION:

$$x(t) = -\frac{1}{\omega_n\sqrt{1-\zeta^2}} \int_0^t a(\tau)e^{-\omega_n\zeta(t-\tau)} \sin \omega_n\sqrt{1-\zeta^2}(t-\tau)\,d\tau$$

DEFINITION OF RESPONSE SPECTRA:

$SD = |x(t)|_{max}$ = RELATIVE DISPLACEMENT RESPONSE SPECTRUM

$SV = |\dot{x}(t)|_{max}$ = RELATIVE VELOCITY RESPONSE SPECTRUM

$SA = |\ddot{y}(t)|_{max}$ = ABSOLUTE ACCELERATION RESPONSE SPECTRUM

$PSV = \omega_n SD = \frac{2\pi}{T} SD$ = PSEUDOVELOCITY SPECTRUM

$PSA = \omega_n^2 SD = \left(\frac{2\pi}{T}\right)^2 SD$ = PSEUDOACCELERATION SPECTRUM

after Bolt

Some terminology

Hazard: A dangerous phenomenon, substance, human activity or condition that may cause loss of life injury, or other health impacts, property damage, loss of livelihoods and services, social and economic disruption, or environmental damage (UNISDR, 2009).

Exposure: People, property, systems or other elements present in hazard zones that are thereby subject to potential losses (UNISDR, 2009).

Vulnerability: Characteristics and circumstances of a community, system or asset that make it susceptible to the damaging effects of a hazard (UNISDR, 2009).

Risk: The combination of the consequences of an event (hazard) and the associated likelihood/probability of its occurrence (ISO 31010, 2009).

Global Earthquake Model

Global Seismic Hazard Map

Version 2018.1

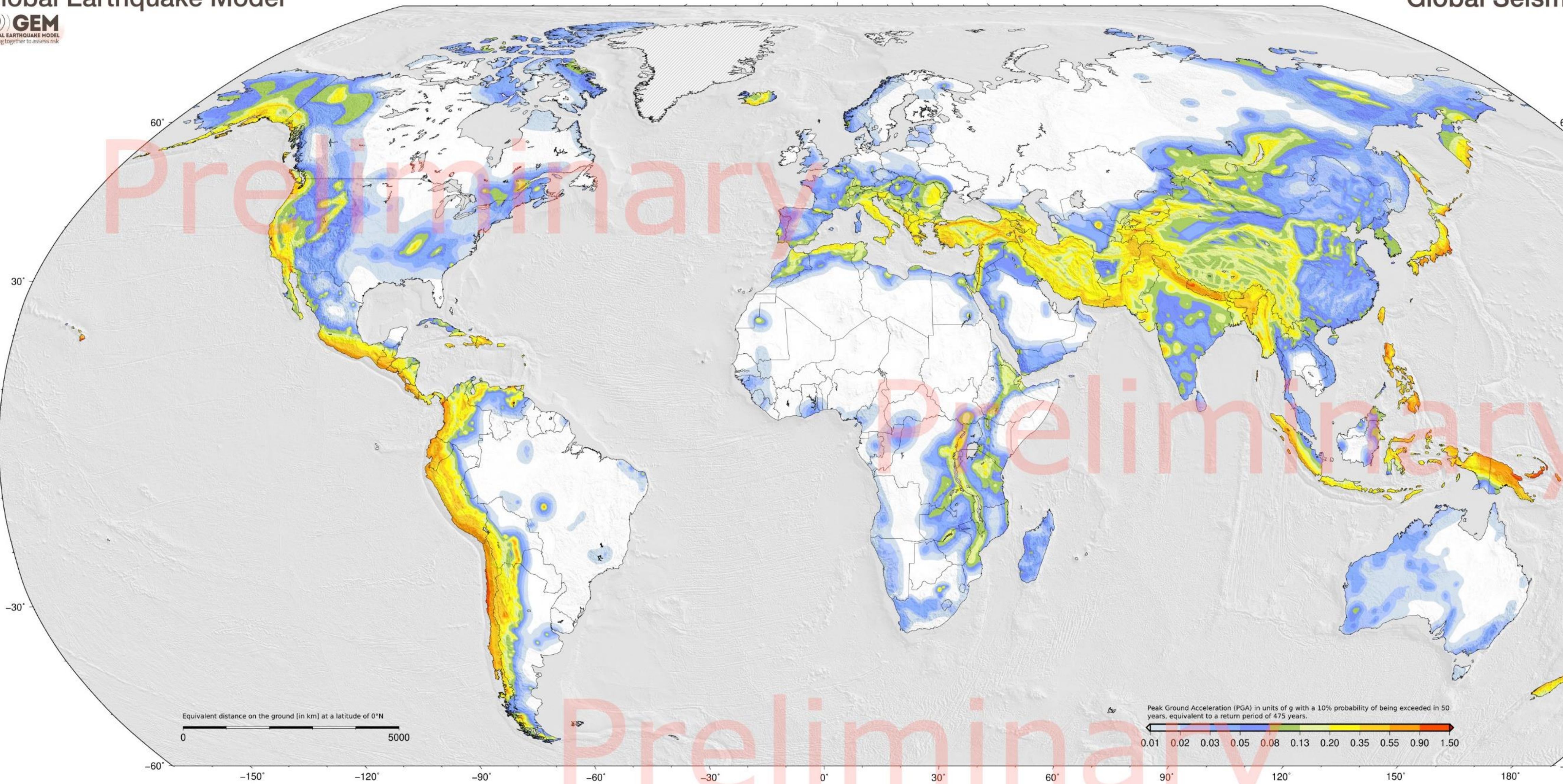

Global Earthquake Model (GEM) Seismic Hazard Map

The Global Earthquake Model (GEM) Seismic Hazard Map depicts the geographic distribution of the Peak Ground Acceleration (PGA) with a 10% probability of being exceeded in 50 years, equivalent to a return period of about 475 years, the internationally agreed reference for building safety regulation. The map was created by collating maps computed using national and regional probabilistic seismic hazard models developed by various institutions and projects, and by scientists working at the GEM Foundation. The OpenQuake engine, an open source seismic hazard and risk calculation software principally developed by the GEM Foundation, was used to calculate the hazard values. A smoothing methodology was applied to homogenise hazard values between adjacent models within buffer zones symmetrically distributed across the model borders. The map is based on a database of hazard models described using the OpenQuake engine and data format. Scientists working at the GEM Secretariat converted the models originally described using other formats. The models that were translated are: Alaska, Arabian Peninsula, Canada (translation completed by the Canada Geological Survey), China (translation completed by CEA in collaboration with GEM and the Swiss Seismological Service), Hawaii, India (translation completed by Nick Ackerley), Japan (translation completed by GEM in collaboration with NIED), New Zealand (translation completed by GNS Science), and United States of America. While translating these models various checks were performed to test the compatibility between the original results and the new results computed using the OpenQuake engine. Overall the differences between the original and translated model results are small, notwithstanding some diversity in modelling methodologies implemented in different hazard modelling software. The map and the underlying database of models are designed as a dynamic framework, capable to incorporate the most recent open models. The GEM Foundation plans to release future updates of this map on a regular basis as new information becomes available.

Acknowledgements

This map is the result of a collaborative effort and extensively relies on the determination of various organisations and projects to openly share resources. The creation of this map would not have been possible without the support provided by several public and private organisations during GEM's second implementation phase (2015-2018). These key contributions are profoundly acknowledged. The map was plotted using the GMT plotting software; the authors of this tool are acknowledged.

How to use and cite this work

Please cite this work as: M. Pagani, L. Danciu, J. Garcia, R. Gee, K. Johnson, D. Monelli, V. Poggi, R. Styron, G. Weatherill (2018). Global Earthquake Model (GEM) Seismic Hazard Map (version 2018.1 - December 2018). doi:

Contacts:

Fondazione GEM
via Ferrata, 127100 Pavia, Italy
info@globalquakemodel.org

More information available at:
http://www.globalquakemodel.org/gem

→ **Alaska (US) [ALS] - 2007**
Developed by the United States Geological Survey and converted into the OpenQuake engine by GEM.
• Authors: R.L. Wesson, O.S. Boyd, C.S. Mueller, C.G. Bufe, A.D. Frankel, M.D. Petersen
• Website: https://earthquake.usgs.gov/hazards/hazmaps/

→ **Arabian Peninsula [ARB] - 2018**
Developed by the Saudi Geological Survey and converted into the OpenQuake engine by GEM.
• Authors: H. Zahran, V. Sokolov, S. El-Hadidy Youssef, W. W. Alraddadi, M. J. Rodgers, I. C. F. Stewart, M. El-Hadidy
• Website: https://www.sgs.org.sa/english/naturalhazards/pages/nsce.aspx

→ **Australia [AUS] - 2018**
Developed by Geoscience Australia.
• Authors: T. Allen, J. Griffin, M. Leonard, D. Clark, H. Ghasemi
• Website: https://www.ga.gov.au/about/projects/safety/nsha

→ **Canada [CAN] - 2015**
Developed by Natural Resources Canada, partly adapted to the OpenQuake engine by GEM.
• Authors: J. Adams, S. Halchuk, T. Allen, G. Rogers
• Website: http://www.earthquakescanada.nrcan.gc.ca

→ **Caribbean and Central America [CCA] - 2018**
Developed within the USAID-funded project CCARA. Cuba and Puerto Rico were included a posteriori by GEM. Organisations involved in CCARA: GEM - University of Costa Rica, Costa Rica - Costa Rican Institute of Electricity, Costa Rica - Nicaraguan Institute of Territorial Studies, Nicaragua - Catholic University of El Salvador, El Salvador - Ministry of Environment and Natural Resources, El Salvador - Panama University, Panama.
• Authors: J. Garcia-Pelaez, R. Gee, R. Styron, V. Poggi
• Website: https://www.globalquakemodel.org/

→ **Central Asia [CEA] - 2018**
Developed within the EMCA project. Organisations involved: Helmholtz German Research Centre for Geosciences, Germany - Institute of Geology, Earthquake Engineering and Seismology of the Academy of Sciences of the Republic of Tajikistan - Institute of Geophysical Research, Kazakhstan - International University of Innovation Technologies, Kyrgyzstan - Kyrgyzstan Institute of Seismology, Kyrgyzstan - Central-Asian Institute of Applied Geosciences, Kyrgyzstan - Institute of Mechanics and Seismic Stability of Structures of the Academy of Sciences of Uzbekistan, Uzbekistan - Mavlyanov Institute of Seismology, Uzbekistan.
• Authors: S. Ullah, D. Bindi, M. Pilz, L. Danciu, G.A. Weatherill, E. Zuccolo, A. Ischuk, N.N. Mikhailova, K. Abdrakhmatov, S. Parolai, K. Fleming
• Website: http://www.emca-gem.org/

→ **China [CHN] - 2015**
Developed by the Institute of Geophysics of the China Earthquake Administration and converted into the OpenQuake engine by Changlong Li within a collaboration between the Institute of Geophysics of the China Earthquake Administration, the Swiss Seismological Service, Swiss Federal Institute of Technology, Switzerland and GEM.
• Authors: M. Gao, G. Chen, F. Xie, X. Xu, X. Li, Y. Yu, S. Li, B. Zhou, H. Pan, Y. Lu, F. Zhao, J. Wu
• Website: http://www.gb18306.cn/

→ **Europe [EUR] - 2013**
Developed within the EU-funded SHARE project, coordinated by the Swiss Federal Institute of Technology, Zurich, Switzerland. Organisations involved: Helmholtz Zentrum Potsdam Deutsches GeoForschungsZentrum GFZ - Istituto Nazionale di Geofisica e Vulcanologia, Italy - Université Joseph Fourier Grenoble, France - Università degli Studi di Pavia, Italy - Aristotelio Panepistimio Thessalonikis, Greece - Bureau de Recherches Géologiques et Minières, France - Centre de Recherche en Astronomie Astrophysique et Géophysique, Algeria - Instituto Superior Tecnico, Portugal - Bogazici University, Turkey - Laboratorio Nacional de Engenharia Civil, Portugal - Middle East Technical University, Turkey - Seizmoloski Zavod Crne Gore, Montenegro - Natural Environment Research Council, United Kingdom - Institutul National de Cercetare-Dezvoltare Pentru Fizica Pamantului, Romenia - Ethniko kai Kapodistriako Panepistimio Athinon, Greece - Stiftelsen Norsar, Norway - Koninklijke Sterrenwacht van Belgie, Belgium
• Authors: J. Woessner, L. Danciu, D. Giardini, H. Crowley, F. Cotton, G. Grünthal, G. Valensise, R. Arvidsson, R. Basili, M. Betül Demircioglu, S. Hiemer, Carlo Meletti, R. W. Musson, A.N. Rovida, K. Sesetyan, M. Stucchi
• Website: http://www.share-eu.org/

→ **Hawaii (US) [HAW] - 1998**
Developed by the United States Geological Survey and converted into the OpenQuake engine by GEM.
• Authors: F. W. Klein, A.D. Frankel, C.S. Mueller, R.L. Wesson, P.G. Okubo
• Website: https://earthquake.usgs.gov/hazards/hazmaps/

→ **Indonesia [IDN] - 2017**
National seismic hazard model for Indonesia created by the Team for Updating of Seismic Hazard Maps of Indonesia. The team belongs to the National Center for Earthquake Studies under the Center for Research and Development of Housing and Settlements of the Ministry of Public Works and People Housing. Ministries involved: Ministry of Public Works and People Housing; Ministry of Energy and Mineral resources; Ministry of Transportation; Ministry of Research, Technology and Higher Education; and National Disaster Management Authority of Indonesia. Organizations involved: Bureau of Meteorology, Climatology and Geophysics; Indonesian Research Institute; Geospatial Information Agency; Center for Research and Development of Housing and Settlements; Centre of Volcanology and Geological Hazard Mitigation; Indonesian Academy of Sciences; Bandung Institute of Technology; University of Indonesia; University of Gajah Mada; University of Diponegoro; Indonesian Society for Geotechnical Engineering; and Indonesian Disaster Expert Association. The team collaborated internationally with Geoscience Australia, Australia.
• Authors: M. Irsyam., L. Faizal, D. Natawidjaja, I. Meilano, S. Widiyantoro, W. Triyoso, A. Rudiyanto, S. Hidayati, M. Asrurifak, M. Ridwan, P. Cummins

→ **India and surroundings [IND] - 2012**
Developed by Thingbaijam and Nath (2012), revised and implemented in OpenQuake by N. Ackerley (Natural Resources Canada).
• Authors: N. Ackerley, K.K.S. Thingbaijaim, and S.K. Nath

→ **Japan [JPN] - 2014**
National hazard model implemented by the Headquarters for Earthquake Research Promotion (HERP) and converted into the OpenQuake engine format within a collaboration between the National Research Institute for Earth Science and Disaster Resilience (NIED), Japan, and GEM.
• Authors: - H. Fujiwara, N. Morikawa, S. Kawai, S. Aoi, S. Senna, T. Maeda, H. Azuma, K. X. Hao, A. Iwaki, K. Wakamatsu, M. Imoto, N. Hasegawa, T. Okumura, T. Hayakawa, and M. Takahashi
• Website: http://www.j-shis.bosai.go.jp/en/

→ **Korean Peninsula [KOR] - 2018**
Assembled by GEM.
• Website: https://www.globalquakemodel.org/

→ **Mexico [MEX] - 2018**
Developed by GEM.
• Authors: J. Garcia-Pelaez, R. Gee, R. Styron
• Website: https://www.globalquakemodel.org/

→ **Middle East [MIE] - 2016**
Developed within the EMME project, jointly coordinated by the Swiss Federal Institute of Technology, Switzerland, and the Kandilli Observatory and Earthquake Research Institute, Turkey. Institutions involved:International Institute for Earthquake Engineering ans Seismology, Iran; Middle East Technical University, Turkey; Sakarya University, Turkey; University of Peshawar, Pakistan; Yarmouk University, Jordan; American University of Beirut, Lebanon; Ivane Javakhishvili Tbilisi State University, Georgia; National Academy of Sciences, Armenia; National Academy of Sciences, Azerbaijan.
• Authors: D. Giardini, L. Danciu, M. Erdik, K. Sesetyan, MB Demircioğlu, S. Akkar, L. Gulen, M. Zare, S. Adamia, A. Ansari, A. Arakelyan, A. Askan, M. Avanesyan, H. Babayan, T. Chelidze, R. Durgaryan, A. Elias, H. Hamzehloo, K. Hessami, D. Kalafat, O. Kale, A. Karakhanyan, MA. Khan, T. Mamadli, M. Al-Qarouti, M. Sayab, N. Tsereteli, M. Utkucu, O. Varazanashvili, M. Waseem, H. Yalçın, MT. Yilmaz
• Website: http://www.efehr.org

→ **Northern Africa [NAF] - 2018**
Developed by GEM.
• Authors: V. Poggi, J. Garcia-Pelaez, R. Styron
• Website: https://www.globalquakemodel.org/

→ **Northeast Asia [NEA] - 2018**
Developed by GEM.
• Authors: V. Poggi, J. Garcia-Pelaez, R. Styron
• Website: https://www.globalquakemodel.org/

→ **Northwestern Asia [NWA] - 2018**
Developed by GEM and the Swiss Federal Institute of Technology, Switzerland.
• Authors: V. Poggi, L. Danciu
• Website: https://www.globalquakemodel.org/

→ **New Zealand [NZL] - 2010 corrected**
GNS Science led the development of the model and converted it into the OpenQuake engine.
• Authors: E.R. Abbott, N. Horspool, M. Gerstenberger, R. Huso, C. Van Houtte, G. McVerry, S. Canessa
• Website: https://www.gns.cri.nz/

→ **Pacific Islands [PAC] - 2018**
Developed by GEM.
• Authors: K. Johnson
• Website: https://www.globalquakemodel.org/gem

→ **Philippines [PHL] - 2018**
Developed jointly by the Philippine Institute of Volcanology and Seismology and GEM.
• Authors: PHIVOLCS, K. Johnson and R. Styron
• Website: https://www.phivolcs.dost.gov.ph/ and https://www.globalquakemodel.org/gem

→ **Papua New Guinea [PNG] - 2015**
Developed within a collaboration between the Port Moresby Geophysical Observatory and Geoscience Australia.
• Authors: H. Ghasemi, C. McKee, M. Leonard, P. Cummins, M. Moihoi, S. Spiliopoulos, F. Taranu, E. Buri

→ **South America [SAM] - 2018**
Initially developed within the Swiss Re Foundation sponsored project SARA and updated by GEM. Organisations involved: GEM, Colombian Geological Survey, Colombia - National University of Colombia, Colombia - University of Valle, Colombia - Venezuelan Foundation for Seismological Research, Venezuela - University of Merida, Venezuela - National Observatory, Brazil, Institute of Astronomy, Geophysics and Atmospheric Sciences, Brazil - Federal University of Rio Grande do Norte, Brazil - National Polytechnic University, Ecuador - San Calixto Observatory - Bolivia - University of Chile, Chile - University of Concepción, Chile - Pontifical Catholic University of Chile, Chile - Research Center for Disaster Risk Management, Chile - Peruvian Geological Service, Peru - University of San Luis, Argentina - University of Antofagasta, Argentina - National Institute of Seismic Prevention, Argentina - National Institute of Geophysics and Volcanology, Italy.
• Authors: J. Garcia-Pelaez, M. Pagani, K. Johnson, R. Styron, V. Poggi
• Website: https://www.globalquakemodel.org/gem

→ **Continental Southeast Asia [SEA] - 2018**
Developed by the Earth Observatory of Singapore and Mahidol University.
• Authors: C.-H. Chan, T. Ornthammarath

→ **Sub-Saharan Africa [SSA] - 2018**
Developed by GEM in collaboration with AfricaArray within the USAID sponsored project SSAHARA.
• Authors: V. Poggi, R. Durrheim, G.M. Tuluka, G.A. Weatherill, R. Gee, M. Pagani, A. Nyblade, D. Delvaux
• Website: https://www.globalquakemodel.org/

→ **Taiwan [TWN] - 2015**
Developed within the Taiwan Earthquake Model initiative, a collaboration between various Taiwanese research institutions operating in the field of seismic hazard and risk assessment.
• Authors: Y.-J. Wang, C.-H. Chan, Y.-T. Lee, K.-F. Ma, J.-H. Shyu, R.-J. Rau, and C.-T. Cheng
• Website: http://tec.earth.sinica.edu.tw/TEM/index.php

→ **California (US) [UCF] - 2014**
Developed within a project supported by the United States Geological Survey, the Southern California Earthquake Center, the California Geological Survey and the California Earthquake Authority. The model was converted into the OpenQuake engine by GEM.
• Authors: E.H. Field, G.P. Biasi, P. Bird, T.E. Dawson, K.R. Felzer, D.D. Jackson, K.M. Johnson, T.H. Jordan, C. Madden, A.J. Michael, K.R. Milner, M.T. Page, T. Parsons, P.M. Powers, B.E. Shaw, W.R. Thatcher, R.J. Weldon II, Y. Zeng
• Website: http://wgcep.org/ucerf3

→ **United States of America [USA] - 2014**
Developed the United States Geological Survey and converted into the OpenQuake engine by GEM.
• Authors: M.D. Petersen, M.P. Moschetti, P.M. Powers, C.S. Mueller, K. M. Haller, A.D. Frankel, Y. Zeng, S. Rezaeian, S.C. Harmsen, O.S. Boyd, E.H. Field, R. Chen, K.S. Rukstales, N. Luco, R.L. Wheeler, R.A. Williams, A.H. Olsen
• Website: https://earthquake.usgs.gov/hazards/hazmaps/

→ **Western Africa [WAF] - 2018**
Developed by GEM.
• Authors: V. Poggi
• Website: https://www.globalquakemodel.org/

→ **South Africa [ZAF] - 2018**
Developed by scientists working at the Council of Geoscience, South Africa.
• Authors: V. Midzi, B. Manzunzu, T. Mulabisana, B.S. Zulu, T. Pule, S. Myendeki, G. W. Rathod
• Website: http://www.geoscience.org.za/

Contributing models

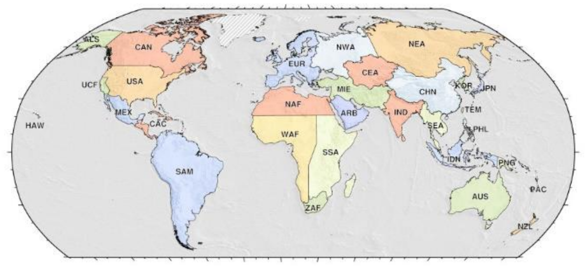

Global Earthquake Model (GEM) Foundation

The GEM Global Seismic Hazard Map is a product of the GEM Foundation. Initiated by the OECD's Global Science Forum in 2006, GEM was formed in 2009 as a non-profit foundation in Pavia, Italy, funded through a public-private sponsorship with the vision to create a world that is resilient to earthquakes. Participants represent national research, applied science or disaster management institutions, the private sector and international organisations. GEM continues the tradition of the Global Seismic Hazard Assessment Program (GSHAP), which produced the first global seismic hazard map arising from a global collaborative effort of scientists in 1999 in support of the UN International Decade of Natural Disaster Reduction (IDNDR). GEM's collaborative network comprises more than 70 public and private institutions organized under more than 25 regional, national and multilateral projects. Observing its core values of collaboration, transparency, openness, credibility and serving the public good, the GEM initiative extends the scope of work of GSHAP to the risk domain, providing an institutional framework for continuous updates and fostering direct applications to risk reduction and prevention projects. GEM's OpenQuake platform provides access to data, models, tools and software behind the maps. GEM's heart is the open-source OpenQuake engine, which enables probabilistic hazard and risk calculations worldwide and at all scales, from global down to regional, national, local, and site-specific in a single software package.

The Sendai Framework for Disaster Risk Reduction (SFDRR) calls for "decision-making on disaster risk reduction to be based on solid and openly accessible scientific work". GEM supports the SFDRR goals by contributing its openly accessible products, its capabilities for hazard and risk assessment, for training and capacity development, and for application in risk reduction projects. GEM also serves as a baseline or exemplar for the development of a broader multi-hazard framework for risk assessment in support of a holistic and comprehensive approach to disaster risk reduction. Technical details on the compilation of the hazard and risk maps and the underlying models are available on GEM's website at http://www.globalquakemodel.org/gem

Legal statements

Sponsors and major contributors:

UNIVERSITÀ DEGLI STUDI DI TRIESTE

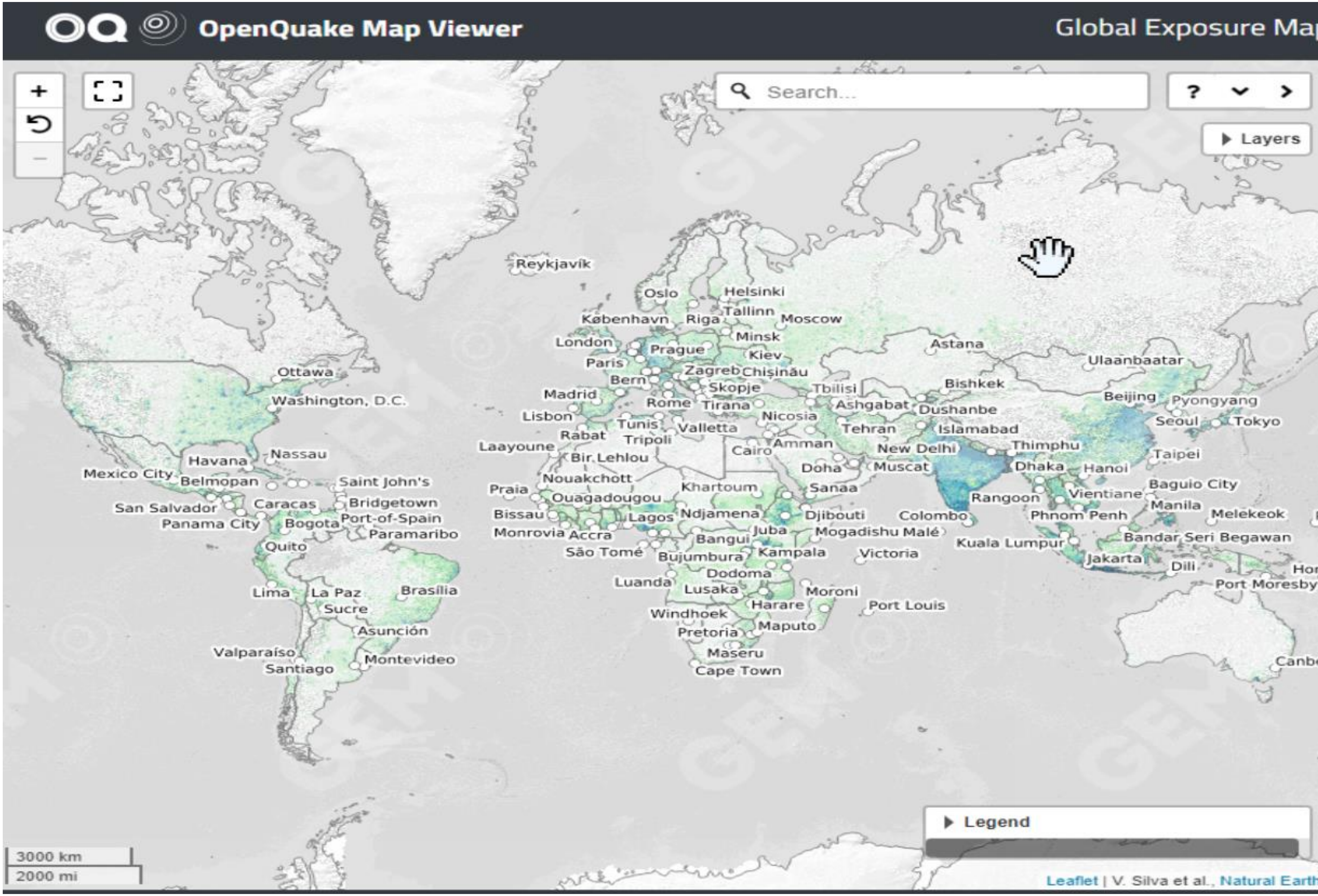

OpenQuake Map Viewer
Global Exposure Map
Search...
Layers
Legend
3000 km
2000 mi
Leaflet | V. Silva et al., Natural Earth
Reykjavík
Oslo
Helsinki
Tallinn
København
Riga
Moscow
Minsk
London
Prague
Kiev
Paris
Zagreb
Chișinău
Bern
Skopje
Madrid
Rome
Tirana
Lisbon
Tunis
Valletta
Nicosia
Rabat
Tripoli
Laayoune
Bir Lehlou
Cairo
Amman
Tbilisi
Ashgabat
Dushanbe
Tehran
Islamabad
Astana
Bishkek
Ulaanbaatar
Beijing
Pyongyang
Seoul
Tokyo
New Delhi
Thimphu
Taipei
Doha
Muscat
Dhaka
Hanoi
Baguio City
Nouakchott
Khartoum
Sanaa
Praia
Ouagadougou
Rangoon
Vientiane
Manila
Bissau
Lagos
Ndjamena
Djibouti
Colombo
Phnom Penh
Melekeok
Monrovia
Accra
Bangui
Juba
Mogadishu
Malé
Bandar Seri Begawan
São Tomé
Bujumbura
Kampala
Victoria
Kuala Lumpur
Jakarta
Dili
Dodoma
Luanda
Lusaka
Moroni
Port Moresby
Harare
Port Louis
Windhoek
Maputo
Pretoria
Maseru
Cape Town
Ottawa
Washington, D.C.
Havana
Nassau
Mexico City
Belmopan
Saint John's
Bridgetown
San Salvador
Caracas
Port-of-Spain
Panama City
Bogota
Paramaribo
Quito
Lima
La Paz
Brasília
Sucre
Asunción
Valparaíso
Santiago
Montevideo

Global Earthquake Model

GEM
GLOBAL EARTHQUAKE MODEL
working together to assess risk

Global Seismic Risk Map

OQ OPENQUAKE

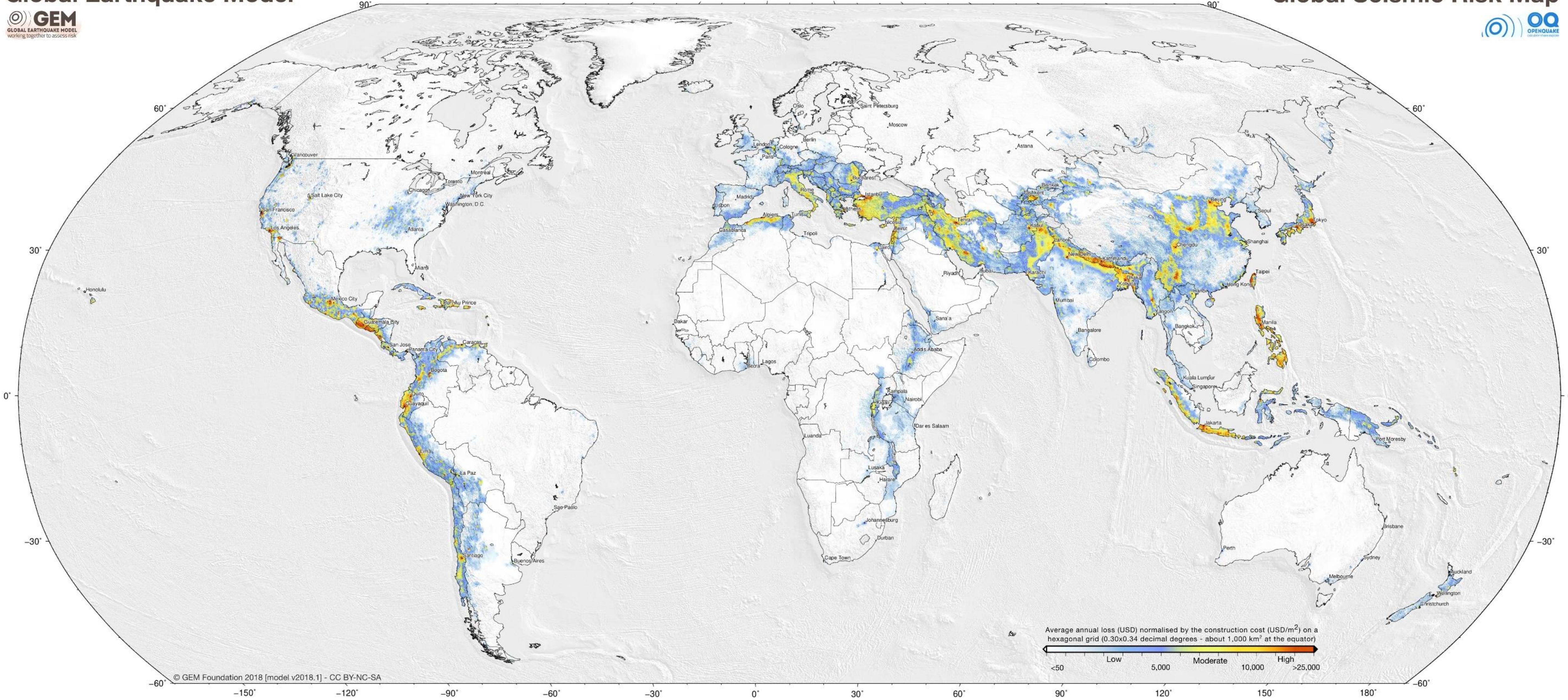

Global Seismic Hazard Map

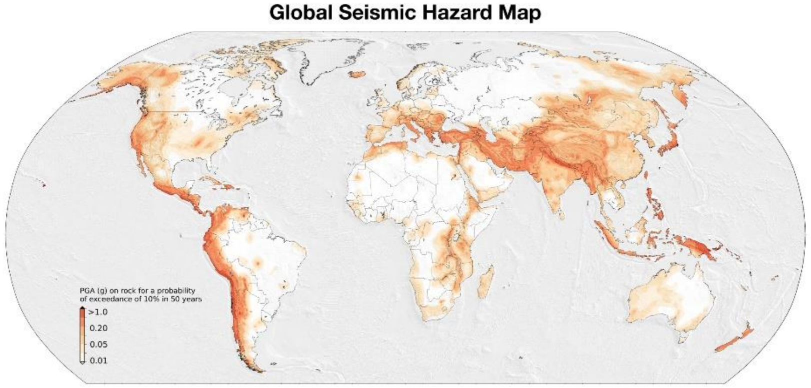

Global Exposure Map

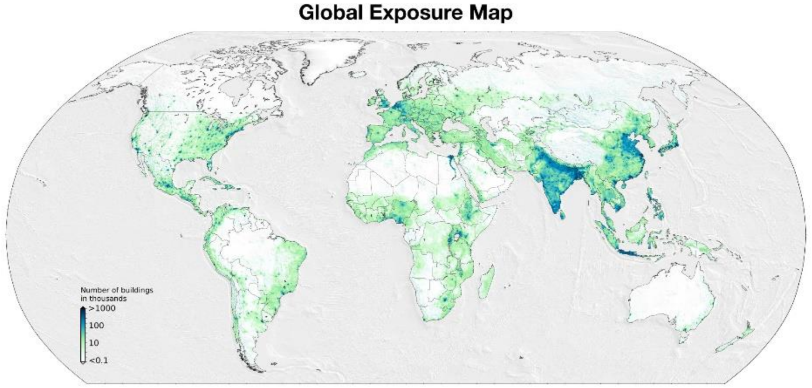

Global Seismic Fatalities Map

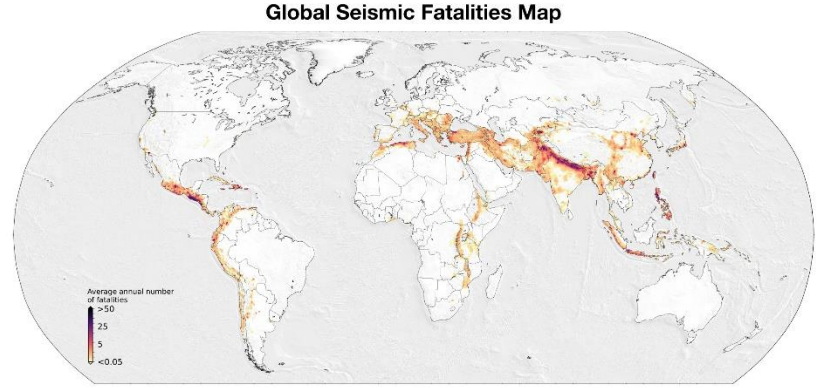

Global Earthquake Model (GEM) Global Seismic Risk Map

The Global Seismic Risk Map (v2018.1) comprises four global maps. The main map presents the geographic distribution of average annual loss (USD) normalised by the average construction costs of the respective country (USD/m^2) due to ground shaking in the residential, commercial and industrial building stock, considering contents, structural and non-structural components. The normalised metric allows a direct comparison of the risk between countries with widely different construction costs. It does not consider the effects of tsunamis, liquefaction, landslides, and fires following earthquakes. The loss estimates are from direct physical damage to buildings due to shaking, and thus damage to infrastructure or indirect losses due to business interruption are not included. The Global Seismic Hazard Map depicts the geographic distribution of the Peak Ground Acceleration (PGA) with a 10% probability of being exceeded in 50 years, computed for reference rock conditions (shear wave velocity of 760-800 m/s). The Global Exposure Map depicts the geographic distribution of residential, commercial and industrial buildings. The Global Seismic Fatalities Map depicts an estimate of average annual human losses due to earthquake-induced structural collapse of buildings. The results for human losses do not consider indirect fatalities such as those from post-earthquake epidemics. The average annual losses and number of buildings are presented on a hexagonal grid, with a spacing of 0.30 x 0.34 decimal degrees (approximately 1,000 km^2 at the equator). The average annual losses were computed using the event-based calculator of the OpenQuake engine, an open-source software for seismic hazard and risk analysis developed by the GEM Foundation. The seismic hazard, exposure and vulnerability models employed in these calculations were provided by national institutions, or developed within the scope of regional programs or bilateral collaborations. These global maps and the underlying databases are based on best available and publicly accessible datasets and models. Due to possible model limitations, regions portrayed with low risk may still experience potentially damaging earthquakes. The GEM Risk Map is intended to be a dynamic product, such that it may be updated when new datasets and models become available. Releases of updated versions of the seismic risk map are anticipated on a regular basis. Additional hazard and risk metrics for each country can be explored at globalquakemodel.org/gem.

The Global Earthquake Model (GEM) Foundation

The Earthquake Risk Map 2018 is a product of the GEM Foundation. Initiated by the Organisation for Economic Co-operation and Development (OECD) Global Science Forum in 2006, GEM was formed in 2009 as a non-profit foundation in Pavia (Italy), funded through a public-private sponsorship with the vision to create a world that is resilient to earthquakes. Participants represent national research or disaster management institutions, the private sector and international organisations. GEM expands the assessment of seismic hazard at the global scale initially started by the Global Seismic Hazard Assessment Program (GSHAP) in support of the UN International Decade of Natural Disaster Reduction in 1999 to the consideration of direct economic and human losses. Observing its core values of collaboration, transparency, openness, credibility, and serving the public good, GEM goes beyond GSHAP by extending the scope of work to the risk domain, providing an institutional framework for continuous updates, and fostering direct applications to risk reduction and prevention projects. GEM's collaborative network comprises more than 70 public and private institutions organised under more than 25 regional, national and multilateral projects.

GEM's OpenQuake platform (platform.openquake.org) provides access to all data, models, tools and software behind the maps. GEM's open-source OpenQuake engine enables probabilistic hazard and risk calculations worldwide and at all scales, from global down to regional, national, local, and site-specific in a single software package.

The Sendai Framework for Disaster Risk Reduction (SFDRR) calls for "decision-making on disaster risk reduction to be based on solid and openly accessible scientific work". GEM supports the SFDRR goals by contributing openly accessible products for hazard and risk assessment and capacity development in risk reduction projects. GEM also serves as a baseline or exemplar for the development of a broader multi-hazard framework for risk assessment in support of a holistic and comprehensive approach to disaster risk reduction. Technical details on the development and compilation of the hazard and risk maps, underlying models and the list of contributors can be found at globalquakemodel.org/gem.

How to use and cite this work

Please cite this work as: V. Silva, D. Amo-Oduro, A. Calderon, J. Dabbeek, V. Despotaki, L. Martins, A. Rao, M. Simionato, D. Viganò, C. Yepes-Estrada, A. Acevedo, H. Crowley, N. Horspool, K. Jaiswal, M. Journeay, M. Pittore (2018). Global Earthquake Model (GEM) Seismic Risk Map (version 2018.1), DOI: 10.13117/GEM-GLOBAL-SEISMIC-RISK-MAP-2018.

Acknowledgements

This map is the result of a collaborative effort and extensively relies on the enthusiasm and commitment of various organisations to openly share and collaborate. The creation of this map would not have been possible without the support provided by several public and private organisations during GEM's second working programme (2014-2018). None of this would have been possible without the extensive support of all GEM Secretariat staff. These key contributions are profoundly acknowledged. A complete list of the contributors can be found at globalquakemodel.org/gem.

Legal statements

This map is an informational product created by the GEM Foundation for public dissemination purposes. The information included in this map must not be used for the design of earthquake-resistant structures or to support any important decisions involving human life, capital and movable and immovable properties. The values of seismic hazard and risk in this map do not constitute an alternative nor do they replace building actions defined in national building codes or earthquake risk estimates derived nationally. Readers seeking this information should contact the national authorities tasked with seismic hazard and risk assessment. The seismic risk map results from an integration process that is solely the responsibility of the GEM Foundation.

Contacts

GEM (Global Earthquake Model) Foundation
Via Ferrata, 1 – 27100, Pavia, Italy
info@globalquakemodel.org

More information available at globalquakemodel.org/gem

Sponsors and major contributors

AIR ARUP UNIVERSIDAD EAFIT EUCENTRE FM Global GFZ Helmholtz Centre Potsdam Australian Government Geoscience Australia GNS hannover re Munich RE Canada Nanyang Technological University Singapore Institute of Catastrophe Risk Management Nephila NERC Science of the Environment NIED NSET OYO PartnerRe Protezione Civile Servicio Geológico Colombiano sura The Research Council of Norway Swiss Re Foundation USAID USGS science for a changing world Willis Towers Watson ZURICH

SHA dualism: P & D

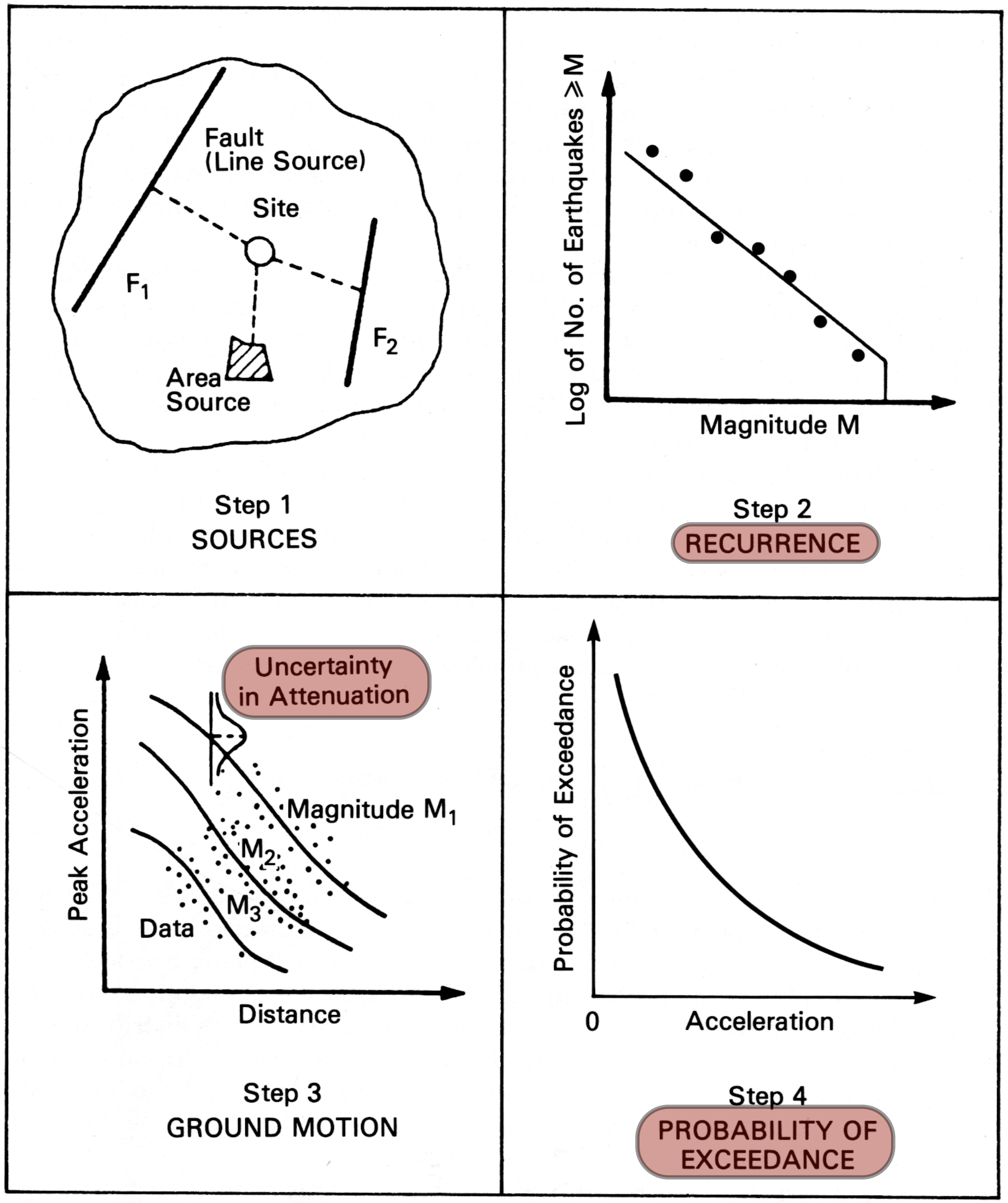

FIGURE 10.2 Basic steps of probabilistic seismic hazard analysis (after TERA Corporation 1978).

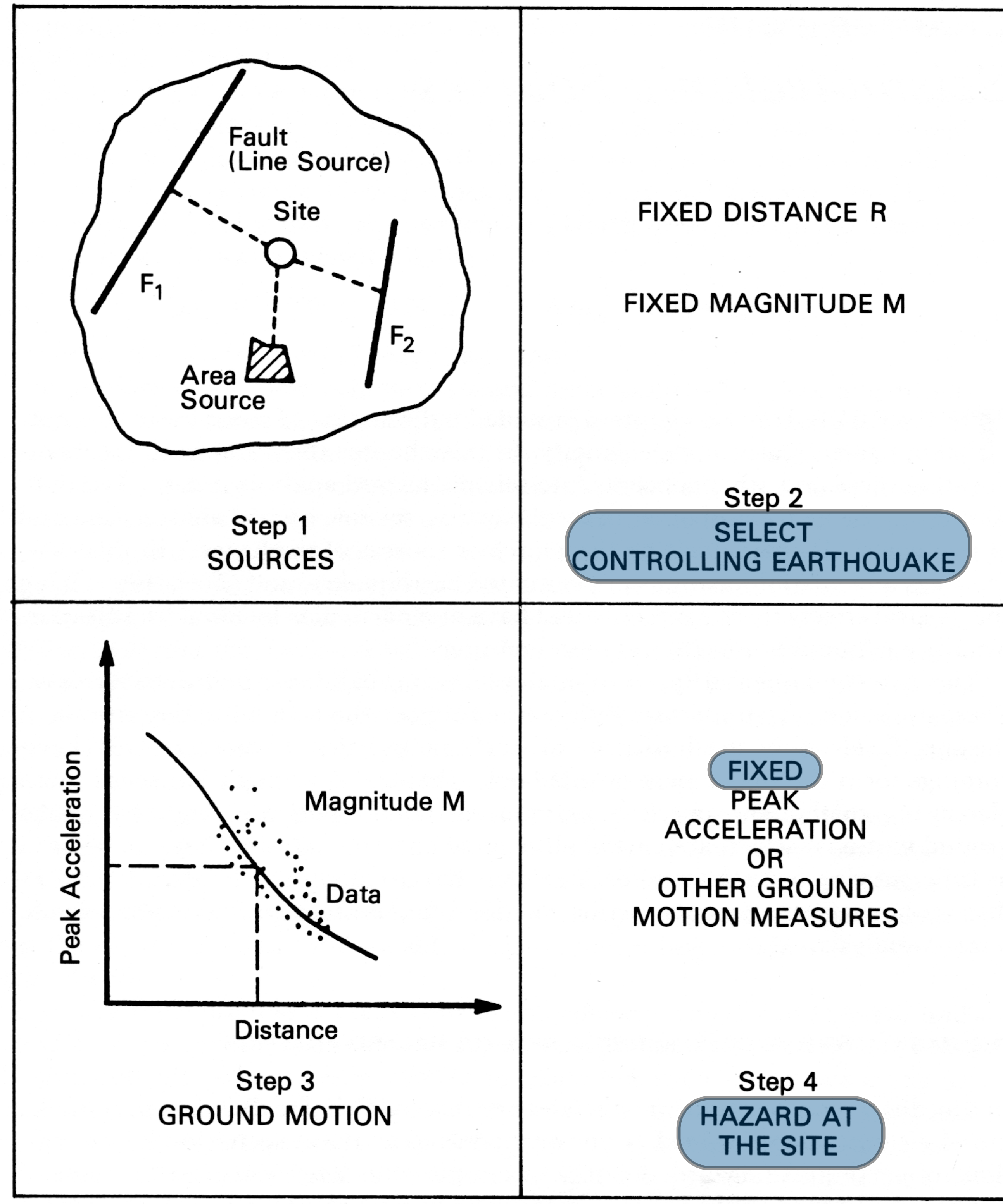

FIGURE 4.1 Basic steps of deterministic seismic hazard analysis (after TERA Corporation 1978).

"Earthquake Hazard Analysis", Reiter, 1990

Seismic Zonation and Catalogs

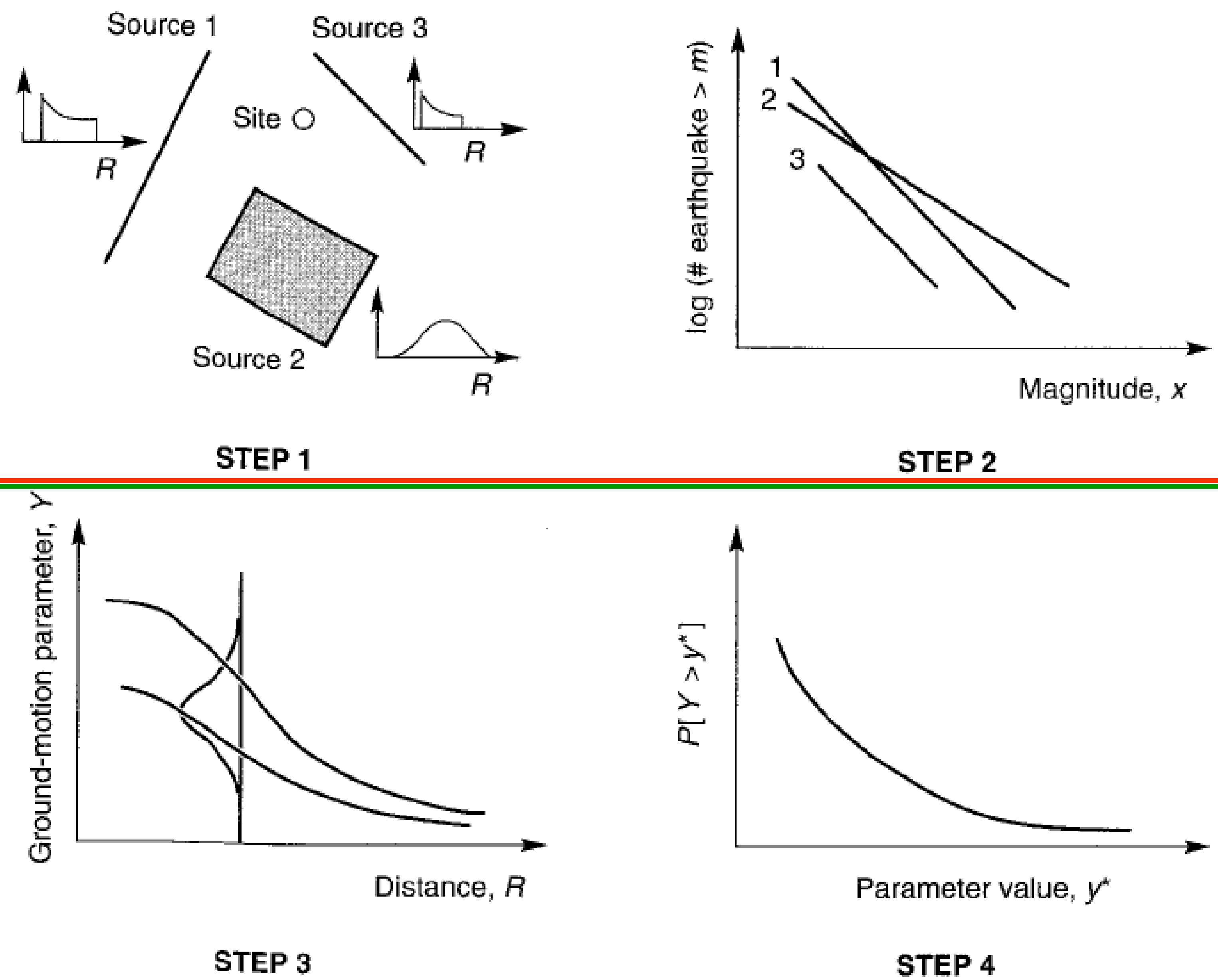

GMPEs and Probability of execeedance

Credit to Kramer's book

Issues regarding magnitude

The **advantages** of magnitude scales are

They can be determined directly from the seismogram, without the need for sophisticated processing.

The units of order 1 are intuitively attractive.

to 2.9	Minor	Generally not felt but recorded	1000/day
3 to 3.9	Minor	Often felt, but rarely cause damage.	49000/year
4 to 4.9	Light	Noticeable shaking, damage unlikely.	6200/year
5 to 5.9	Moderate	Can cause damage to poor quality buildings	800/year
6 to 6.9	Strong	Destructive in areas up to *ca.*160 km.	120/year
7 to 7.9	Major	Serious damage over larger areas.	18/year
8 to 8.9	Great	Serious damage over areas of 100's km.	1/year
9 to 9.9	Great	Serious damage over areas of 1000' s km.	1/20 years

Earthquake distribution

AS noted, the numbers of earthquakes of a given size decreases by about an order of magnitude per magnitude unit increase.

Quantified by the ***Gutenberg-Richter*** relation:

$$\log N = a_1 - bM$$

where *N* is the number of earthquakes with a magnitude greater than *M* occurring in a given time (cumulative) or

$$\log n = a_2 - bM$$

n is (*dN/dM*), and a_1, a_2 and *b* are constants for a given

Right: Frequency-magnitude for all earthquakes M>5 between 1968-97.

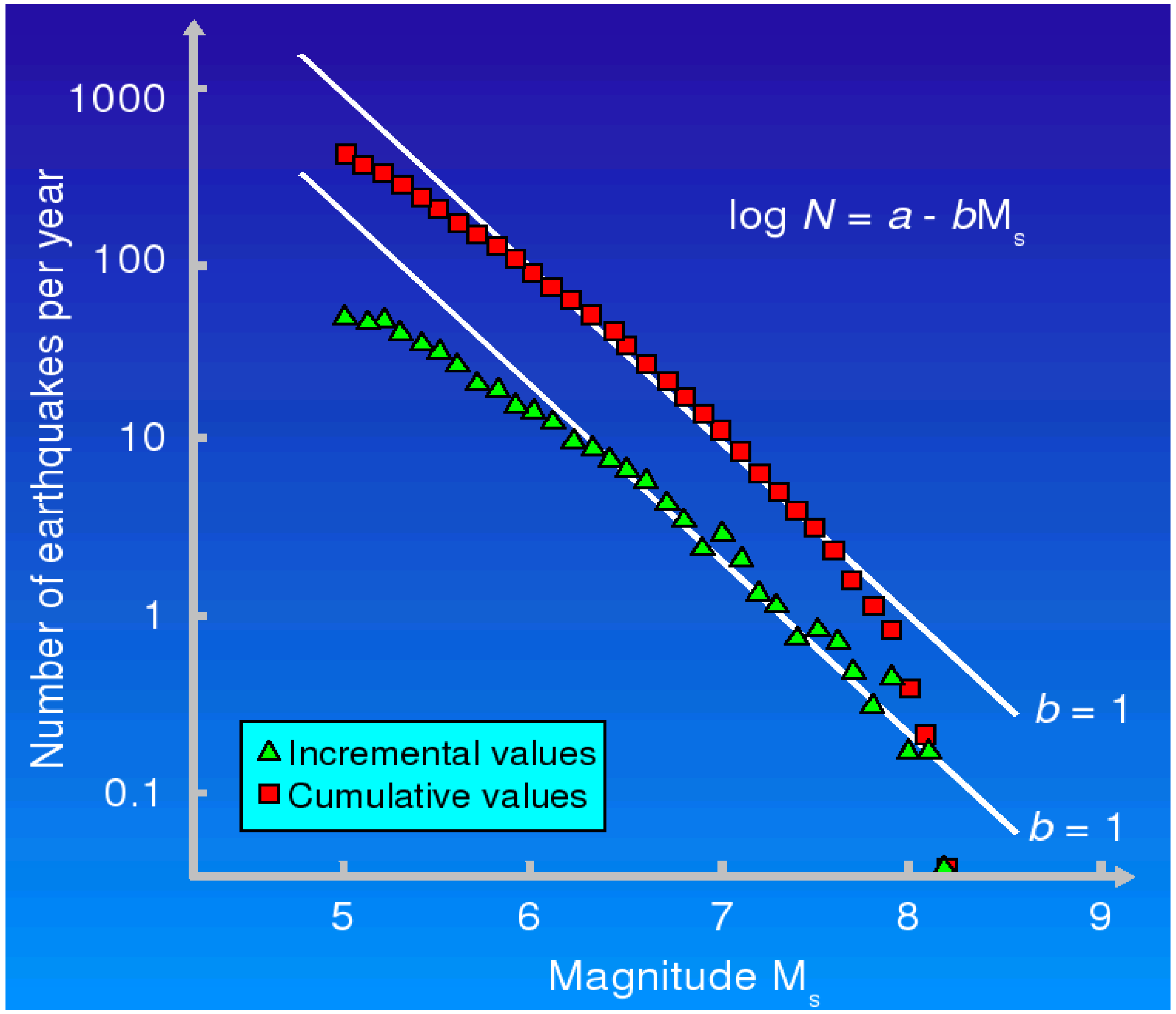

The value of *b* is generally about 1, even for individual seismic areas.

(*Stein & Wysession, 2003*

Probabilistic Seismic Hazard Analysis

All possible distances are considered - contribution of each is weighted by its probability of occurrence

$$\lambda_{y^*} = \sum_{i=1}^{N_S} \sum_{j=1}^{N_M} \sum_{k=1}^{N_R} \nu_i \int\int P[Y > y^* \mid m_j, r_k] P[M = m_j] P[R = r_k]$$

All sites are considered

All possible effects are considered - each weighted by its conditional probability of occurrence

All possible magnitudes are considered - contribution of each is weighted by its probability of occurrence

Probabilistic Seismic Hazard Analysis

$$\lambda_{y^*} = \sum_{i=1}^{N_S} \sum_{j=1}^{N_M} \sum_{k=1}^{N_R} \nu_i \int\int P[Y > y^* \mid m_j, r_k] P[M = m_j] P[R = r_k]$$

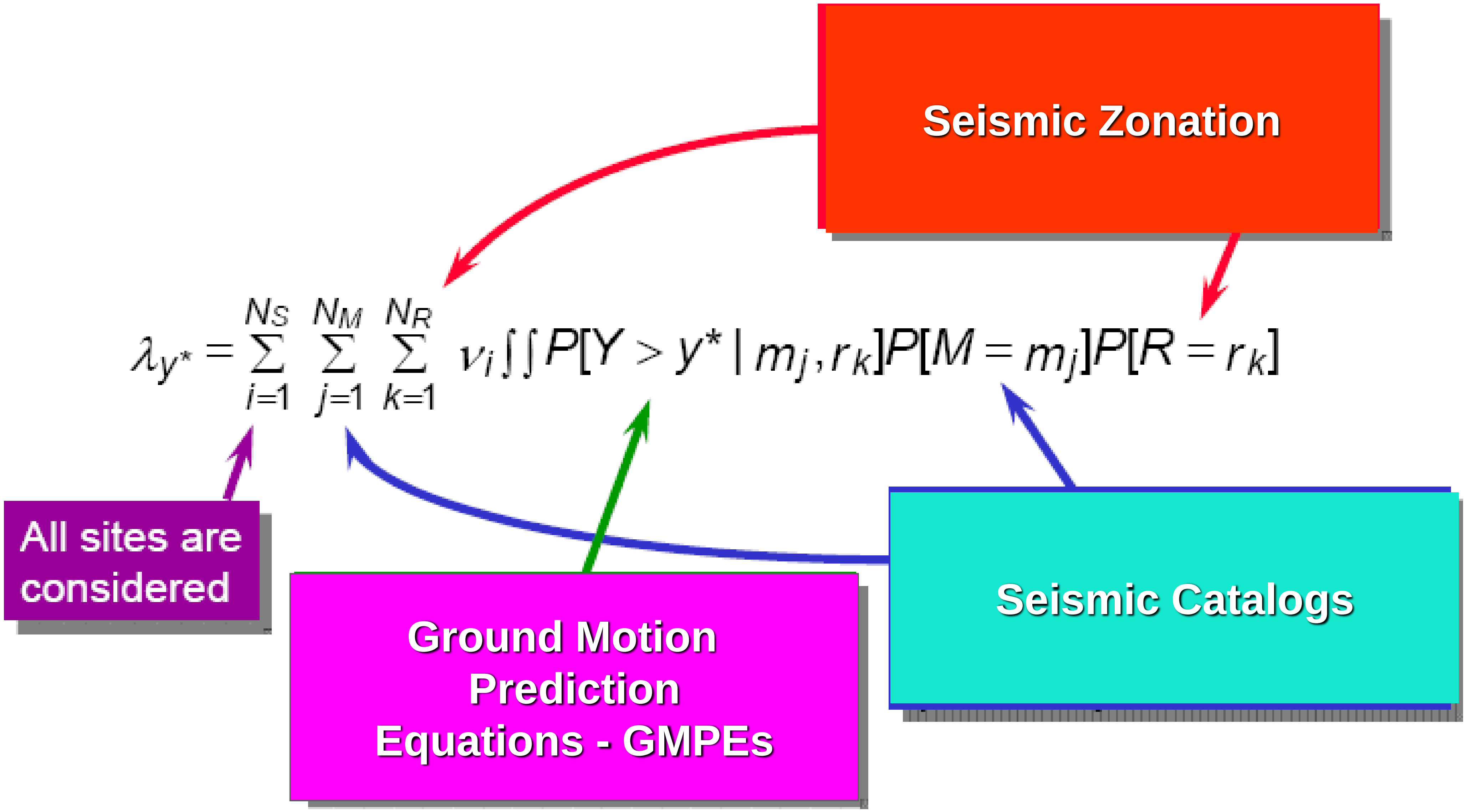

Random events

Sample Space

$S = \{1, 2, 3, 4, 5, 6\}$

$E_1 = \{1, 3, 5\}$ $E_2 = \{4, 5, 6\}$

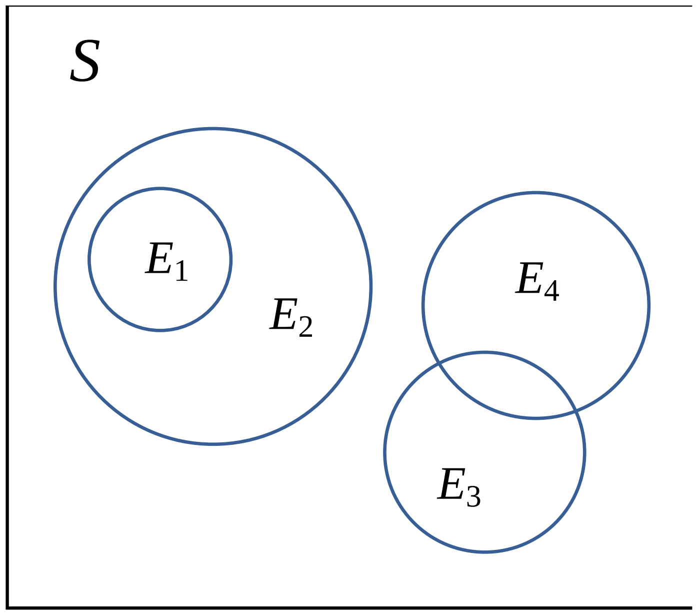

Baker, Bradley and Stafford (2021), "Seismic Hazard and Risk Analysis." These images are provided for instructional and research use, with attribution. Not for commercial use.

Union

$E_1 \cup E_2 = \{1, 3, 4, 5, 6\}$

Intersection

$E_1 \cap E_2 = \{5\}$

Or E_1E_2

1. Events E_1 and E_2 are *mutually exclusive* when they have no common outcomes (i.e., $E_1E_2 = \phi$, where ϕ is the *null event*).
2. Events $E_1, E_2 \ldots E_n$ are *collectively exhaustive* when their union contains every possible outcome of the random event (i.e., $E_1 \cup E_2 \cup, \ldots, \cup E_n = S$).
3. The *complementary event*, $\overline{E_1}$, of an event E_1, contains all outcomes in the sample space that are not in event E_1. By this definition, $\overline{E_1} \cup E_1 = S$ and $\overline{E_1}E_1 = \phi$. That is, $\overline{E_1}$ and E_1 are mutually exclusive and collectively exhaustive.

Random events

We will be interested in the probabilities of occurrence of various events. These probabilities must follow three axioms of probability:

$$0 \leq P(E) \leq 1, \tag{A.1}$$

$$P(S) = 1, \tag{A.2}$$

and, for mutually exclusive events E_1 and E_2,

$$P(E_1 \cup E_2) = P(E_1) + P(E_2). \tag{A.3}$$

$$P(\bar{E}) = 1 - P(E) \tag{A.4}$$

$$P(\phi) = 0 \tag{A.5}$$

$$P(E_1 \cup E_2) = P(E_1) + P(E_2) - P(E_1 E_2). \tag{A.6}$$

Conditional Probability

$$P(E_1|E_2) = \begin{cases} \frac{P(E_1 E_2)}{P(E_2)} & \text{if } P(E_2) > 0 \\ 0 & \text{if } P(E_2) = 0. \end{cases}$$

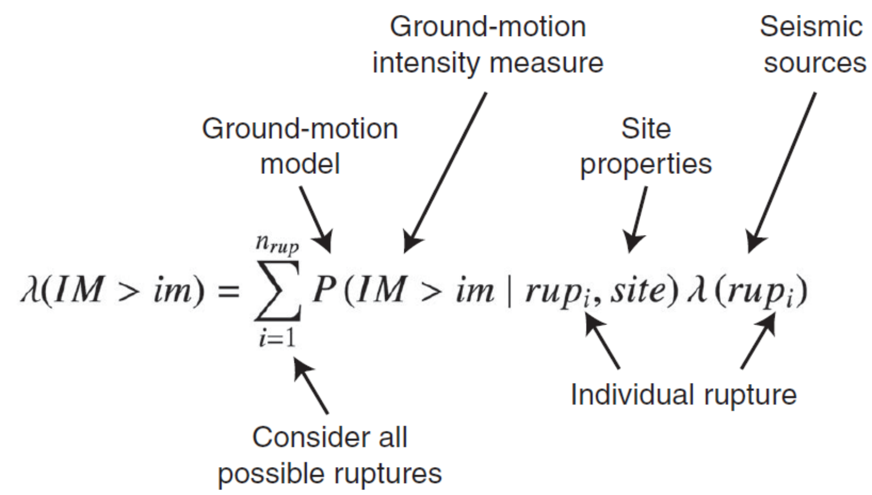

for the nontrivial case of $P(E_2) > 0$, gives

$$P(E_1 E_2) = P(E_1|E_2)P(E_2).$$

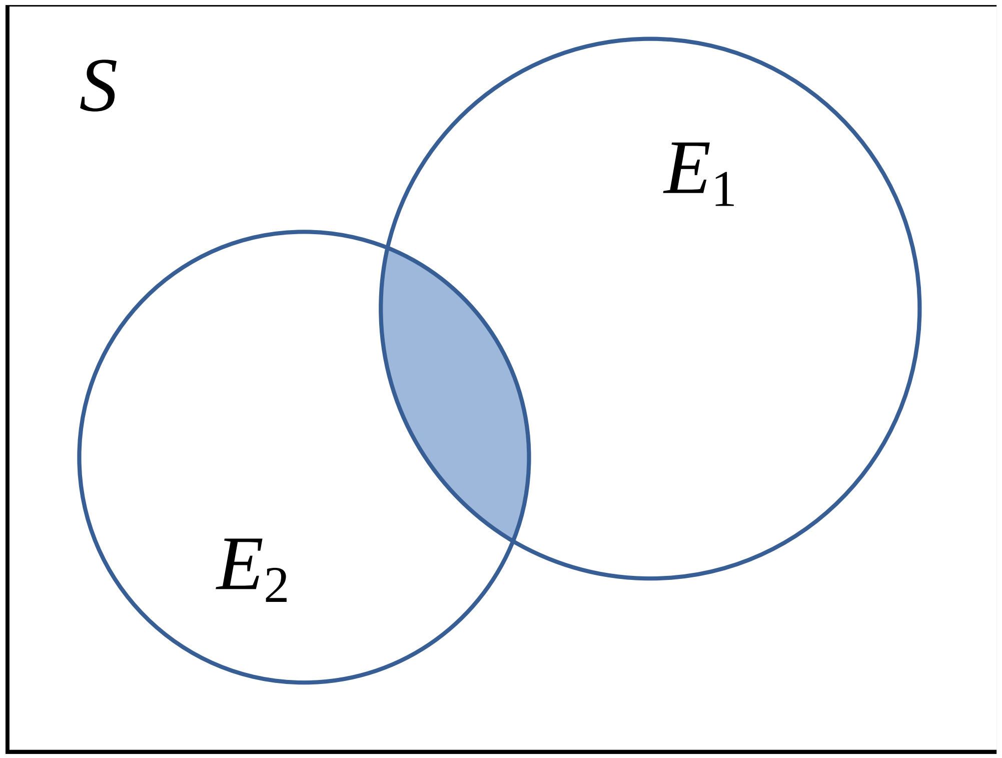

Independence

$$P(E_1|E_2) = P(E_1). \qquad \text{(A.9)}$$

$$P(E_1 E_2) = P(E_1)P(E_2),$$

Conditional Probability

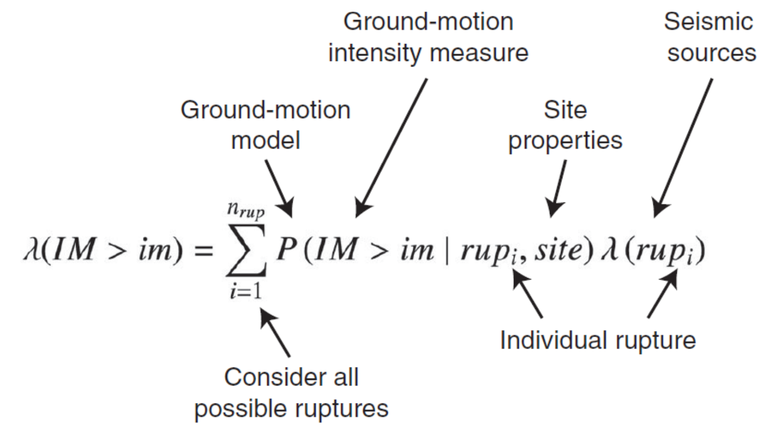

$$\lambda(IM > im) = \sum_{i=1}^{n_{rup}} P(IM > im \mid rup_i, site)\, \lambda(rup_i)$$

Total Probabilty Theorem

Consider an event A and a set of mutually exclusive and collectively exhaustive events $E_1, E_2, \ldots, E_n$. The Total Probability Theorem states that

$$P(A) = \sum_{i=1}^{n} P(A|E_i)P(E_i). \tag{A.11}$$

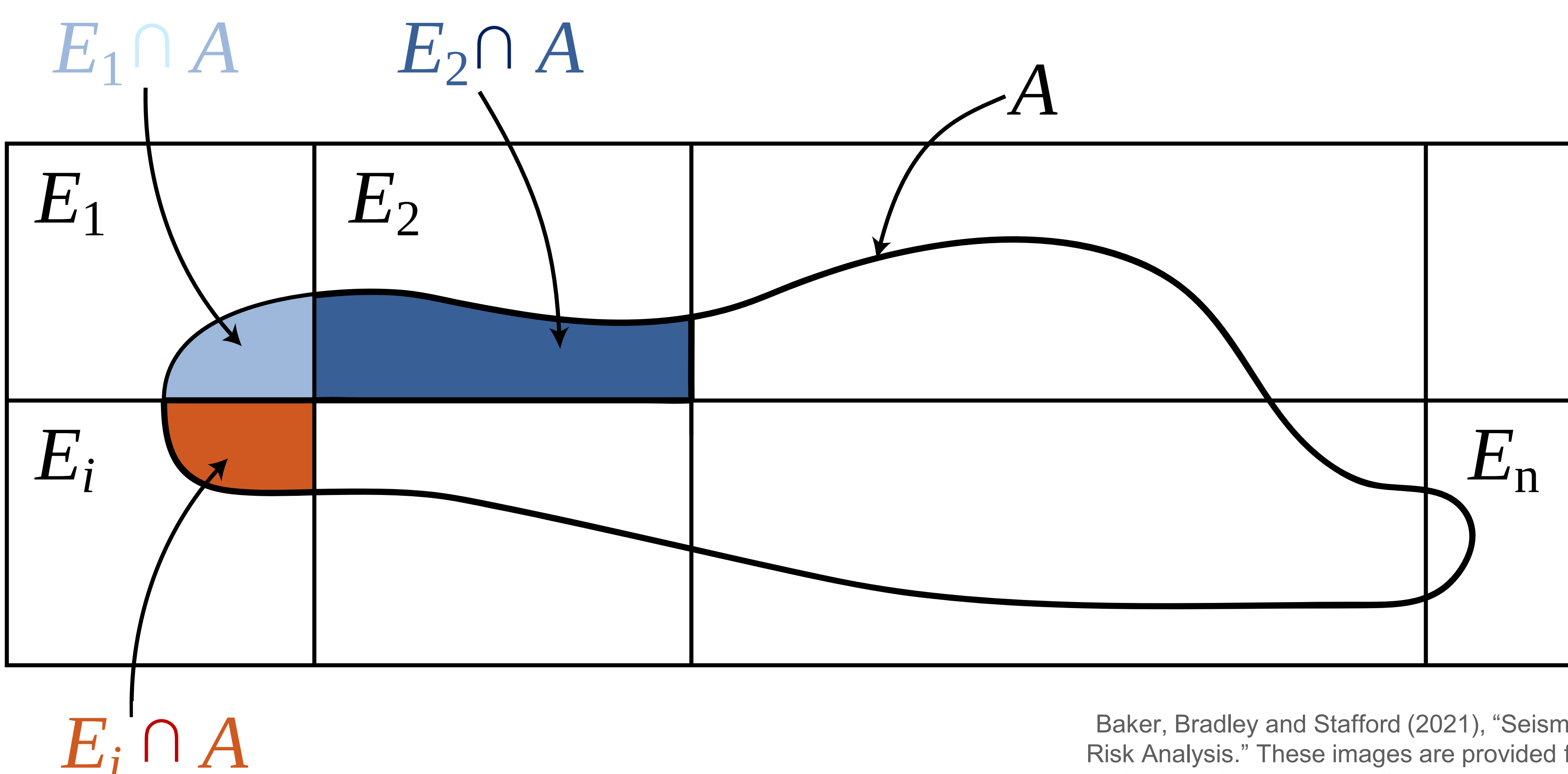

Baker, Bradley and Stafford (2021), "Seismic Hazard and Risk Analysis." These images are provided for instructional and research use, with attribution. Not for commercial use.

Conditional Probability

Bayes' Rule

$$P(E_1|E_2) = P(E_1). \qquad \text{(A.9)}$$

Consider an event A and a set of mutually exclusive and collectively exhaustive events $E_1, E_2, \ldots, E_n$. Using Equation A.9, we can write

$$P(AE_j) = P(E_j|A)P(A) = P(A|E_j)P(E_j). \qquad \text{(A.12)}$$

Rearranging the last two terms gives

$$P(E_j|A) = \frac{P(A|E_j)P(E_j)}{P(A)}. \qquad \text{(A.13)}$$

Random Variables

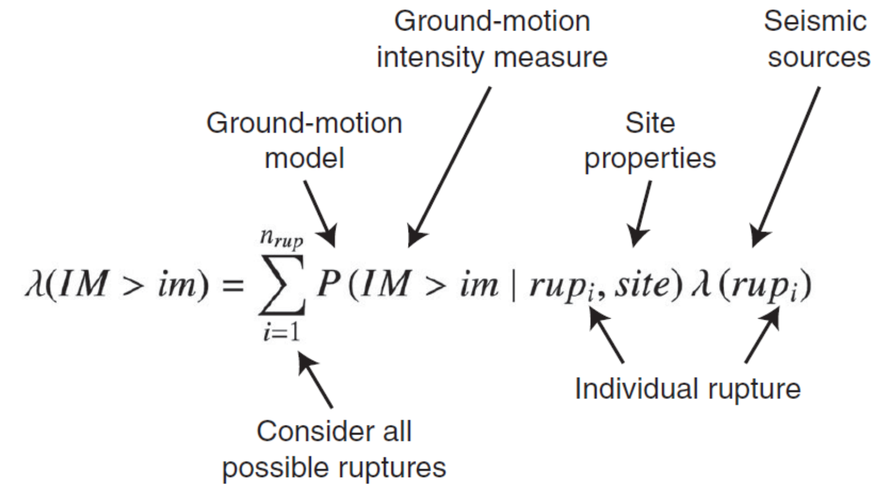

A **random variable** is a numerical variable whose specific value cannot be predicted with certainty before the occurrence of an event

x1,x2,x3 …denote possible outcome of X

P(X=x1) is the probability of X of assuming the value x1

Random variable can be **discrete** (e.g. number of earthquakes occurring in a region in a certain amount of time) or **continuous**

The probabilty distribution of a discrete random variable is quantified by the **probability mass function (PMF):**

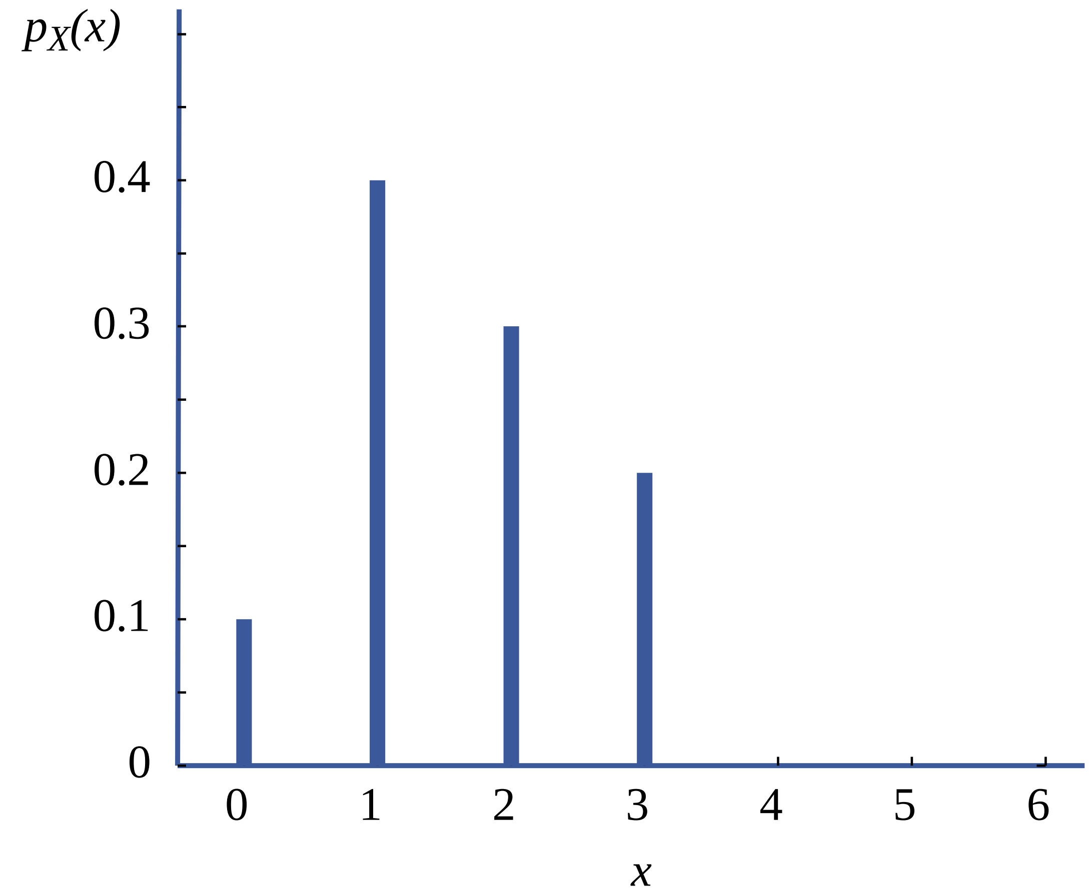

(a)

$$p_X(x) = P(X = x).$$

Random Variables

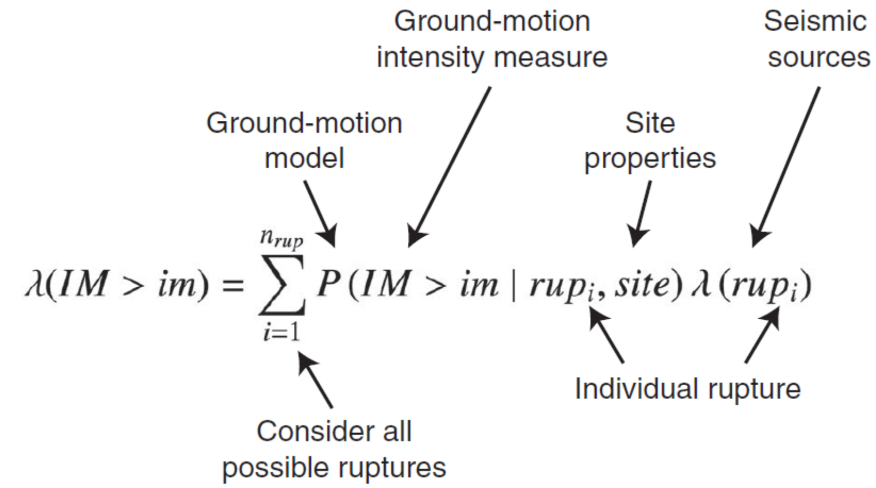

The **cumulative distribution function (CDF)** is defined as the probability of the event that the random variable takes a value less than or equal to the value of the argument:

$$F_X(x) = P(X \leq x).$$

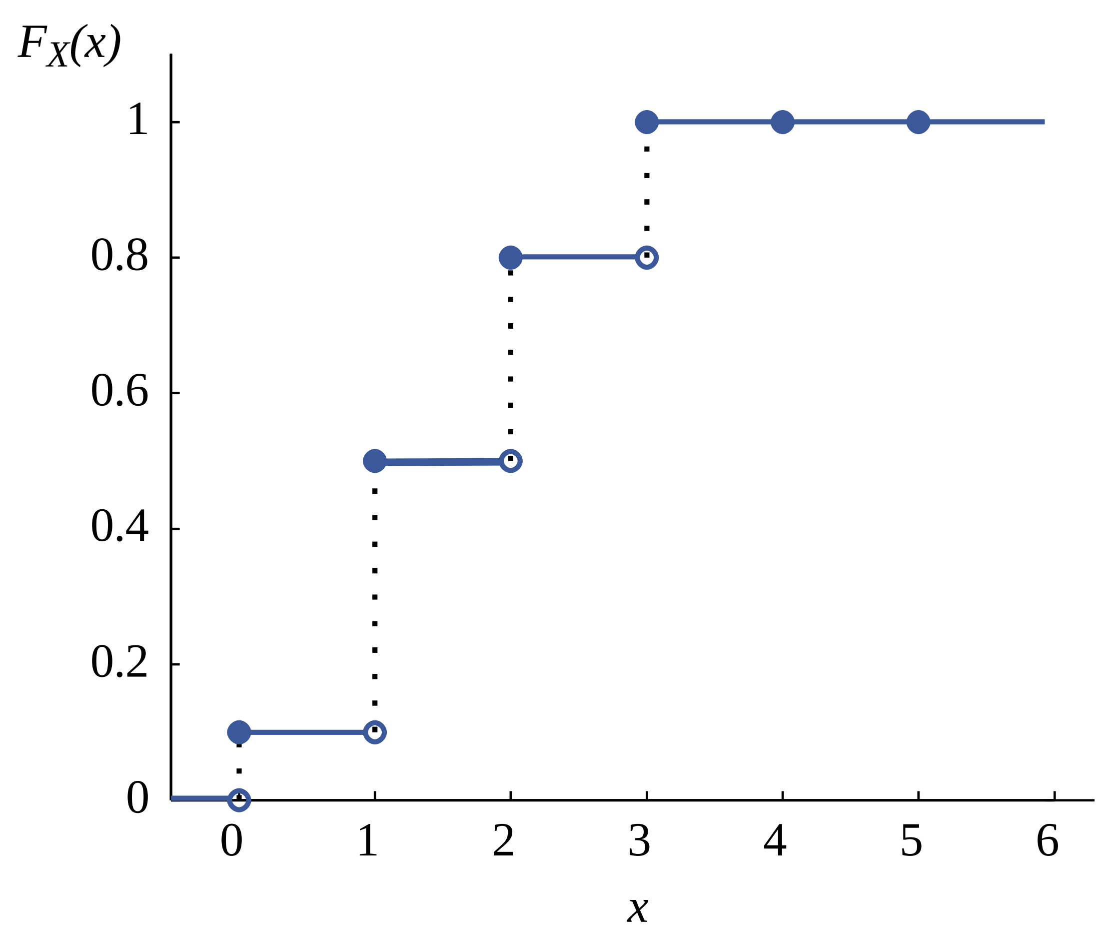

(b)

PMF and **CDF** are related by:

$$F_X(a) = \sum_{\text{all } x_i \leq a} p_X(x_i).$$

In many cass (see equation on the top right) we are interested in the probability of **X** $\geq$ **x**:

$$P(X > x) = 1 - P(X \leq x)$$

Random Variables

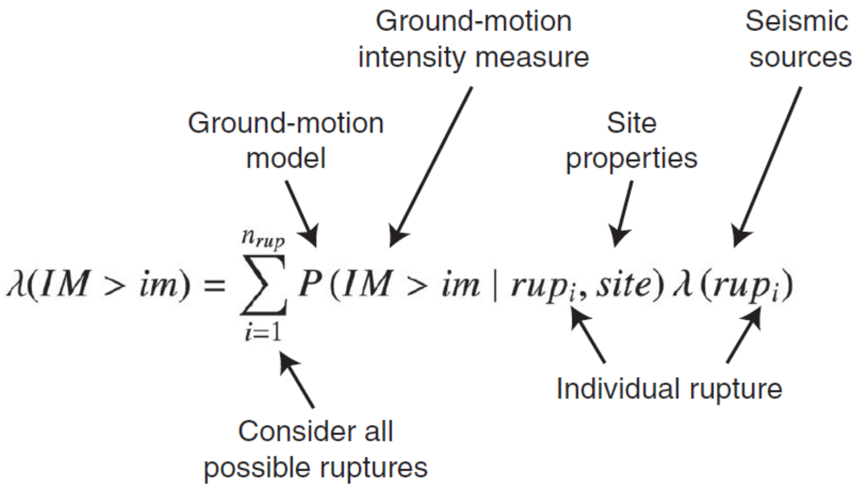

In the case of a **continuous** variable the **Probability Density Function (PDF)** is defined:

$$f_X(x)\,dx = P(x < X \leq x + dx)$$

$f_X(x)\,dx$ represents the probability of the random variable X taking values between x and x+dx

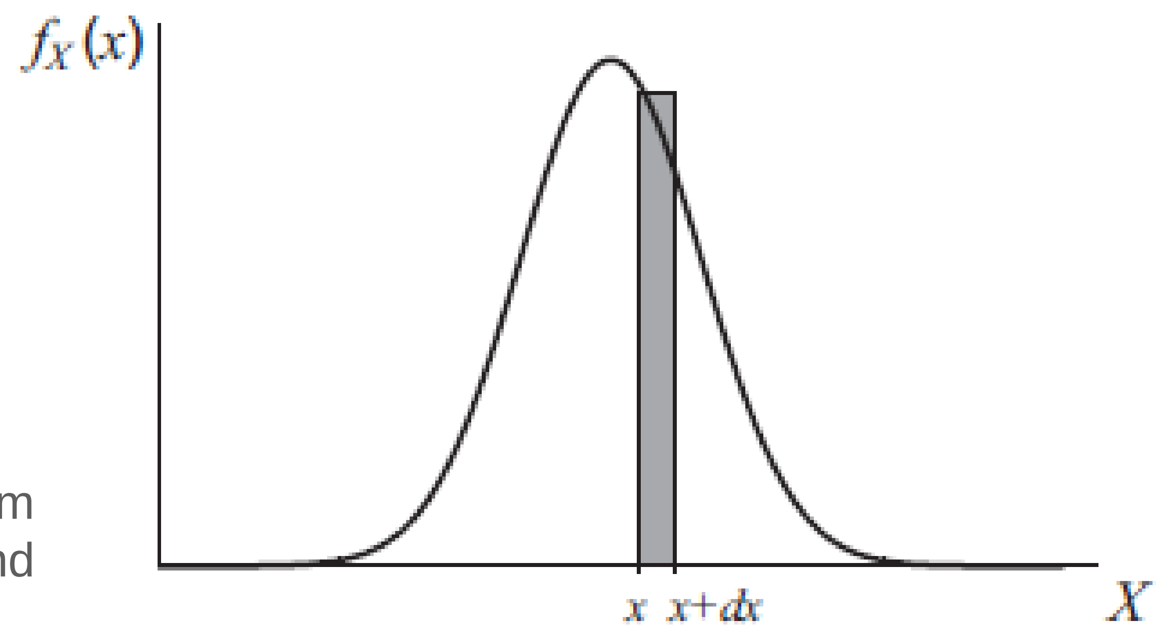

Baker, Bradley and Stafford (2021), "Seismic Hazard and Risk Analysis." These images are provided for instructional and research use, with attribution. Not for commercial use.

Random Variables

Probability that the outcome of X is in the interval between and **b**

$$P(a < X \leq b) = \int_a^b f_X(x)\,dx.$$

For discrete random variables

$$p_{\tilde{X}}(x) = f_X(x)\,\Delta x = P(x < X \leq x + \Delta x)$$

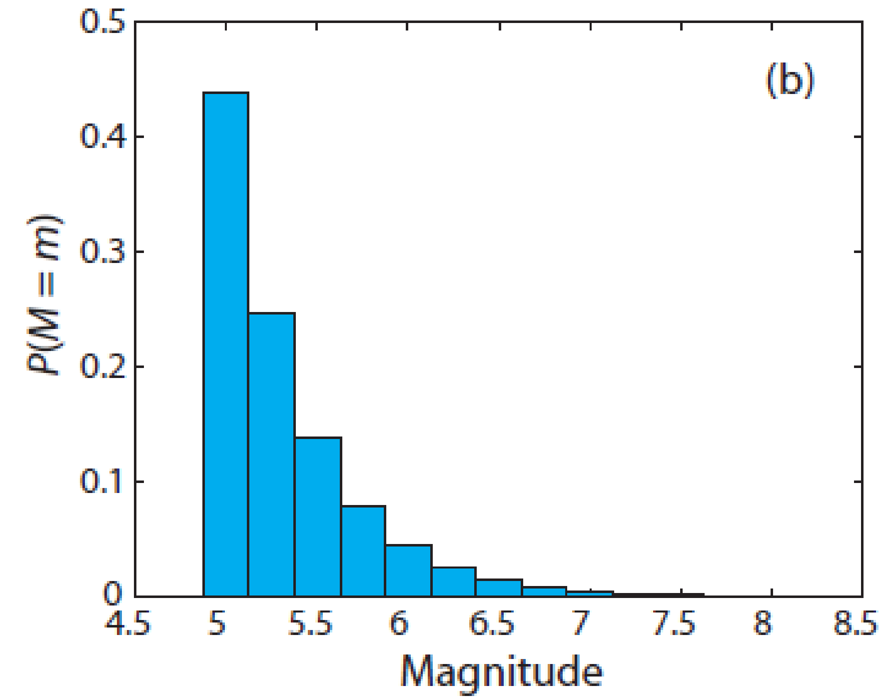

Relation between PDF and CDF

CDF

$$F_X(x) = P(X \leq x).$$

CDF

$$F_X(x) = P(X \leq x) = \int_{-\infty}^{x} f_X(u)\,du$$

$-\infty$

PDF

$$f_X(x) = \frac{d}{dx}F_X(x).$$

Common Probability Distributions

Normal Distribution

PDF $$f_X(x) = \frac{1}{\sigma_X\sqrt{2\pi}}\exp\left(-\frac{1}{2}\left(\frac{x-\mu_X}{\sigma_X}\right)^2\right) \qquad -\infty \leq x \leq \infty$$

where μ_X and σ_X denote the mean value and standard deviation, respectively, of X.

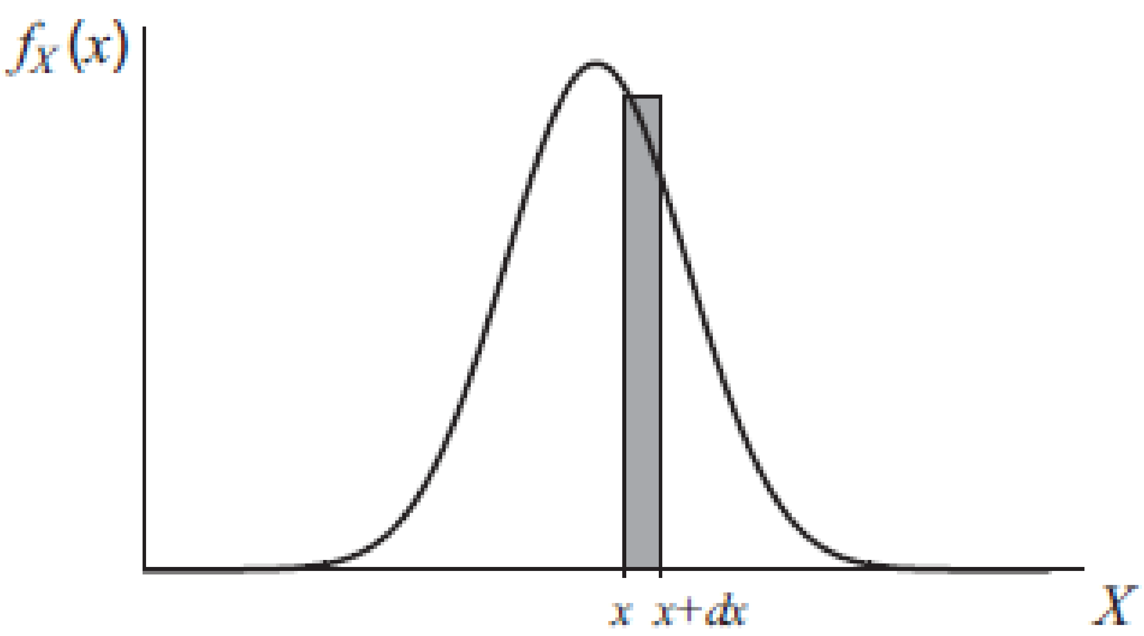

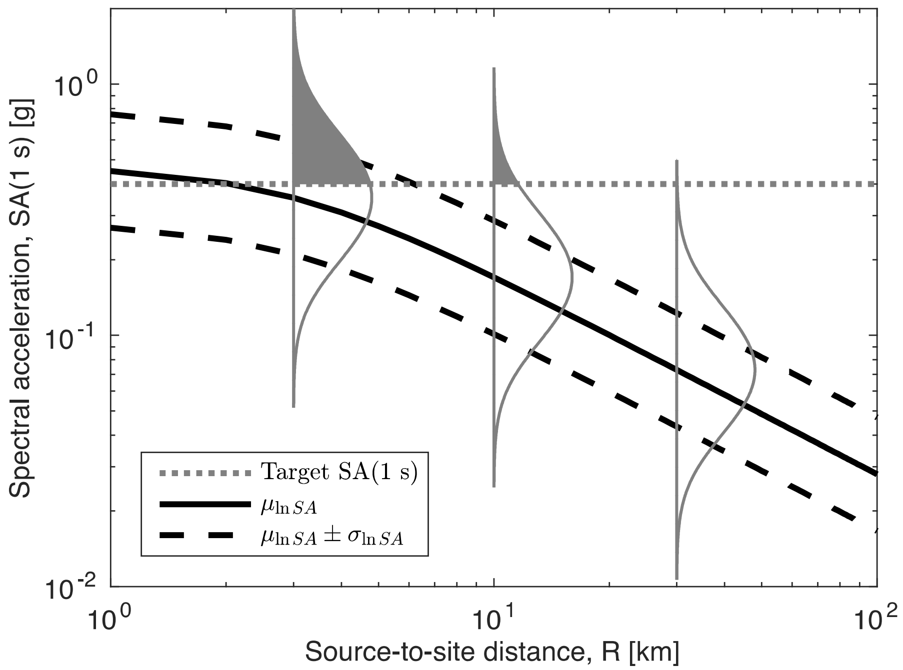

UNIVERSITÀ DEGLI STUDI DI TRIESTE

Common Probability Distributions

Normal Distribution

A normal random variable, X, can be transformed into a standard normal random variable as

$$U = \frac{X - \mu_X}{\sigma_X} \tag{A.51}$$

where U is a standard normal random variable.

The CDF for general normal random variable can be written as:

$$P(X \leq x) = \Phi\left(\frac{X - \mu_X}{\sigma_X}\right)$$

Common Probability Distributions

Bivariate Normal Distribution

Normal distribution of 2 random variables

$$f_{X,Y}(x,y) = \frac{1}{2\pi\sigma_X\sigma_Y\sqrt{1-\rho_{X,Y}^2}} \exp\left\{-\frac{z}{2(1-\rho_{X,Y}^2)}\right\} \qquad -\infty \le x, y \le \infty$$

where $\rho_{X,Y}$ is the correlation coefficient between X and Y, and

$$z = \frac{(x-\mu_X)^2}{\sigma_X^2} - \frac{2\rho_{X,Y}(x-\mu_X)(y-\mu_Y)}{\sigma_X\sigma_Y} + \frac{(y-\mu_Y)^2}{\sigma_Y^2}.$$

A useful property of random variables having this distribution is that if X and Y are jointly normal, then their marginal distributions ($f_X(x)$ and $f_Y(y)$) are normal, and their conditional distributions are also normal. Specifically, the distribution of X given $Y = y$ has conditional mean

$$\mu_{X|Y=y} = \mu_X + \rho_{X,Y}\,\sigma_X\left(\frac{y-\mu_Y}{\sigma_Y}\right) \qquad \text{(A.55)}$$

and conditional standard deviation

$$\sigma_{X|Y=y} = \sigma_X\sqrt{1-\rho_{X,Y}^2}. \qquad \text{(A.56)}$$

These properties are convenient when computing joint distributions of ground-motion parameters.

Common Probability Distributions

Lognormal Distribution

A random variable Y has a lognormal distribution if its logarithm, X=ln Y has a normal distribution

$$f_Y(y) = \frac{1}{y\sigma_{\ln Y}\sqrt{2\pi}} \exp\left(-\frac{1}{2}\left(\frac{\ln y - \mu_{\ln Y}}{\sigma_{\ln Y}}\right)^2\right) \quad 0 \le y \le \infty$$

$$F_Y(y) = \Phi\left(\frac{\ln y - \mu_{\ln Y}}{\sigma_{\ln Y}}\right) \quad 0 \le y \le \infty$$

Relation to the mean and standard deviation of Y

$$\mu_Y = e^{\mu_{\ln Y}} e^{\frac{1}{2}\sigma^2_{\ln Y}}$$

$$\sigma_Y = \mu_Y \sqrt{e^{\sigma^2_{\ln Y}} - 1}.$$

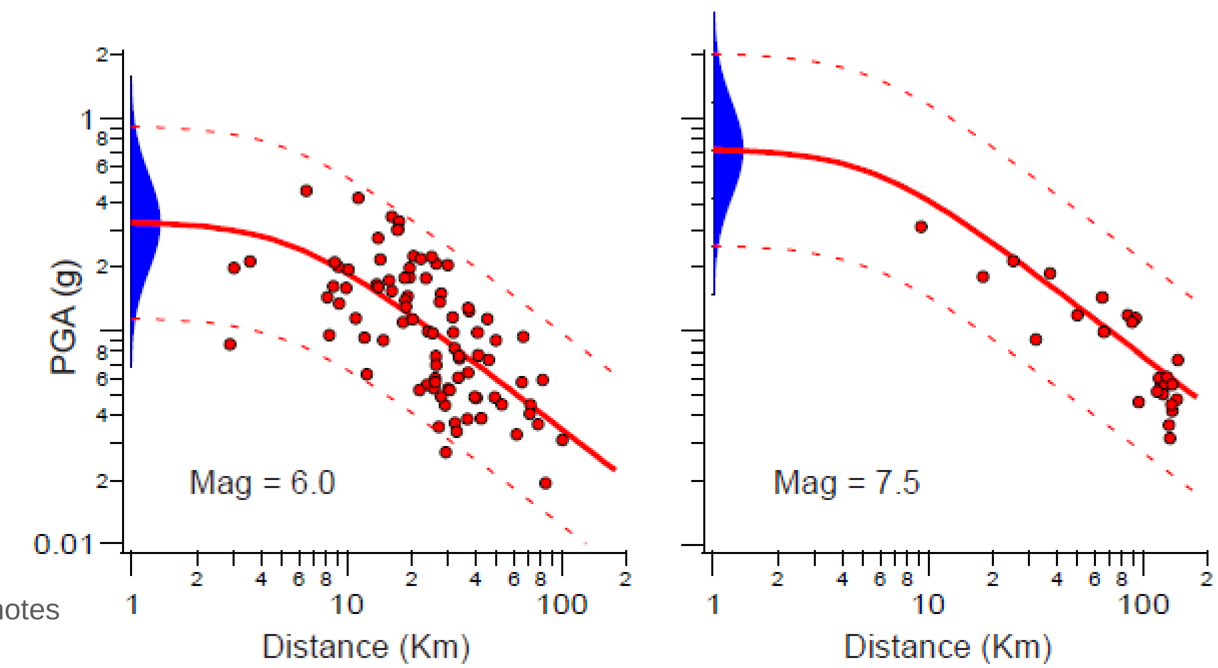

E.H. Field notes

The relationship between the median of Y, y_{50}, and $\mu_{\ln Y}$ can be determined by setting the CDF of Equation A.69 equal to 0.5 when y equals the median, y_{50}:

$$0.5 = \Phi\left(\frac{\ln y_{50} - \mu_{\ln Y}}{\sigma_{\ln Y}}\right) \quad \rightarrow \quad y_{50} = e^{\mu_{\ln Y}}. \qquad \text{(A.72)}$$

The equivalence of $\ln y_{50}$ and $\mu_{\ln Y}$ can be stated in words as "the log of the median is equal to the logarithmic mean."

UNIVERSITÀ DEGLI STUDI DI TRIESTE

Common Probability Distributions

The poisson process

A *Poisson process* is a sequence of discrete events having the following properties:

1. Stationarity: the probability of an event in a short interval from time t to $t + h$ is approximately λh, for any t.
2. Nonmultiplicity: the probability of two or more events in a short time interval is negligible compared with λh.
3. Independence: the number of events in any interval of time is independent of the number of events in any other (nonoverlapping) interval of time.

The number of events observed in time t froma poisson process has a Poisson distribution.

Poisson PMF $$p_X(x) = \frac{(\lambda t)^x}{x!}\exp(-\lambda t), \qquad x = 0, 1, 2, \ldots$$

X is the number of success in time t
The process has a mean rate of events λ

Mean $$\mu_X = \lambda t$$

Standard deviation $$\sigma_X = \sqrt{\lambda t}.$$

Baker, Bradley and Stafford (2021), "Seismic Hazard and Risk Analysis." These images are provided for instructional and research use, with attribution. Not for commercial use.

E.H. Field notes

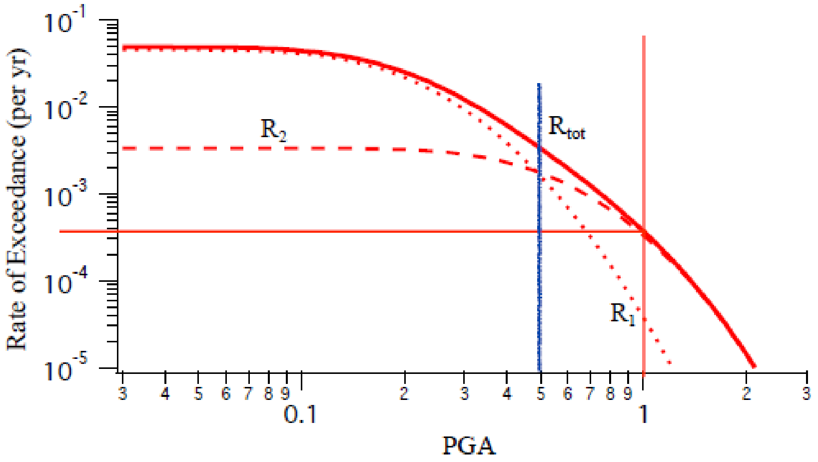

Poissonian probability of exceeding each ground motion level in the next T years from the annual rate

UNIVERSITÀ DEGLI STUDI DI TRIESTE

Modified from Probabilistic Seismic Hazard Analysis (PSHA)
A Primer Written by Edward (Ned) H. Field

Basic of Probabilistic Seismic Hazard Assessment (1)

Hazard is the mean rate of exceedence of a certain ground motion measure (PGA, SA, PGV) etc   UNIT is $(\text{years})^{-1}$

Risk is the mean annual loss (dollars, properties, lives) UNITS dollars/years lives/years

Sesimic Source Zone (SSZ) $=5X10^{6}$ km^{2}

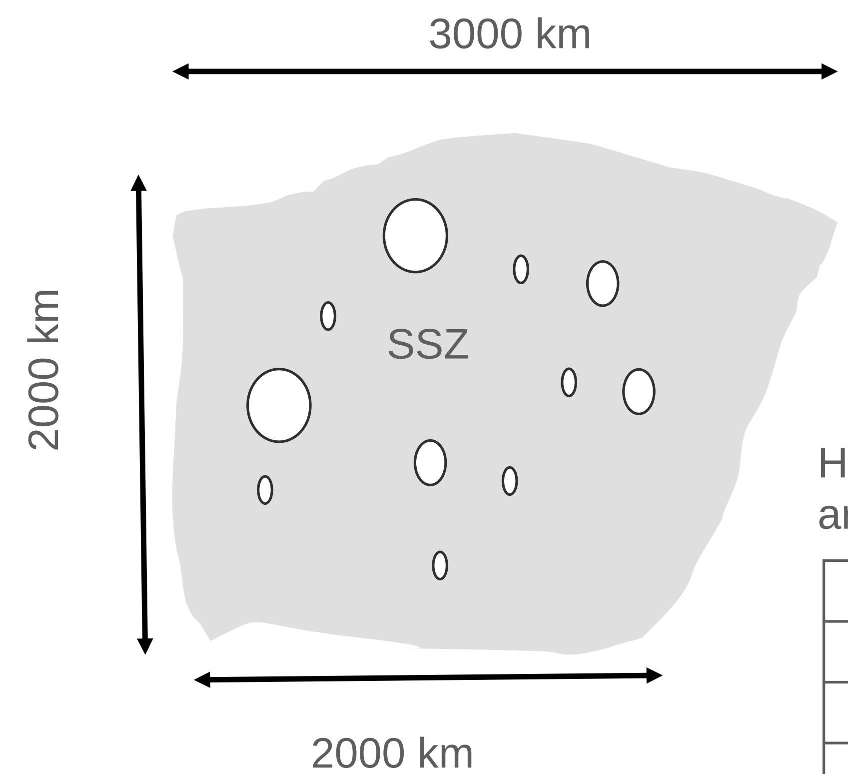

One M=5   per year
One M=6 per decade
One M=7 per century

Horizontal distance (km) within which the given pga's are achieved or exceeded for the given magnitudes

	M=5	M=6	M=7
0.1 g	14	25	41
0.2 g	3.2	12	22
0.4 g	0	0	10

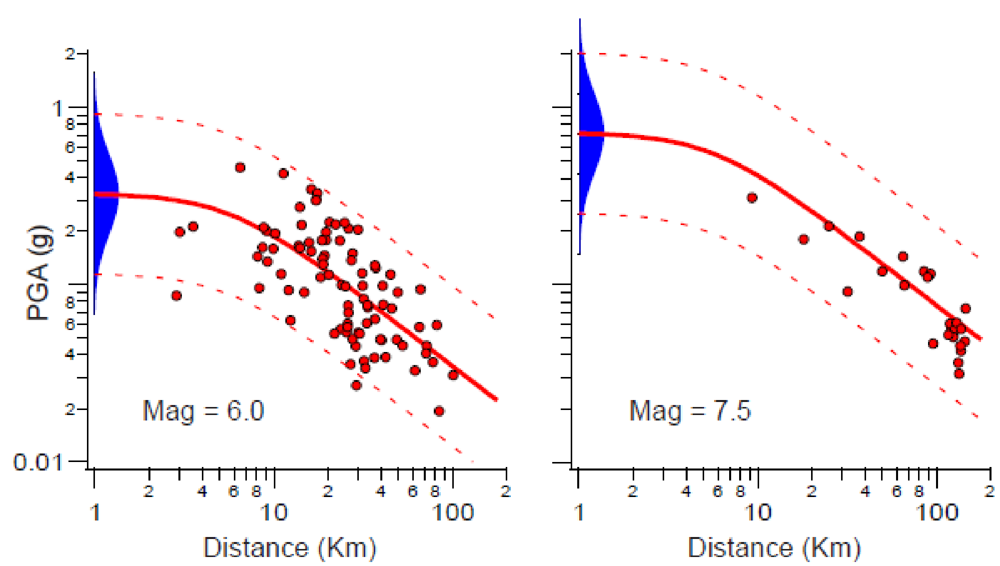

Mean rate of exceedance (MROES) x 10-4 per year, for given pga's for the given magnitudes

	M=5	M=6	M=7	$\sum$	$\sum^{\sigma}$
0.1 g	1.23	0.39	0.11	1.73	1.47
0.2 g	0.06	0.09	0.03	0.18	0.41
0.4 g	0	0	0.006	0.006	0.034

Modified from probabilistic seismic hazard analysis: a beginner's guide T.C Hanks, C.A. Cornell

Basic of Probabilistic Seismic Hazard Assessment (1)

Example for MROE
M=5
Pga=0.1

The PGA will be greater than or equal to the given value of PGA within each distance R
That is where exceedance comes!

Likelihood that the place of interest will be affected by the level of pga or higher

$$MROE=((\pi 14^2)\ km^2/(5X10^6)\ km^2)*1/year = 1.23x10^{-4}$$

Occurrence rate of each Magnitude

One M=5 per year
One M=6 per decade
One M=7 per century

Horizontal distance R (km) within which the given pga's are achieved or exceeded for the given magnitudes

	M=5	M=6	M=7
0.1 g	14	25	41
0.2 g	3.2	12	22
0.4 g	0	0	10

Mean rate of exceedance (MROES) x 10-4 per year, for given pga's for the given magnitudes

	M=5	M=6	M=7	$\sum$	$\sum^{\sigma}$
0.1 g	1.23	0.39	0.11	1.73	1.47
0.2 g	0.06	0.09	0.03	0.18	0.41
0.4 g	0	0	0.006	0.006	0.034

Numerical integration with $\Delta M=1$

Modified from probabilistic seismic hazard analysis: a beginner's guide T.C Hanks, C.A. Cornell

Basic of Probabilistic Seismic Hazard Assessment (1)

Example for MROE
M=5
Pga=0.1

The mean rate in the order of 10^{-4} /year does not mean that we need data for 10.000 year.

The small value is not due to the seismicity rate but to the ratio of the area!

The earthquakes are occurring at the rate of 1/year for M=5 and 10^{-2} year for M=7

One M=5 per year
One M=6 per decade
One M=7 per century

Horizontal distance R (km) within which the given pga's are achieved or exceeded for the given magnitudes

	M=5	M=6	M=7
0.1 g	14	25	41
0.2 g	3.2	12	22
0.4 g	0	0	10

Mean rate of exceedance (MROES) x 10-4 per year, for given pga's for the given magnitudes

	M=5	M=6	M=7	$\sum$	$\sum^{\sigma}$
0.1 g	1.23	0.39	0.11	1.73	1.47
0.2 g	0.06	0.09	0.03	0.18	0.41
0.4 g	0	0	0.006	0.006	0.034

Numerical integration with ΔM=1

UNIVERSITÀ DEGLI STUDI DI TRIESTE

Modified from probabilistic seismic hazard analysis: a beginner's guide T.C Hanks, C.A. Cornell

Basic of Probabilistic Seismic Hazard Assessment (1)

Consider that two subregions are more active than the rest

Three different seismicty rate but with whole region with the same value as in the previous case

In Region 1 the seismicity rate is dow by **0.5** but the (area)-1 is up (for example) of a factor **100**

Therefore, for this region the exceedence rate is **50** time larger with respect to the previous case

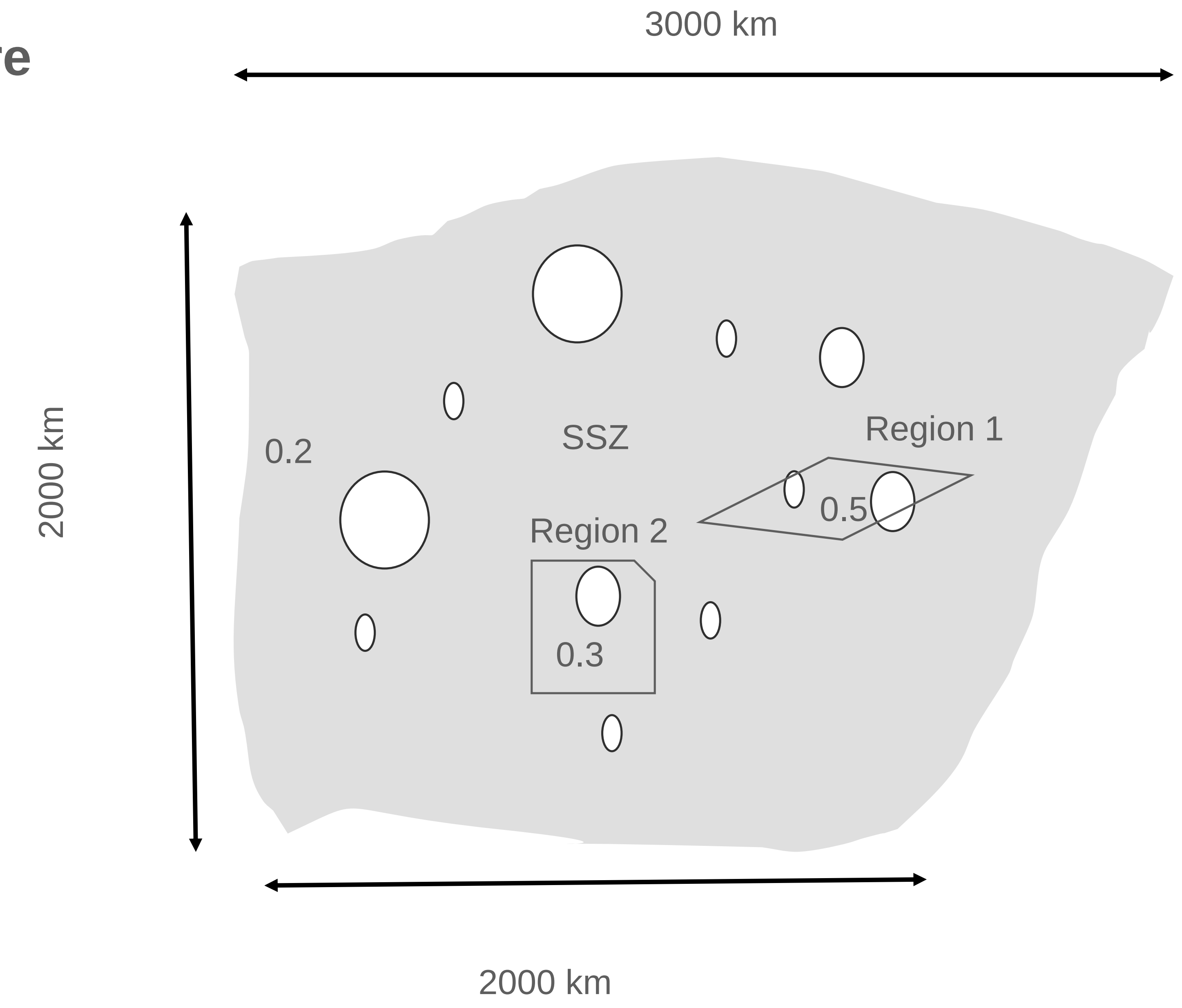

Modified from probabilistic seismic hazard analysis: a beginner's guide T.C Hanks, C.A. Cornell

Basic of Probabilistic Seismic Hazard Assessment (2)

Consider that the source model is made by N earthquake scenarion E_n, each one with its magnitude (m_n,) location (L_n) and rate (r_n)

$$E_n = E(m_n, L_n, r_n).$$

r_n represents the annual rate of the earthquake scenario

The probability of the scenario over some specified time period should be given; this would allow the implementation of time-dependent models.

Time dependent models are usually implemented by converting the conditional probability into an equivalent Poissonian time-dependent rate

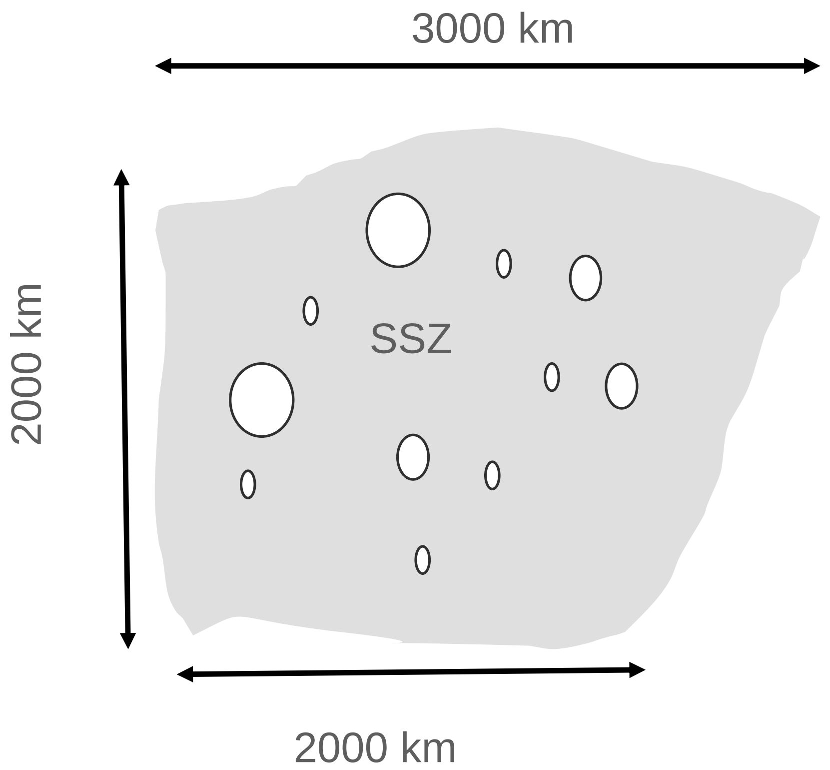

Example

An average repeat time of an earthquake ona fault is 147 years→ r=0.007 events per year

The Poissonian probability of having more than one event over T years is:

$$P_{pois} = 1 - \exp(-r T)$$

The Poissonian probability for an event in the next 30 years is 19%

Basic of Probabilistic Seismic Hazard Assessment (2)

The target is to calculate the PSHA at a certain site
The Seismic source model provide the N earthquake scenarios E_n, each one with its magnitude (m_n,) location (L_n) and rate (r_n)

From the scenario L_n we can calculate the distance D_n to the target site.

Given m_n and D_n and using a Ground Motion Prediction equation.

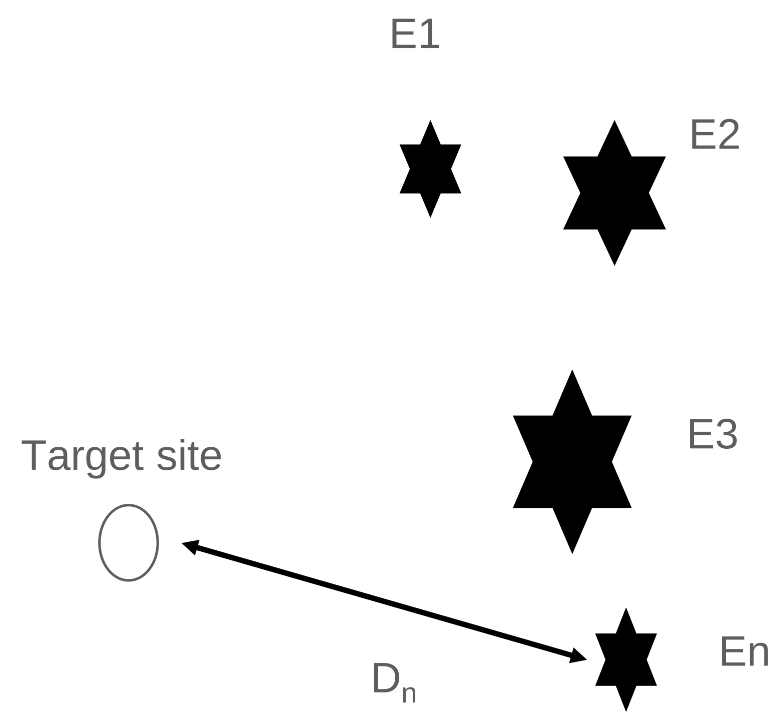

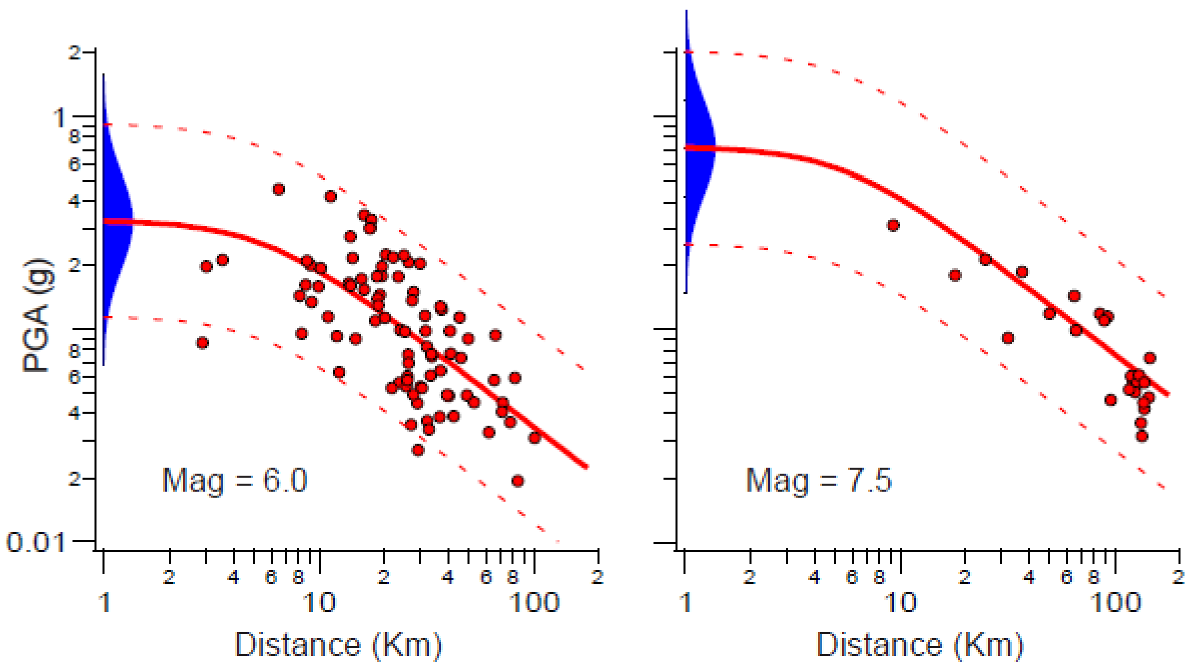

$$p_n(\ln PGA) = \frac{1}{\sigma_n\sqrt{2\pi}} e^{-(\ln PGA - g(m_n, D_n))^2/2\sigma_n} =$$

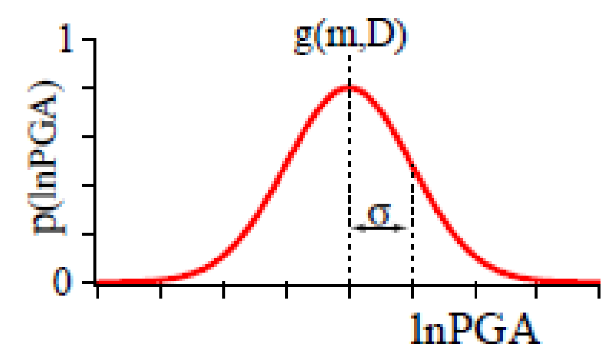

Basic of Probabilistic Seismic Hazard Assessment (2)

Probabiliy of exceeding a certain lnPGA

$$P_n(> \ln PGA) = \frac{1}{\sigma_n \sqrt{2\pi}} \int_{\ln PGA}^{\infty} e^{-(\ln PGA - g(m_n, D_n))^2 / 2\sigma_n} d\ln PGA =$$

Modified from Probabilistic Seismic Hazard Analysis (PSHA)
A Primer Written by Edward (Ned) H. Field

Basic of Probabilistic Seismic Hazard Assessment (2)

Multiplying for the annual rate r_n one get **annual rate R_n at which a certain lnPGA will be exceeded** for that specific M and Location scenario at the considered site

$$R_n(>\ln PGA) = r_n P_n(>\ln PGA)$$

Summing over the N scenarios (all considered Magnitudes and locations, and rates) one get the

Total annual rate of exceeding a certain ln PGA

$$R_{tot}(>\ln PGA) = \sum_{n=1}^{N} R_n(>\ln PGA) = \sum_{n=1}^{N} r_n P_n(>\ln PGA)$$

Modified from Probabilistic Seismic Hazard Analysis (PSHA)
A Primer Written by Edward (Ned) H. Field

Basic of Probabilistic Seismic Hazard Assessment (2)

Considering the Poissonian distribution one can compute the **Probability of exceeding each ground motion level in T years** using the total annual rate

$$P_{pois}(> \ln PGA, T) = 1 - e^{-R_{tot}T}$$

If P_{pois}=10% in 50 years

T= 50 years

R_{tot}=(-ln(1-0.1))/T=0.00210721

From which one get a **return period of 475 years**

Modified from Probabilistic Seismic Hazard Analysis (PSHA)
A Primer Written by Edward (Ned) H. Field

Basic of Probabilistic Seismic Hazard Assessment (2)

Example
Two scenarios only

R1=M=6 every 22 years

R2=M= 7.8 every 300 years

Both at 10 km from the target site

$$\ln(PGA) = 0.53(M-6) - 0.39\ln(D^2+31) + 0.25$$

→ 0.19 g

→ 0.5 g

σ (lnpga)= 0.52

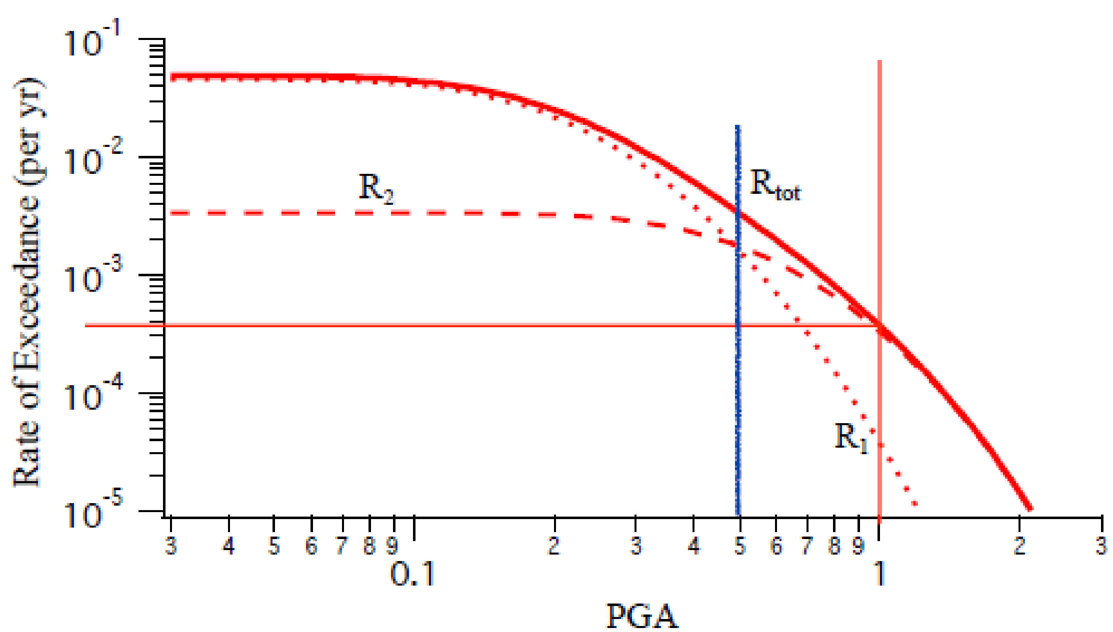

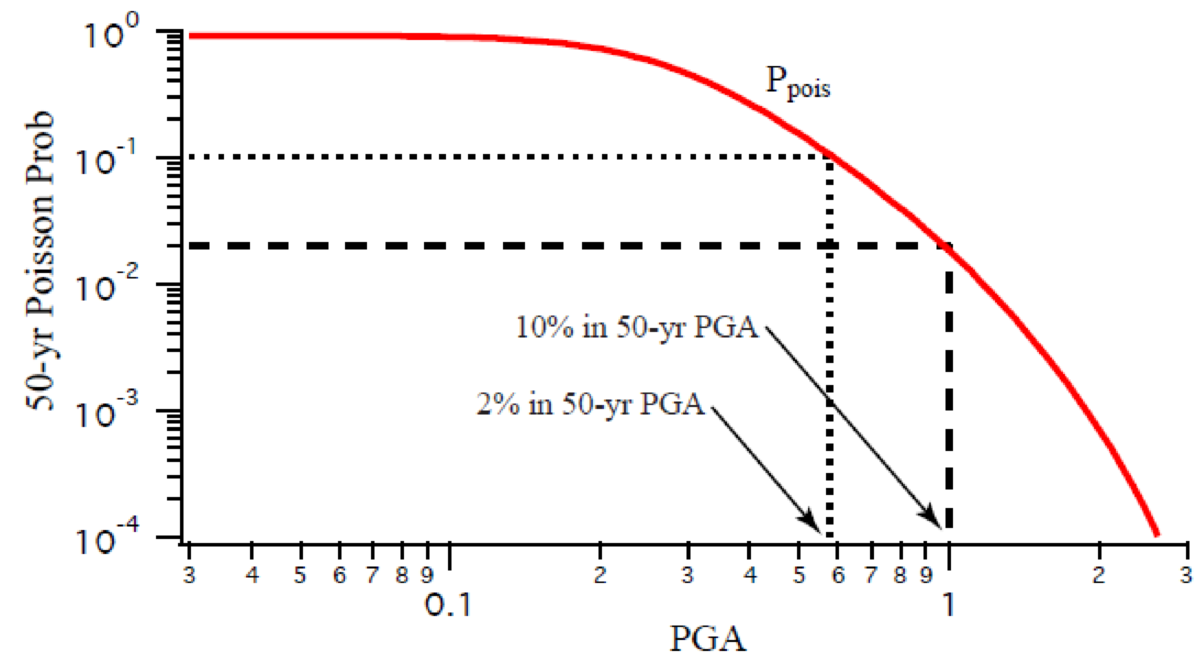

Modified from Probabilistic Seismic Hazard Analysis (PSHA)
A Primer Written by Edward (Ned) H. Field

Basic of Probabilistic Seismic Hazard Assessment (2)

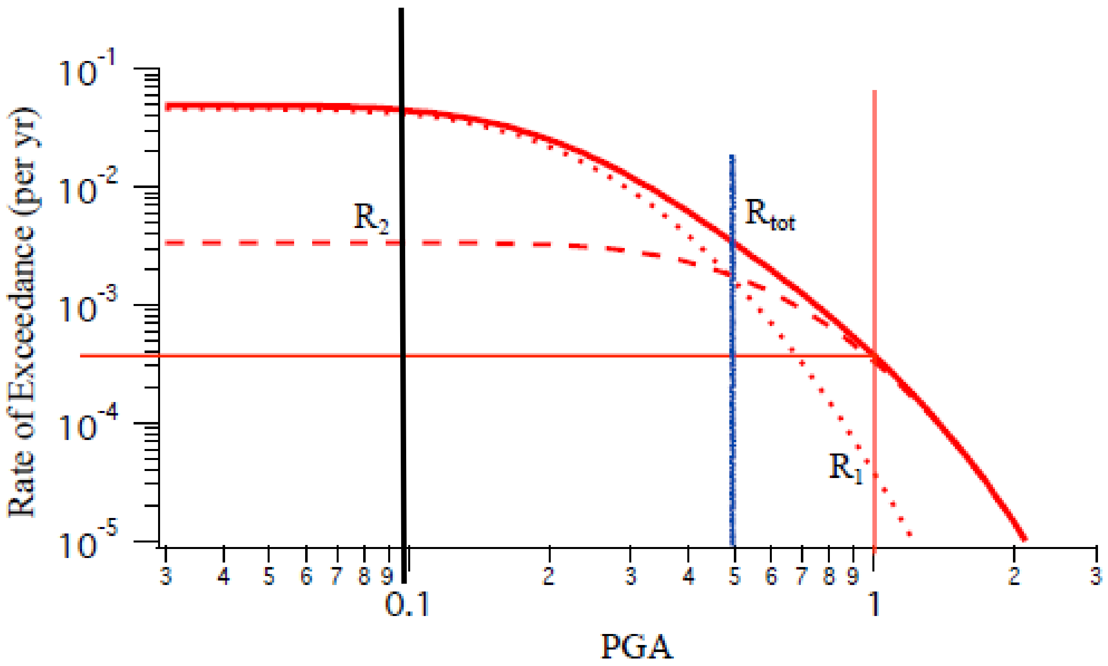

R1

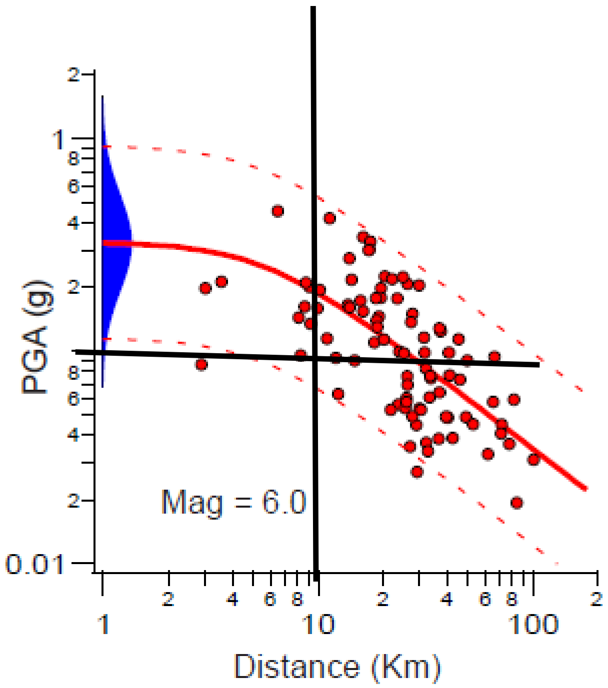

R2

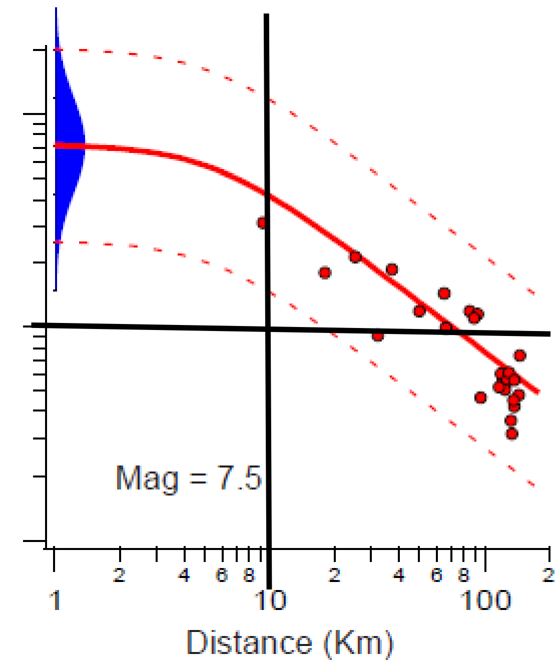

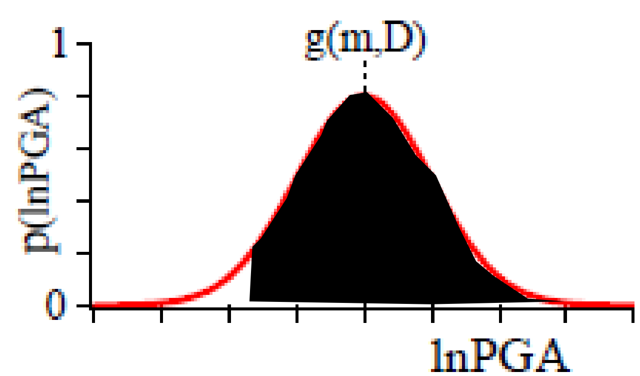

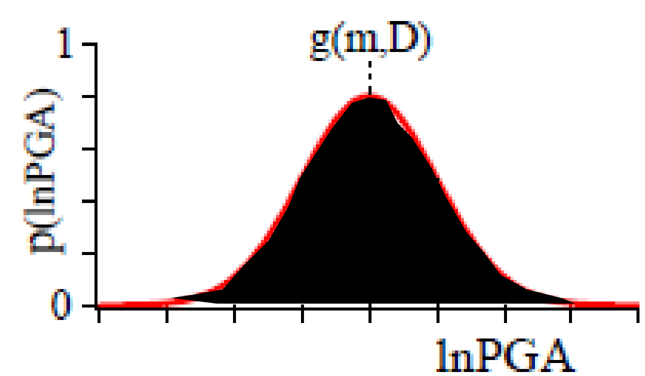

For small PGA (e.g. 0.1 g) although the **probability of exceedence** is larger for the M6, the **annual rate of exceedence** of R1 is larger than that of R2 because the **annual rate** of R1, r1=1/22 is much larger than the **annual rate** of R2, r2=1/300!

UNIVERSITÀ DEGLI STUDI DI TRIESTE

Modified from Probabilistic Seismic Hazard Analysis (PSHA)
A Primer Written by Edward (Ned) H. Field

Basic of Probabilistic Seismic Hazard Assessment (2)

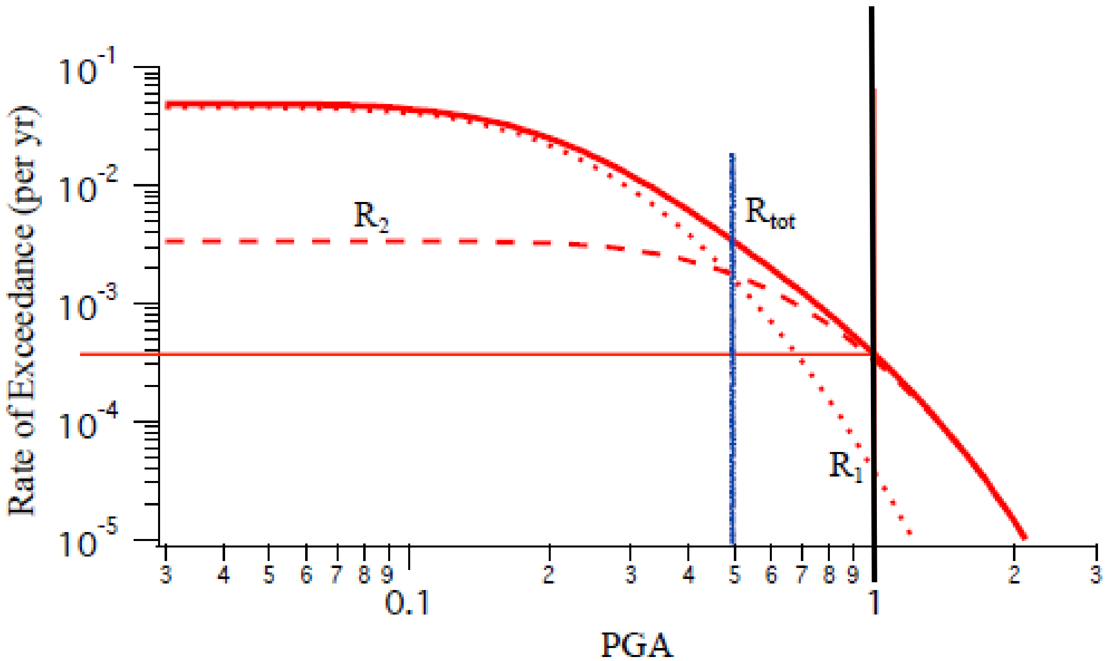

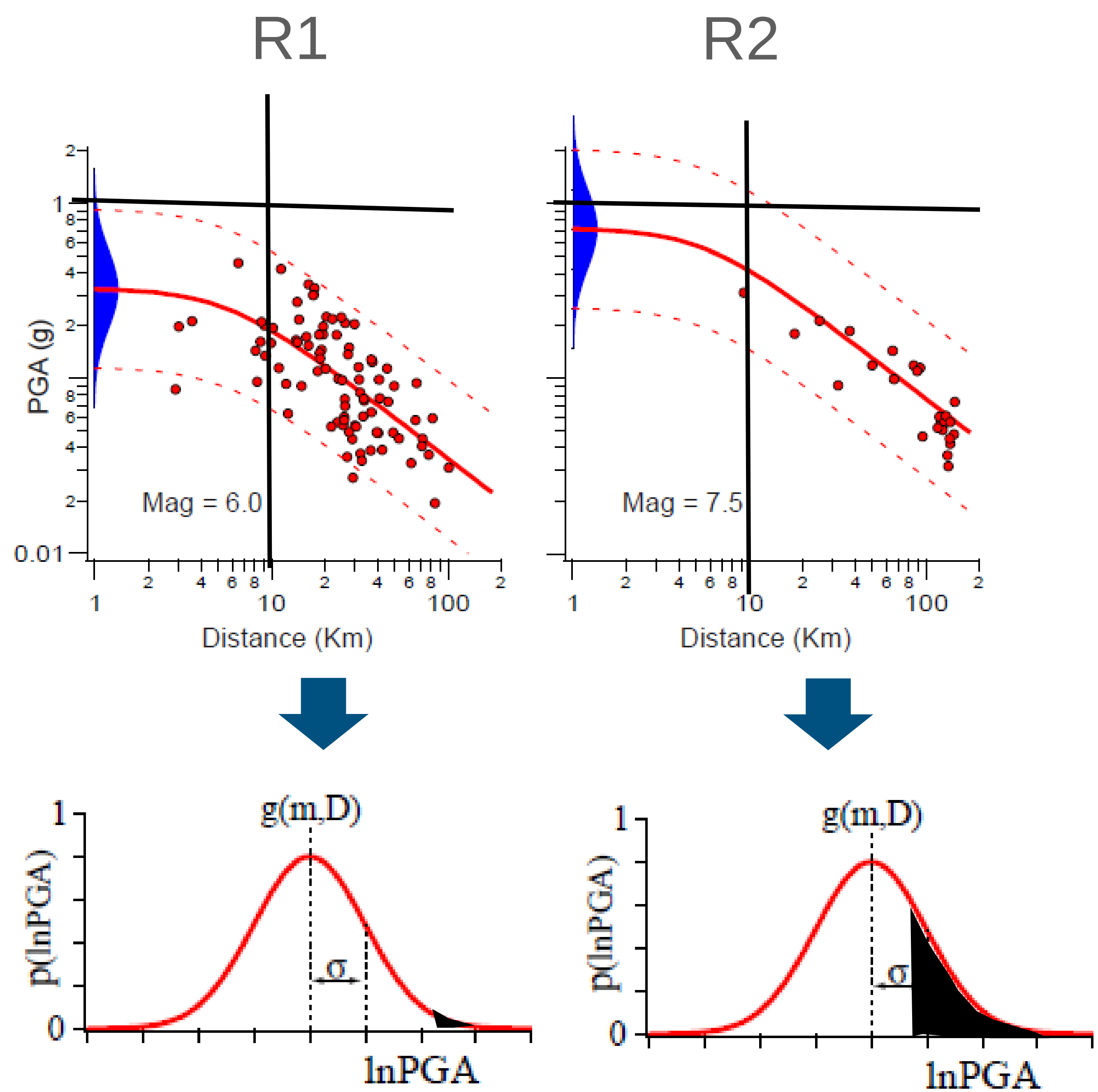

For large PGA (e.g. 1 g) the **probability of exceedence** is larger for the M7.8, **although** the **annual rate** of R1 is larger than that of R2, because **probability of exceedence** of R1 is very small

Basic of Probabilistic Seismic Hazard Assessment (2)

Rtot=sum of the two scenario is dominated at low PGA by the small but frequent events and for high pga by the strong but rare events

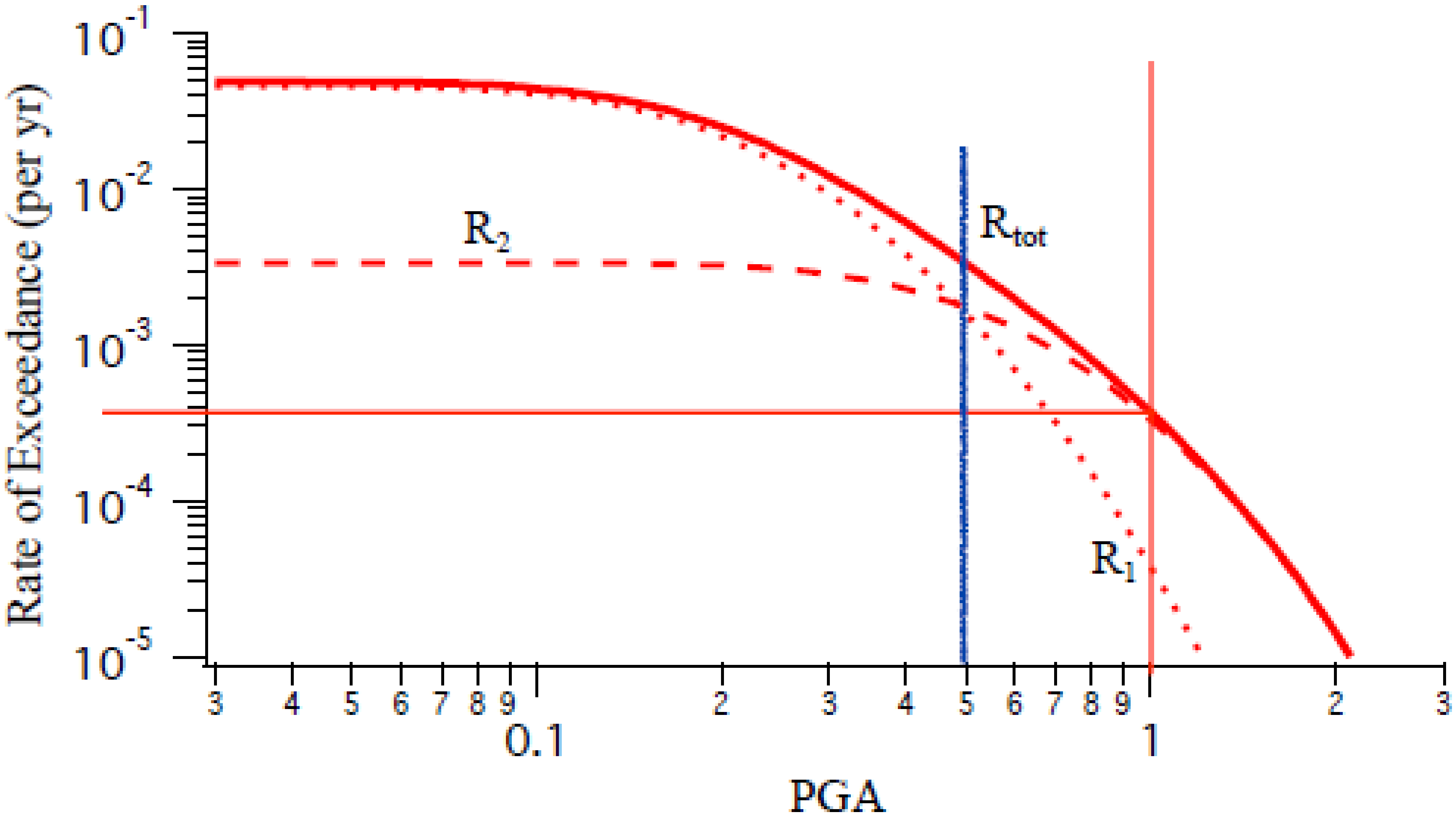

Modified from Probabilistic Seismic Hazard Analysis (PSHA)
A Primer Written by Edward (Ned) H. Field

Basic of Probabilistic Seismic Hazard Assessment (2)

$$P_{pois}(> \ln PGA, T) = 1 - e^{-R_{tot}T}$$

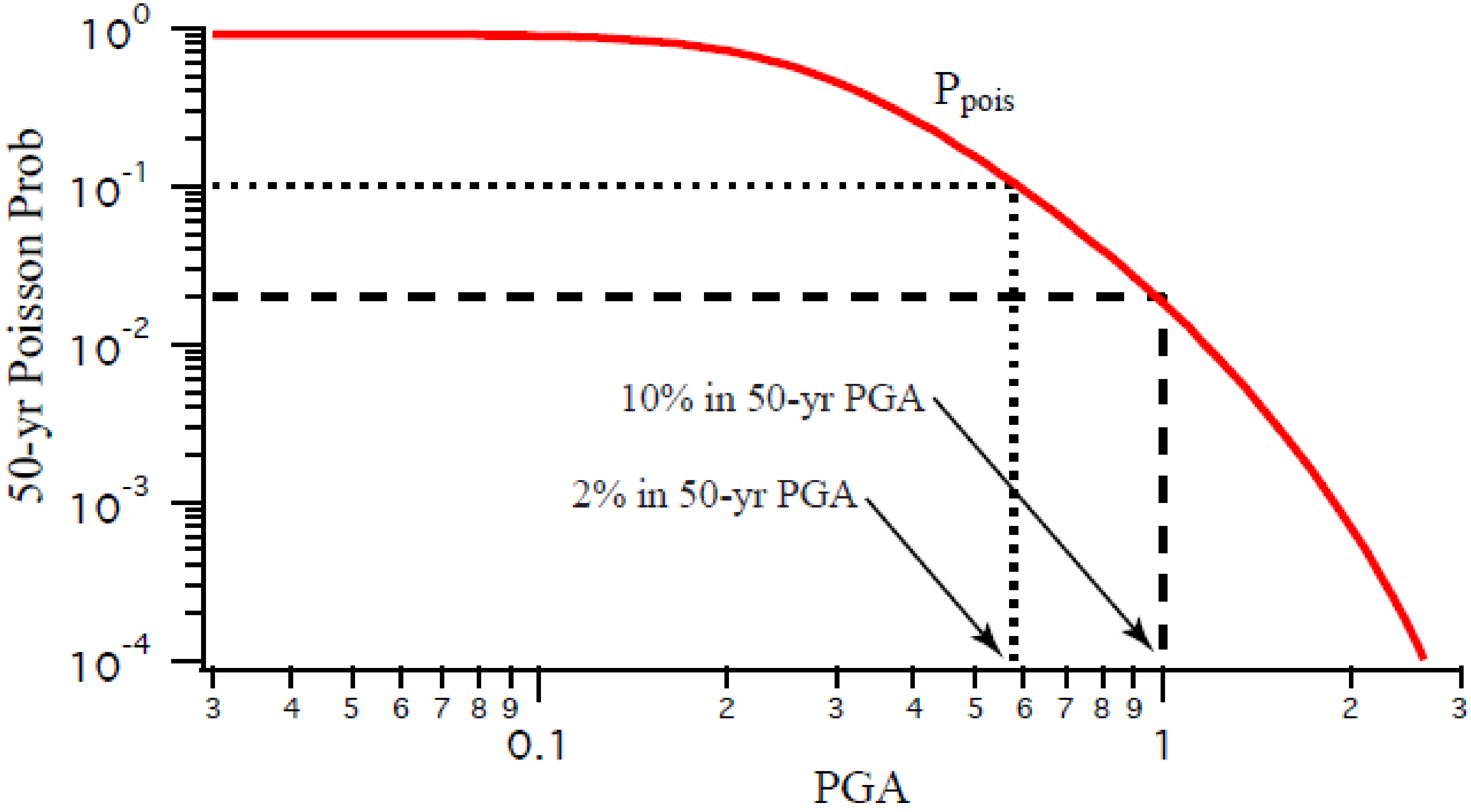

Extending this analysis for several sites we obtain the seismic hazard maps

Modified from Probabilistic Seismic Hazard Analysis (PSHA)
A Primer Written by Edward (Ned) H. Field

Italian building code (NTC08/18)

- Seismic classification

  https://rischi.protezionecivile.gov.it/it/sismico/attivita/classificazione-sismica

- Seismic hazard

  http://esse1.mi.ingv.it

- NTC08 Seismic code (§ 2.*; 3.2; 7.*)

  https://www.gazzettaufficiale.it/eli/id/2008/02/04/08A00368/sg

- NTC18 Seismic code (§ 2.*; 3.2; 7.*)

  https://www.gazzettaufficiale.it/eli/gu/2018/02/20/42/so/8/sg/pdf

  https://www.gazzettaufficiale.it/eli/id/2019/02/11/19A00855/sg

Italian code NTC18 - Seismic Action

L'azione sismica è caratterizzata da 3 componenti traslazionali, due orizzontali contrassegnate da X ed Y ed una verticale contrassegnata da Z, da considerare tra di loro indipendenti. Le componenti possono essere descritte, in funzione del tipo di analisi adottata, mediante una delle seguenti rappresentazioni:

- accelerazione massima in superficie;

- accelerazione massima e relativo spettro di risposta in superficie;

- storia temporale del moto del terreno.

Le due componenti ortogonali indipendenti che descrivono il moto orizzontale sono caratterizzate dallo stesso spettro di risposta o dalle due componenti accelerometriche orizzontali del moto sismico.

Italian code NTC18 - Elastic spectra

Lo spettro di risposta elastico in accelerazione è espresso da una forma spettrale (spettro normalizzato) riferita ad uno smorzamento convenzionale del 5%, moltiplicata per il valore della accelerazione orizzontale massima a_g su sito di riferimento rigido orizzontale.

Sia la forma spettrale che il valore di a_g variano al variare della probabilità di superamento nel periodo di riferimento P_{VR} (vedi § 2.4 e § 3.2.1).

Gli spettri così definiti possono essere utilizzati per strutture con periodo fondamentale minore o uguale a 4,0 s. Per strutture con periodi fondamentali superiori lo spettro deve essere definito da apposite analisi oppure l'azione sismica deve essere descritta mediante storie temporali del moto del terreno.

Italian code NTC18 - Elastic spectra

Lo spettro di risposta (componente orizzontale) è definito a partire dai valori dei seguenti parametri, validi per sito di riferimento su suolo rigido:

- a_g accelerazione orizzontale massima al sito
- F_0 è il fattore che quantifica l'amplificazione spettrale massima, su sito di riferimento rigido orizzontale, ed ha valore minimo pari a 2,2
- T_C^* (valore di riferimento per la determinazione del) periodo di inizio del tratto a velocità costante dello spettro in accelerazione orizzontale.

  Viene quindi definito: $T_C = C_C\, T_C^*$

  dove C_C dipende dalla categoria del sottosuolo

I valori di tali parametri sono forniti dalla NTC18, per tutti i siti considerati, in forma tabellare. Per la pericolosità in particolare (a_g):http://esse1.mi.ingv.it

Italian code NTC18 - Elastic spectra

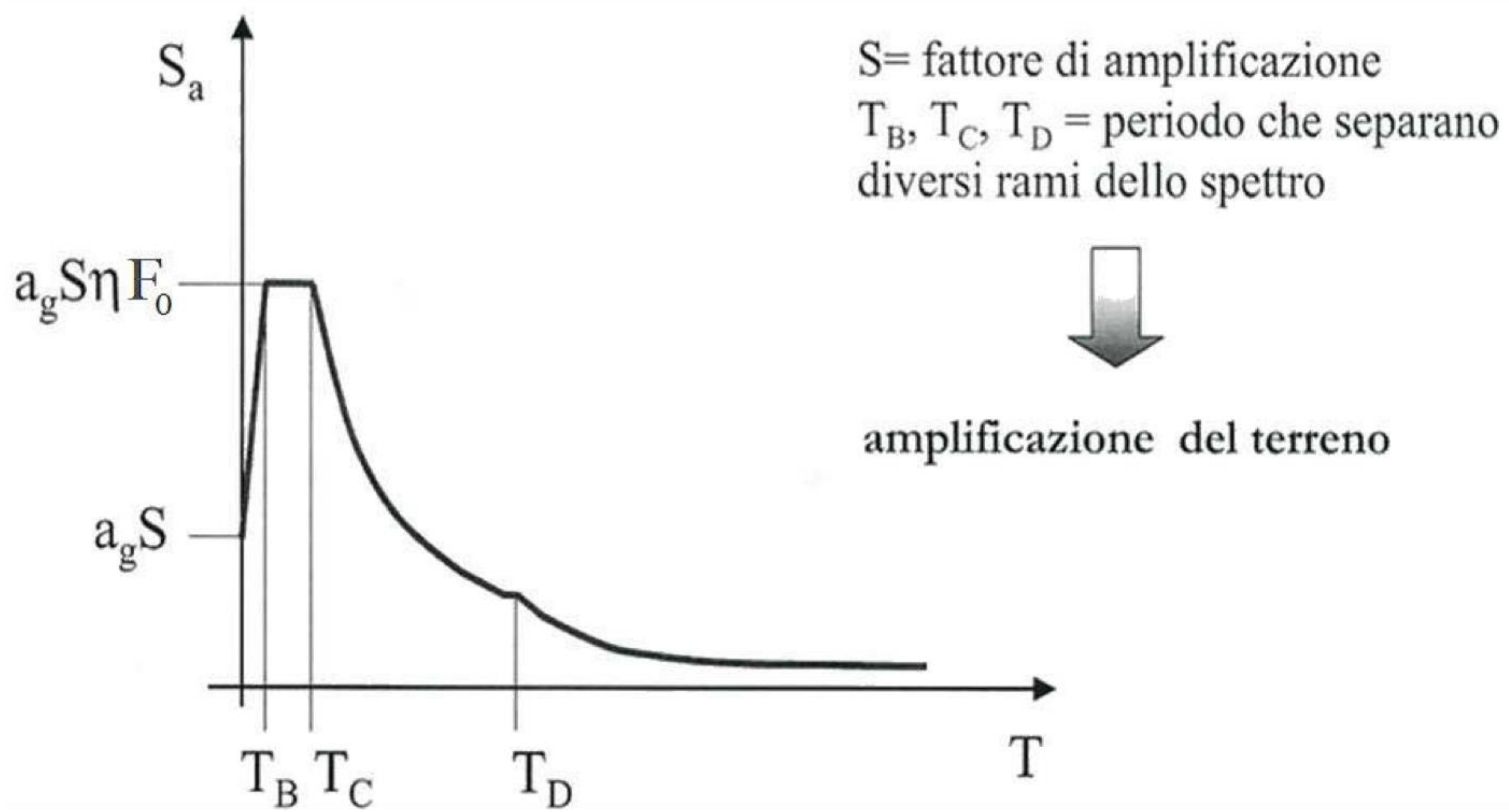

$$S_e(T) = a_g \cdot S \cdot \eta \cdot F_0 \cdot \left[\frac{T}{T_B} + \frac{1}{\eta \cdot F_0} \cdot \left(1 - \frac{T}{T_B}\right)\right]$$

$$S_e(T) = a_g \cdot S \cdot \eta \cdot F_0 \cdot \left(\frac{T_C}{T}\right)$$

$$S_e(T) = a_g \cdot S \cdot \eta \cdot F_0$$

$$S_e(T) = a_g \cdot S \cdot \eta \cdot F_0 \cdot \left(\frac{T_C \cdot T_D}{T^2}\right)$$

- T_B è il periodo corrispondente all'inizio del tratto dello spettro ad accelerazione costante, $T_B = T_C/3$; T_D è il periodo corrispondente all'inizio del tratto a spostamento costante dello spettro, espresso in secondi mediante la relazione: $T_D = 4.0 * a_g/g + 1.6$
- η è il fattore che altera lo spettro elastico per coefficienti di smorzamento viscosi convenzionali ξ diversi dal 5%, ($\eta = [10/(5+\xi)]^{0.5} \geq 0,55$), e valutato sulla base di materiali, tipologia strutturale e terreno di fondazione

Italian code NTC18 - from hazard to “design”

- Per ciascun nodo del reticolo di riferimento e per ciascuno dei periodi di ritorno T_R considerati dalla pericolosità sismica, i tre parametri si ricavano riferendosi ai valori corrispondenti al 50–esimo percentile ed attribuendo a F_0 e T_C^* i valori ottenuti imponendo che...

- le forme spettrali in accelerazione, velocità e spostamento previste dalle NTC scartino al minimo dalle corrispondenti forme spettrali previste dalla pericolosità sismica (la condizione di minimo è imposta operando ai minimi quadrati, su spettri di risposta normalizzati ad uno, per ciascun sito e ciascun periodo di ritorno).

Site effects and NTC18 - Elastic spectra & soil

S è il coefficiente che tiene conto della categoria di sottosuolo e delle condizioni topografiche mediante la relazione: $S = S_S \cdot S_T$

S_S è il coefficiente di amplificazione stratigrafica
S_T è il coefficiente di amplificazione topografica

Tab. 3.2.V – *Valori massimi del coefficiente di amplificazione topografica S_T*

Categoria topografica	Ubicazione dell'opera o dell'intervento	S_T
T1	-	1,0
T2	In corrispondenza della sommità del pendio	1,2
T3	In corrispondenza della cresta di un rilievo con pendenza media minore o uguale a 30°	1,2
T4	In corrispondenza della cresta di un rilievo con pendenza media maggiore di 30°	1,4

Tab. 3.2.IV – *Espressioni di S_S e di C_C*

Categoria sottosuolo	S_S	C_C
A	1,00	1,00
B	$1{,}00 \le 1{,}40 - 0{,}40 \cdot F_o \cdot \frac{a_g}{g} \le 1{,}20$	$1{,}10 \cdot (T_C^*)^{-0{,}20}$
C	$1{,}00 \le 1{,}70 - 0{,}60 \cdot F_o \cdot \frac{a_g}{g} \le 1{,}50$	$1{,}05 \cdot (T_C^*)^{-0{,}33}$
D	$0{,}90 \le 2{,}40 - 1{,}50 \cdot F_o \cdot \frac{a_g}{g} \le 1{,}80$	$1{,}25 \cdot (T_C^*)^{-0{,}50}$
E	$1{,}00 \le 2{,}00 - 1{,}10 \cdot F_o \cdot \frac{a_g}{g} \le 1{,}60$	$1{,}15 \cdot (T_C^*)^{-0{,}40}$

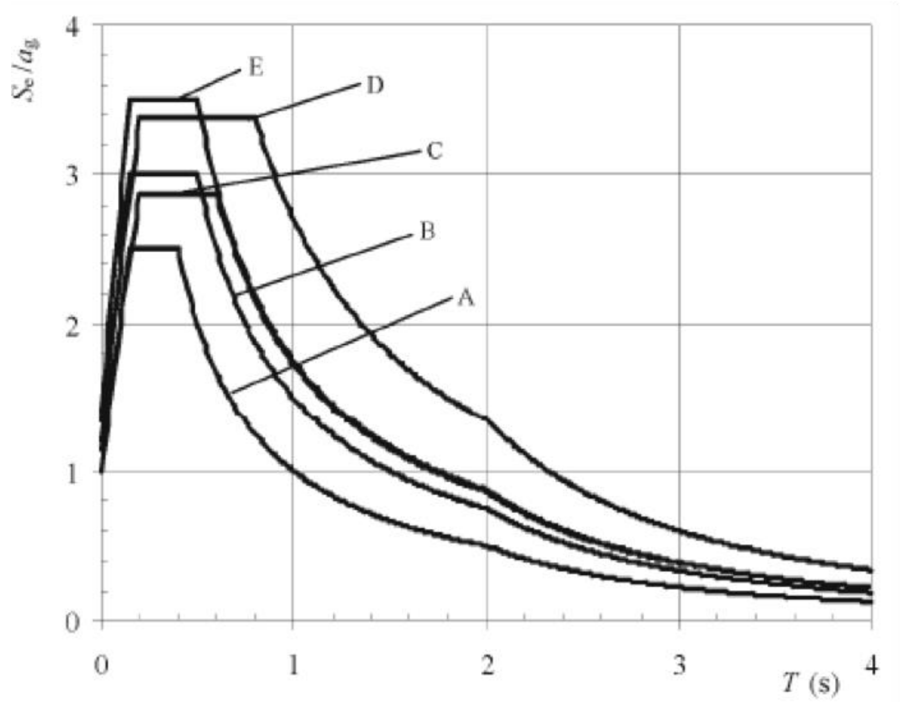

Site effects and NTC18 - Soil classification

3.2.2 CATEGORIE DI SOTTOSUOLO E CONDIZIONI TOPOGRAFICHE

Categorie di sottosuolo

Ai fini della definizione dell'azione sismica di progetto, l'effetto della risposta sismica locale si valuta mediante specifiche analisi, da eseguire con le modalità indicate nel § 7.11.3. In alternativa, qualora le condizioni stratigrafiche e le proprietà dei terreni siano chiaramente riconducibili alle categorie definite nella Tab. 3.2.II, si può fare riferimento a un approccio semplificato che si basa sulla classificazione del sottosuolo in funzione dei valori della velocità di propagazione delle onde di taglio, V_S. I valori dei parametri meccanici necessari per le analisi di risposta sismica locale o delle velocità V_S per l'approccio semplificato costituiscono parte integrante della caratterizzazione geotecnica dei terreni compresi nel volume significativo, di cui al § 6.2.2.

Tab. 3.2.II – *Categorie di sottosuolo che permettono l'utilizzo dell'approccio semplificato.*

Categoria	Caratteristiche della superficie topografica
A	*Ammassi rocciosi affioranti o terreni molto rigidi* caratterizzati da valori di velocità delle onde di taglio superiori a 800 m/s, eventualmente comprendenti in superficie terreni di caratteristiche meccaniche più scadenti con spessore massimo pari a 3 m.
B	*Rocce tenere e depositi di terreni a grana grossa molto addensati o terreni a grana fina molto consistenti*, caratterizzati da un miglioramento delle proprietà meccaniche con la profondità e da valori di velocità equivalente compresi tra 360 m/s e 800 m/s.
C	*Depositi di terreni a grana grossa mediamente addensati o terreni a grana fina mediamente consistenti* con profondità del substrato superiori a 30 m, caratterizzati da un miglioramento delle proprietà meccaniche con la profondità e da valori di velocità equivalente compresi tra 180 m/s e 360 m/s.
D	*Depositi di terreni a grana grossa scarsamente addensati o di terreni a grana fina scarsamente consistenti*, con profondità del substrato superiori a 30 m, caratterizzati da un miglioramento delle proprietà meccaniche con la profondità e da valori di velocità equivalente compresi tra 100 e 180 m/s.
E	*Terreni con caratteristiche e valori di velocità equivalente riconducibili a quelle definite per le categorie C o D*, con profondità del substrato non superiore a 30 m.

Site effects and NTC18 - $V_{S,eq}$

La classificazione del sottosuolo si effettua in base alle condizioni stratigrafiche ed ai valori della velocità equivalente di propagazione delle onde di taglio, $V_{S,eq}$ (in m/s), definita dall'espressione:

$$V_{S,eq} = \frac{H}{\sum_{i=1,N} \frac{h_i}{V_{S,i}}} \quad [m/s]$$

con h_i spessore dell'i-esimo strato; $V_{S,i}$ velocità delle onde di taglio nell'i-esimo strato; N numero di strati; H profondità del substrato, definito come quella formazione costituita da roccia o terreno molto rigido, caratterizzata da V_S non inferiore a 800 m/s.

Per depositi con profondità H del substrato superiore a 30 m, la velocità equivalente delle onde di taglio $V_{S,eq}$ è definita dal parametro $V_{S,30}$, ottenuto ponendo H=30 m nella precedente espressione e considerando le proprietà degli strati di terreno fino a tale profondità.

V_{S30}

Nelle definizioni precedenti V_{S30} è la velocità media di propagazione dei primi 30 m di profondità delle onde di taglio e viene calcolata con la seguente espressione:

$$V_{S30} = \frac{30}{\sum_{i=1,N} \frac{h_i}{V_i}} \quad [m/s]$$

dove h_i e V_i indicano lo spessore (in m) e la velocità delle onde di taglio (per deformazioni di taglio $\gamma < 10^{-6}$) dello strato i-esimo, per un totale di N strati presenti nei 30 m superiori.

Site effects and NTC18 - Topography

Per condizioni topografiche complesse è necessario predisporre specifiche analisi di risposta sismica locale. Per configurazioni superficiali semplici si può adottare la seguente classificazione (Tab. 3.2.III):

T1 Superficie pianeggiante, pendii e rilievi isolati con inclinazione media i≤15°

T2 Pendii con inclinazione media i>15°

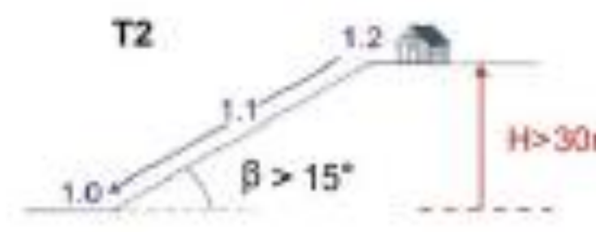

T3 Rilievi con larghezza in cresta molto minore che alla base e inclinazione media 15≤i≤30°

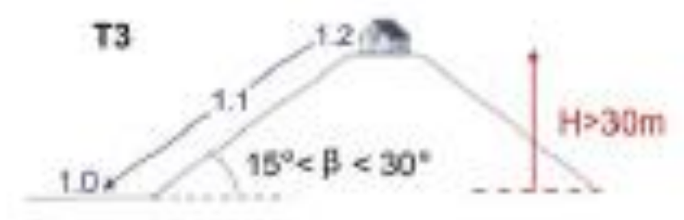

T4 Rilievi con larghezza in cresta molto minore che alla base e inclinazione media i>30°

Le su esposte categorie topografiche si riferiscono a configurazioni geometriche prevalentemente bidimensionali, creste o dorsali allungate, e devono essere considerate nella definizione dell'azione sismica se di altezza maggiore di 30 m.

Site effects and NTC18 - Topography

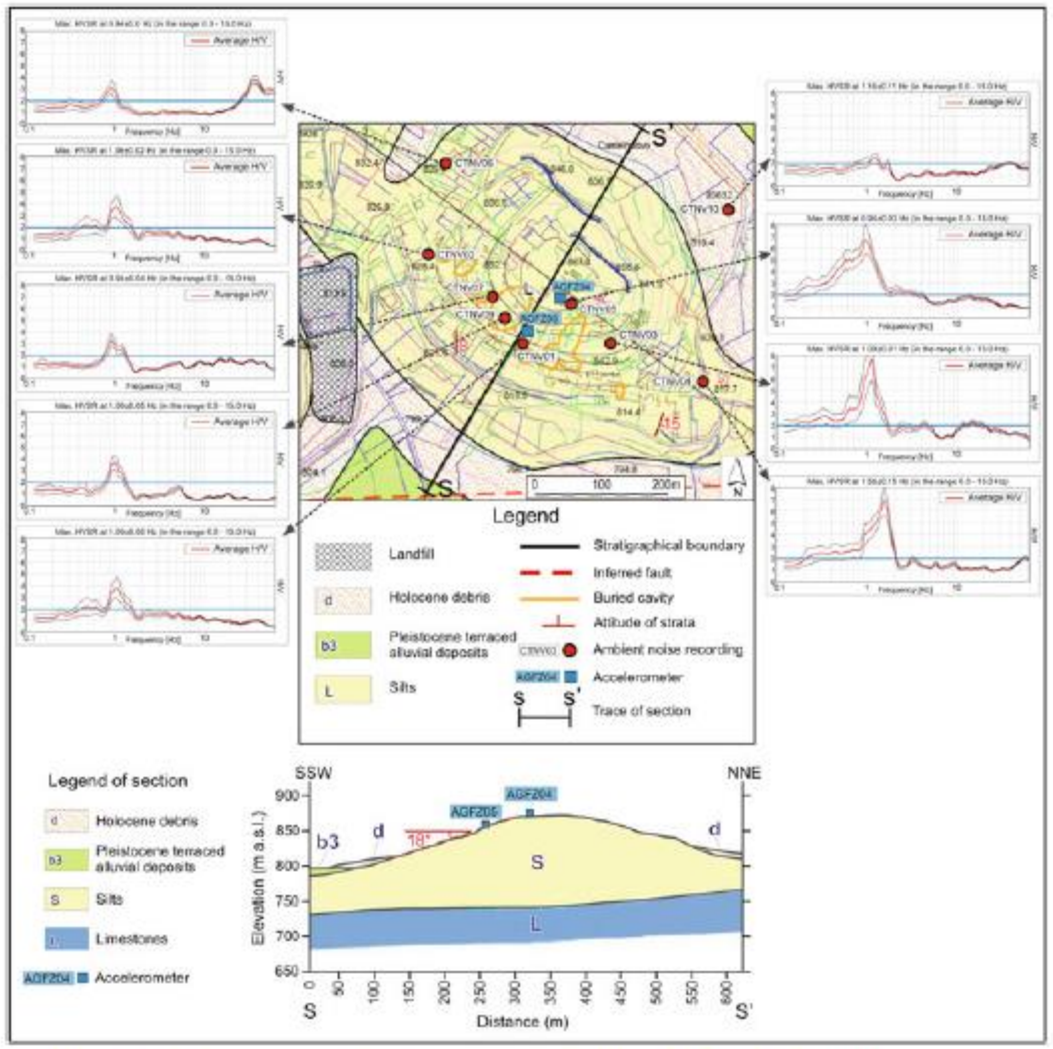

Fig. 2 Geological map and section for Castelnuovo (modified from Gallipoli et al. 2011)

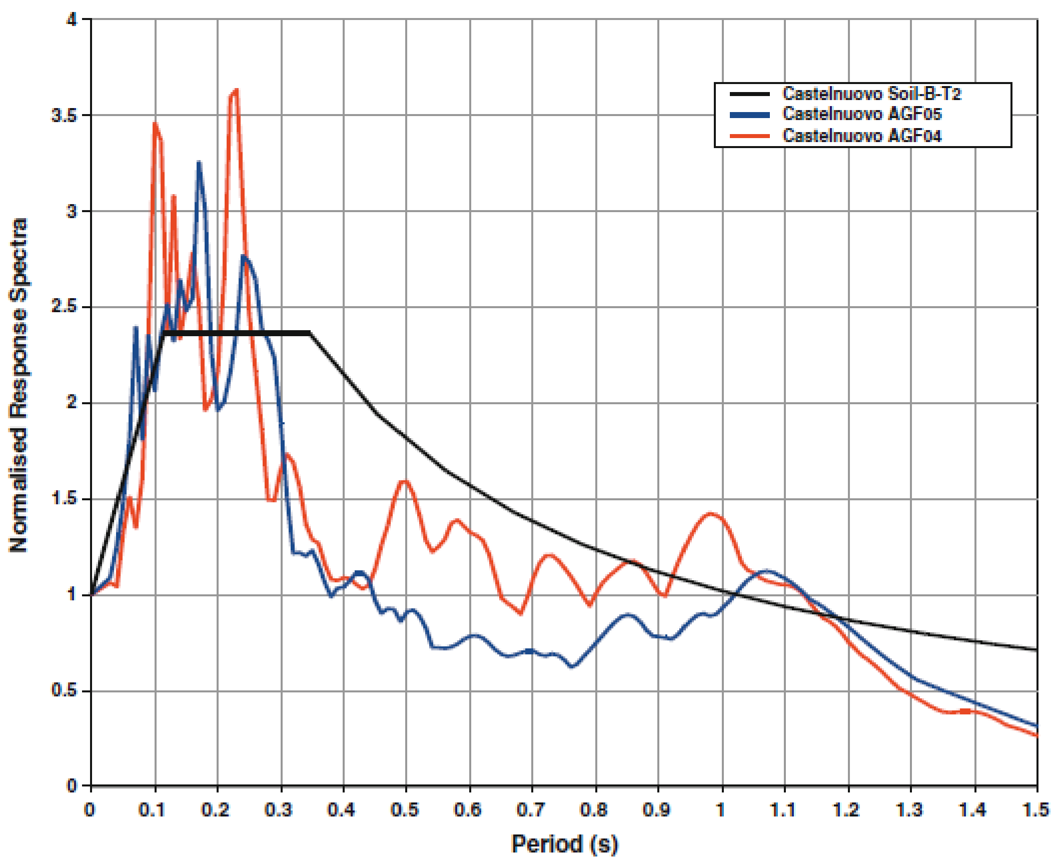

Fig. 5 Normalised Response spectra of the M 5.1 event of April 9, 2009 recorded at two sites in Castelnuovo compared with code provision

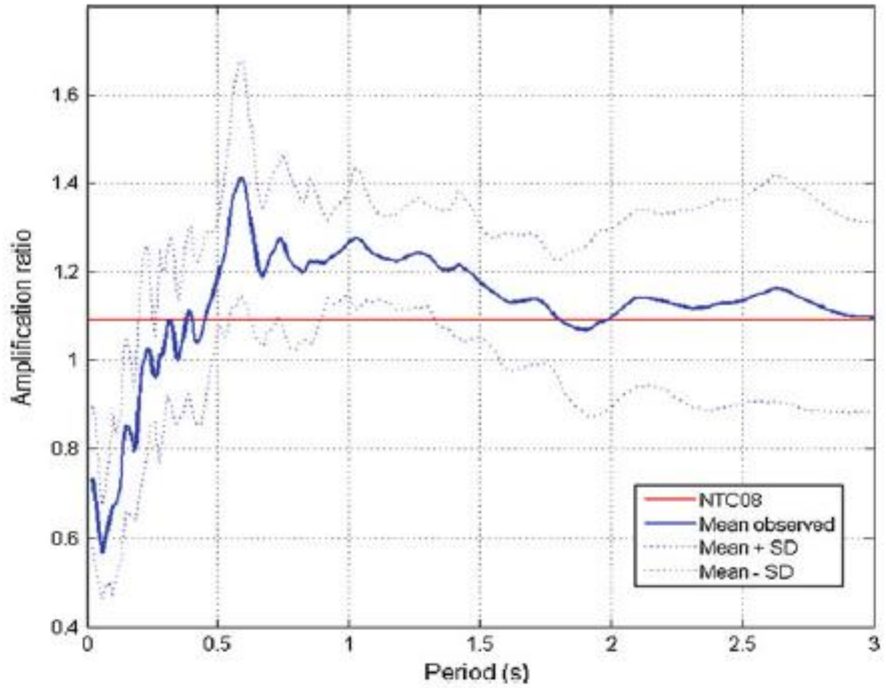

Fig. 6 Comparison between code provisions ratio (*red*) and observed amplification ratio (*blue*) in Castelnuovo

Site effects and NTC18 - Topography

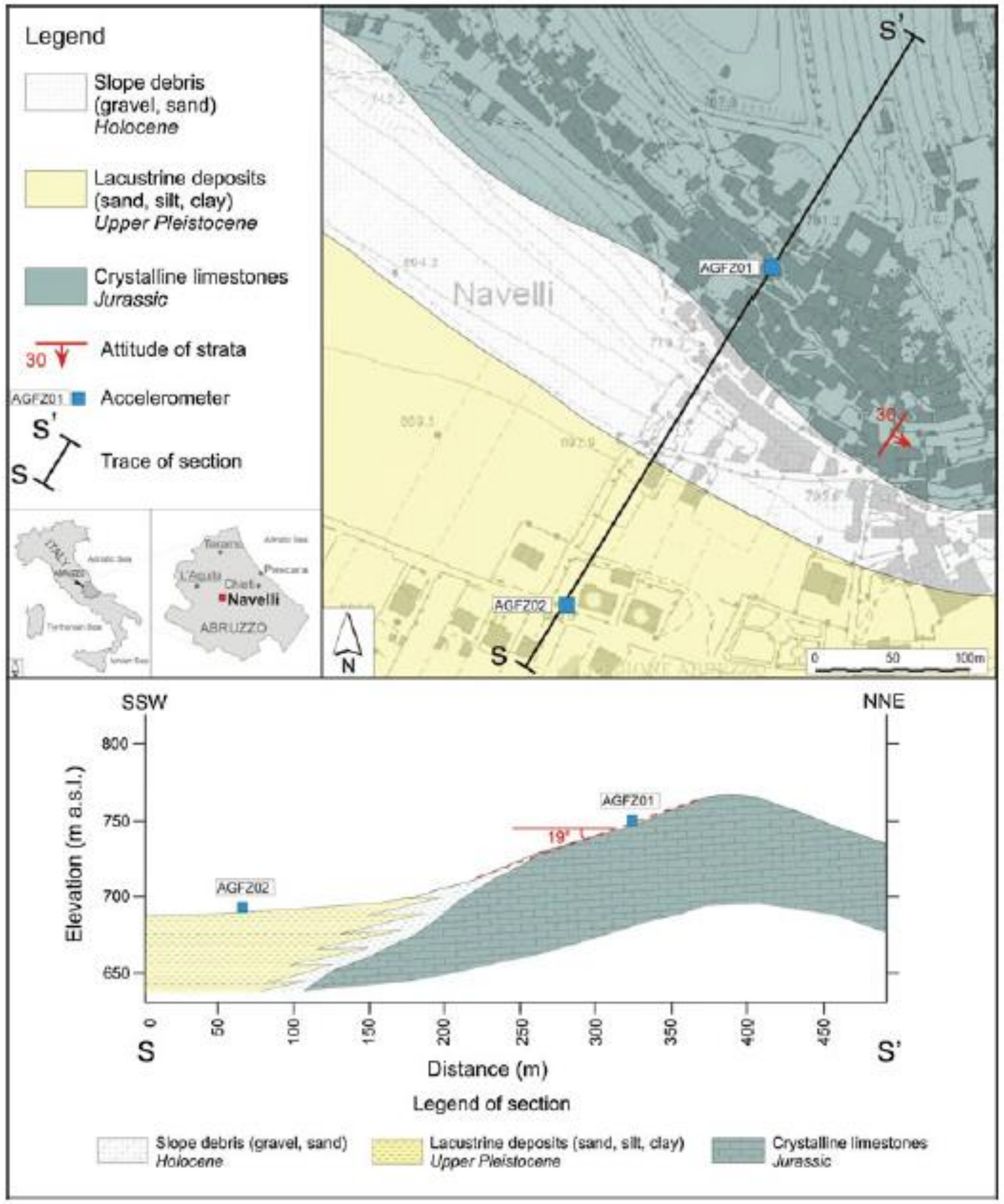

Fig. 7 Geological map and section for Navelli

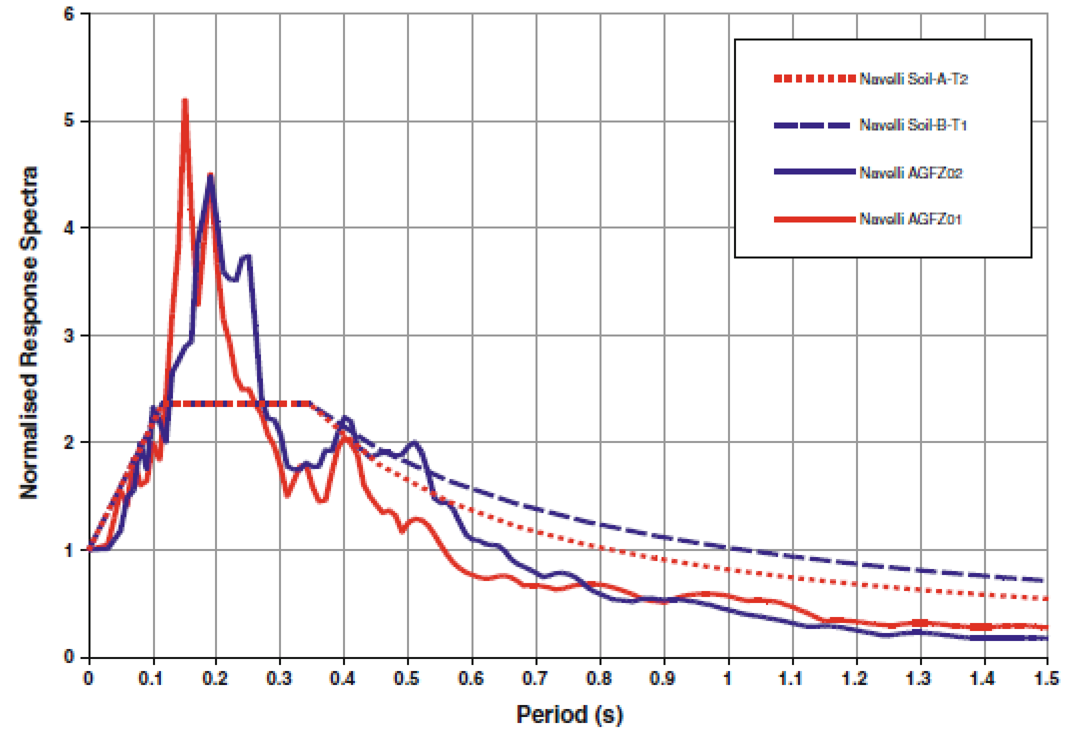

Fig. 10 Normalised Response spectra of the M 5.1 event of April 9, 2009 recorded at two sites in Navelli compared with code provision

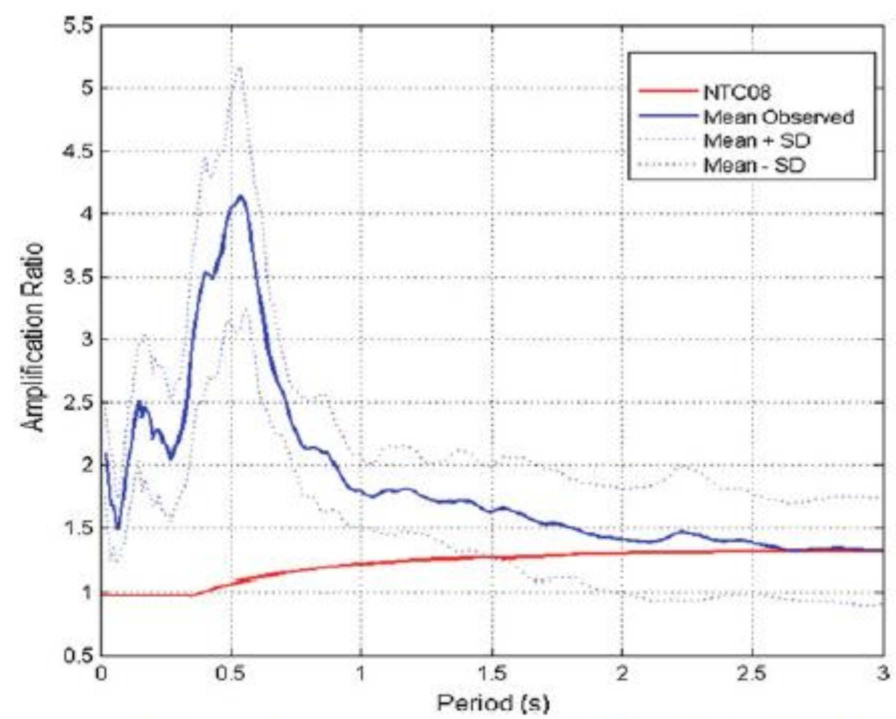

Fig. 11 Comparison between code provisions (*red*) and observed amplification ratio (*blue*) in Navelli

NTC18 - Time histories (3.2)

Gli stati limite, ultimi e di esercizio, possono essere verificati mediante l'uso di storie temporali del moto del terreno artificiali o naturali...
L'uso di storie temporali del moto del terreno artificiali non è ammesso nelle analisi dinamiche di opere e sistemi geotecnici.

L'uso di storie temporali del moto del terreno generate mediante simulazione del meccanismo di sorgente e della propagazione è ammesso a condizione che siano adeguatamente giustificate le ipotesi relative alle caratteristiche sismogenetiche della sorgente e del mezzo di propagazione e che, negli intervalli di periodo sopraindicati, l'ordinata spettrale media non presenti uno scarto in difetto superiore al 20% rispetto alla corrispondente componente dello spettro elastico.

L'uso di storie temporali del moto del terreno naturali o registrate è ammesso a condizione che la loro scelta sia rappresentativa della sismicità del sito e sia adeguatamente giustificata in base alle caratteristiche sismogenetiche della sorgente, alle condizioni del sito di registrazione, alla magnitudo, alla distanza dalla sorgente e alla massima accelerazione orizzontale attesa al sito.

NTC18 - Space variability (3.2.4.1)

Nei punti di contatto con il terreno di opere con sviluppo planimetrico significativo, il moto sismico può avere caratteristiche differenti, a causa del carattere asincrono del fenomeno di propagazione, delle disomogeneità e delle discontinuità eventualmente presenti, e della diversa risposta locale del terreno.

Degli effetti sopra indicati deve tenersi conto quando essi possono essere significativi e in ogni caso quando le condizioni di sottosuolo siano così variabili lungo lo sviluppo dell’opera da richiedere l’uso di accelerogrammi o di spettri di risposta diversi.

NTC18 - Local response (7.11.3)

Il moto generato da un terremoto in un sito dipende dalle particolari condizioni locali, cioè dalle caratteristiche topografiche e stratigrafiche del sottosuolo e dalle proprietà fisiche e meccaniche dei terreni e degli ammassi rocciosi di cui è costituito. Alla scala della singola opera o del singolo sistema geotecnico, l'analisi della risposta sismica locale consente quindi di definire le modifiche che il segnale sismico di ingresso subisce, a causa dei suddetti fattori locali.

...

Nelle analisi di risposta sismica locale, l'azione sismica di ingresso è descritta in termini di storia temporale dell'accelerazione (accelerogrammi) su di un sito di riferimento rigido ed affiorante con superficie topografica orizzontale.

L'applicazione del metodo richiede la valutazione dell'accelerazione critica, che deve essere valutata con i valori caratteristici dei parametri di resistenza, e dell'azione sismica di progetto, che deve essere rappresentata mediante storie temporali delle accelerazioni. Gli accelerogrammi impiegati nelle analisi, in numero non inferiore a 7, devono essere rappresentativi della sismicità del sito e la loro scelta deve essere adeguatamente giustificata (vedi § 3.2.3.6). Non è ammesso l'impiego di accelerogrammi artificiali.

SURFACE TOPOGRAPHY EFFECTS

(convexity) sensitivity to:
a) type of wavefield
b) angle of incidence
c) shape and sharpness

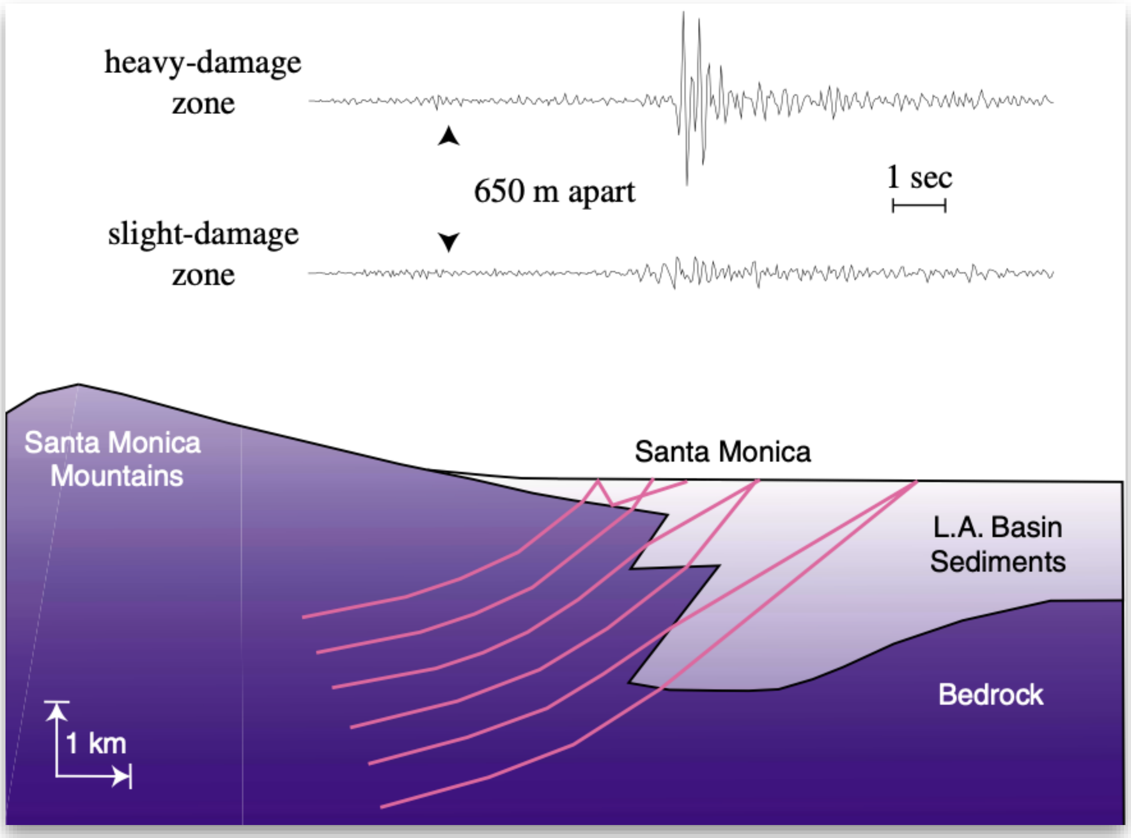

GROUNDSHAKING SITE EFFECTS

SOFT SURFACE LAYERING

a) 1-D: trapping of waves for impedance contrast; vertical resonances

$$f_n=[(2n+1)\beta]/4H; \quad A\approx(\rho_2 v_2)/(\rho_1 v_1)$$

b) 2-D, 3-D: complex energy focusing; diffraction effects; basin edge waves

Effetti di sito 1D

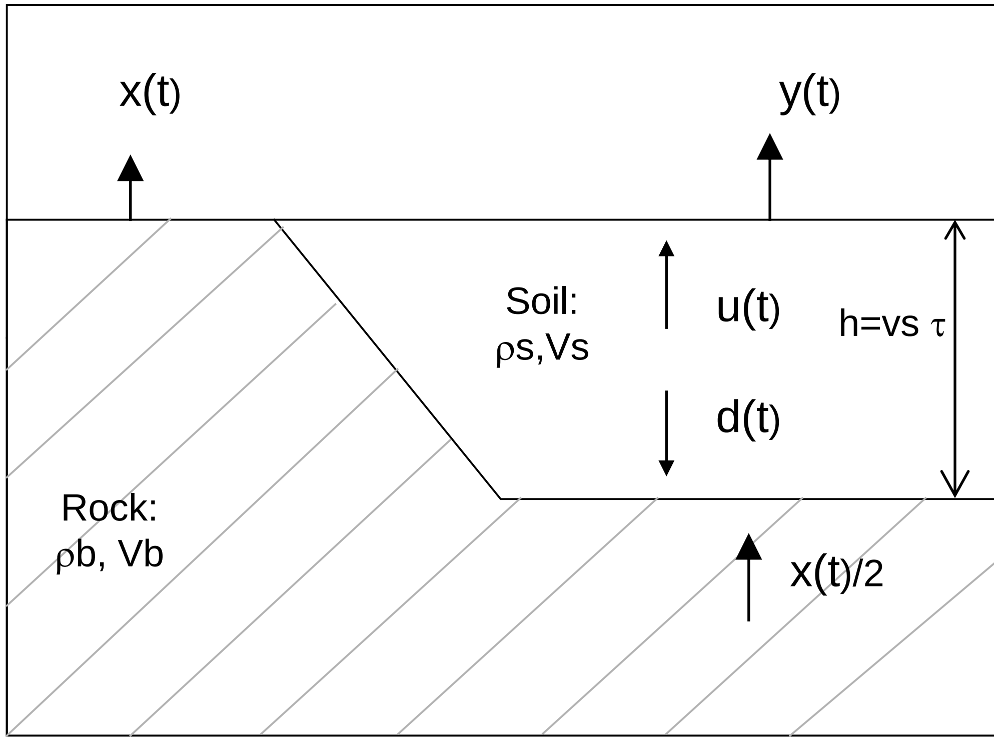

$$|H(f)| = \left(\frac{(1+r)^2}{1+2r\cos(4\pi f \tau)+r^2} \right)^{1/2}$$

$$r = \frac{p_b V_b - p_s V_s}{p_b V_b + p_s V_s} = \frac{c-1}{1+c}$$

$\tau = h/V_s$

$f_o = 400/(4*100) = 1Hz$

$C = \left(\frac{2800*1200}{2600*400} \right) \sim 3.23$

$|H(f)|$ Massimo per $f=f_o$
Tale che $\cos(4\pi f\tau)=-1$

$$f_o = \frac{1}{4\tau} = \frac{V_s}{4h}$$

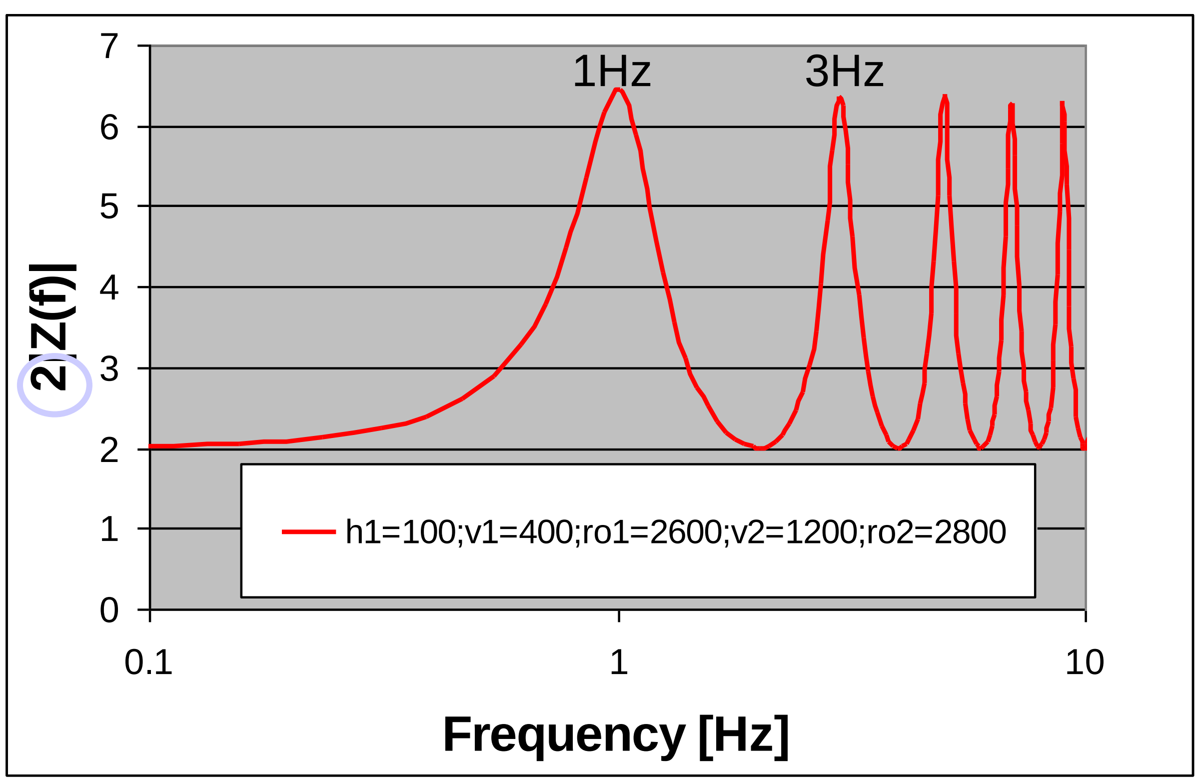

Esistono diversi massimi a frequenze:

$$f_n = \frac{V_s}{4h}(2n+1) \quad \text{with } n = 0,1,2,3,\ldots$$

(n=0 modo fondamentale
n>0 modi superiori)

UNIVERSITÀ DEGLI STUDI DI TRIESTE

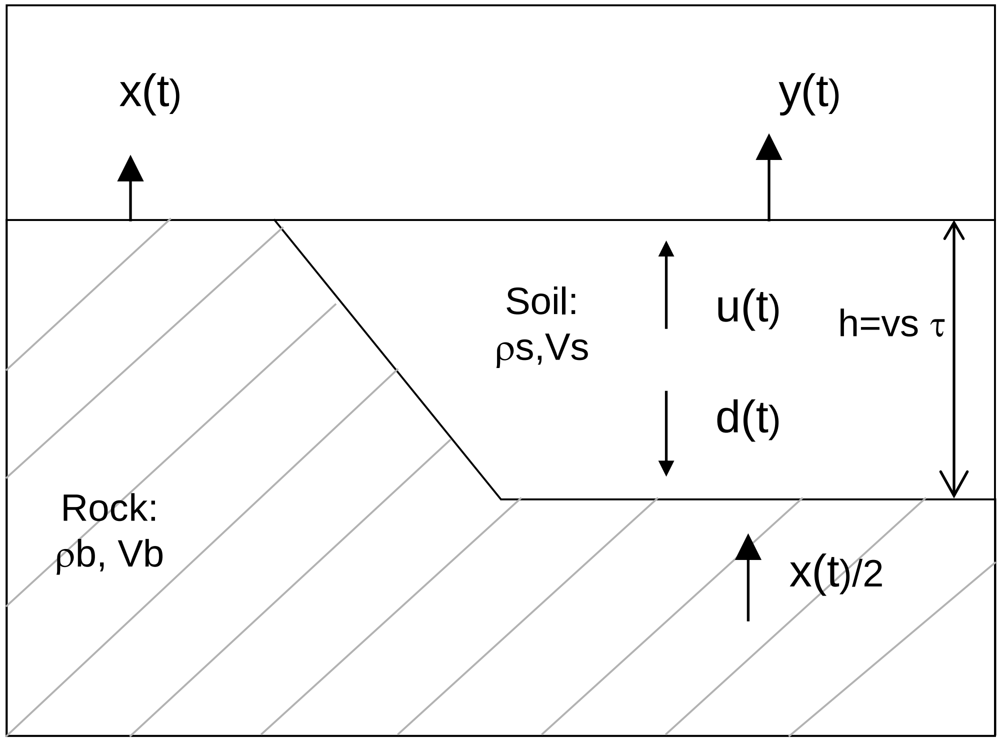

$$|H(f)| = \left(\frac{(1+r)^2}{1+2r\cos(4\pi f t)+r^2} \right)^{1/2}$$

Per f=f_n $|H(f)|$ diventa

$$|H(f_n)| = \left(\frac{(1+r)^2}{1-2r+r^2} \right)^{1/2} = \frac{1+r}{1-r} = c$$

f_o=400/(4*100)=1Hz

$C = \left(\frac{2800*1200}{2600*400} \right) \sim 3.23$

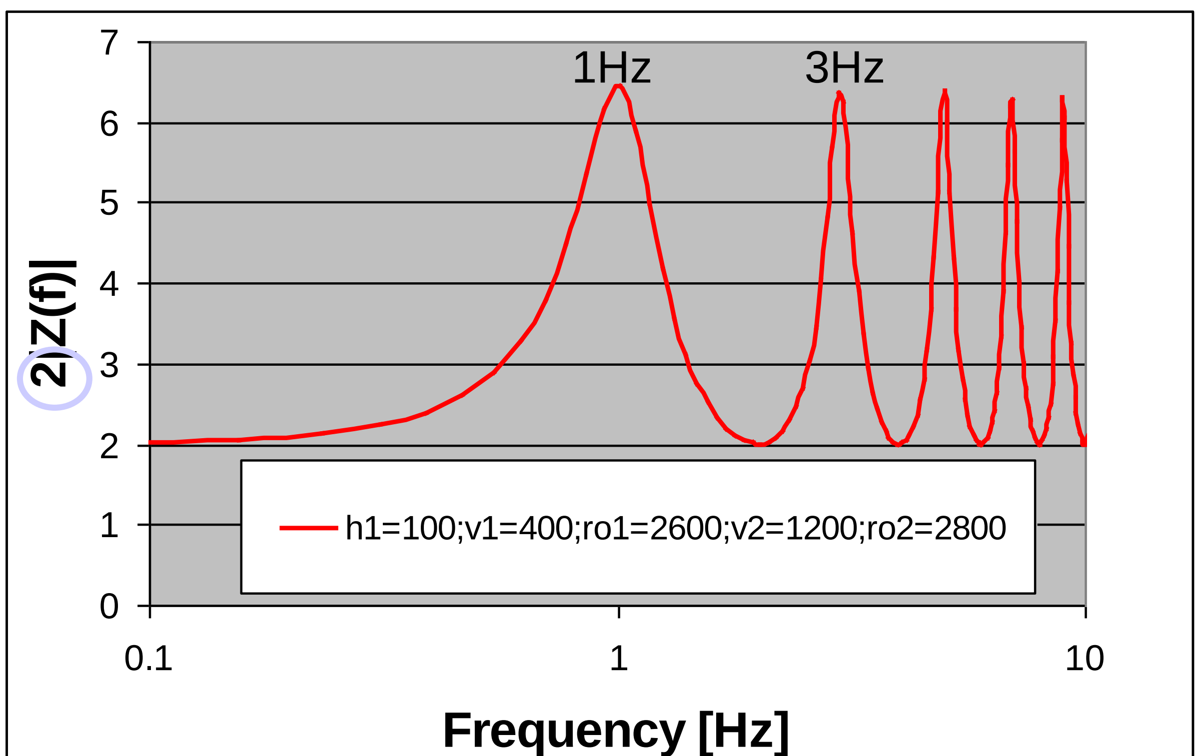

Il contrasto di impedenza determina l'ampiezza del picco (modello elastic)

1D site effects

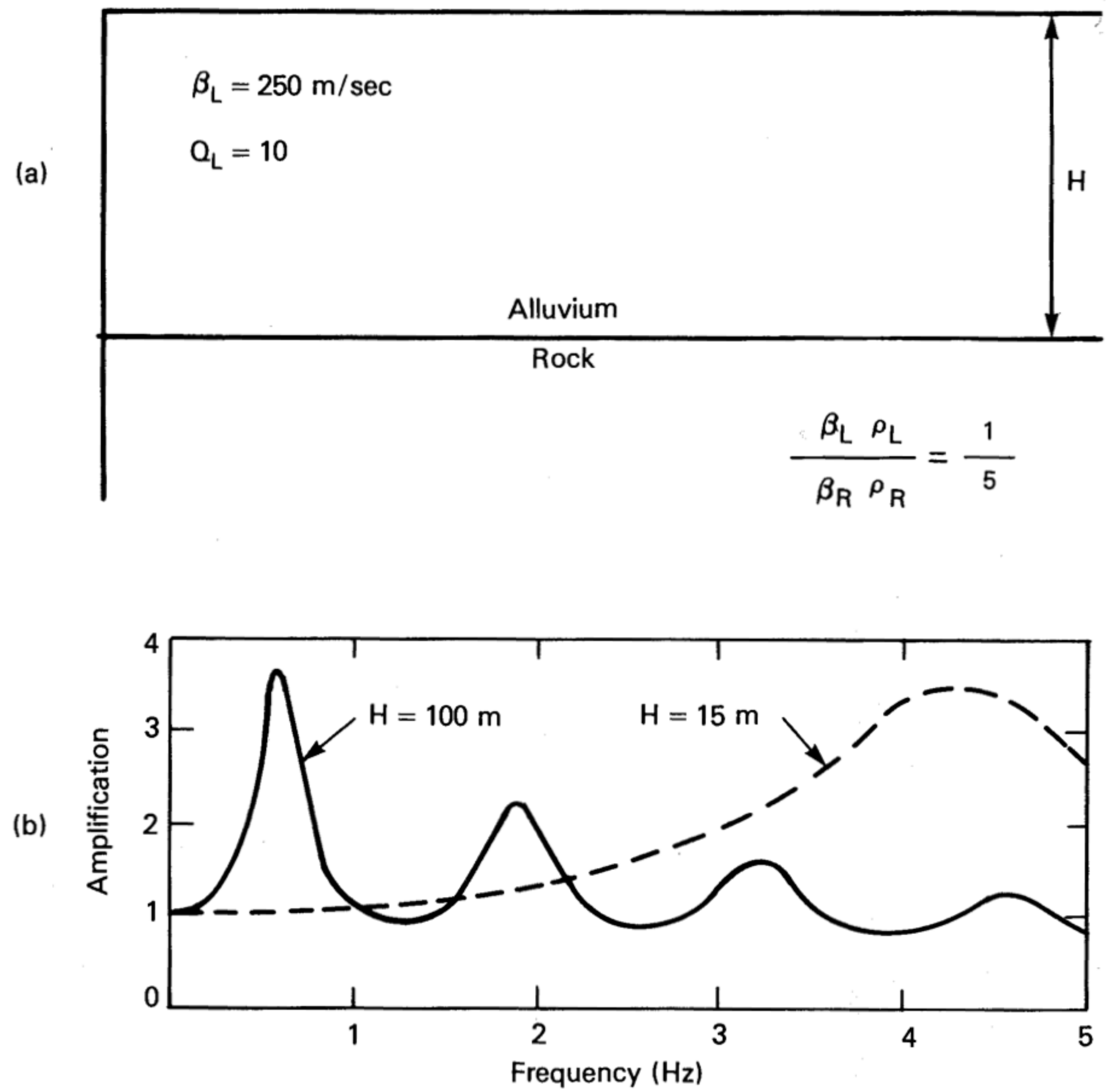

FIGURE 8.2 Model of site amplification. (a) Crossection of alluvial layer of thickness H overlying rock. Impedance of rock is five times impedance of alluvium. (b) Amplification factors in the frequency domain for two thicknesses of alluvium (after Murphy and O'Brien 1978).

$$|U_L(\omega)| = 2.0\left[\cos^2(k_L H) + \left(\frac{\rho_L v_L}{\rho_H v_H}\right)\sin^2(k_L H)^2\right]^{-1/2}$$

Site effect estimation

1) <u>Direct methods</u>:

Earthquake based:

<u>With reference site</u>: Standard Spectral Ratio (SSR), Generalised Inversion Technique (GIT),

<u>Without a reference site</u>: Horizontal-to-Vertical Spectral Ratio (H/V)

Seismic noise based:

<u>With reference site</u>: Standard Spectral Ratio (SSR), Spectra analysis,

<u>Without a reference site</u>: Horizontal-to-Vertical Spectral Ratio (H/V)

2) *<u>Indirect methods</u>*: active (SASW, MASW) and passive (seismic noise) array analysis. Numerical simulations

WEAK (AND STRONG) MOTION

EMPIRICAL TECHNIQUES FOR SITE EFFECT ESTIMATION

a) S/B spectral ratio (Borcherdt, 1970)

b) generalized inversion scheme (Andrews, 1986)

c) coda waves analysis (Margheriti et al., 1994)

d) parametrized source and path inversion (Boatwright et al., 1991)

e) H/V spectral ratio (receiver function) (Lermo et al., 1993)

$$R_{ij}(\omega) = E_i(\omega) \cdot P_{ij}(\omega) \cdot S_j(\omega)$$

MICROTREMORS

a) peak frequencies examination

b) S/B spectral ratio

c) H/V spectral ratio (Nagoshi, 1971; Nakamura, 1989)

d) array analysis (Malagnini et al., 1993)

Earthquake based Reference Site methods

1) *Standard spectral ratio*: spectral ratio between the same ground motion components of 2 close stations

2) *Generalized inversion techniques*: a spectral inversion is performed in order to correct for the path effects if the reference station is faraway from the actual one.

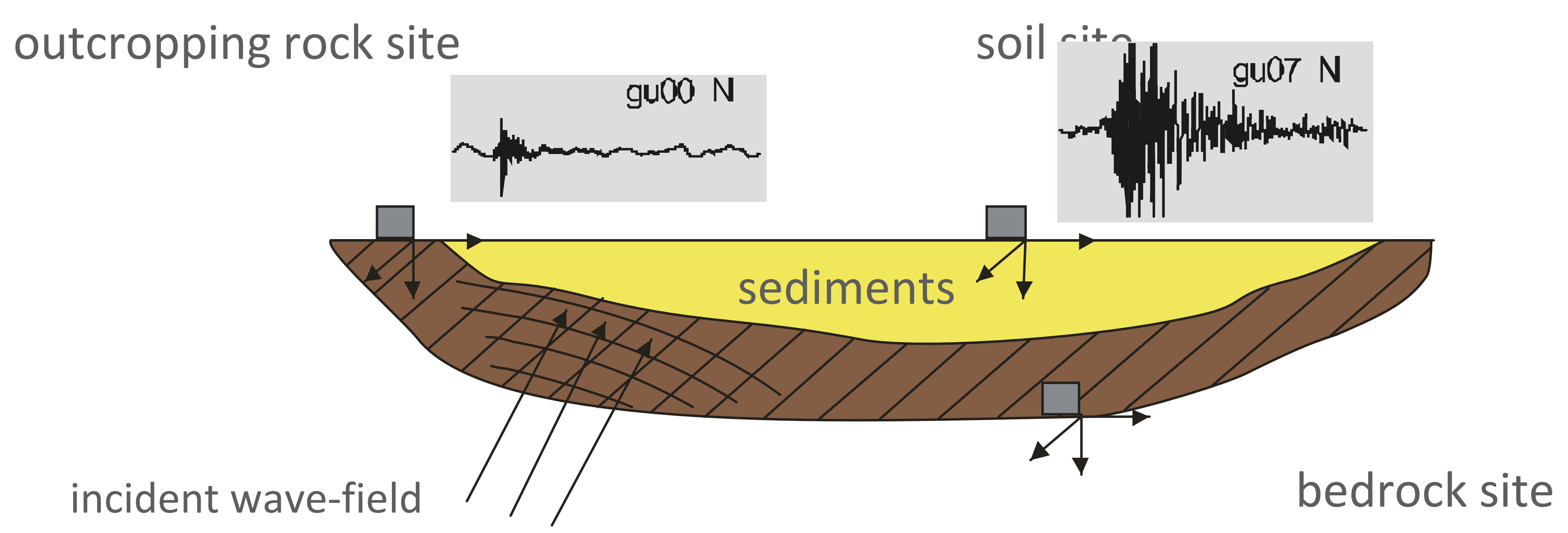

Fourier Amplitude Spectra A(f)

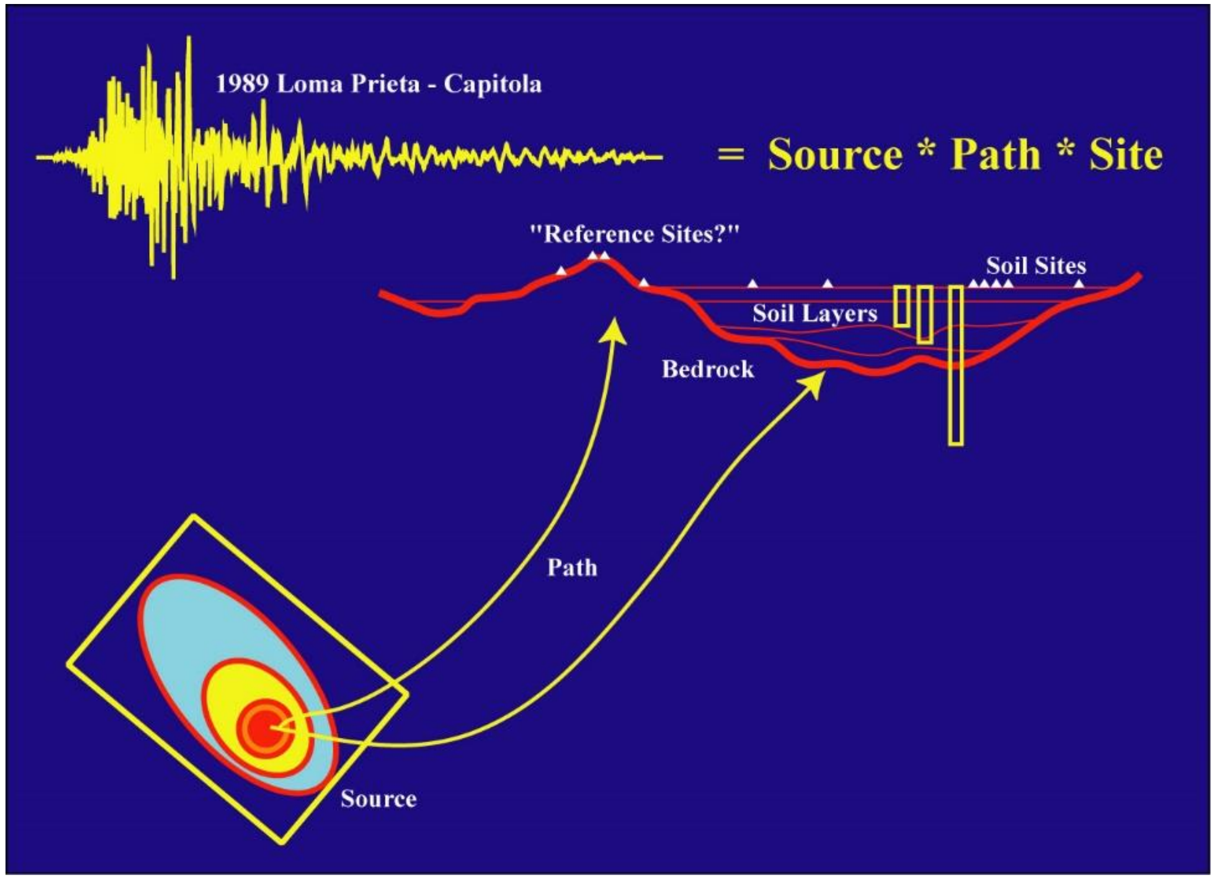

Amplitude

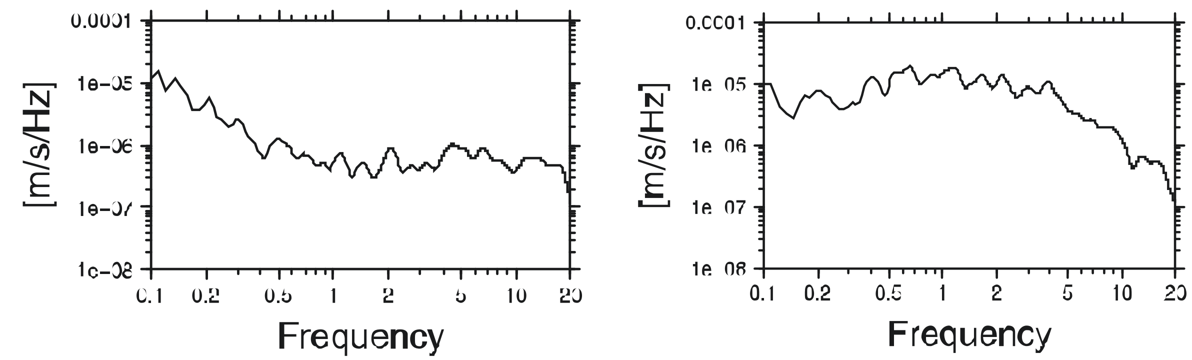

Amplification function

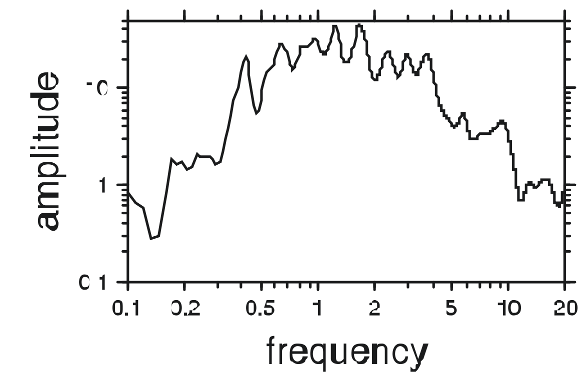

$$\frac{A_{soil}(f)}{A_{rock}(f)} = \frac{\cancel{Source_{soil}}\, Path_{soil}\, Site_{soil}}{\cancel{Source_{rock}}\, Path_{rock}\, Site_{rock}} = \frac{\cancel{Path_{soil}}\, Site_{soil}}{\cancel{Path_{rock}}} = Site_{soil}$$

$Site_{rock}$ =1 (reference)

Window selection in time domain → Fourier amplitude and smoothing

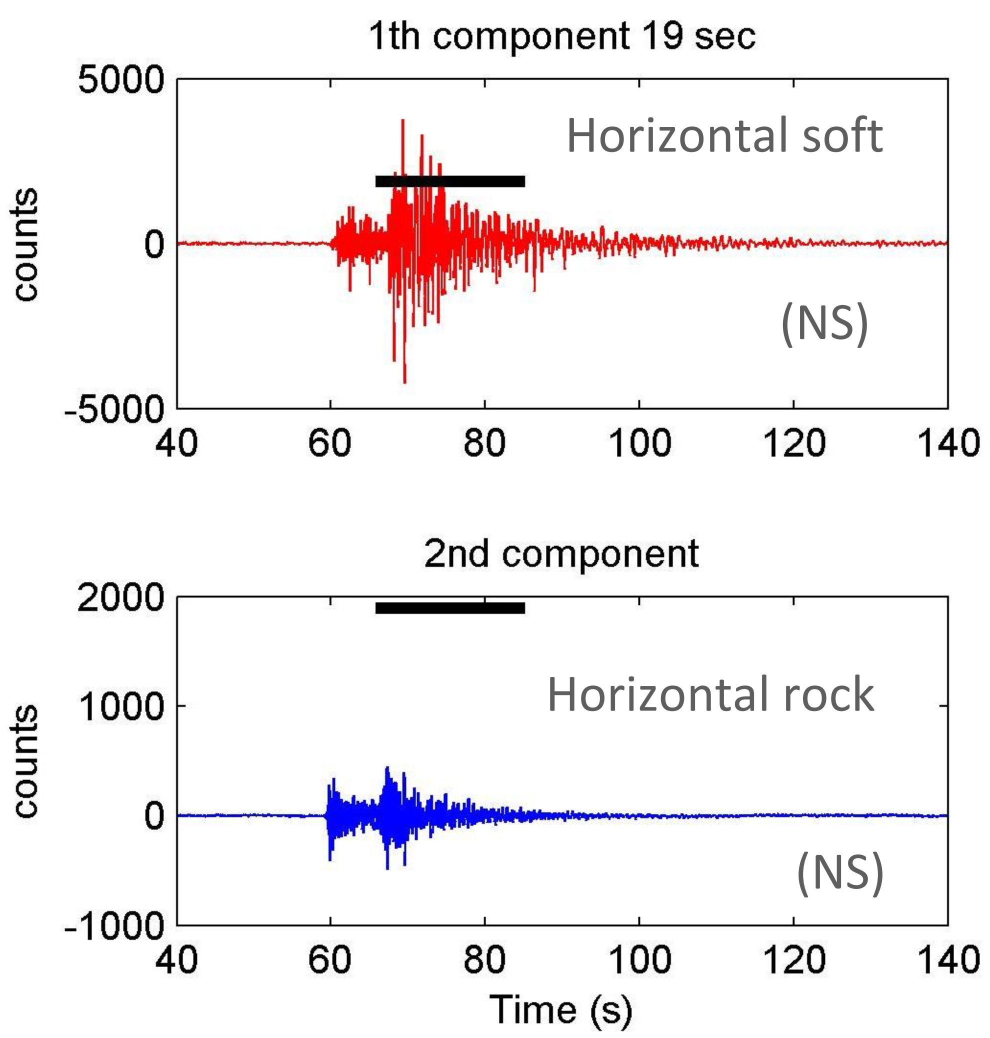

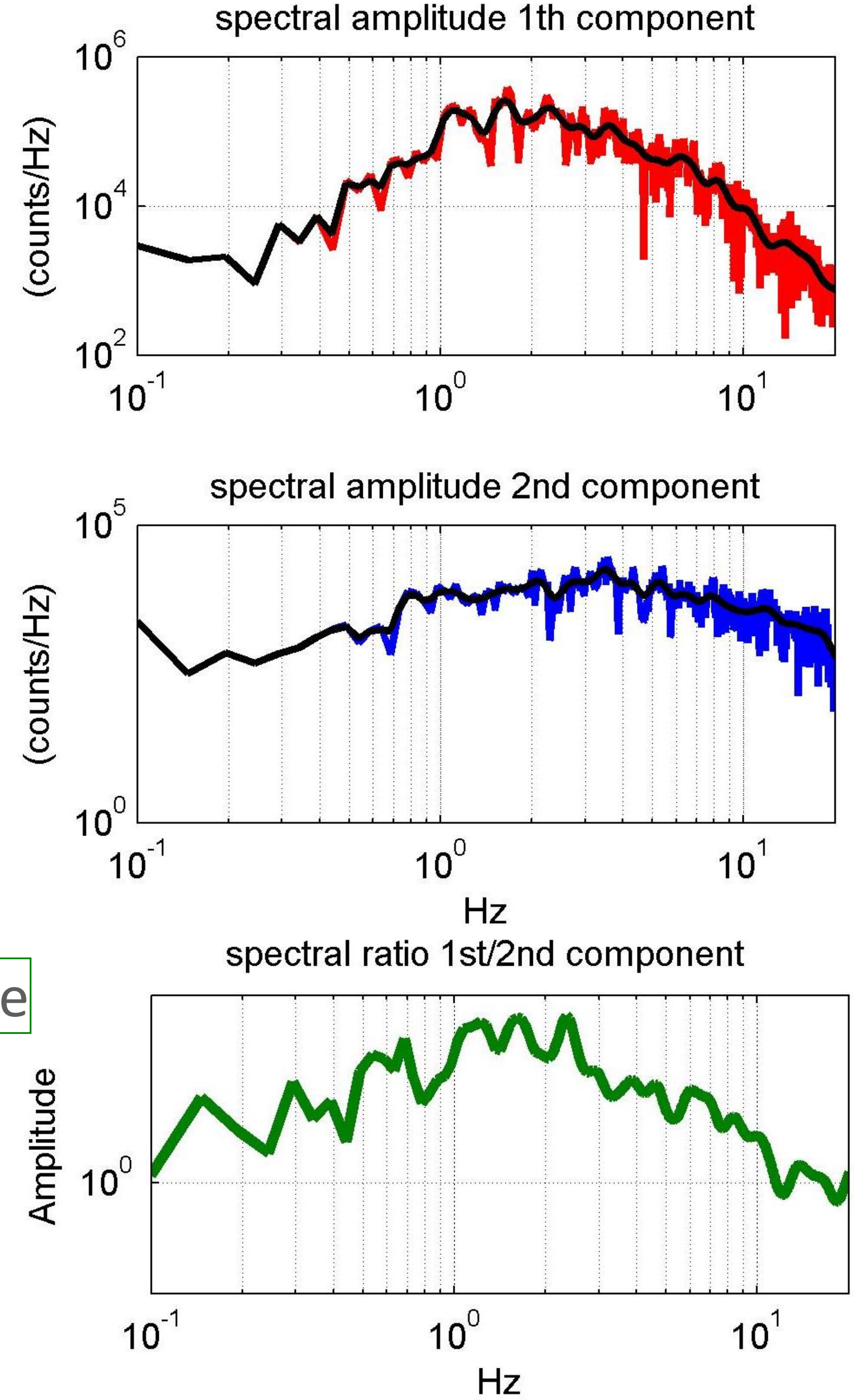

Average

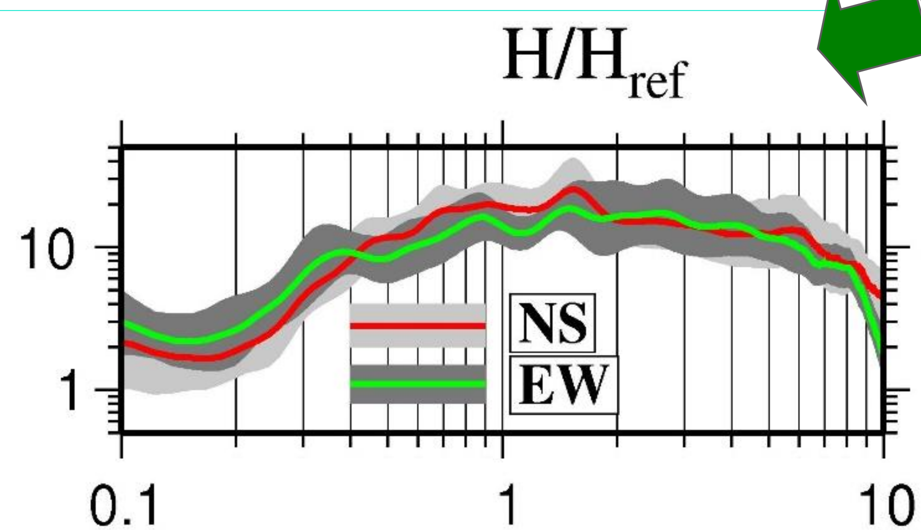

H(f)

H(f)

=

|SSR(f)|

Standard spectral ratios: the example of Gubbio basin (Italy)

“Good” reference site

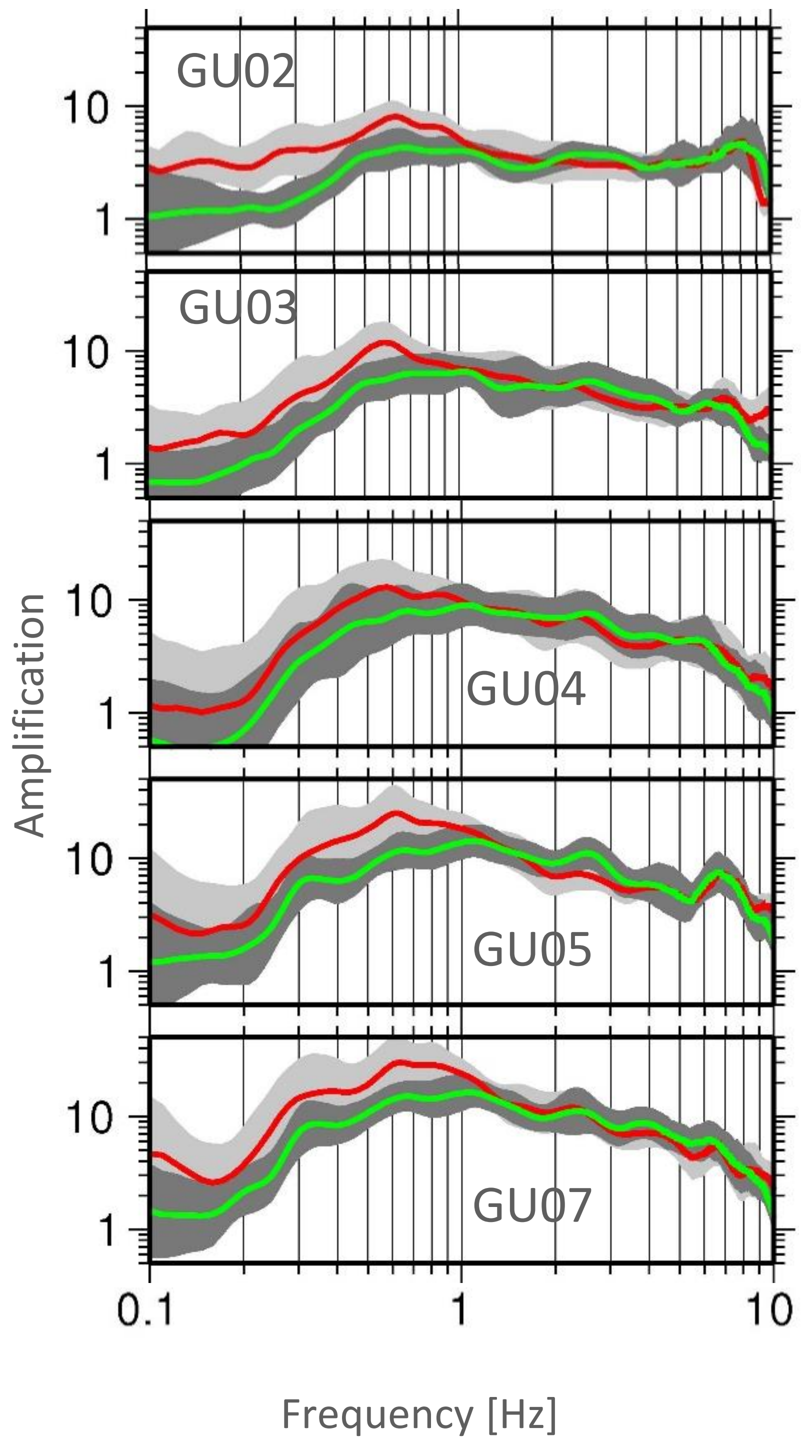

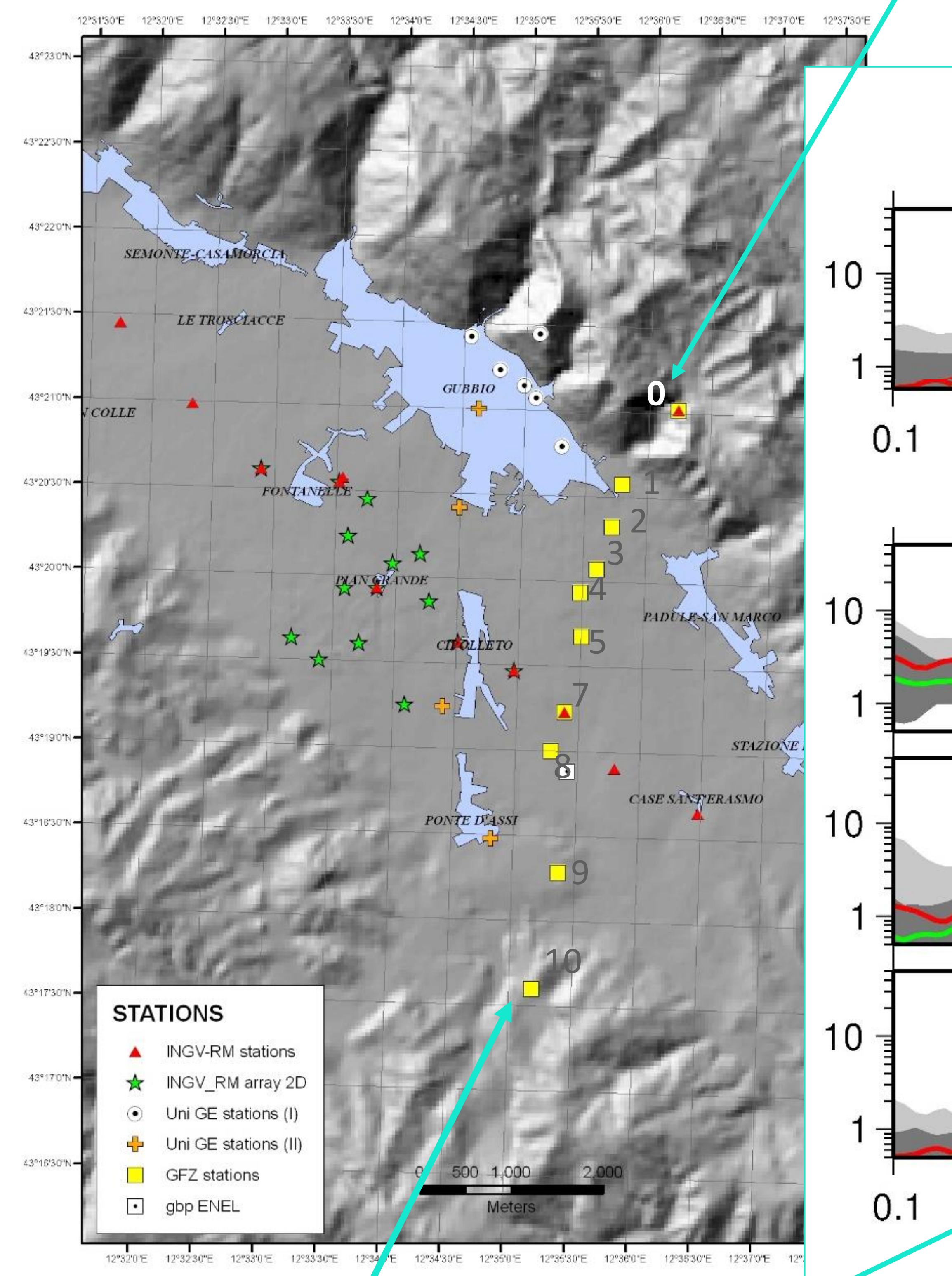

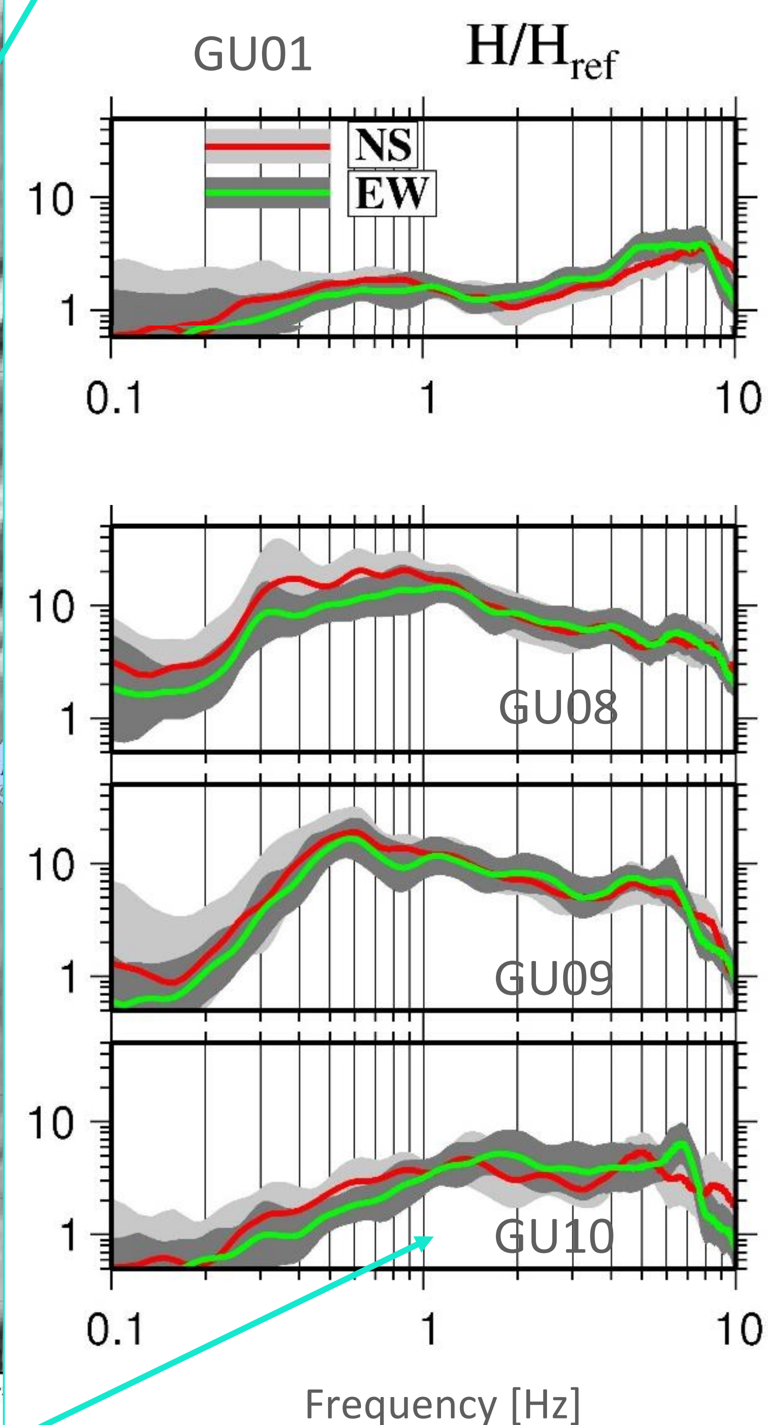

another rock station but ……

Bindi et al. (2009)

Important issues in SRE

- Near surface effects: impedance contrast, velocity
  - geological maps, V_{S30}
  - Basin effects
- Basin-edge induced waves
  - Subsurface focusing

In SHA the site effect should be defined as the average behavior, relative to other sites, given all potentially damaging earthquakes.

This produces an intrinsic variability with respect to different earthquake locations, that cannot exceed the difference between sites

Amplification patterns...

....may vary greatly among the earthquake scenarios, considering different source locations (and rupture ...)

SCEC Phase 3 Report

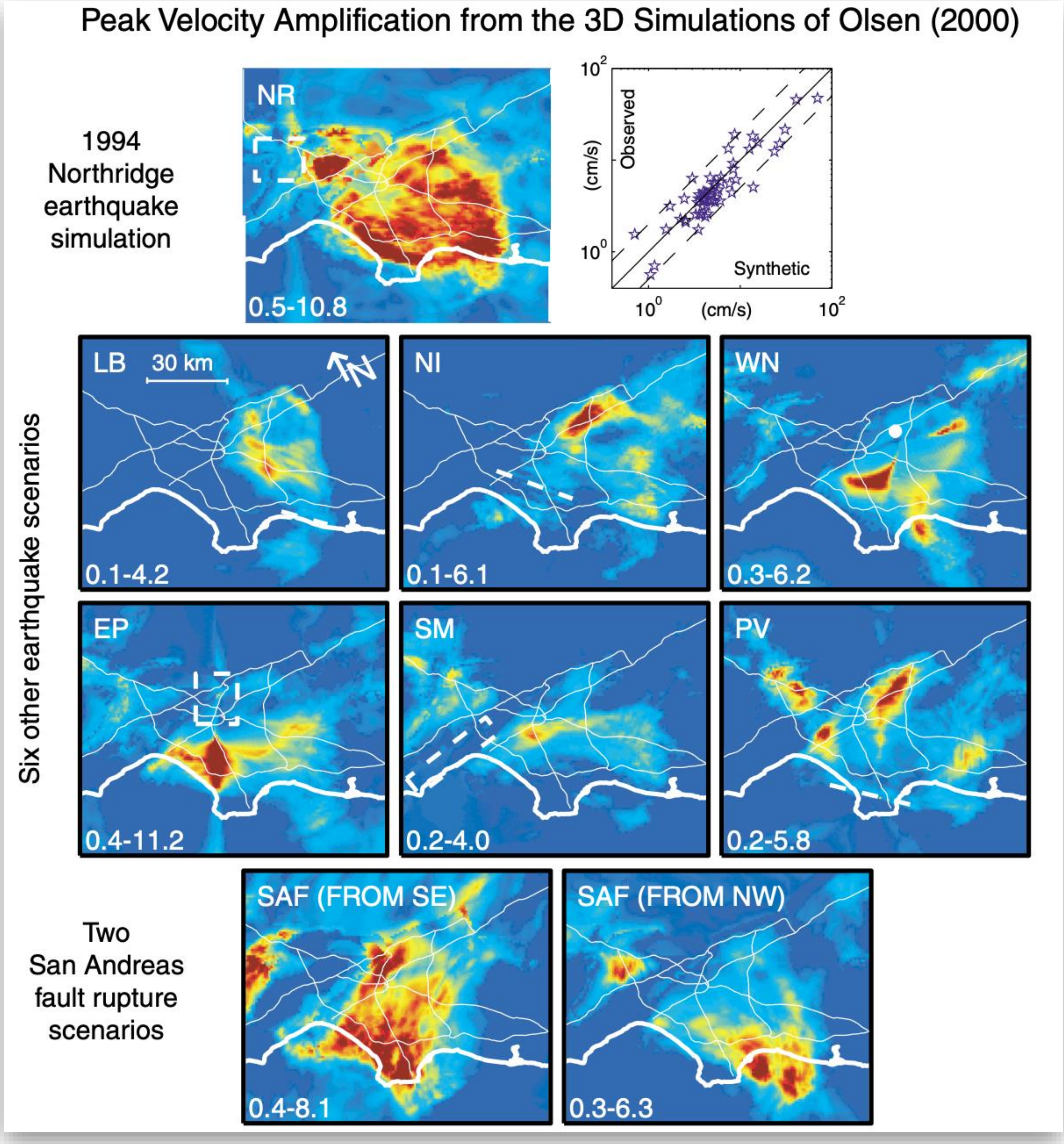

Seismic Source effects

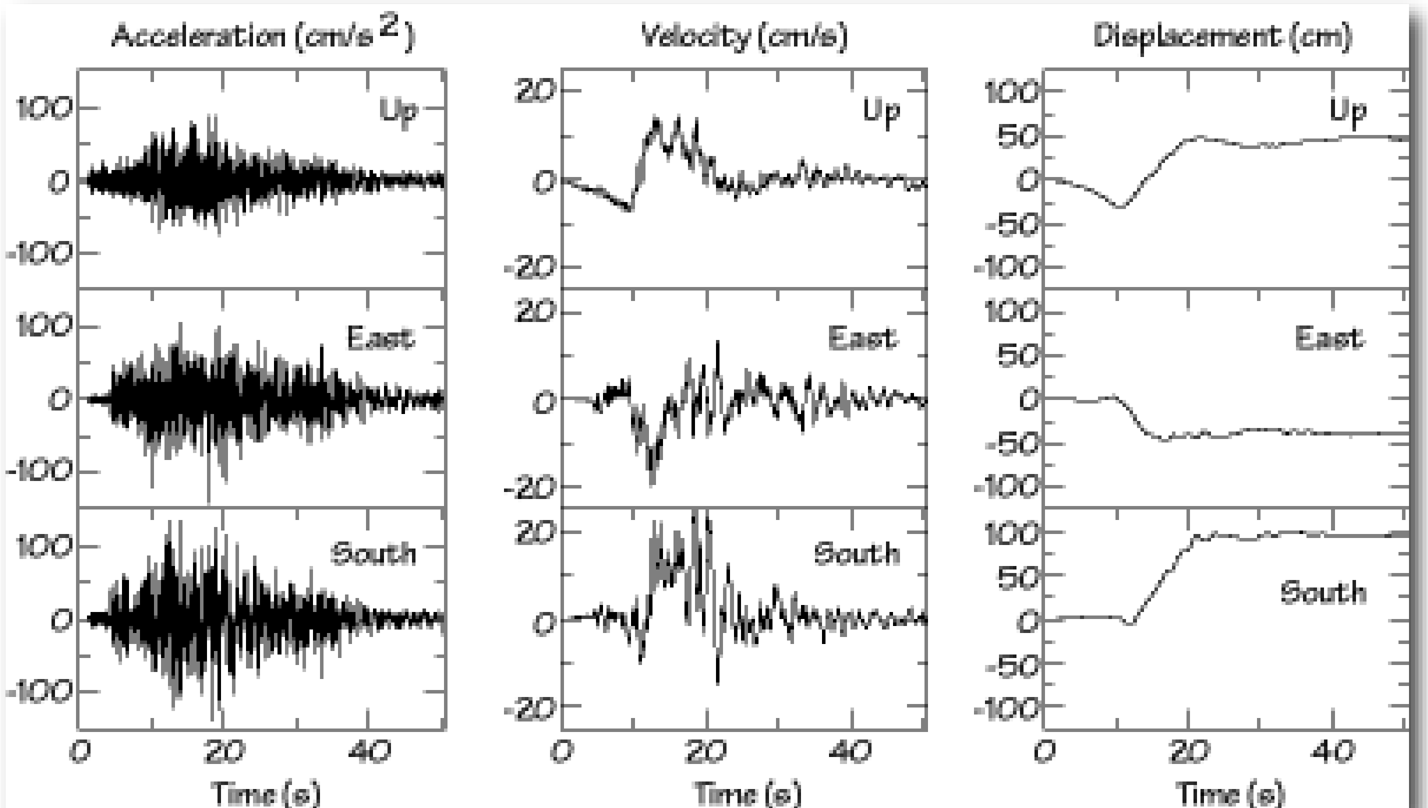

Michoacan, 1985

Fling & Directivity

aka

Near-field & Near-source

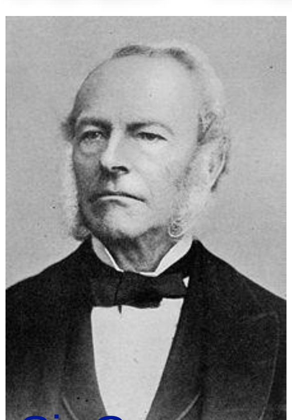

Sir Georges Stokes

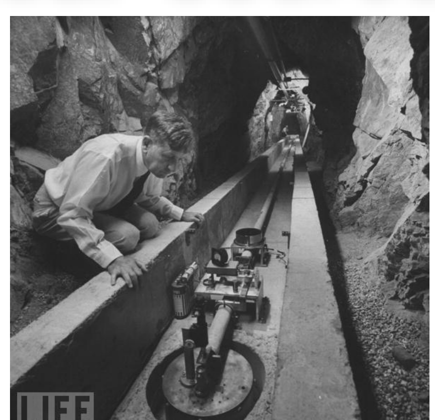

Hugo Benioff

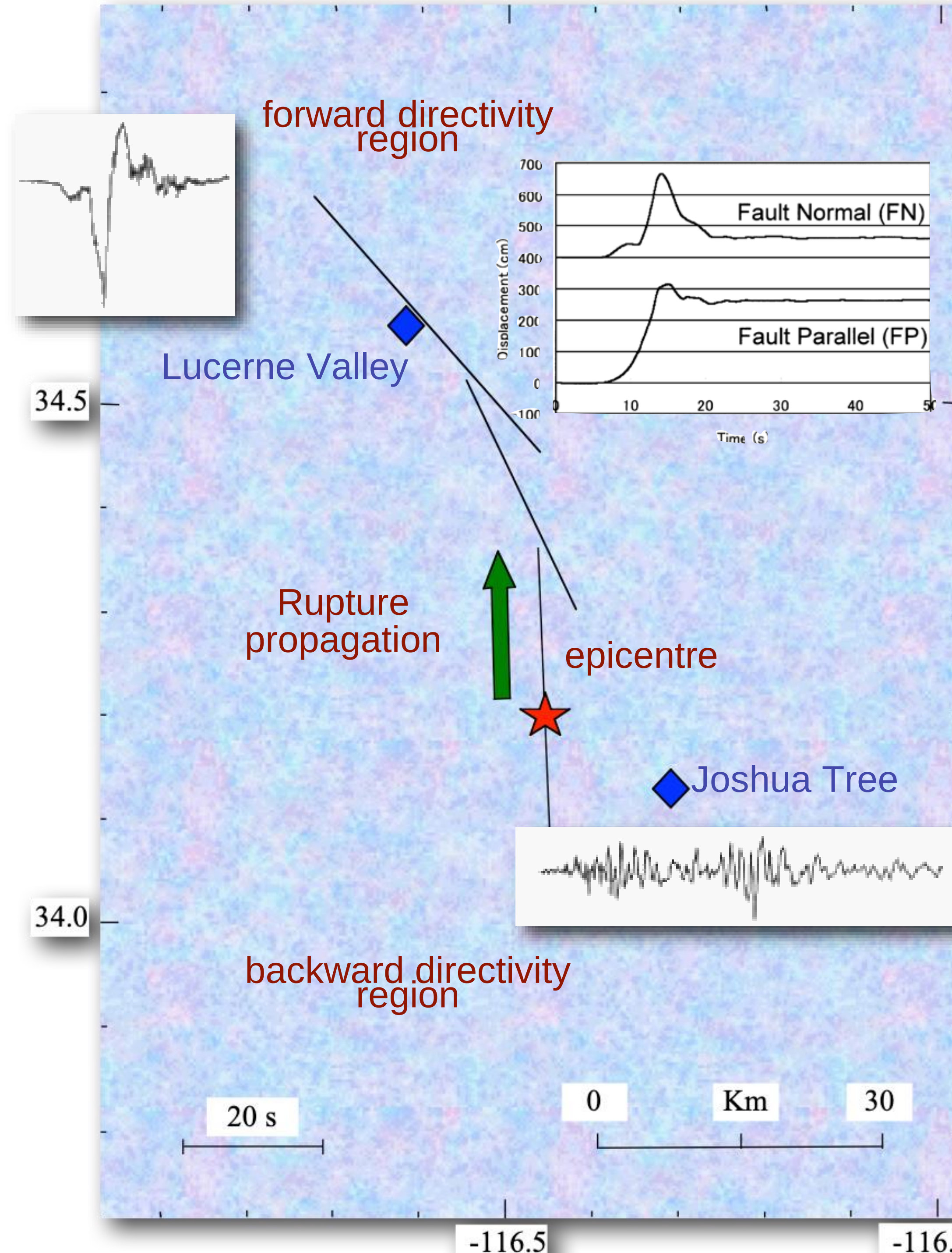

Landers, 1992

Seismic source: Friction & Stresses

A number of factors can control friction: temperature, slip rate and slip history. Many materials become weaker with repeated slip (slip weakening).
They may exhibit an inverse dependence of friction on slip velocity (velocity weakening).
Stick slip behaviour is observed only at temperatures below 300°C.

Anderson's theory of faulting: he recognized that principal stress orientations could vary among geological provinces within the upper crust of the earth. He deduced the connection between three common fault types: normal, strike-slip, and thrust and the three principal stress systems arising as a consequence of the assumption that one principal stress must be normal to the earth's surface.

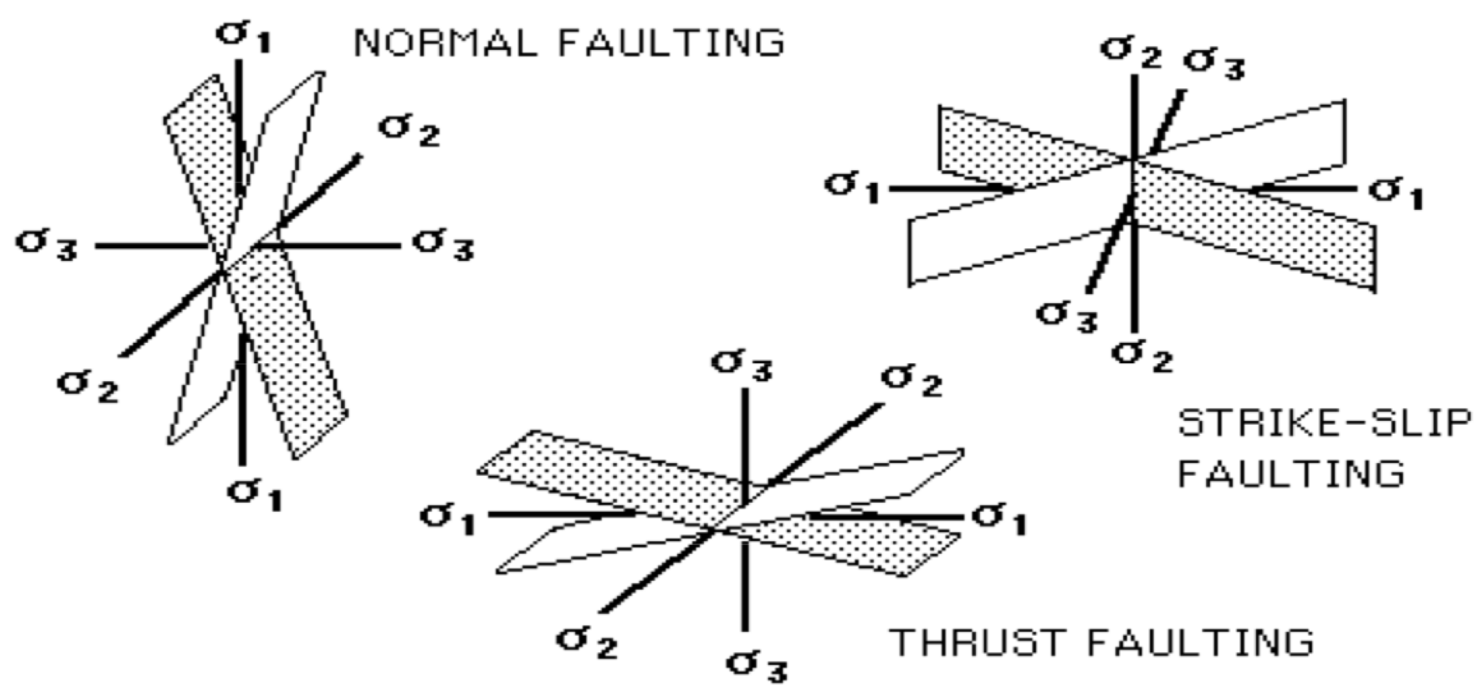

Rupture process

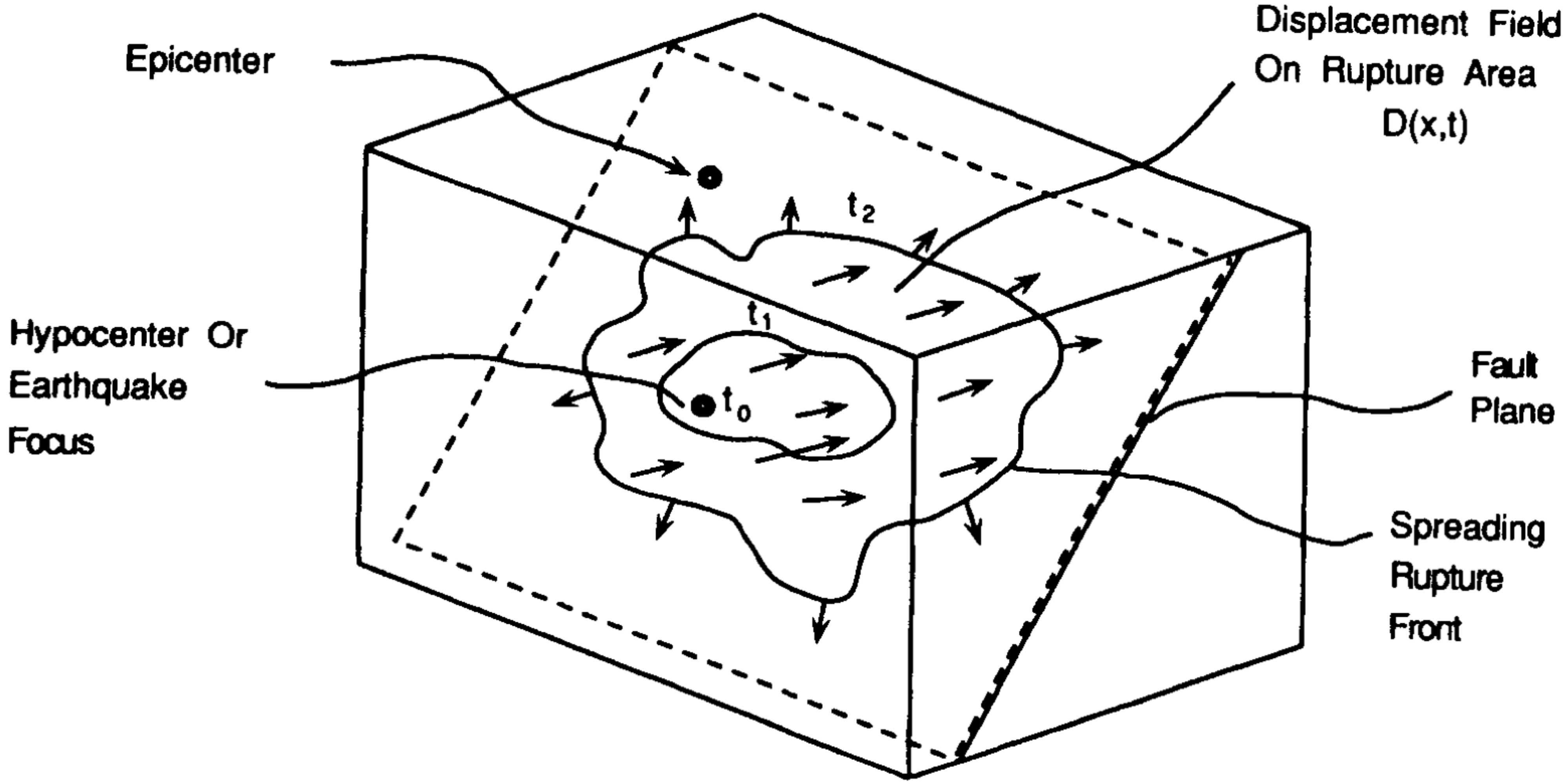

Schematic diagram of rupture on a fault plane. Slipping points radiate outgoing P- and S-waves. In general, rupture wavefront is not regular and slip vector, as well as slipping time, is different for the points on the fault.

Fault slip involves three main stages:

1) initiation of fault sliding
2) rupture front expansion
3) termination of rupture process.

Equivalent Forces

The observable seismic radiation is through energy release as the fault surface moves: formation and propagation of a crack. This complex dynamical problem can be studied by kinematical equivalent approaches.

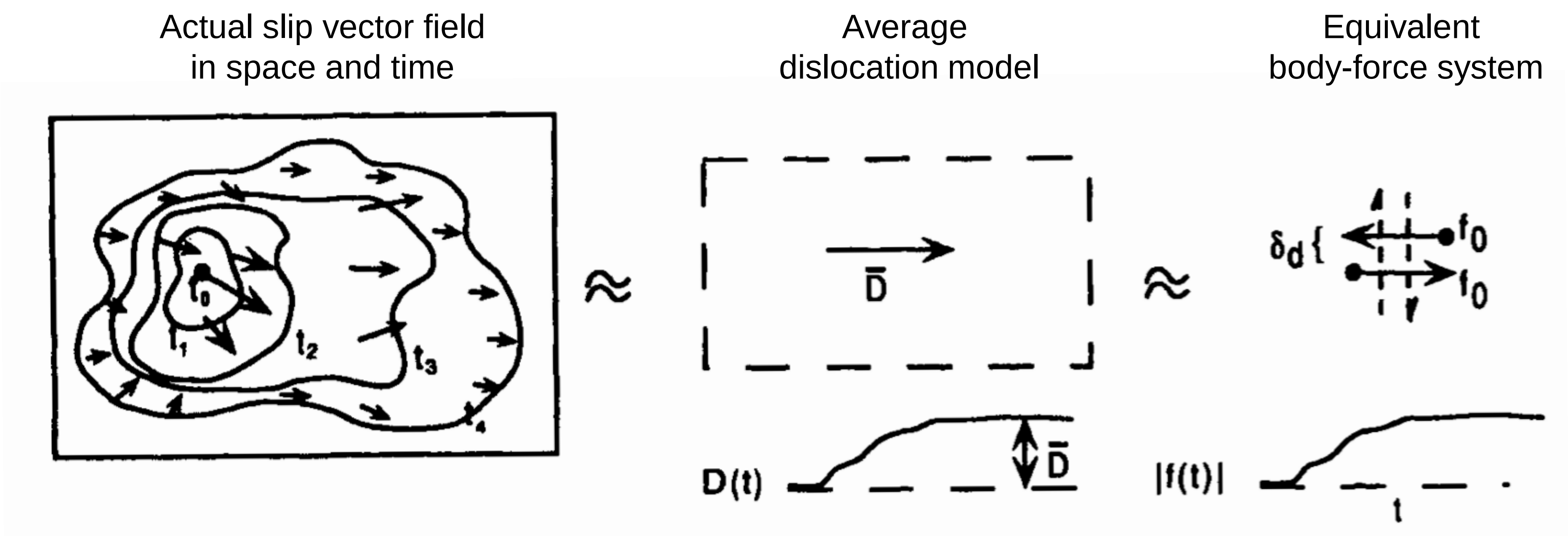

The scope is to develop a representation of the displacement generated in an elastic body in terms of the quantities that originated it: body forces and applied tractions and displacements over the surface of the body.

The actual slip process will be described by superposition of equivalent body forces acting in space (over a fault) and time (rise time).

Fundamental papers

- Maruyama T. (1963). On the force equivalents of dynamical elastic dislocations with reference to the earthquake mechanism. Bulletin of the Earthquake Research Institute 41: 467–486.

- Burridge R. and Knopoff L. (1964). Body force equivalents for seismic dislocations. Bulletin of the Seismological Society of America 54: 1875–1878.

“An explicit expression is derived for the body force to be applied in the absence of a dislocation, which produces radiation identical to that of the dislocation. This equivalent force depends only upon the source and the elastic properties of the medium in the immediate vicinity of the source and not upon the proximity of any reflecting surfaces. The theory is developed for dislocations in an anisotropic inhomogeneous medium; in the examples isotropy is assumed. For displacement dislocation faults, the double couple is an exact equivalent body force.”

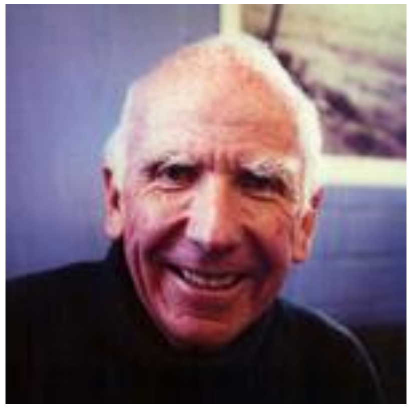

Leon Knopoff

Fault plane and slip vector

Figure 4.2-2: Fault geometry used in earthquake studies.

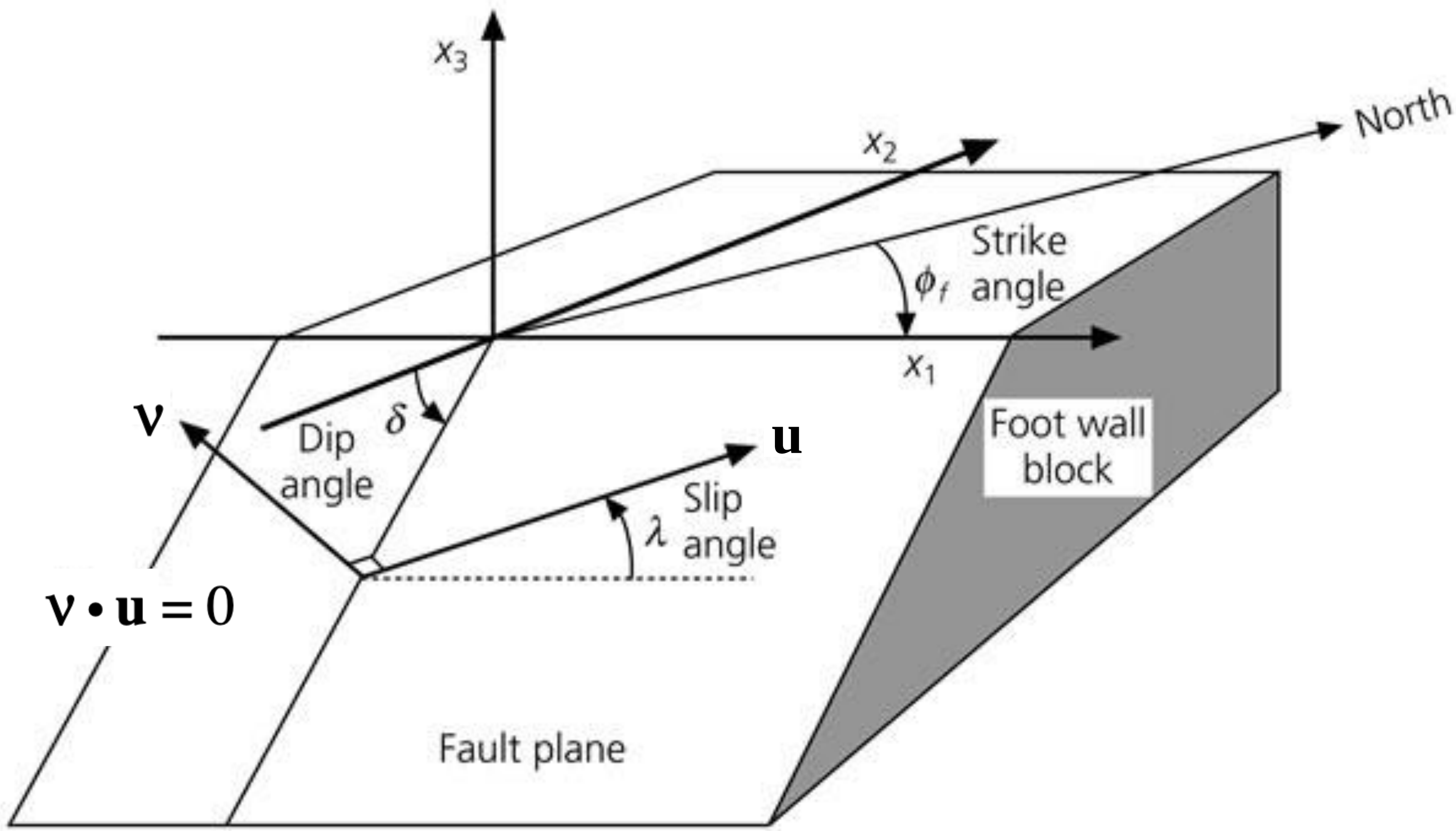

Final (point) source representation

And if the source can be considered a point-source (for distances greater than fault dimensions), the contributions from different surface elements can be considered in phase.

Thus for an effective point source, one can define the moment tensor, to be convolved with the (spatially derived) Green's function of the medium:

$$u_n(x,t) = M_{pq} * G_{np,q}$$

For a shear dislocation, the equivalent point force is a **double-couple**, since internal faulting implies that the total force $\mathbf{f}^{[u]}$ and its total moment are null. The seismic moment has a **null trace** and **one of the eigenvalues is 0**.

$$M_{pq}(\text{doublecouple}) = \begin{pmatrix} M_0 & 0 & 0 \\ 0 & 0 & 0 \\ 0 & 0 & -M_0 \end{pmatrix} \quad \text{with } M_0 = \mu A[\bar{u}]$$

M_0 is called **seismic moment**, a scalar quantity related to the area of the fault and to the slip, averaged over the fault plane.

Moment tensor components

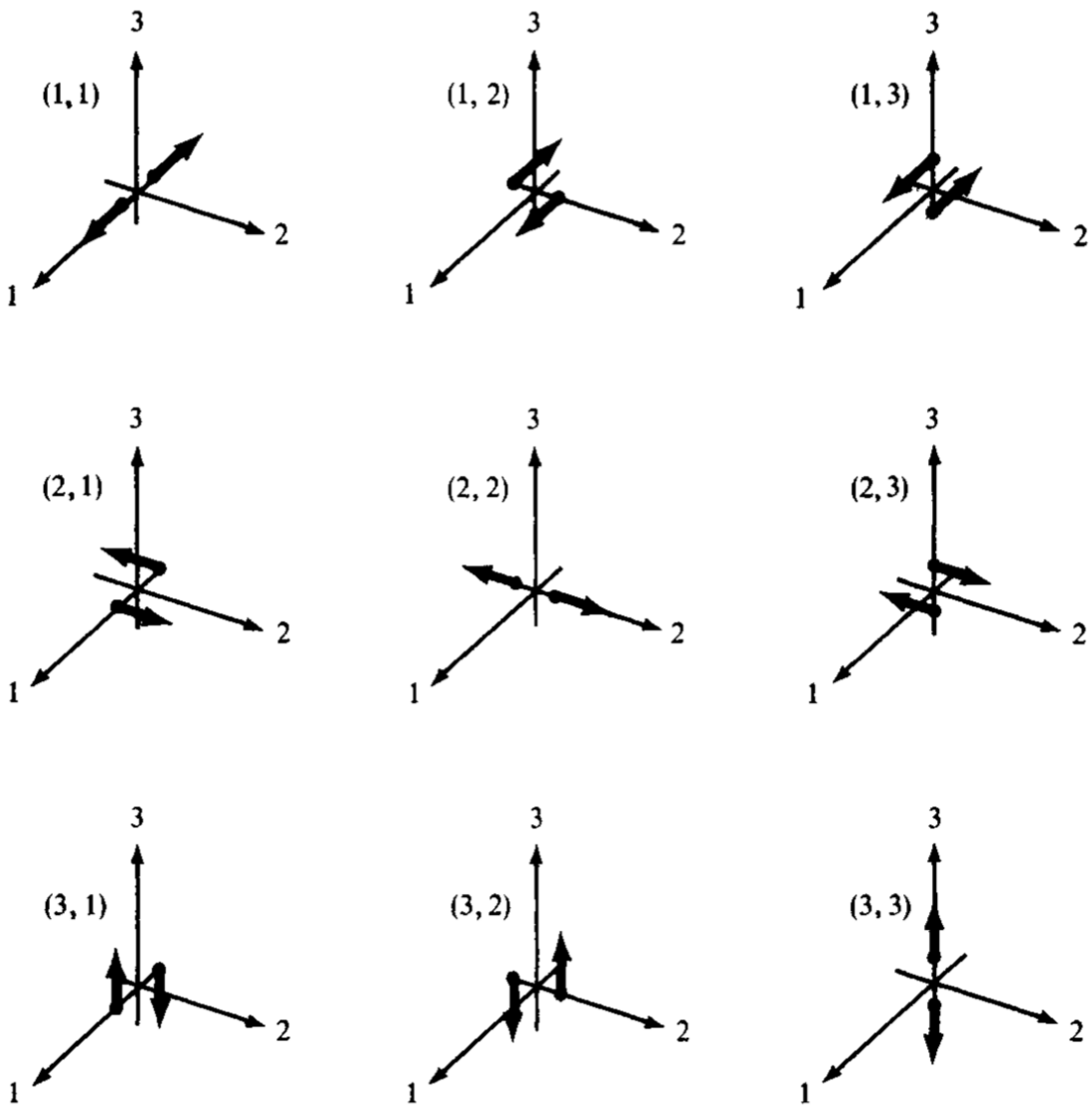

The nine possible couples that are required to obtain equivalent forces for a generally oriented displacement discontinuity in anisotropic media.

Point sources can be described by the seismic moment tensor **Mpq**, whose elements have clear physical meaning of **forces acting on particular planes**.

The Principal Focal Mechanisms

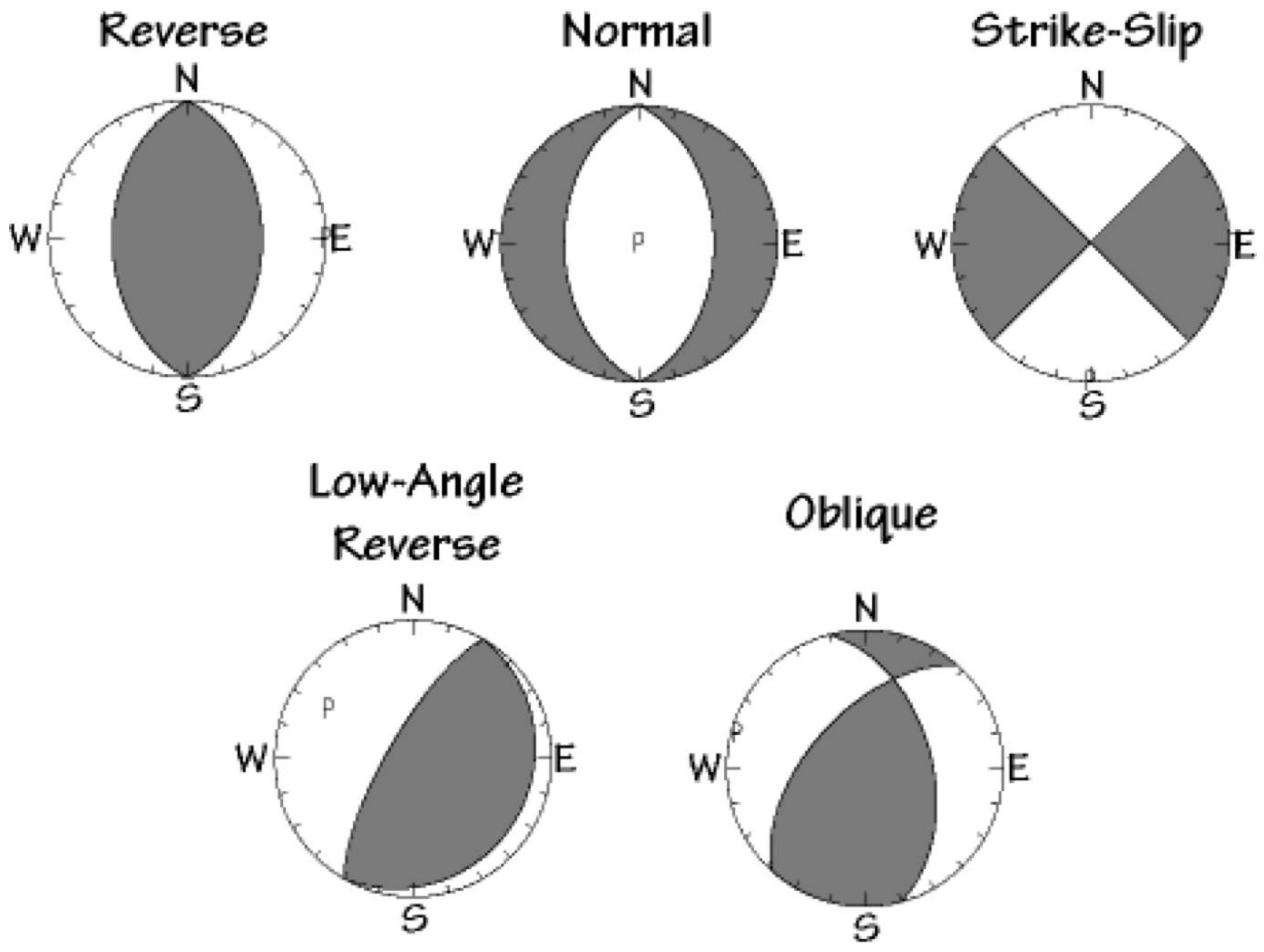

FM & stress axes

Figure 4.2-16: Relation between fault planes and stress axes.

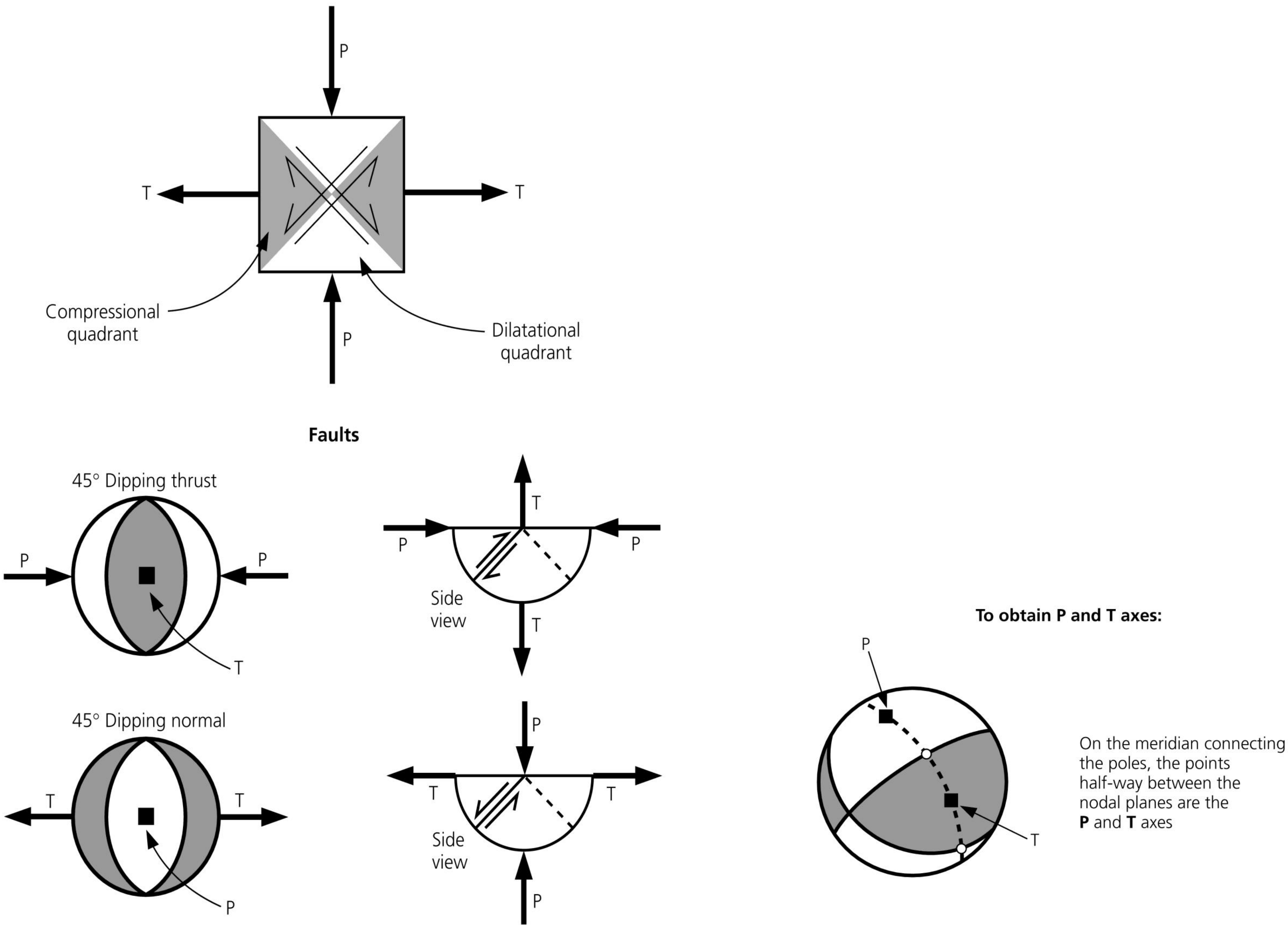

Radiation pattern & surface waves

Figure 4.3-12: Surface wave amplitude radiation patterns for several focal mechanisms.

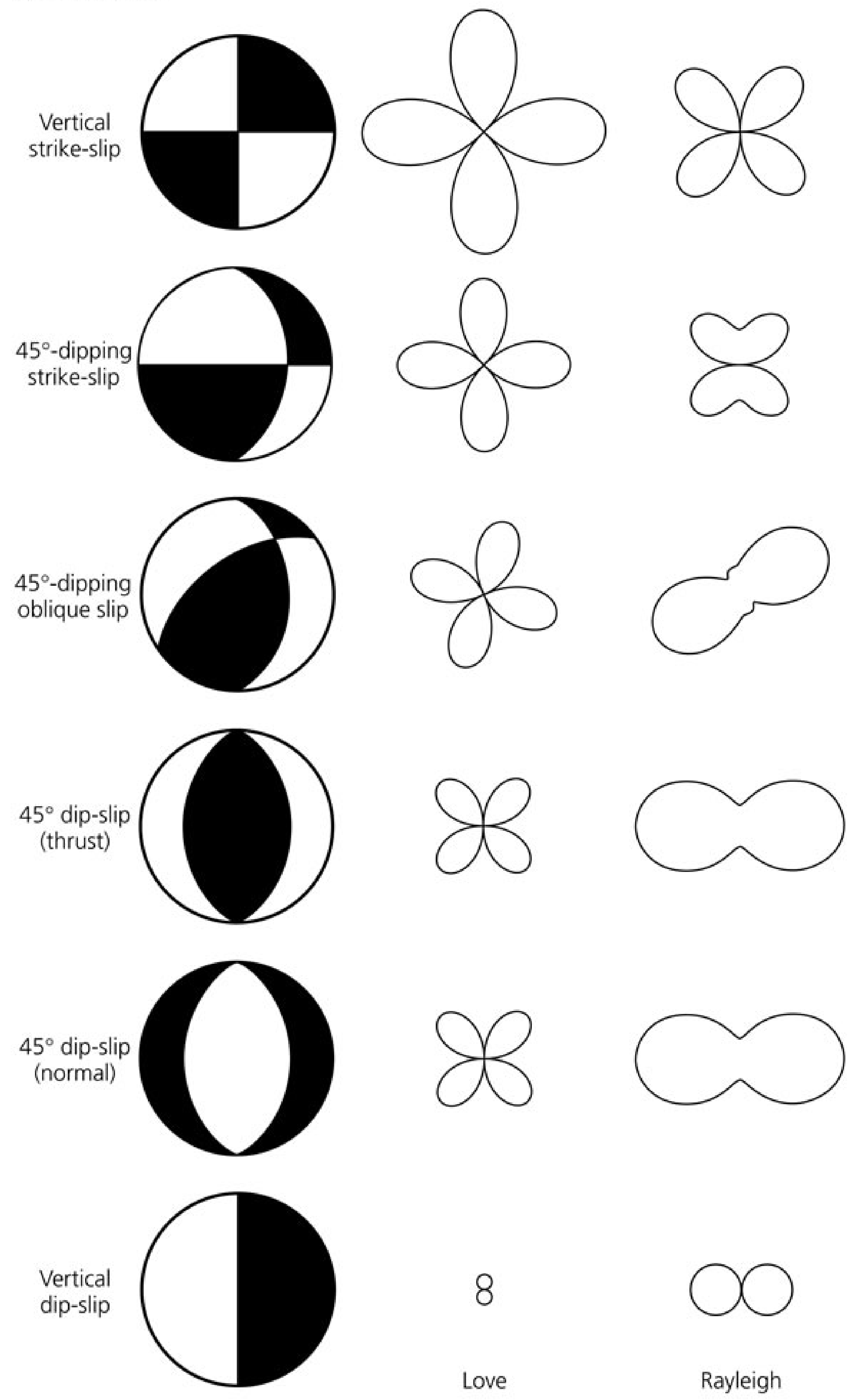

Haskell dislocation model

Haskell N. A. (1964). Total energy spectral density of elastic wave radiation from propagating faults, Bull. Seism. Soc. Am. **54**, 1811-1841

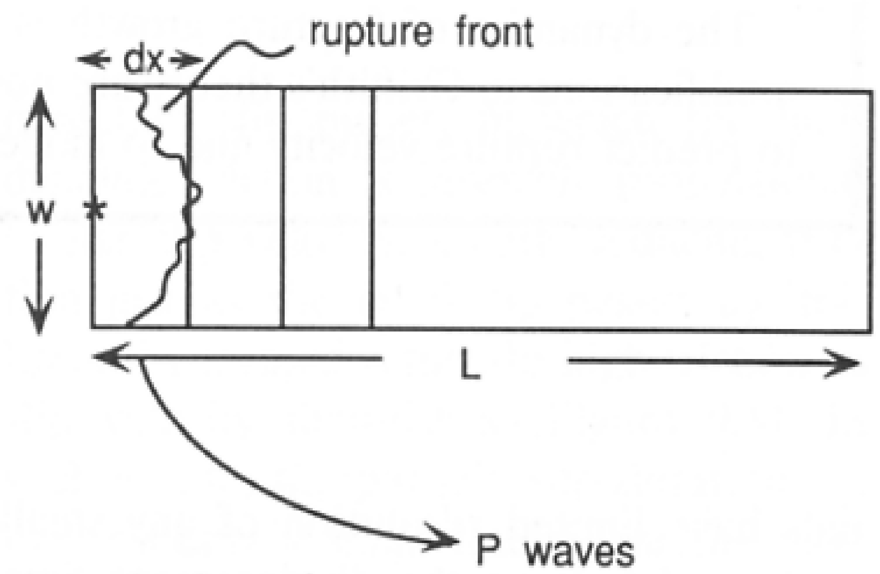

FIGURE 9.5 Geometry of a one-dimensional fault of width w and length L. The individual segments of the fault are of length dx, and the moment of a segment is $m\,dx$. The fault ruptures with velocity v_r.

Sumatra earthquake, Dec 26, 2004

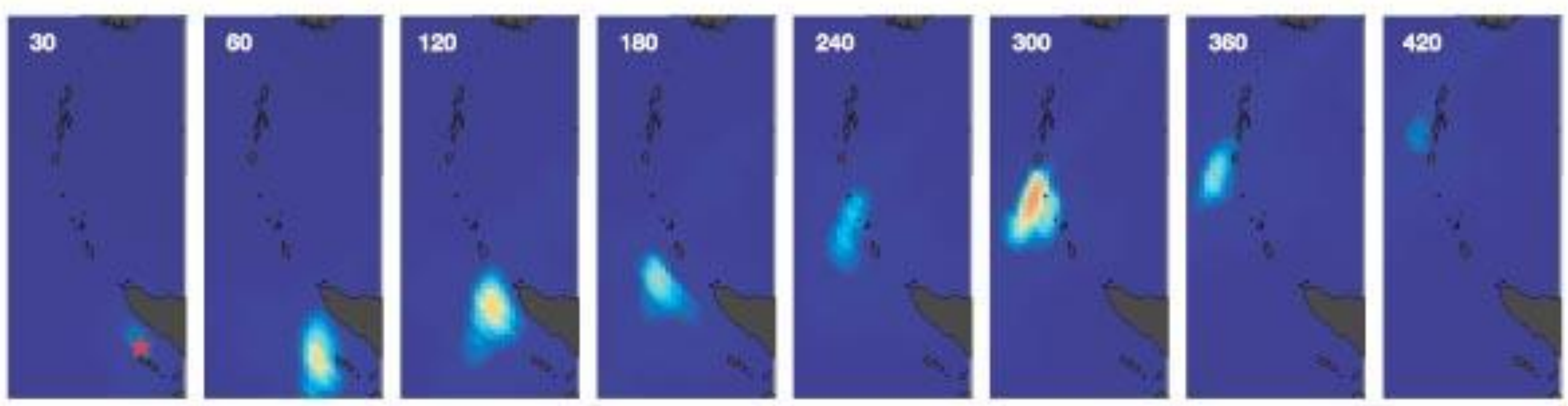

Ishii et al., Nature 2005 doi:10.1038/nature03675

Haskell source model: far field

resulting in the convolution of two boxcars: the first with duration equal to the rise time and the second with duration equal to the **rupture time** (L/v_r)

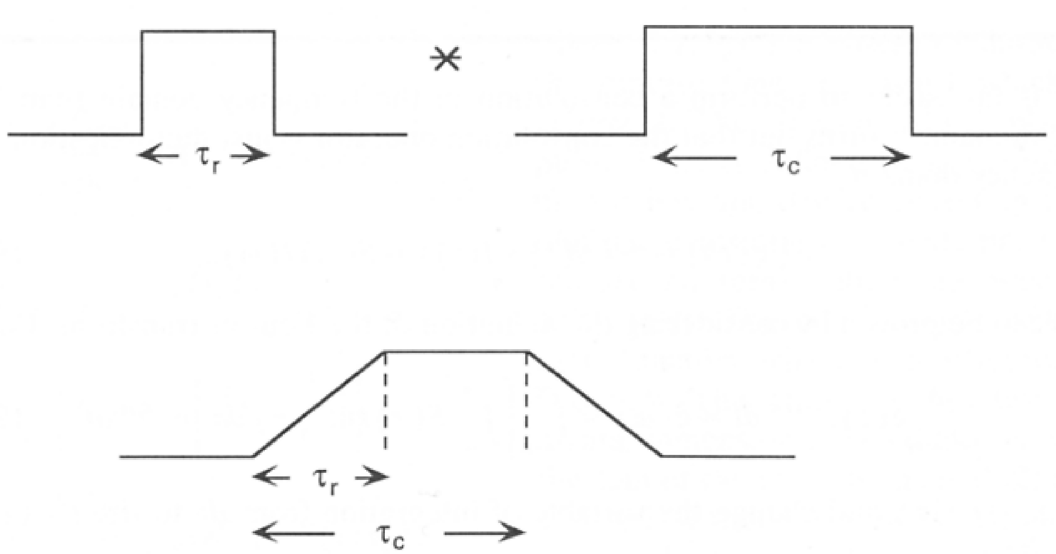

FIGURE 9.6 The convolution of two boxcars, one of length τ_r and the other of length τ_c ($\tau_c > \tau_r$). The result is a trapezoid with a rise time of τ_r, a top of length $\tau_c - \tau_r$, and a fall of width τ_r.

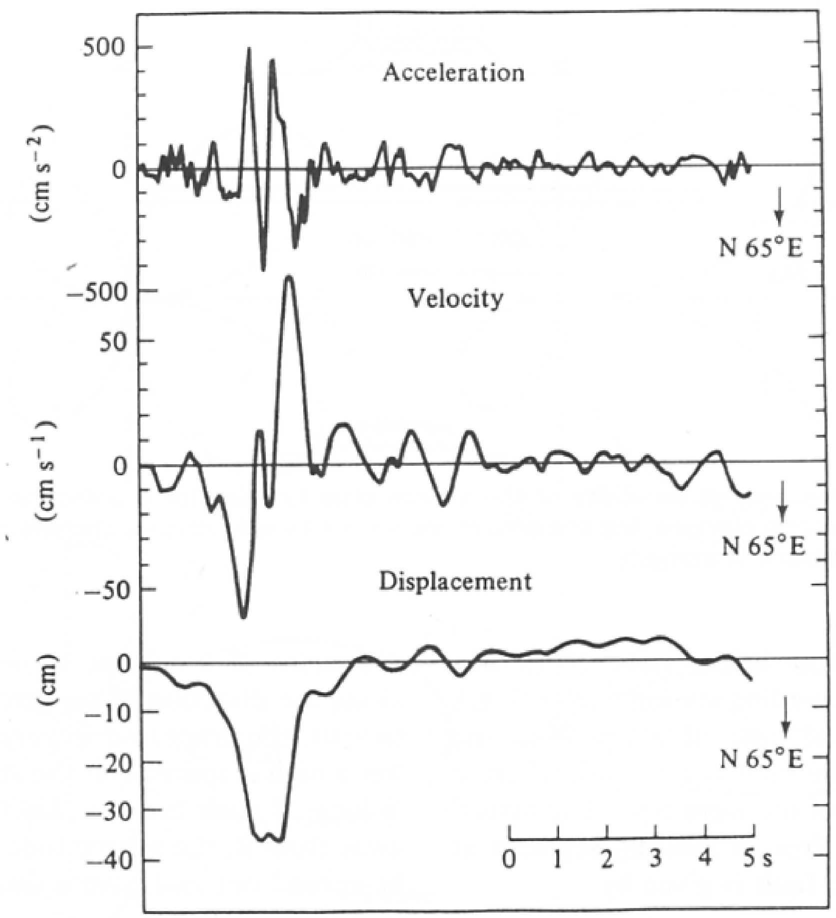

FIGURE 9.7 A recording of the ground motion near the epicenter of an earthquake at Parkfield, California. The station is located on a node for *P* waves and a maximum for *SH*. The displacement pulse is the *SH* wave. Note the trapezoidal shape. (From Aki, *J. Geophys. Res.* 73, 5359–5375, 1968; © copyright by the American Geophysical Union.)

Haskell source model: directivity

The body waves generated from a breaking segment will arrive at a receiver before than those that are radiated by a segment that ruptures later.

If the path to the station is not perpendicular, the waves generated by different segments will have different path lengths, and then unequal travel times.

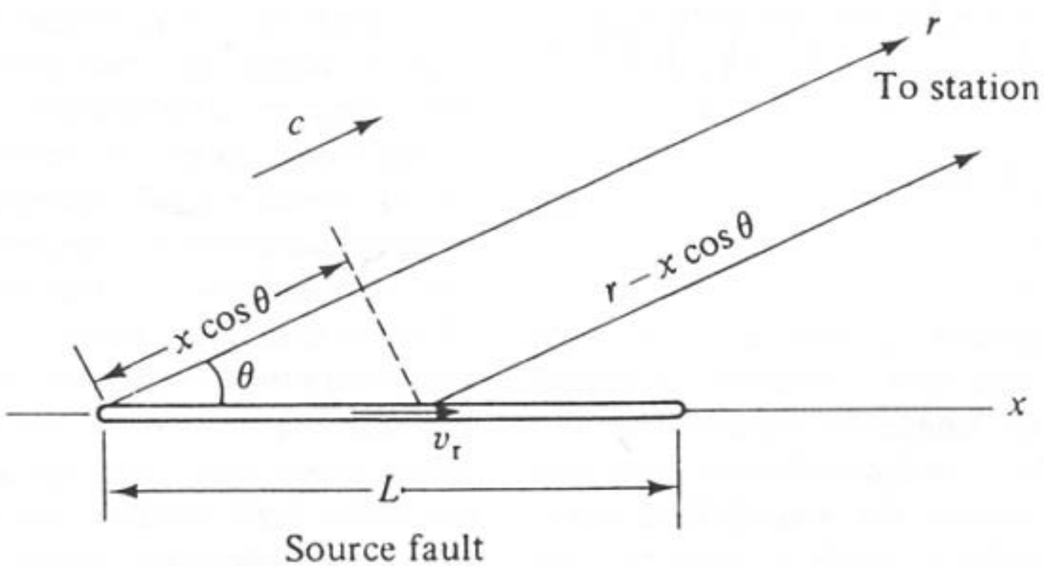

FIGURE 9.8 Geometry of a rupturing fault and the path to a remote recording station. (From Kasahara, 1981.)

$$T_r = \left[\frac{L}{v_r} + \left(\frac{r - L\cos\theta}{c}\right)\right] - \frac{r}{c} =$$

$$= \frac{L}{v_r} - \left(\frac{L\cos\theta}{c}\right) = \frac{L}{v_r}\left(1 - \frac{v_r}{c}\cos\theta\right)$$

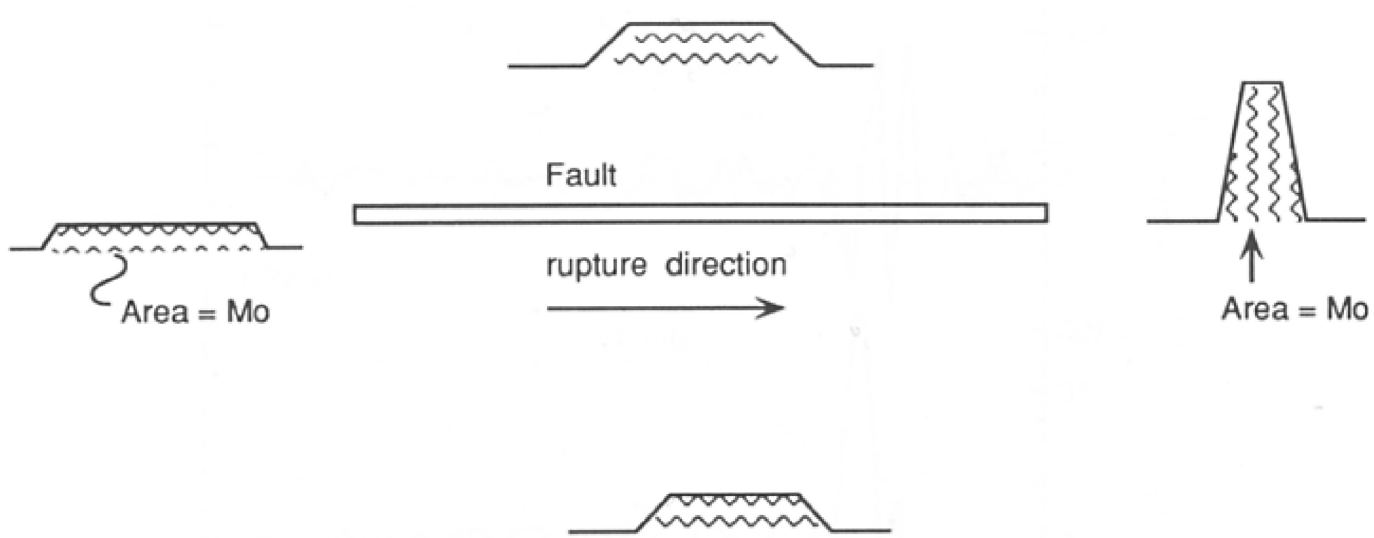

FIGURE 9.9 Azimuthal variability of the source time function for a unilaterally rupturing fault. The duration changes, but the area of the source time function is the seismic moment and is independent of azimuth.

Directivity example

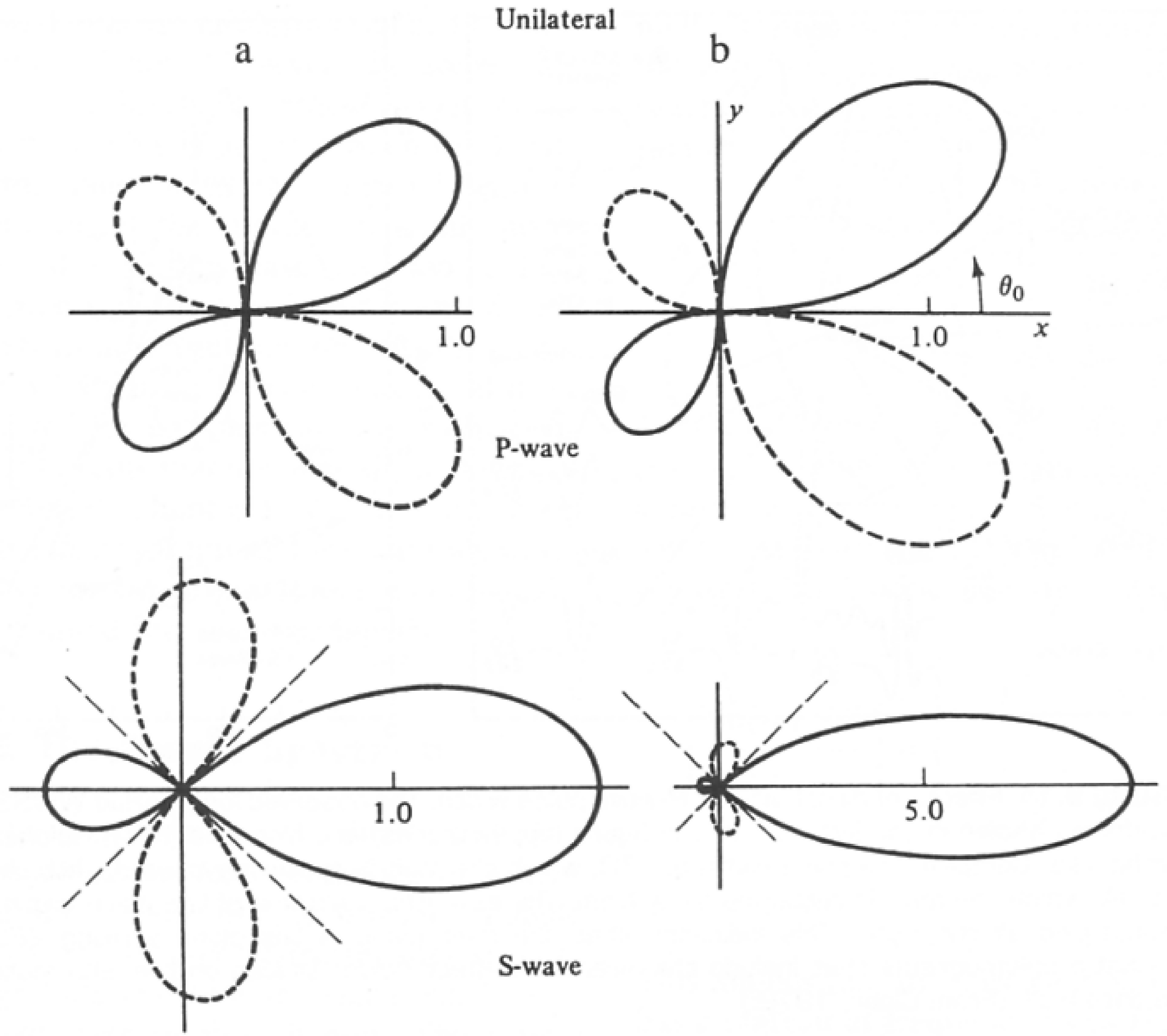

FIGURE 9.10 The variability of *P*- and *SH*-wave amplitude for a propagating fault (from left to right). For the column on the left $v_r/v_s = 0.5$, while for the column on the right $v_r/v_s = 0.9$. Note that the effects are amplified as rupture velocity approaches the propagation velocity. (From Kasahara, 1981.)

Source spectrum (amplitude)

The displacement pulse, corrected for the geometrical spreading and the radiation pattern can be written as:

$$U(\omega) \approx \begin{cases} M_0 & \omega < \dfrac{2}{T_r} \\ \dfrac{2M_0}{\omega T_R} & \dfrac{2}{T_r} < \omega < \dfrac{2}{\tau} \\ \dfrac{4M_0}{\omega^2 \tau T_R} & \omega > \dfrac{2}{\tau} \end{cases}$$

Figure 4.6-4: Approximation of the (sin *x*)/*x* function, and derivation of corner frequencies.

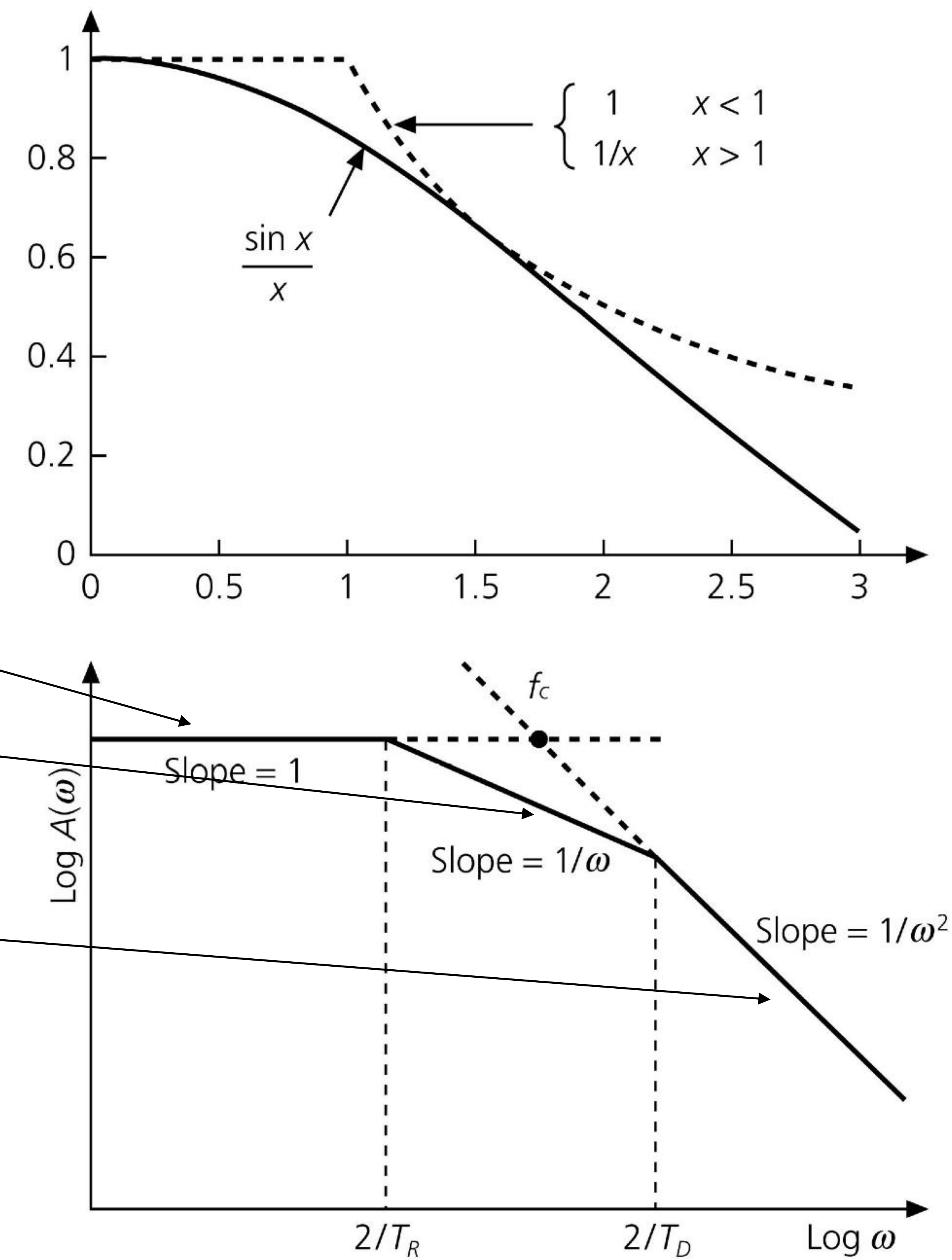

Magnitude Scales - Richter

The concept of magnitude was introduced by Richter (1935) to provide an objective instrumental measure of the size of earthquakes. Contrary to seismic intensity, I, which is based on the assessment and classification of shaking damage and human perceptions of shaking, the magnitude M uses instrumental measurements of earth ground motion adjusted for epicentral distance and source depth.

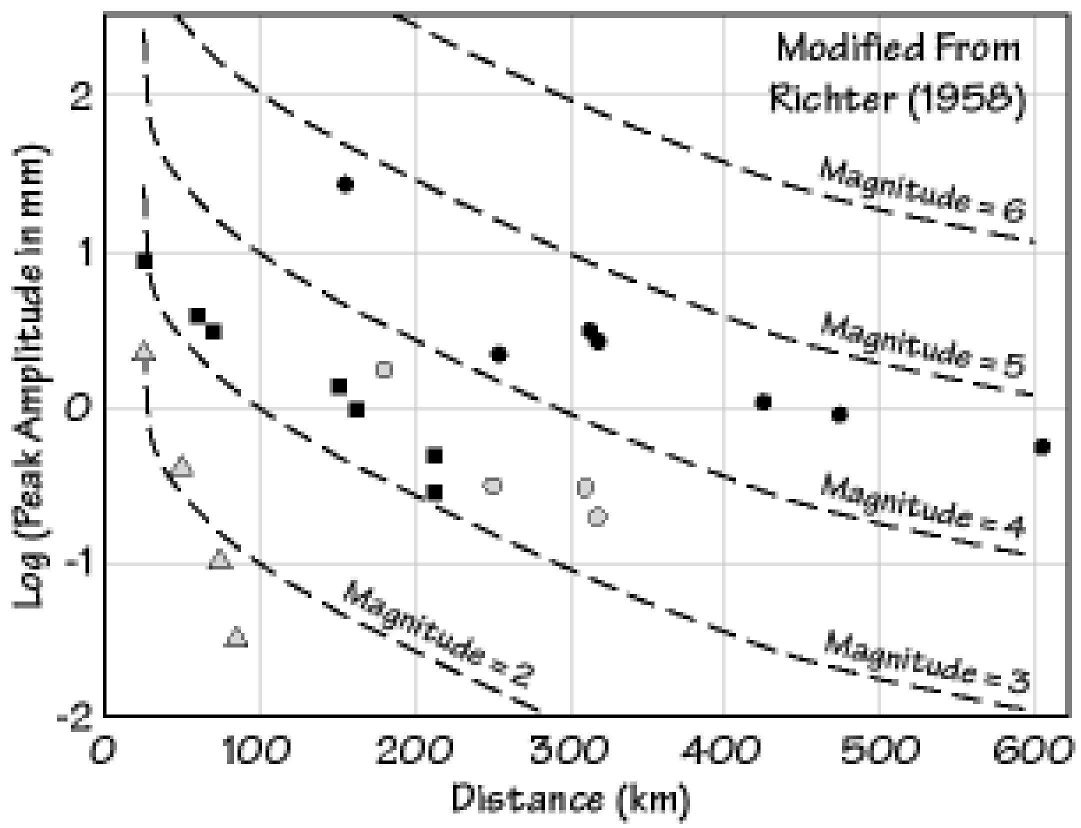

The original Richter scale was based on the observation that the amplitude of seismic waves systematically decreases with epicentral distance.

Data from local earthquakes in California

The relative size of events is calculated by comparison to a reference event, with M_L=0, such that A_0 was 1 μm at an epicentral distance, Δ, of 100 km with a Wood-Anderson instrument:

$$M_L=\log(A/A_0)=\log A-2.48+2.76\Delta.$$

Magnitude Scales - Richter

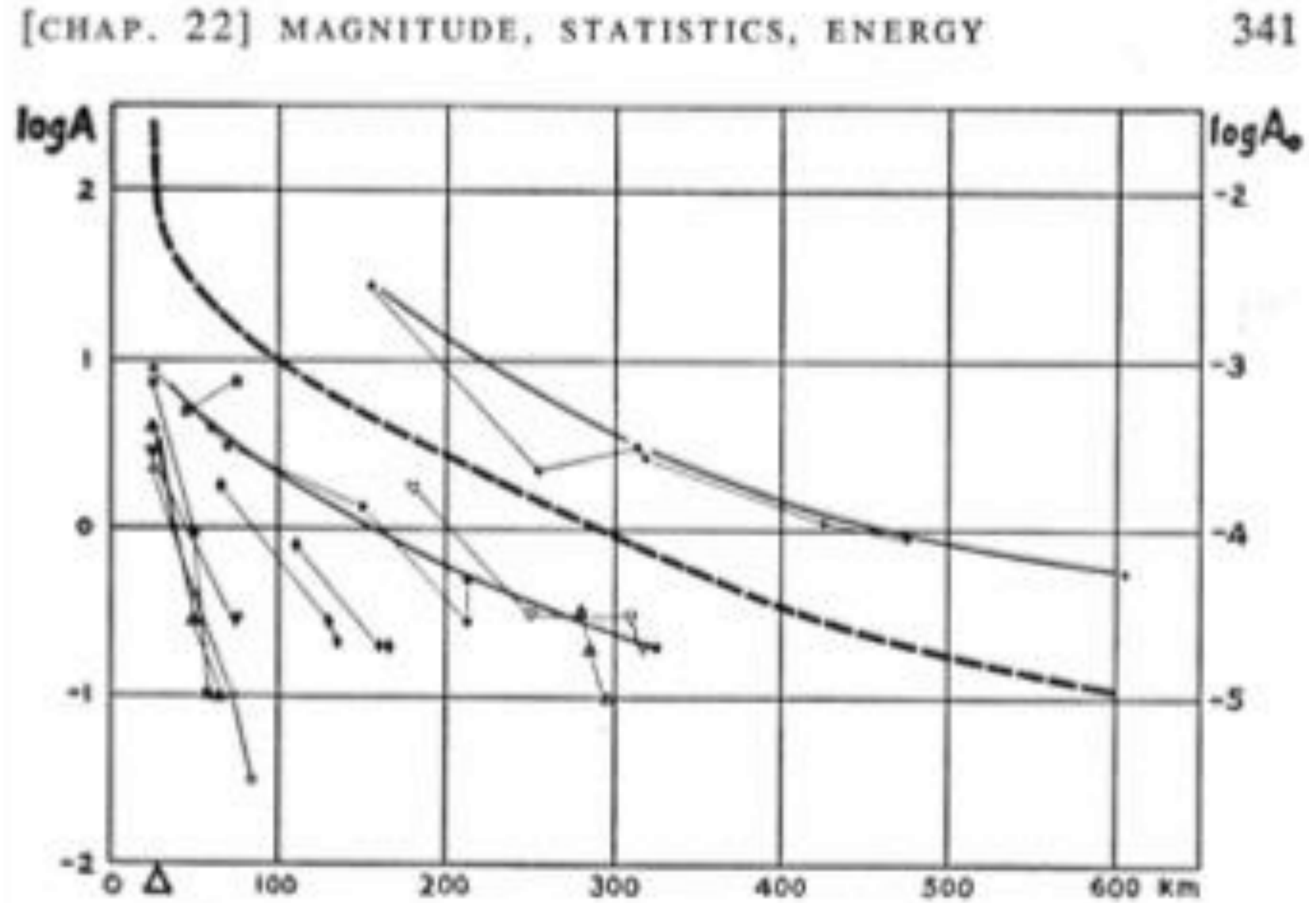

FIGURE 22-2 *Origin of the magnitude scale. Data for Southern California earthquakes of January, 1932. [Redrafted from the original notes.]*

“I found a paper by Professor K. Wadati of Japan in which he compared large earthquakes by plotting the maximum ground motion against distance to the epicenter. I tried a similar procedure for our stations, but the range between the largest and smallest magnitudes seemed unmanageably large. Dr. Beno Gutenberg then made the natural suggestion to plot the amplitudes logarithmically. I was lucky because **logarithmic plots are a device of the devil**. I saw that I could now rank the earthquakes one above the other. Also, quite unexpectedly the attenuation curves were roughly parallel on the plot. By moving them vertically, a representative mean curve could be formed, and individual events were then characterized by individual logarithmic differences from the standard curve. This set of logarithmic differences thus became the numbers on a new instrumental scale. Very perceptively, Mr. Wood insisted that this new quantity should be given a distinctive name to contrast it with the intensity scale. My amateur interest in astronomy brought out the term "magnitude," which is used for the brightness of a star.”

Charles F. Richter - An Interview by Henry Spall, Earthquake Information Bulletin. Vol. 12, No. 1, January - February, 1980

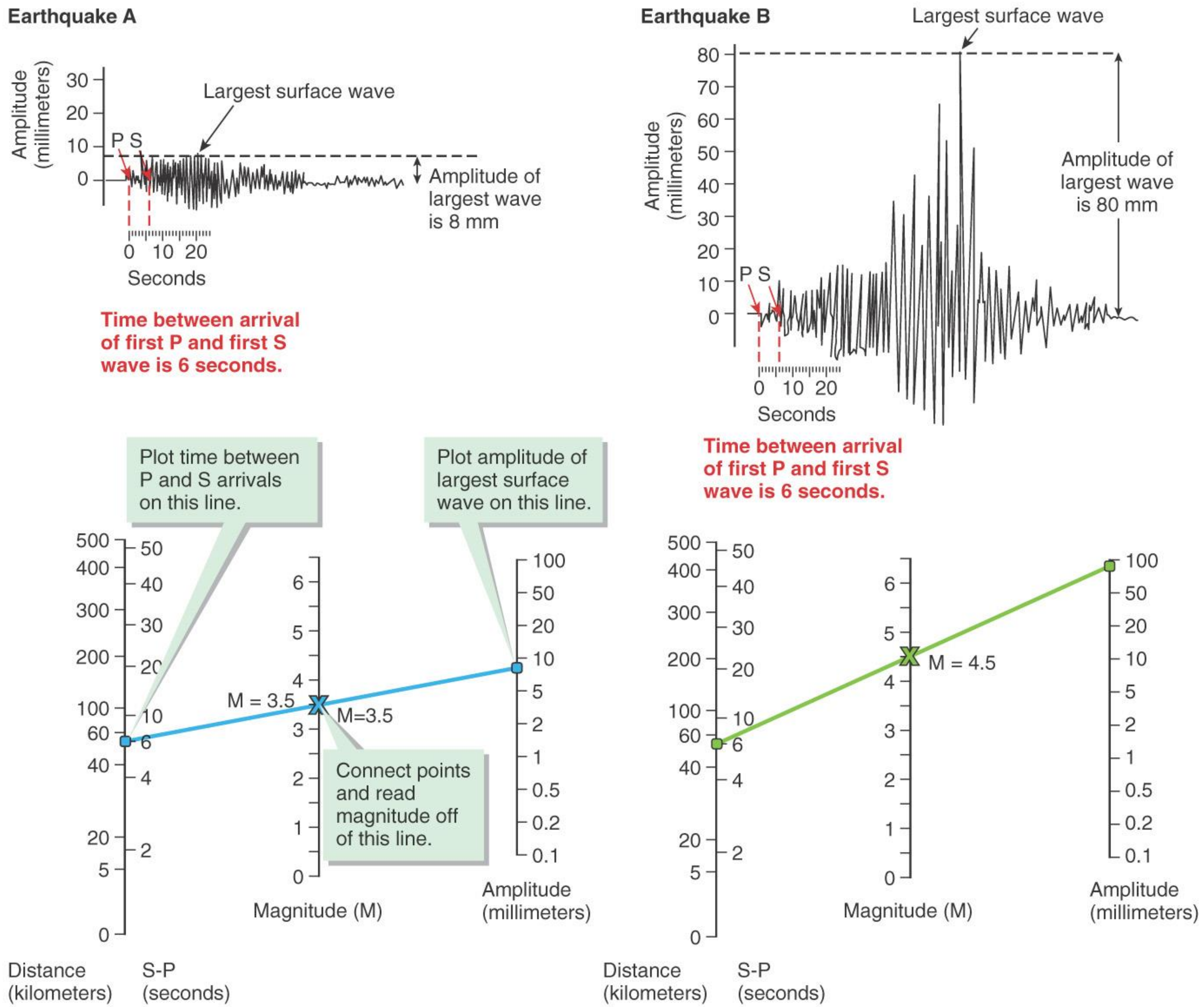

Earthquake A
Amplitude (millimeters)
30
20
10
0
P S
Largest surface wave
Amplitude of largest wave is 8 mm
0 10 20
Seconds
Time between arrival of first P and first S wave is 6 seconds.
Earthquake B
Largest surface wave
80
70
60
50
40
30
20
10
0
Amplitude (millimeters)
Amplitude of largest wave is 80 mm
P S
0 10 20
Seconds
Time between arrival of first P and first S wave is 6 seconds.
Plot time between P and S arrivals on this line.
Plot amplitude of largest surface wave on this line.
Connect points and read magnitude off of this line.
M = 3.5
M=3.5
M = 4.5
500 400 300 200 100 60 40 20 5 0
50 40 30 20 10 6 4 2
6 5 4 3 2 1 0
100 50 20 10 5 2 1 0.5 0.2 0.1
Distance (kilometers)
S-P (seconds)
Magnitude (M)
Amplitude (millimeters)

Wood-Anderson Seismometer

Richter also tied his formula to a specific seismic instrument.

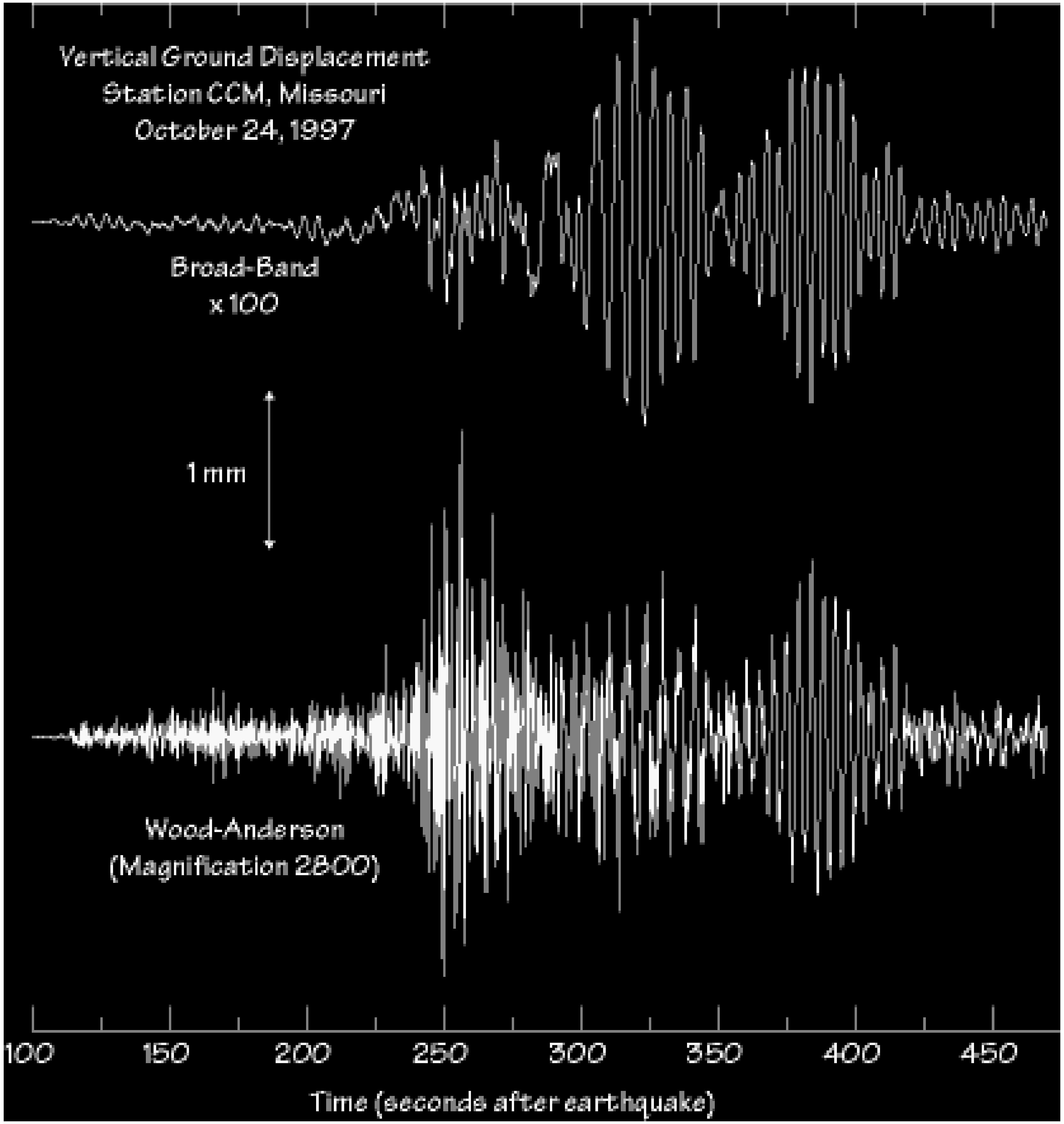

Magnitude Scales

The original M_L is suitable for the classification of local shocks in Southern California only since it used data from the standardized short-period Wood-Anderson seismometer network. The magnitude concept has then been extended so as to be applicable also to ground motion measurements from medium- and long-period seismographic recordings of both surface waves (M_s) and different types of body waves (m_b) in the teleseismic distance range.
The general form of all magnitude scales based on measurements of ground displacement amplitudes A and periods T is:

$$M = \log\left(\frac{A}{T}\right) + f(\Delta, h) + C_r + C_s$$

M seismic magnitude
A amplitude
T period
f correction for distance and depth
C_s correction for site
C_r correction for source region

M_L **Local magnitude**
m_b **body-wave magnitude** (1s)
M_s **surface wave magnitude** (20s)

Teleseismic M_S and mb

The two most common modern magnitude scales are:

- M_S, Surface-wave magnitude (Rayleigh Wave, 20s)
- m_b, Body-wave magnitude (P-wave)

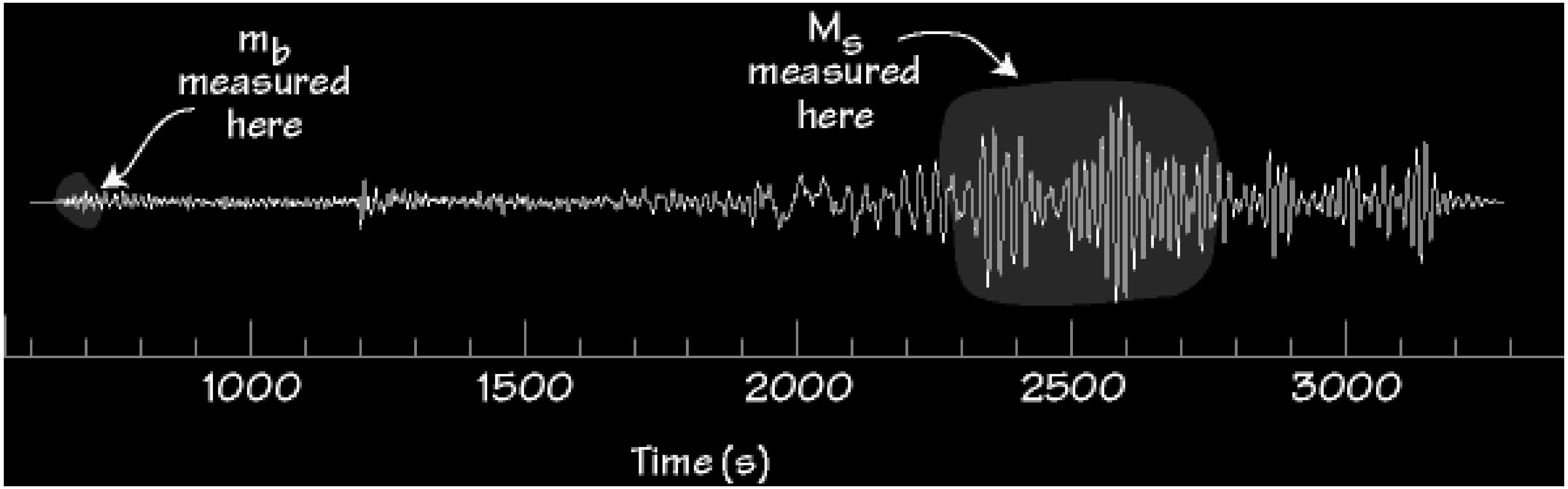

Example: m_b “Saturation”

m_b seldom gives values above 6.7 - it “saturates”.

m_b must be measured in the first 5 seconds - that’s the rule.

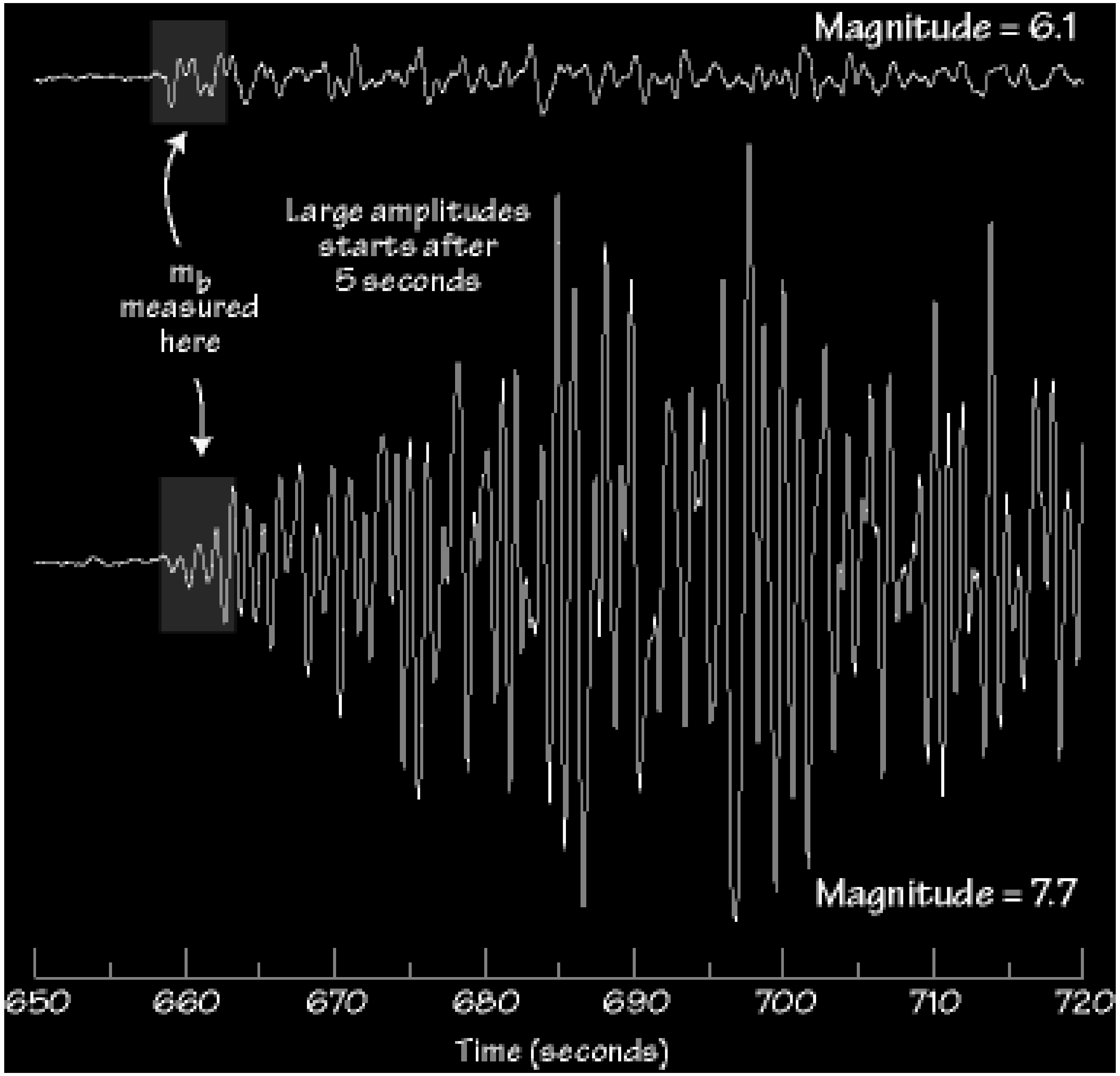

Saturation

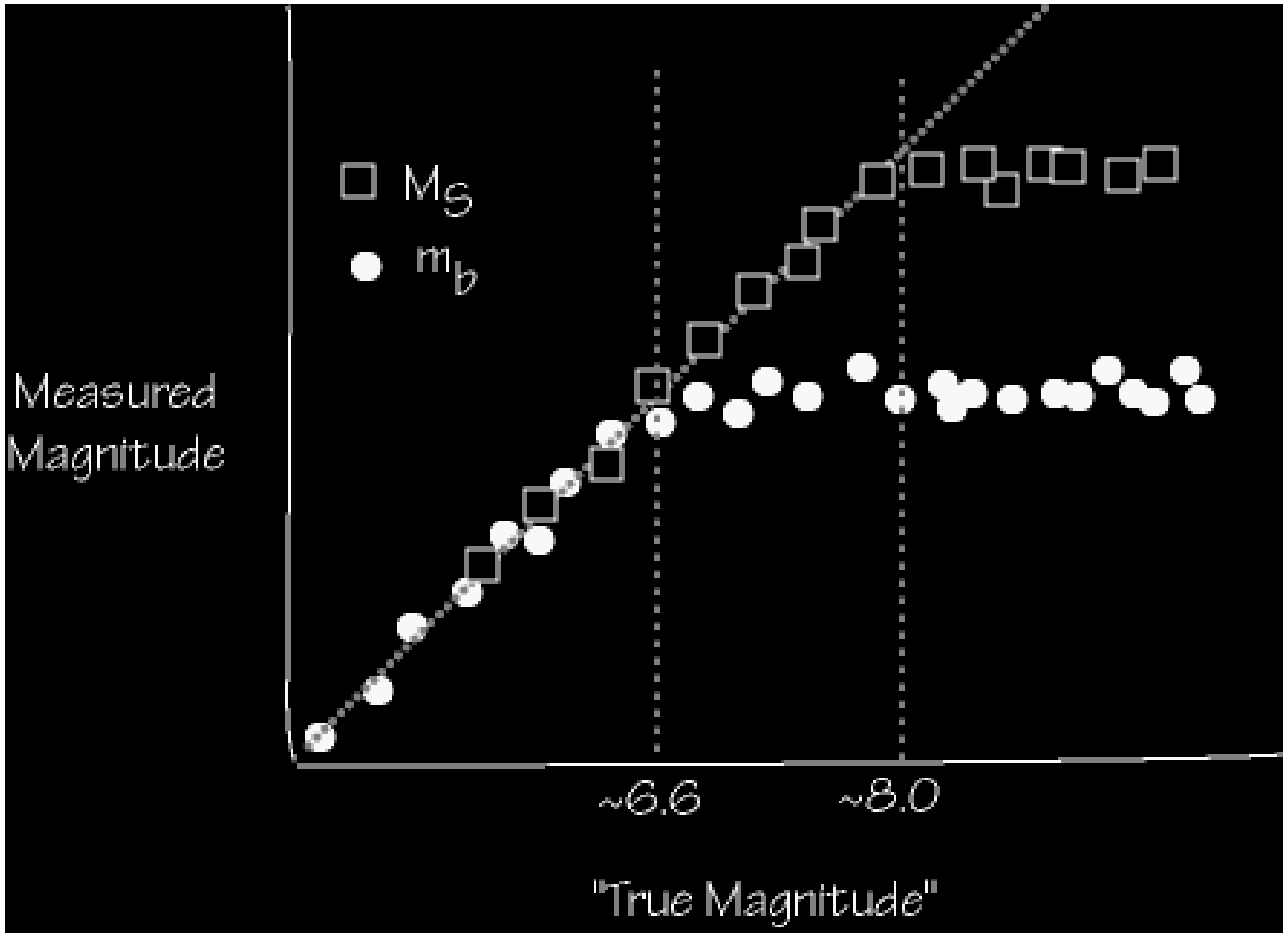

Magnitude saturation

Nature limits the maximum size of tectonic earthquakes which is controlled by the maximum size of a brittle fracture in the lithosphere. A simple seismic shear source with linear rupture propagation has a typical "source spectrum".

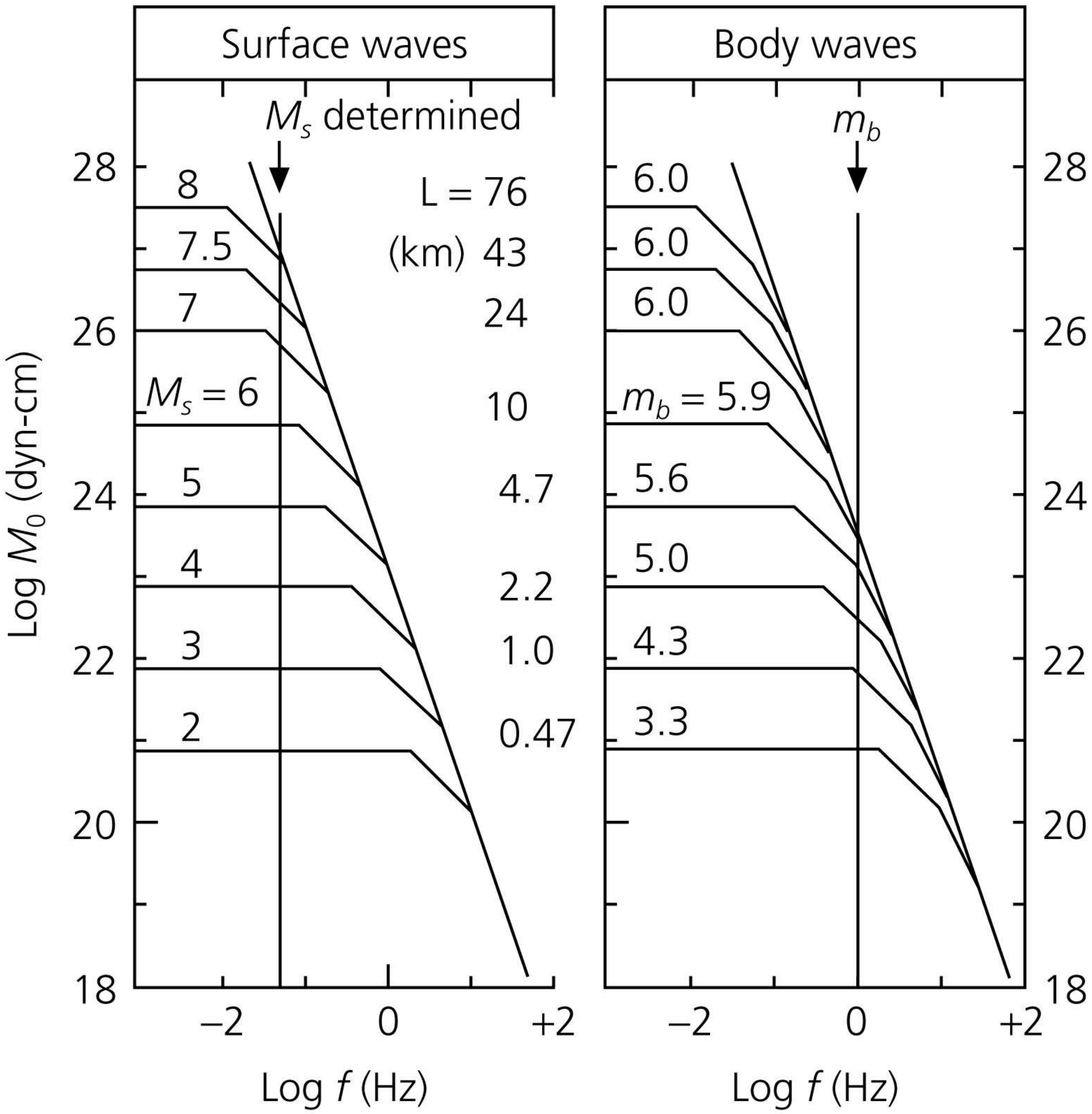

Ms is not linearly scaled with M_0 for $M_S > 6$ due to the beginning of the so-called saturation effect for spectral amplitudes with frequencies $f > f_c$. This saturation occurs already much earlier for m_b which are determined from amplitude measurements around 1 Hz.

Moment magnitude

Empirical studies (Gutenberg & Richter, 1956; Kanamori & Anderson, 1975) lead to a formula for the released seismic energy (in Joule), and for moment, with magnitude:

$\log E = 4.8 + 1.5 M_s$ $\log M_0 = 9.1 + 1.5 M_s$

resulting in

$$M_w = 2/3 \log M_0 - 6.07$$

when the Moment is measured in N·m (otherwise the intercept becomes 10.73); it is related to the final static displacement after an earthquake and consequently to the tectonic effects of an earthquake.

$$u(x,t) = A\cos\left(\frac{2\pi t}{T}\right) \Rightarrow v(x,t) \propto \frac{A}{T} u$$

$$\Rightarrow e \propto v^2 \propto \left(\frac{A}{T}\right)^2 \Rightarrow \log E = C + 2\log\left(\frac{A}{T}\right)$$

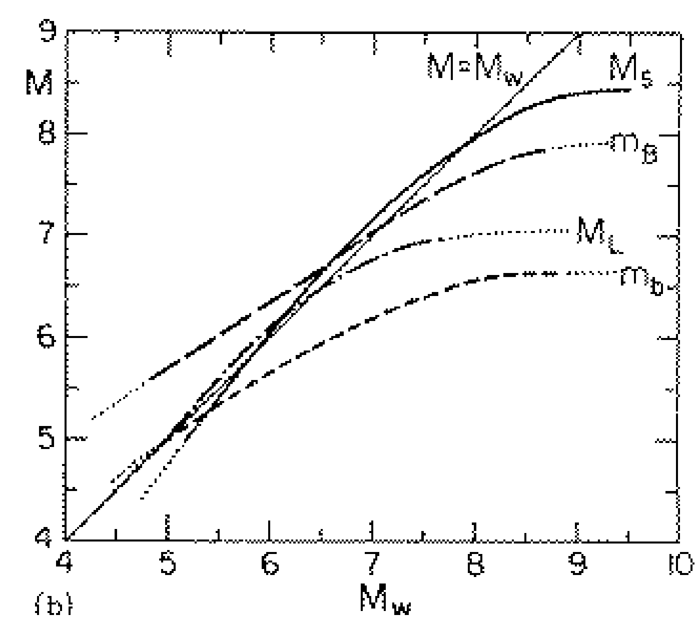

Earthquake	Body wave magnitude m_b	Surface wave magnitude M_s	Fault area (km^2) length × width	Average dislocation (m)	Moment (dyn-cm) M_0	Moment magnitude M_w
Truckee, 1966	5.4	5.9	10 × 10	0.3	8.3×10^{24}	5.8
San Fernando, 1971	6.2	6.6	20 × 14	1.4	1.2×10^{26}	6.7
Loma Prieta, 1989	6.2	7.1	40 × 15	1.7	3.0×10^{26}	6.9
San Francisco, 1906		8.2	320 × 15	4	6.0×10^{27}	7.8
Alaska, 1964	6.2	8.4	500 × 300	7	5.2×10^{29}	9.1
Chile, 1960		8.3	800 × 200	21	2.4×10^{30}	9.5

Seismic moment (1)

Remember . . . the displacement equation for the P and S wave radiation patterns:

$$u_r = \frac{1}{4\pi\alpha^3 r} \dot{M}\left(t - r/\alpha\right) \sin\left(2\theta\right)\cos(\varphi)$$

e.g. P waves

- $\frac{1}{4\pi\alpha^3 r}$ → Amplitude term
- $\dot{M}\left(t - r/\alpha\right)$ → Source time function
- $\sin\left(2\theta\right)\cos(\varphi)$ → Describes the pattern

Considering the ***seismic moment rate function*** or ***source time function***

$$\dot{M}\left(t - r/v\right)$$

which is the time derivative of the ***seismic moment function***

$$M(t) = \mu D(t) S(t)$$

where μ is rigidity, and *D(t)* and *S(t)* are the slip and fault area histories, respectively.

(*Lay & Wallace, 1995; Stein & Wysession, 2003*)

Seismic moment (2)

This leads to the best measure of an earthquake's size and energy,

$$M(t) = \mu D_{av} S$$

the ***seismic moment***, where D_{av} is the average slip or dislocation and *S* is the fault area.

which in turn gives the ***moment magnitude*** M_w

$$M_w = \frac{\log M_o}{1.5} - 10.73$$

where M_o is in dyn-cm.

and which we will discuss again with respect to other magnitude scales.

(*Lay & Wallace, 1995; Stein & Wysession*

Importance of comparing Mw and Me

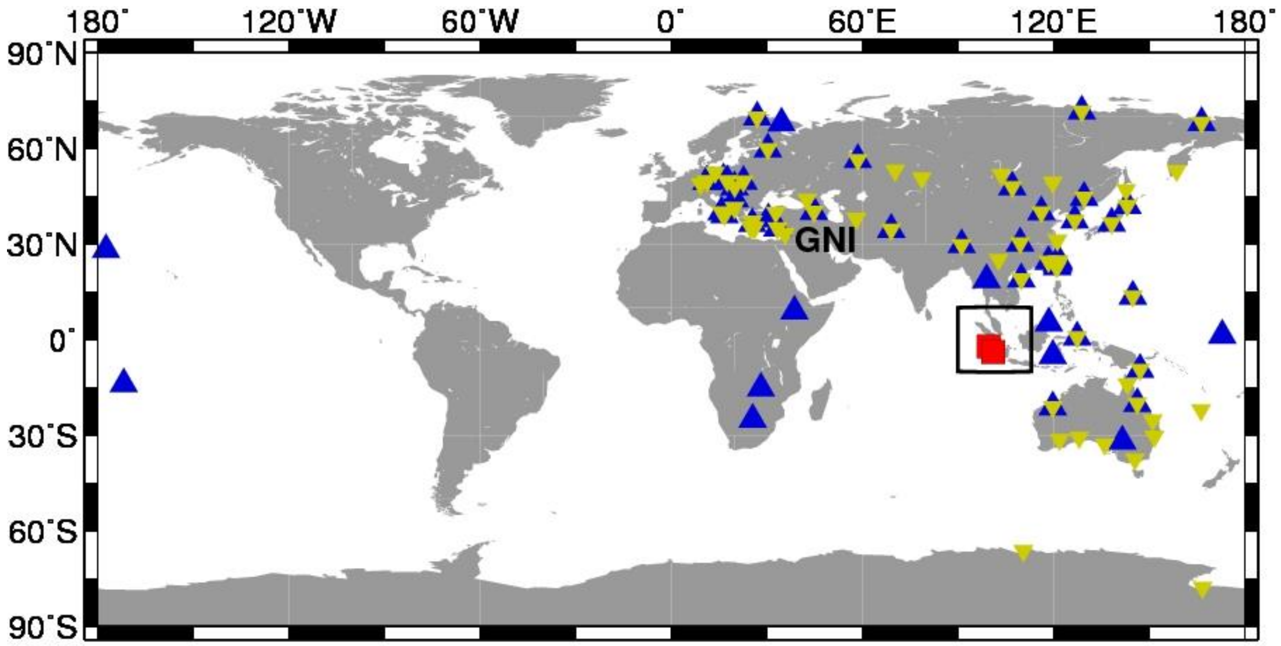

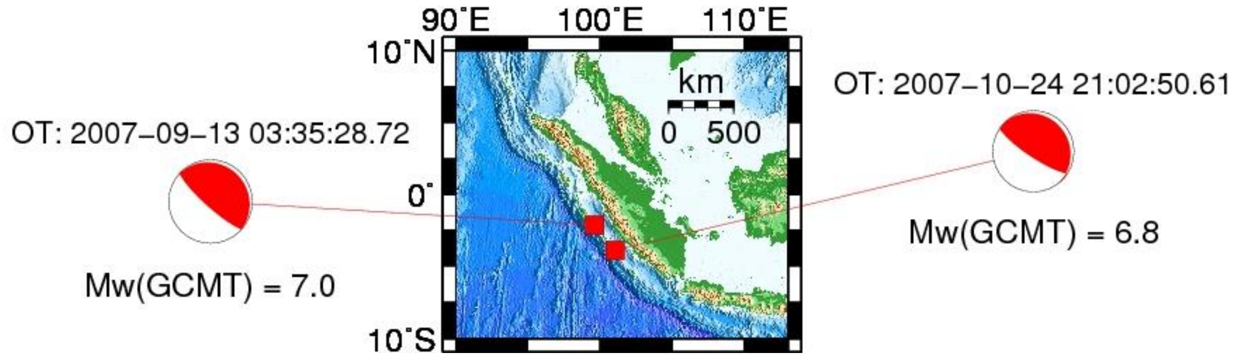

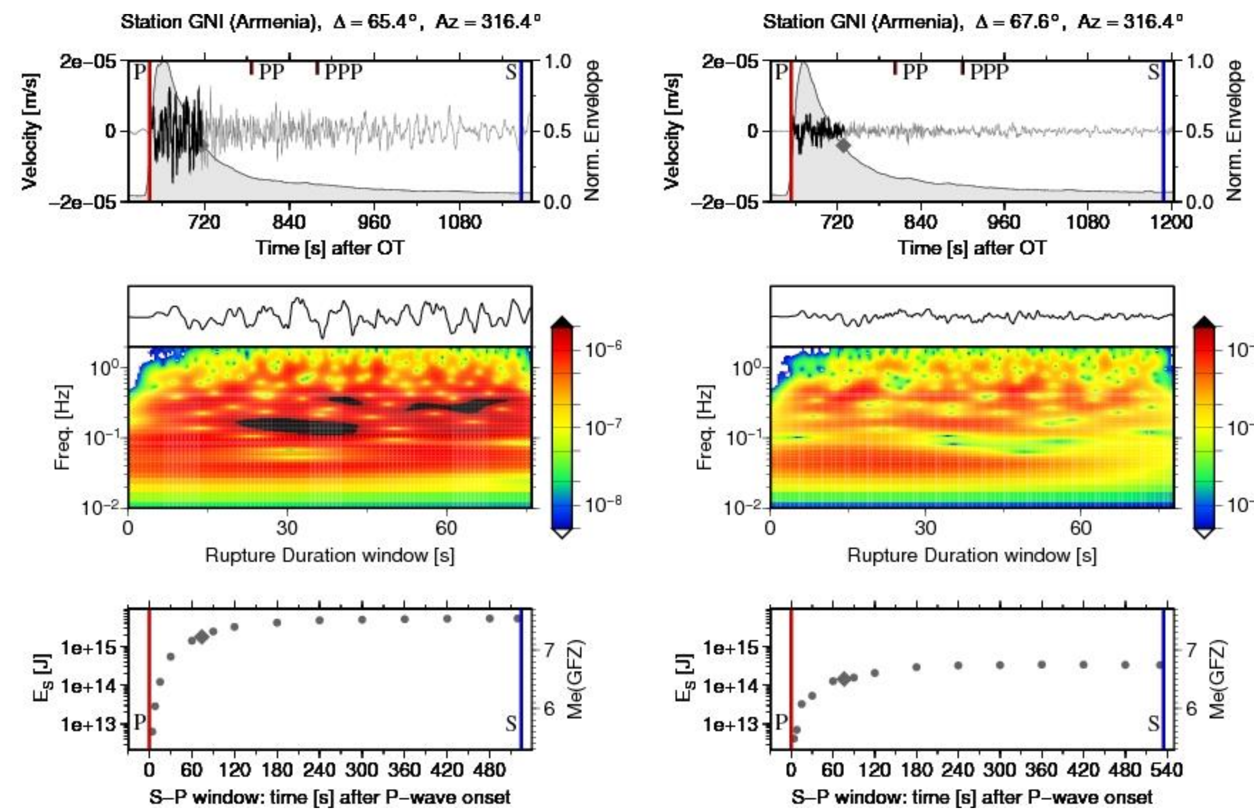

Mw(GCMT) = 7.0
Me(GFZ) = 7.1

Mw(GCMT) = 6.8
Me(GFZ) = 6.4

The locations differ by about 250 km and the moment magnitudes Mw and the fault plane solutions are very similar.

However, the high frequency content observed in the seismograms is significantly different and cannot be explained by Mw only.

Di Giacomo and Bindi (2009)

Importance of comparing Mw and Me

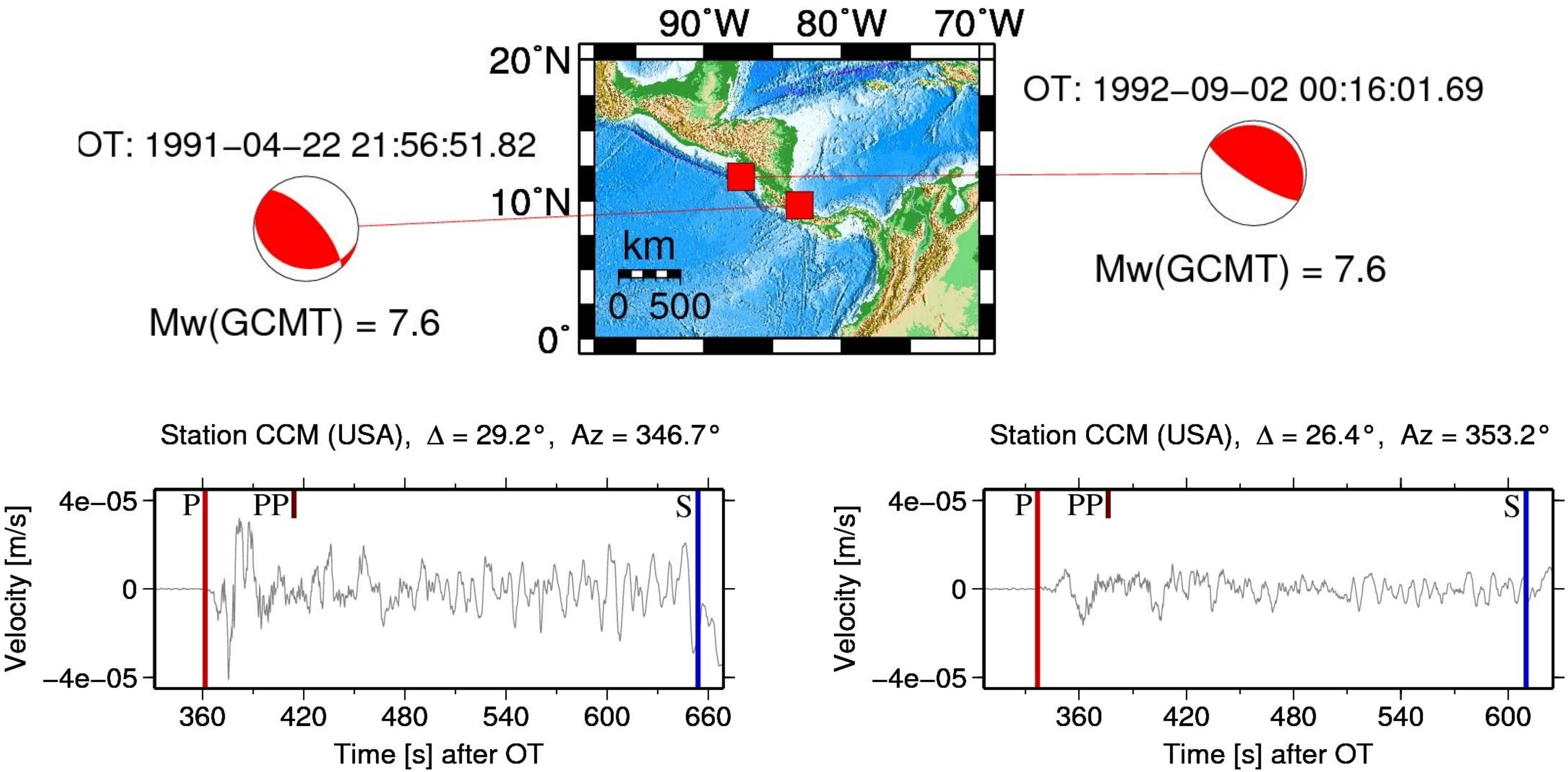

Mw(GCMT) = 7.6, Me(GFZ) = 7.19

Mw(GCMT) = 7.6, Me(GFZ) = 6.75

The locations differ by about 500 km and the moment magnitudes Mw are nearly identical, therefore the differences in the high frequency content observed in the seismograms can be attributed to different source characteristics.

Di Giacomo and Bindi (2009)

Strong motion seismology

- Strong ground motion is an event in which an earthquake cause the ground to shake at least strongly enough for people to feel the motion or to damage or destroy man-made structures.

- The goal of strong motion seismology is to be able to understand and predict seismic motions sufficiently well that the predictions can be used for engineering applications

- The field of strong-motion seismology could initially be identified with a type of instrument, designed to remain on-scale and record the ground motion with fidelity under the conditions of the strongest ground motions experienced in earthquakes.

Anderson J.G Physical Processes That Control Strong Ground Motion. In: Gerald Schubert (editor-in-chief) Treatise on Geophysics, 2nd edition, Vol 4. Oxford: Elsevier; 2015. p. 505-557.

Strong motion seismology

- Early instruments were typically designed so that ground motions up to the acceleration of gravity (1g) would be on-scale.

- The lower limit of ground motion considered by the early strong motion seismology studies was roughly defined by the thickness of the light beam read until the edge of a recorded film. The minimum acceleration resolved is somewhat less than 0.01g, that approximately coincided with minimum ground motions that humans are able to feel.

- Since much smaller ground motions can be recorded on modern instruments, the distinction between strong-motion seismology and traditional seismology is blurred.

Example of Recordings

Ground acceleration, velocity and displacement, recorded at a strong-motion seismometer that was located directly above the part of a fault that ruptured during the 1985 Mw = 8.1, Michaocan, Mexico earthquake.

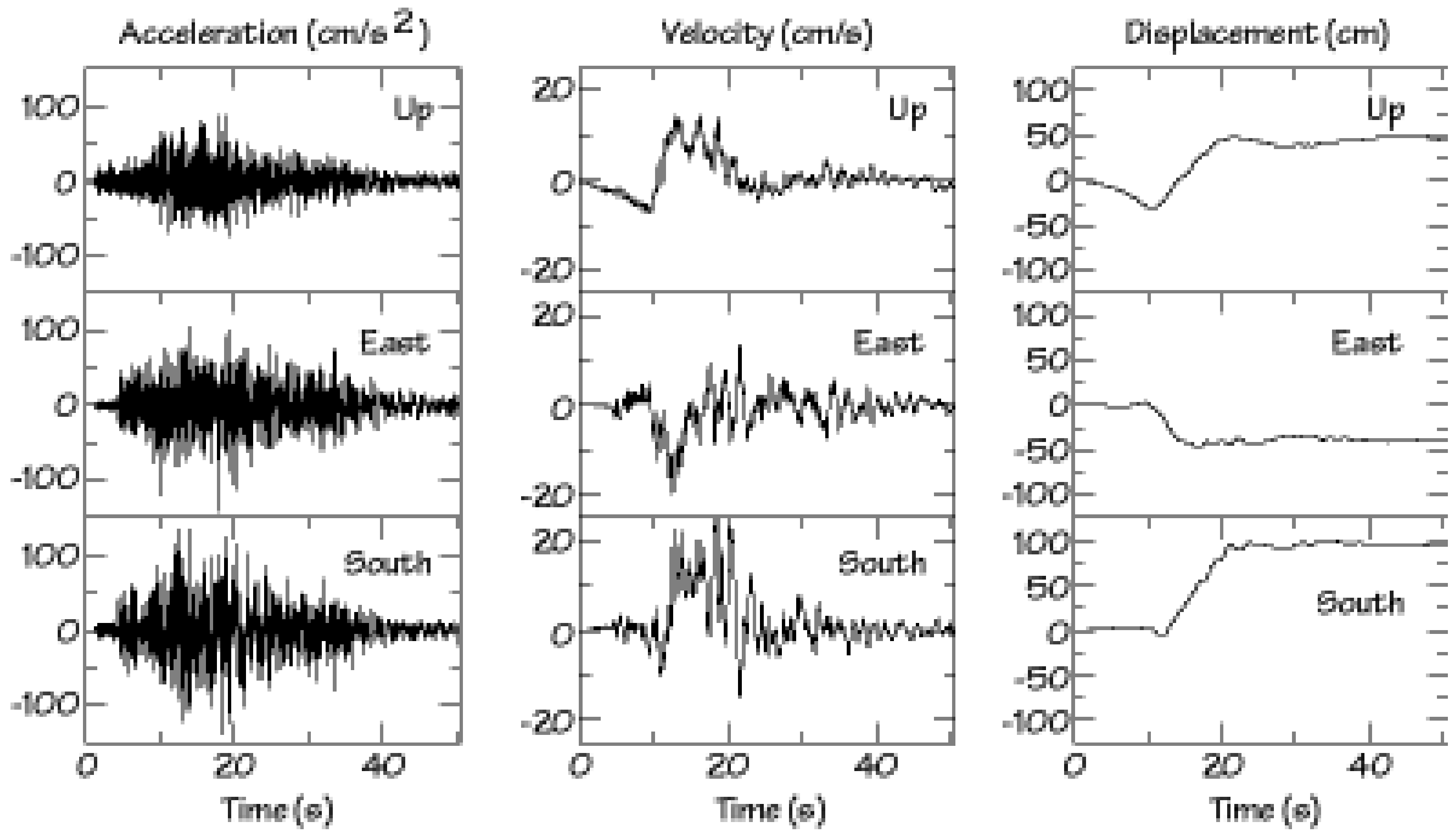

The left panel is a plot of the three components of acceleration: strong, high-frequency shaking lasted almost a minute and the peak acceleration was about 150 cm/s^2 (or about 0.15g). The middle panel shows the velocity of ground movement: the peak velocity for this site during that earthquake was about 20-25 cm/sec. Integrating the velocity, we can compute the displacement, which is shown in the right-most panel: the permanent offsets near the seismometer were up, west, and south, for a total distance of about 125 centimeters.

Maximum Intensity

Maximum Intensity is used to estimate the size of historical earthquakes, but suffers from dependence on depth, population, construction practices, site effects, regional geology, etc.

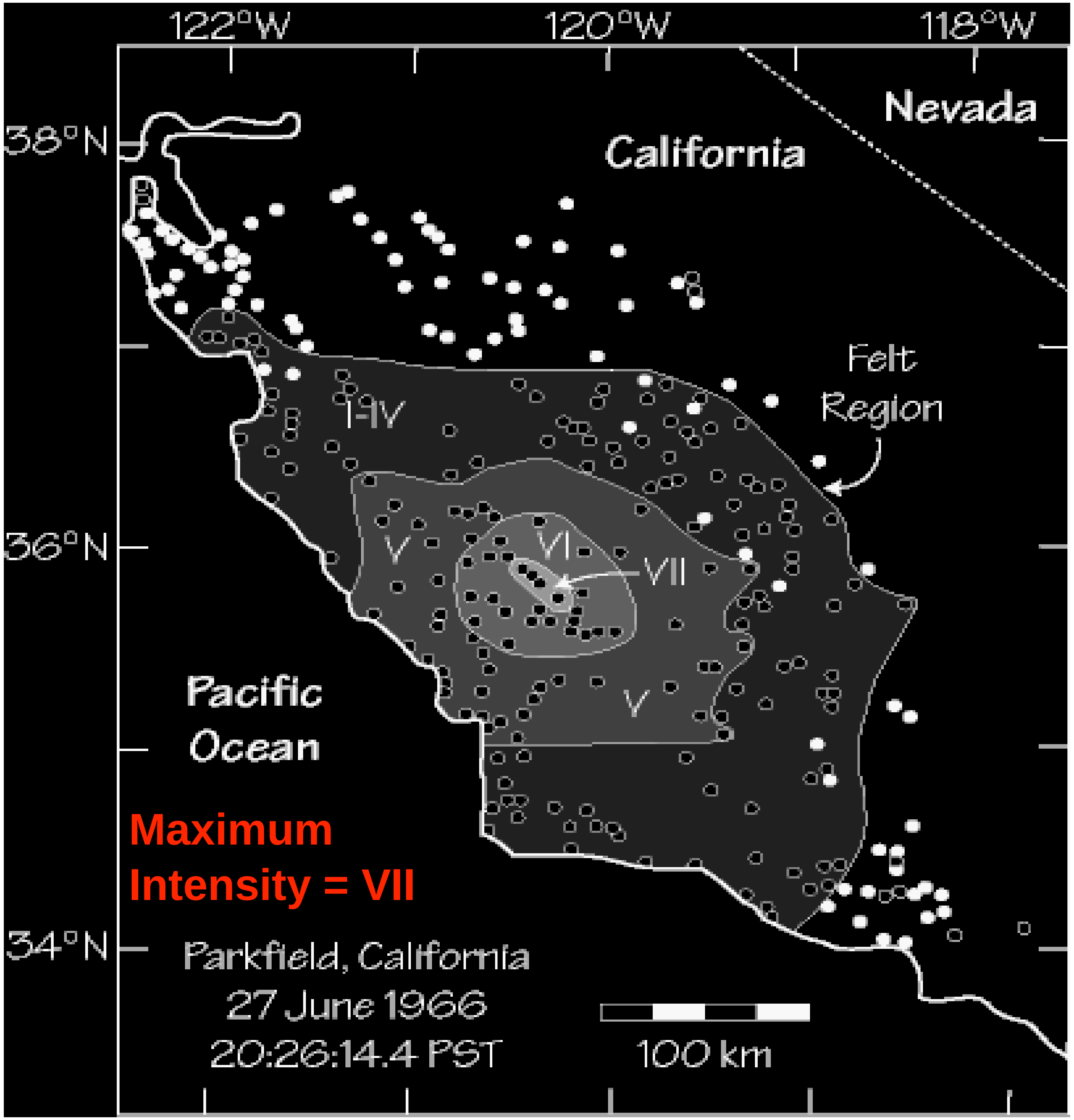

1906 SF and 1811-12 New Madrid

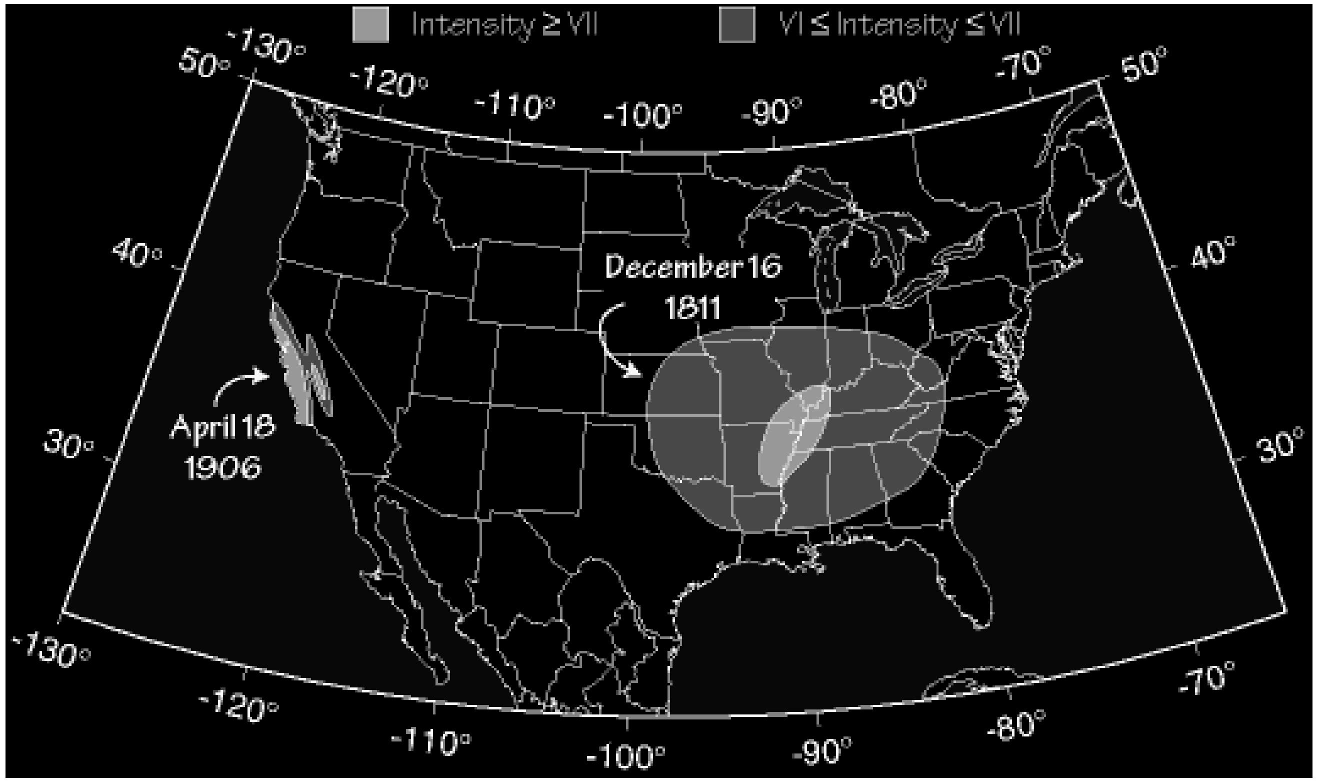

These earthquakes were roughly the same size, but the intensity patterns in the east are broader than in the west (wait for Q...)

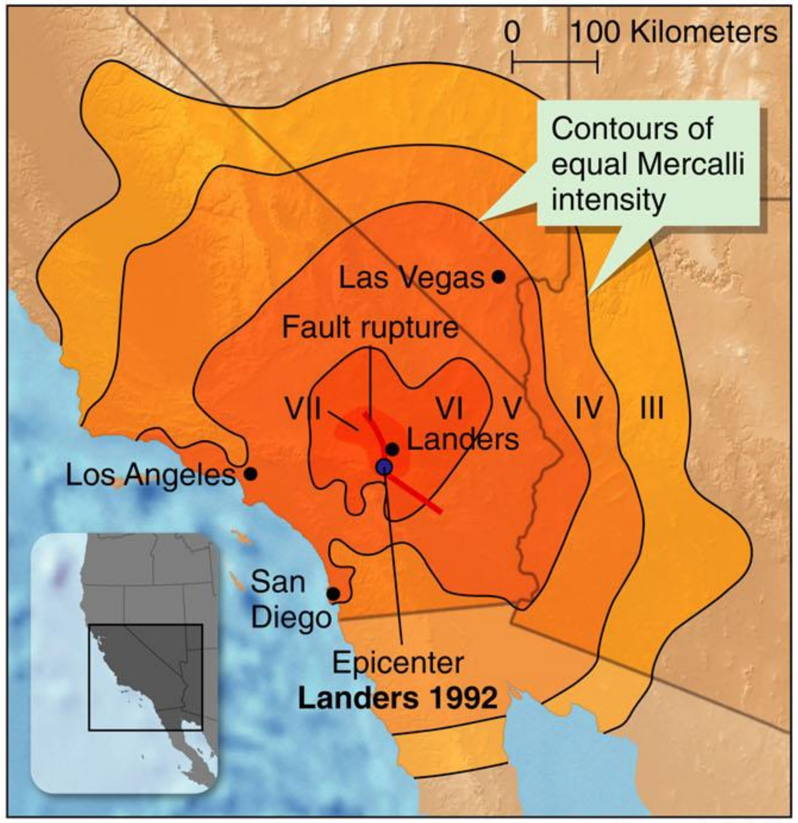

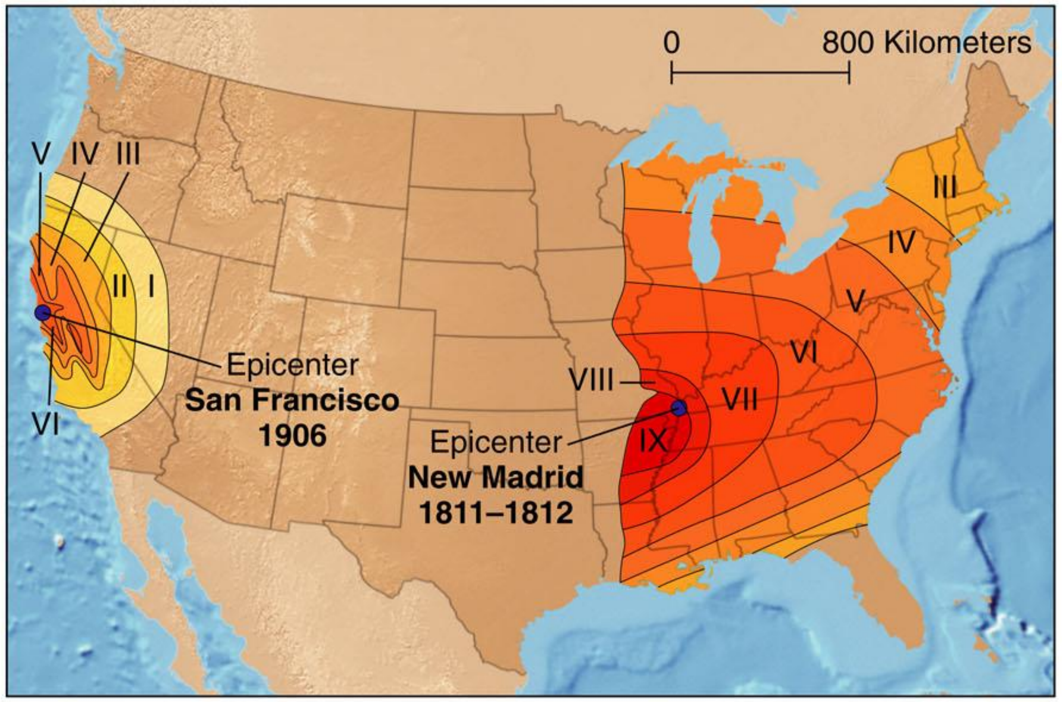

Mercalli Intensity and Richter Magnitude

Magnitude	Intensity	Description
1.0-3.0 **Micro**	**I**	**I.** Not felt except by a very few under especially favorable conditions.
3.0 - 3.9 **Minor**	**II - III**	**II.** Felt only by a few persons at rest, especially on upper floors of buildings. **III.** Felt quite noticeably by persons indoors, especially on upper floors of buildings. Many people do not recognize it as an earthquake. Standing motor cars may rock slightly. Vibrations similar to the passing of a truck. Duration estimated.
4.0 - 4.9 **Light**	**IV - V**	**IV.** Felt indoors by many, outdoors by few during the day. At night, some awakened. Dishes, windows, doors disturbed; walls make cracking sound. Sensation like heavy truck striking building. Standing motor cars rocked noticeably. **V.** Felt by nearly everyone; many awakened. Some dishes, windows broken. Unstable objects overturned. Pendulum clocks may stop.
5.0 - 5.9 **Moderate**	**VI - VII**	**VI.** Felt by all, many frightened. Some heavy furniture moved; a few instances of fallen plaster. Damage slight. **VII.** Damage negligible in buildings of good design and construction; slight to moderate in well-built ordinary structures; considerable damage in poorly built or badly designed structures; some chimneys broken.
6.0 - 6.9 **Strong**	**VII - IX**	**VIII**. Damage slight in specially designed structures; considerable damage in ordinary substantial buildings with partial collapse. Damage great in poorly built structures. Fall of chimneys, factory stacks, columns, monuments, walls. Heavy furniture overturned. **IX.** Damage considerable in specially designed structures; well-designed frame structures thrown out of plumb. Damage great in substantial buildings, with partial collapse. Buildings shifted off foundations.
7.0 and higher **Major great**	**VIII or higher**	**X.** Some well-built wooden structures destroyed; most masonry and frame structures destroyed with foundations. Rails bent. **XI.** Few, if any (masonry) structures remain standing. Bridges destroyed. Rails bent greatly. **XII.** Damage total. Lines of sight and level are distorted. Objects thrown into the air.

Intensity scales

<table>
<tr><th>MM</th><th>RF</th><th>JMA</th><th>MCS</th><th>MSK</th></tr>
<tr><td rowspan="2">I</td><td rowspan="3">I</td><td></td><td rowspan="2">II</td><td rowspan="2">I</td></tr>
<tr><td rowspan="4">I</td></tr>
<tr><td rowspan="2">II</td><td rowspan="2">III</td><td>II</td></tr>
<tr><td>II</td><td rowspan="2">III</td></tr>
<tr><td>III</td><td>III</td><td>IV</td></tr>
<tr><td rowspan="2">IV</td><td>IV</td><td rowspan="2">II</td><td rowspan="2">V</td><td rowspan="2">IV</td></tr>
<tr><td rowspan="2">V</td></tr>
<tr><td rowspan="2">V</td><td rowspan="2">III</td><td rowspan="2">VI</td><td rowspan="2">V</td></tr>
<tr><td rowspan="2">VI</td></tr>
<tr><td rowspan="2">VI</td><td rowspan="2">IV</td><td rowspan="2">VII</td><td rowspan="2">VI</td></tr>
<tr><td>VII</td></tr>
<tr><td rowspan="2">VII</td><td rowspan="3">VIII</td><td rowspan="5">V</td><td>VIII</td><td rowspan="2">VII</td></tr>
<tr><td rowspan="3">IX</td></tr>
<tr><td rowspan="3">VIII</td><td rowspan="3">VIII</td></tr>
<tr><td rowspan="4">IX</td></tr>
<tr><td rowspan="2">X</td></tr>
<tr><td rowspan="2">IX</td><td rowspan="4">VI</td><td rowspan="2">IX</td></tr>
<tr><td rowspan="2">XI</td></tr>
<tr><td rowspan="2">X</td><td rowspan="4">X</td><td rowspan="2">X</td></tr>
<tr><td>XII</td></tr>
<tr><td>XI</td><td rowspan="2">VII</td><td rowspan="2"></td><td>XI</td></tr>
<tr><td>XII</td><td>XII</td></tr>
</table>

MM – Modified Mercalli; RF – Rossi-Forel; JMA – Japanese Meteorological Agency;
MCS – Mercalli-Cancani-Sieberg; MSK – Medvedev-Sponheuer-Karnik

Intensity scales

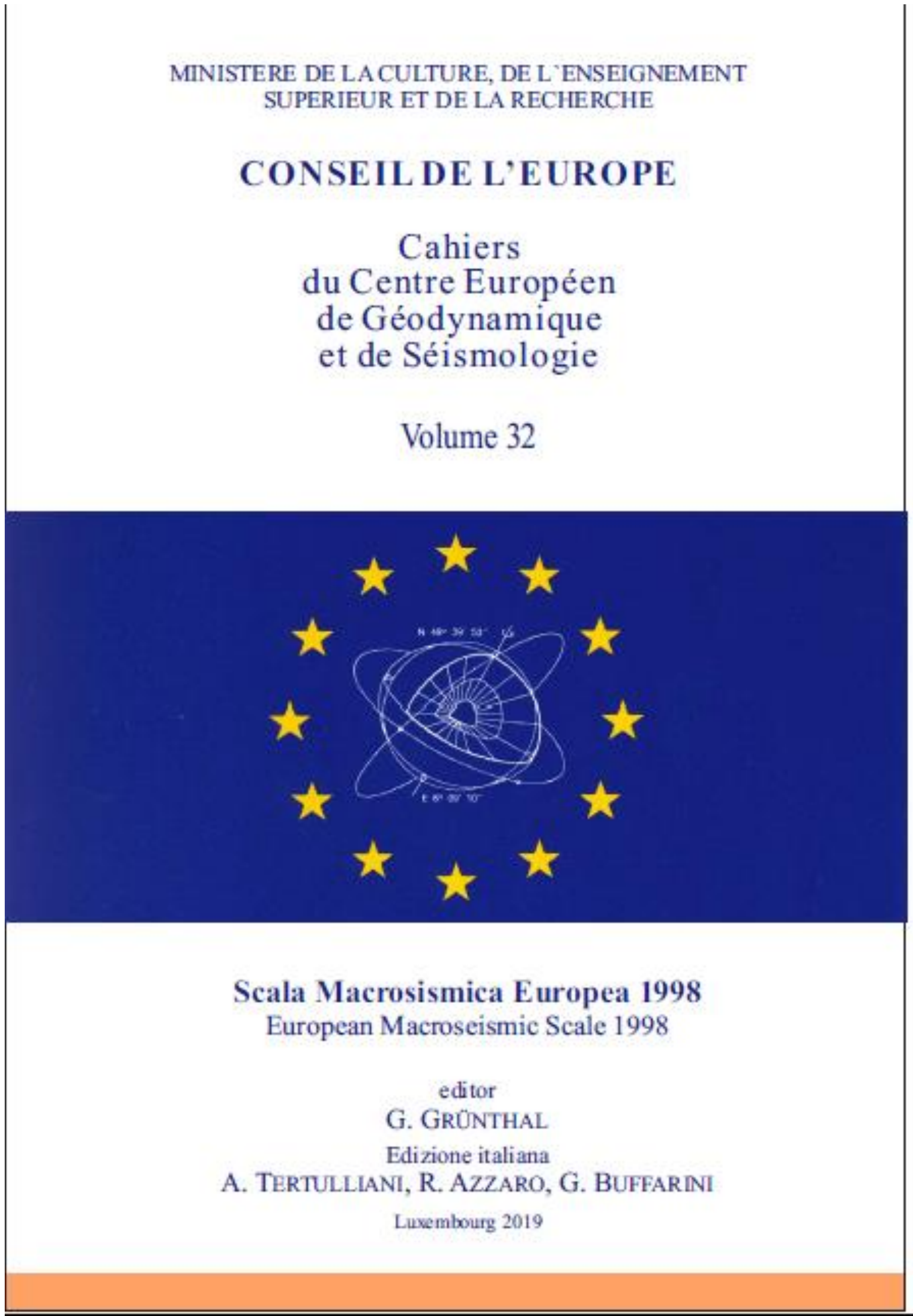

8 Tabella sintetica della EMS-98

La forma sintetica della Scala Macrosismica Europea, estratta dalla parte centrale, è fornita per dare una panoramica molto semplificata e generalizzata della Scala EM. Essa può, per esempio, essere usata per scopi divulgativi. *Questa forma sintetica ma non è adatta per le assegnazioni d'intensità.*

Intensità EMS	Definizione	Descrizione degli effetti tipici osservati (riassunto)
I	**Non avvertito**	Non avvertito.
II	**Appena avvertito**	Avvertito solo da poche persone in stato di riposo al chiuso.
III	**Debole**	Avvertito da alcune persone in casa. Persone a riposo avvertono una oscillazione o un leggero tremore.
IV	**Ampiamente osservato**	Avvertito all'interno da molta gente, da pochissimi all'esterno. Alcune persone si svegliano. Finestre, porte e piatti sbattono.
V	**Forte**	Avvertito all'interno dalla maggior parte delle persone, all'esterno da pochi. Molte persone che dormivano si svegliano. Alcuni si spaventano. Gli edifici tremano nel loro complesso. Oggetti appesi oscillano notevolmente. Piccoli oggetti vengono spostati. Porte e finestre si spalancano o si chiudono.
VI	**Danni lievi**	Molte persone si spaventano e corrono all'aperto. Alcuni oggetti cadono. Molti edifici subiscono leggeri danni non strutturali come sottilissime fessure capillari e caduta di piccoli pezzi di intonaco.
VII	**Danni diffusi**	La maggior parte delle persone si spaventano e corrono fuori. I mobili si spostano e gli oggetti cadono dalle mensole in grande numero. Molti edifici ben costruiti subiscono danni moderati: piccole crepe nei muri, caduta di intonaco, caduta di parti di camini; gli edifici più vecchi possono mostrare grandi crepe nei muri e cedimento dei tramezzi.
VIII	**Danni gravi**	Molte persone hanno difficoltà a stare in piedi. Molti edifici presentano grandi fenditure nei muri. Alcuni edifici ben costruiti mostrano cedimenti gravi dei muri, mentre strutture deboli e più vecchie possono crollare.
IX	**Distruttivo**	Panico generale. Molte costruzioni deboli crollano. Anche edifici ben costruiti mostrano danni molto gravi: gravi lesioni dei muri e parziali cedimenti strutturale.
X	**Molto distruttivo**	Molti edifici ben costruiti crollano.
XI	**Devastante**	La maggior parte degli edifici ben costruiti crollano; anche alcuni con un buon livello di progettazione antisismica vengono distrutti.
XII	**Completamente devastante**	Quasi tutti gli edifici vengono distrutti.

Offline application to Kyrgyzstan: Lead time for Repetition of the M 7.8 1911 Kemin Earthquake

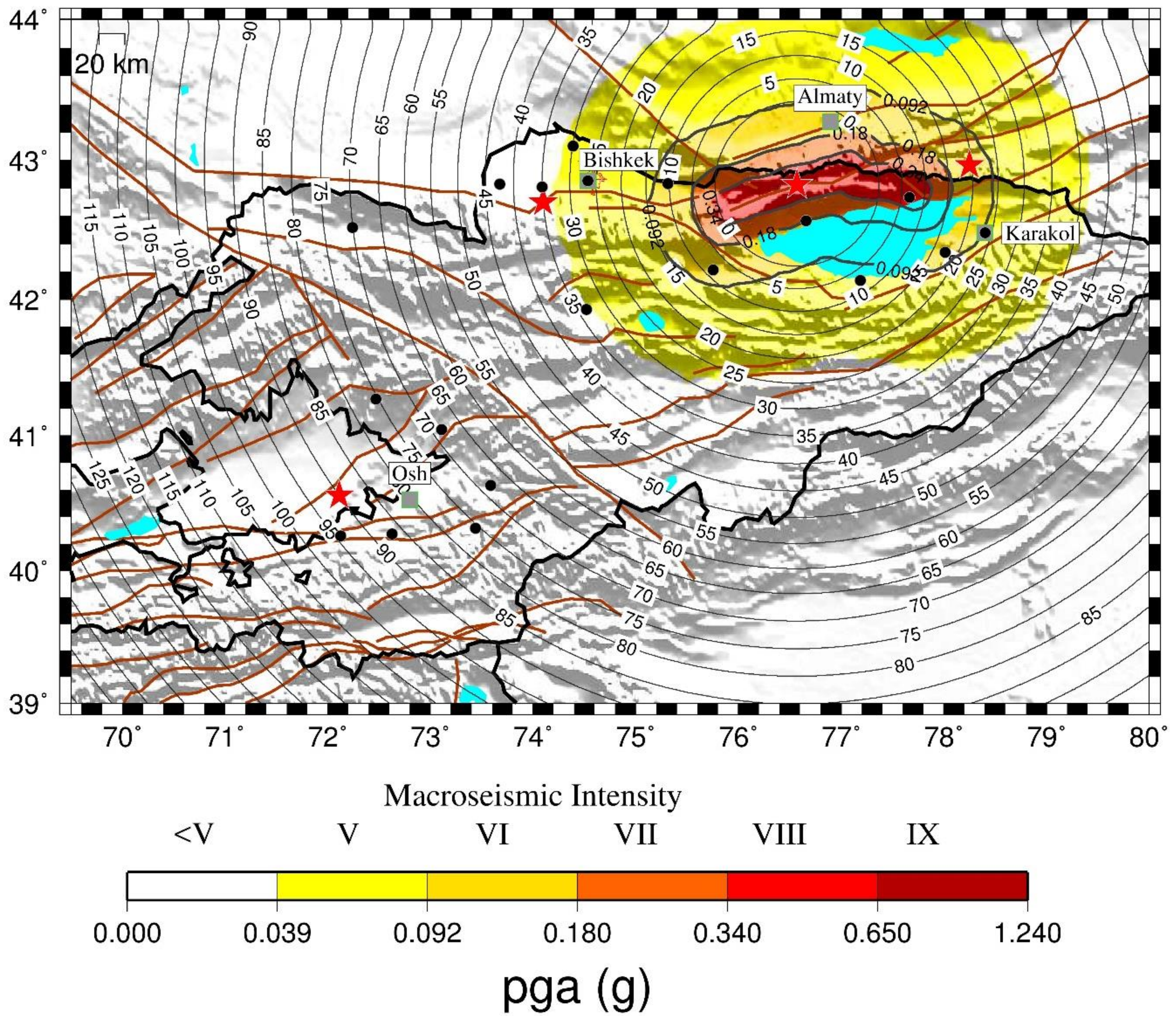

from
Parolai et al.,2017, Frontiers

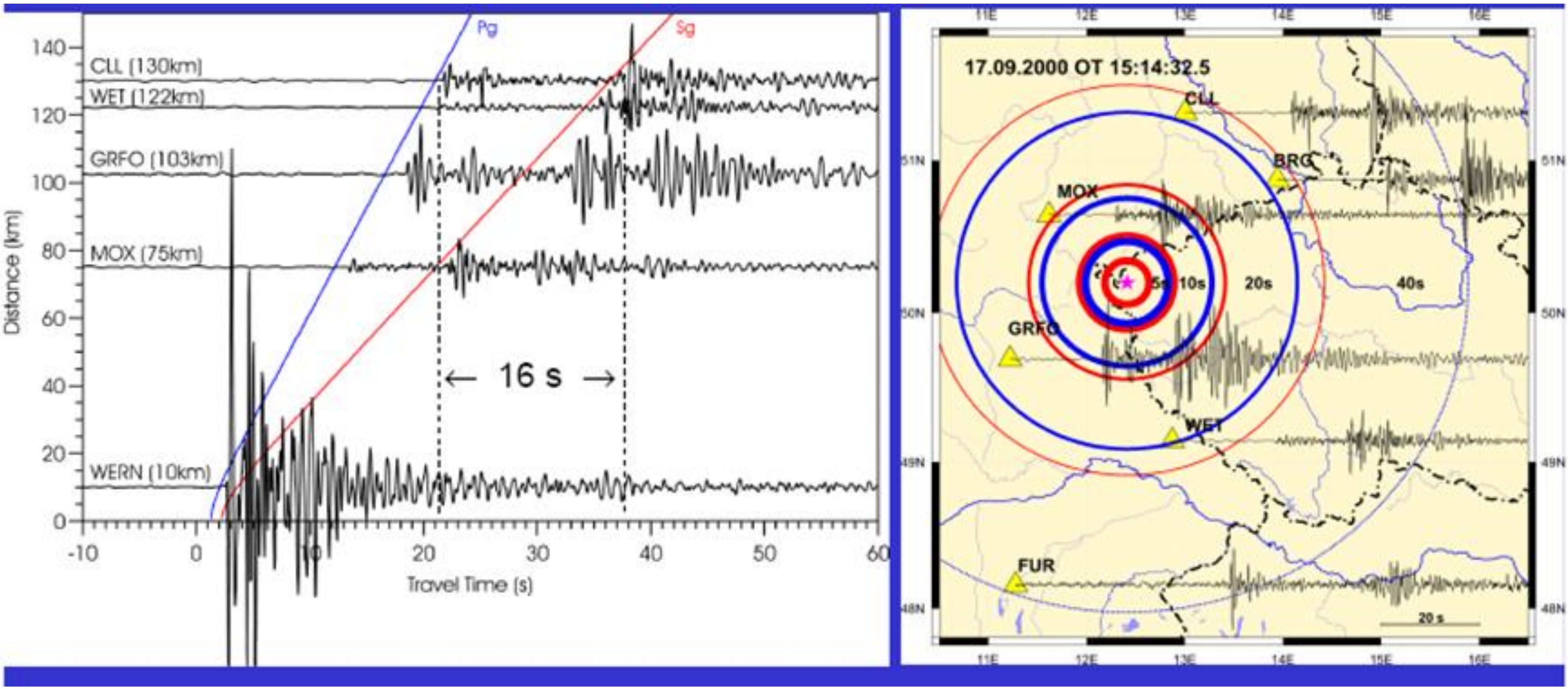

Pg
Sg
CLL (130km)
WET (122km)
GRFO (103km)
MOX (75km)
WERN (10km)
16 s
Distance (km)
Travel Time (s)
17.09.2000 OT 15:14:32.5
CLL
BRG
MOX
GRFO
WET
FUR
5s
10s
20s
40s
20 s

$$Tp = D/Vp$$

$$Ts = D/Vs$$

$$Ts - Tp = D(1/Vs - 1/Vp)$$

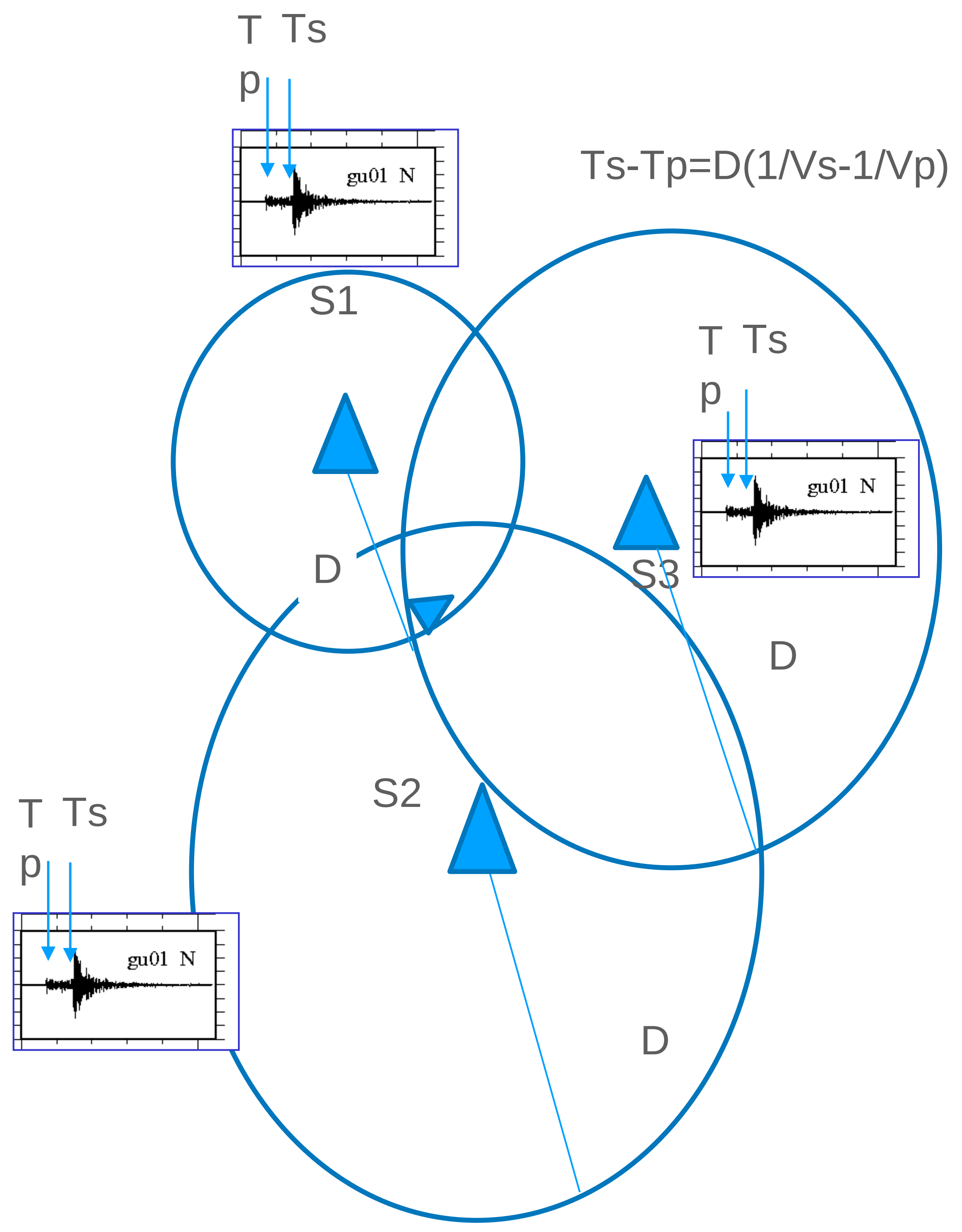

Confronto tra diversi metodi per la localizzazione dei terremoti

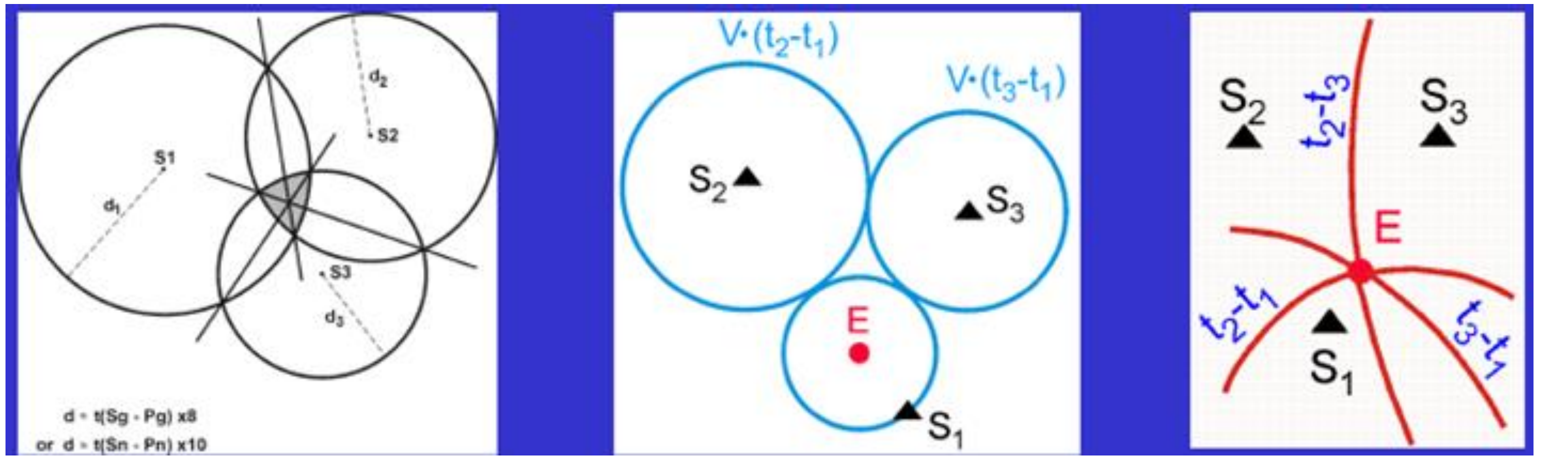

Tutti i metodi illustrati non considerano la forma della terra, e si basano su distanze planari cioè possono essere applicati solo su piccola scala, a livello locale.
Allo stesso modo, tutti i metodi si basano sul modello calcolo dei tempi di percorso mostrato nella diapositiva precedente

PlanetPhysics/Geigers Method

< PlanetPhysics

Geiger's method [1] is an iterative procedure using Gauss-Newton optimization to determine the location of an earthquake, or seismic event. Originally his method was developed to obtain the origin time and Epicentre but it is easily extended to include the Focal Depth for Hypocentre determination.

Given a set of M arrival times t_i find the origin time t_0 and the hypocentre in cartesian coordinatios (x_0, y_0, z_0) which minimize

the objective function

$$F(\mathbf{X}) = \sum_{i=1}^{M} r_i^2.$$

Here, r_i is the difference between observed and calculated arrival times

$$r_i = t_i - t_0 - T_i,$$

and the unknown parameter vector is

$$\mathbf{X} = (t_0, x_0, y_0, z_0)^{\mathrm{T}}$$

In matrix form (1) becomes

$$F(\mathbf{X}) = \mathbf{r}^{\mathrm{T}}\mathbf{r}$$

The Gauss--Newton procedure requires an initial guess of the sought parameters, denoted here as

$$\mathbf{X}^* = (t_0^*, x_0^*, y_0^*, z_0^*)^{\mathbf{T}},$$

which are then used to calculate the adjustment vector

$$\delta\mathbf{X} = (\delta t_0, \delta x_0, \delta y_0, \delta z_0)^{\mathrm{T}}$$

in

$$(1)\mathbf{A}^{\mathrm{T}}\mathbf{A}\delta\mathbf{X} = -\mathbf{A}^{\mathrm{T}}\mathbf{r}.$$

The Jacobian matrix $\mathbf{A}$ is defined as

$$\mathbf{A} = \begin{pmatrix} \partial r_1/\partial t_0 & \partial r_1/\partial x_0 & \partial r_1/\partial y_0 & \partial r_1/\partial z_0 \\ \partial r_2/\partial t_0 & \partial r_2/\partial x_0 & \partial r_2/\partial y_0 & \partial r_2/\partial z_0 \\ \vdots & \vdots & \vdots & \vdots \\ \partial r_M/\partial t_0 & \partial r_M/\partial x_0 & \partial r_M/\partial y_0 & \partial r_M/\partial z_0 \end{pmatrix}.$$

The partial derivatives are evaluated at the initial guess, or trial vector, $\mathbf{X}^*$. Equation (45) can be rewritten as

$$(2)\mathbf{G}\delta\mathbf{X} = \mathbf{g}.$$

Using (46) and an initial guess $\mathbf{X}^*$ an adjustment vector can be calculated. The initial guess can then be updated $\mathbf{X}^* + \delta\mathbf{X}$ and used as the inital guess in the next run of the algorithm. In this manner the sought parameters $\mathbf{X}$ can be determined to some tolerance.

De aggregazione

$$\lambda(IM > x) = \sum_{i=1}^{n_{sources}} \lambda(M_i > m_{\min}) \sum_{j=1}^{n_M} \sum_{k=1}^{n_R} P(IM > x | m_j, r_k) P(M_i = m_j) P(R_i = r_k) \quad (2.25)$$

where the range of possible M_i and R_i have been discretized into n_M and n_R intervals, respectively, using the discretization technique discussed earlier.

One of the primary advantages of PSHA—that it accounts for all possible earthquake sources in an area when computing seismic hazard—is also a disadvantage. Once the PSHA computations are complete, a natural question to ask is "which earthquake scenario is most likely to cause *PGA>x*?" Because we have aggregated all scenarios together in the PSHA calculations, the answer is not immediately obvious. We saw in the example calculations above, however, that some of the intermediate calculation results indicated the relative contribution of different earthquake sources and magnitudes to the rate of exceedance of a given ground motion intensity. Here we will formalize those calculations, through a process known as deaggregation[1] (Bazzurro & Cornell, 1999; McGuire, 1995).

Let us start with magnitude deaggregation. In this case, we are interested in the probability that an earthquake's magnitude is equal to m, given that a ground motion of $IM > x$ has occurred. Intuitively, this is equal to the rate of earthquakes with $IM > x$ and $M = m$, divided by the rate of all earthquakes with $IM > x$

$$P(M = m | IM > x) = \frac{\lambda(IM > x, M = m)}{\lambda(IM > x)} \quad (3.1)$$

$$\lambda(IM > x, M = m) = \sum_{i=1}^{n_{sources}} \lambda(M_i > m_{\min}) \sum_{k=1}^{n_{R_i}} P(IM > x|m, r_k) P(M_i = m) P(R_i = r_k) \quad (3.2)$$

Per Magnitudo e Distanza

$$P(M = m, R = r|IM > x) = \frac{\lambda(IM > x, M = m, R = r)}{\lambda(IM > x)} \quad (3.8)$$

where the numerator of equation 3.8 is computed using the basic PSHA equation but not summing over either M or R

$$\lambda(IM > x, M = m, R = r) = \sum_{i=1}^{n_{sources}} \lambda(M_i > m_{\min}) P(IM > x|m_j, r_k) P(M_i = m) P(R_i = r)$$